REAGENTS AND METHODOLOGIES FOR THE INTRODUCTION OF THIOFLUOROALKYL AND FLUOROSULFUR MOTIFS

Miguel Bernús Pérez

Reduced Manuscript

The current PhD thesis document provided is a condensed version that excludes Chapter 6 due to its confidential nature. Chapter 6 contains research findings that are intended for patent application. In order to protect the intellectual property and potential commercial interests, the decision was made to omit this chapter from the public version of the thesis.

UNIVERSITAT ROVIRA i VIRGILI

Reagents and methodologies for the introduction of thiofluoroalkyl and fluorosulfur motifs

MIGUEL BERNÚS PÉREZ

DOCTORAL THESIS
2023

UNIVERSITAT ROVIRA I VIRGILI
REAGENTS AND METHODOLOGIES FOR THE INTRODUCTION OF THIOFLUOROALKYL AND FLUOROSULFUR MOTIFS
Miguel Bernús Pérez

UNIVERSITAT ROVIRA I VIRGILI
REAGENTS AND METHODOLOGIES FOR THE INTRODUCTION OF THIOFLUOROALKYL AND FLUOROSULFUR MOTIFS
Miguel Bernús Pérez

Miguel Bernús Pérez

Reagents and methodologies for the introduction of thiofluoroalkyl and fluorosulfur motifs

DOCTORAL THESIS

Supervised by

Dr. Omar Boutureira Martín

UNIVERSITAT ROVIRA I VIRGILI

Department of Analytical Chemistry and Organic Chemistry

Tarragona 2023

UNIVERSITAT ROVIRA I VIRGILI
REAGENTS AND METHODOLOGIES FOR THE INTRODUCTION OF THIOFLUOROALKYL AND FLUOROSULFUR MOTIFS
Miguel Bernús Pérez

UNIVERSITAT ROVIRA I VIRGILI

Departament de Química Analítica i Química Orgànica

C/ Marcel·lí Domingo, 1

Campus Sescelades

43007, Tarragona

Dr. Omar Boutureira Martín from the Department of Analytical Chemistry and Organic Chemistry at the University Rovira i Virgili,

I STATE that the present study, entitled "Reagents and methodologies for the introduction of thiofluoroalkyl and fluorosulfur motifs", presented by Miguel Bernús Pérez for the award of the degree of Doctor and European Mention, has been carried out under my supervision at the Department of Analytical Chemistry and Organic Chemistry of this University.

Tarragona, 27th June 2023

Thesis supervisor

Dr. Omar Boutureira Martín

UNIVERSITAT ROVIRA I VIRGILI
REAGENTS AND METHODOLOGIES FOR THE INTRODUCTION OF THIOFLUOROALKYL AND FLUOROSULFUR MOTIFS
Miguel Bernús Pérez

The work performed in the present Doctoral Thesis has been possible thanks to the Martí i Franquès Research Fellowship Program (2018PMF-PIPF-25), the FI fellowship (Personal investigador predoctoral en formació, FI B00254), and the FPU fellowship (Formación de personal Universitario, FPU19/01969 and EST22/00303).

This thesis has been carried out thanks to the funding of the research project: Trifluoromethylated glycoconjugates for cancer diagnosis and treatment (reference: CTQ2017-90088-R) funded by the Ministerio de Ciencia, Innovación y Universidades (MCIU), Agencia Estatal de Investigación (AEI) and Fondo Europeo de Desarrollo Regional (FEDER), and Design and synthesis of polyfluoroalkyl glycopeptides and proteins for cancer diagnosis and treatment (reference: PID2020-120584RB-100) funded by the Ministerio de Ciencia e Innovación (MCIN) and Agencia Estatal de Investigación (AEI).

UNIVERSITAT ROVIRA I VIRGILI
REAGENTS AND METHODOLOGIES FOR THE INTRODUCTION OF THIOFLUOROALKYL AND FLUOROSULFUR MOTIFS
Miguel Bernús Pérez

A testing and a questioning has been all my travelling:—and verily, one must also learn to answer such questioning! That, however,—is my taste:

—Neither a good nor a bad taste, but my taste, of which I have no longer either shame or secrecy.

"This—is now my way,—where is yours?" Thus did I answer those who asked me "the way." For the way—it does not exist!

Thus spoke Zarathustra,
Friedrich Nietzsche

UNIVERSITAT ROVIRA I VIRGILI
REAGENTS AND METHODOLOGIES FOR THE INTRODUCTION OF THIOFLUOROALKYL AND FLUOROSULFUR MOTIFS
Miguel Bernús Pérez

Acknowledgements

I would like to express my heartfelt gratitude to all those who have supported me throughout this journey of pursuing my Ph.D. I am indebted to all individuals who have contributed to the successful completion of this thesis.

In the first place, I extend my appreciation to Omar for giving me the opportunity to grow as a scientist in his lab. I also must thank Sergio, Maribel, and Yolanda for their invaluable contributions in making our research group a collaborative and productive environment. From my Ph.D. placement in Amsterdam, I am deeply grateful to Tim for welcoming me into his lab and providing an encouraging environment for me to develop my ideas.

I would like to also express my gratitude to all my labmates from SintCarb Jordi, Isa, Paula, Albert, Pablo, Javi, Eric, Marc, Cristina, Irene and from the Noël research group, specially to Daniele, Jelena, Arad, Mauro, Cassie, Luca, Zhenghui, Tom, Anto, Stefano, Stefan and Bebo. I am also in debt with all my friends, Enric, Ari, Will, Alba, Luis, Raül, Sergi, Jano for sharing good moments in this way.

Finally, I extend my deepest acknowledgements to my family for their unwavering support throughout this journey. I am incredibly fortunate to have you all by my side.

UNIVERSITAT ROVIRA I VIRGILI
REAGENTS AND METHODOLOGIES FOR THE INTRODUCTION OF THIOFLUOROALKYL AND FLUOROSULFUR MOTIFS
Miguel Bernús Pérez

Abstract

The present thesis has pursued the development of reagents and methodologies for the installation of pharmaceutical relevant motifs containing sulfur and fluorine. The work has been divided into six chapters.

The first chapter provides a general introduction emphasizing the significance of organic synthesis in the exploration of chemical space, with a particular focus on the importance of sulfur and fluorinated motifs. The second one, outlines the objectives of the thesis. The experimental work is presented in the following four chapters.

Chapter III is devoted to a systematic investigation of the medicinal chemistry properties associated with thiofluoroalkyl fragments. In this section, the log*P* and *p*K_a values of a family of fluoroderivated 2-SCH_3 and 2-SCH_2CH_3 pyridines were determined. To provide a rational understanding of the structure-properties relationship, a computational study is also presented. The key findings of this research are the identification of isosteric relationships among the various fluorinated patterns.

Chapter IV presents the development of two saccharin-based reagents for the electrophilic introduction of -SCF_2CF_2H and -SCF_2CF_3 fragments. These electrophilic agents are synthetized in three steps from simple and readily available starting materials and can be obtained in a multigram scale. Electrophilic introduction has been proven successful in a range of different nucleophiles, including blockbuster drugs and natural products. Furthermore, multigram-scale reactions and product derivatization have also been demonstrated.

Chapter V discloses a modular flow platform for the introduction of -SO_2F handles in phenol and amino derivates via click reactions. The microfluidic system is capable of generating on demand, and safely dose, gaseous SO_2F_2 that is next reacted in a second module. This SuFEx (Sulfur(VI) Fluorine Exchange) ligation is exceptionally rapid (2 minutes), and allows the derivatization of various substrates, including therapeutically relevant small molecules, peptides, and proteins. Furthermore, the system can be coupled with other modules to perform telescoped transformations.

Table of contents

Chapter IV: Development of Electrophilic Thiopolifluoroalkylating Reagents

Chapter V: A Modular Flow Platform for Sulfur(VI) Fluorine Exchange (SuFEx) ligation

CHAPTER I

General Introduction

UNIVERSITAT ROVIRA I VIRGILI
REAGENTS AND METHODOLOGIES FOR THE INTRODUCTION OF THIOFLUOROALKYL AND FLUOROSULFUR MOTIFS
Miguel Bernús Pérez

1.1 The importance of organic synthesis in drug discovery

Small molecules have changed the history of human beings.[1] In the field of medicine, small molecule drugs have a major role in the treatment of diseases (Figure 1.1).[2] To put this in perspective, more than 50% of the approved therapeutics in 2022 were small molecules.[3]

This general introduction aims to highlight the crucial role of organic methodologies and reagents in the development of new therapeutics with special focus to sulfur and fluorine-containing motifs.

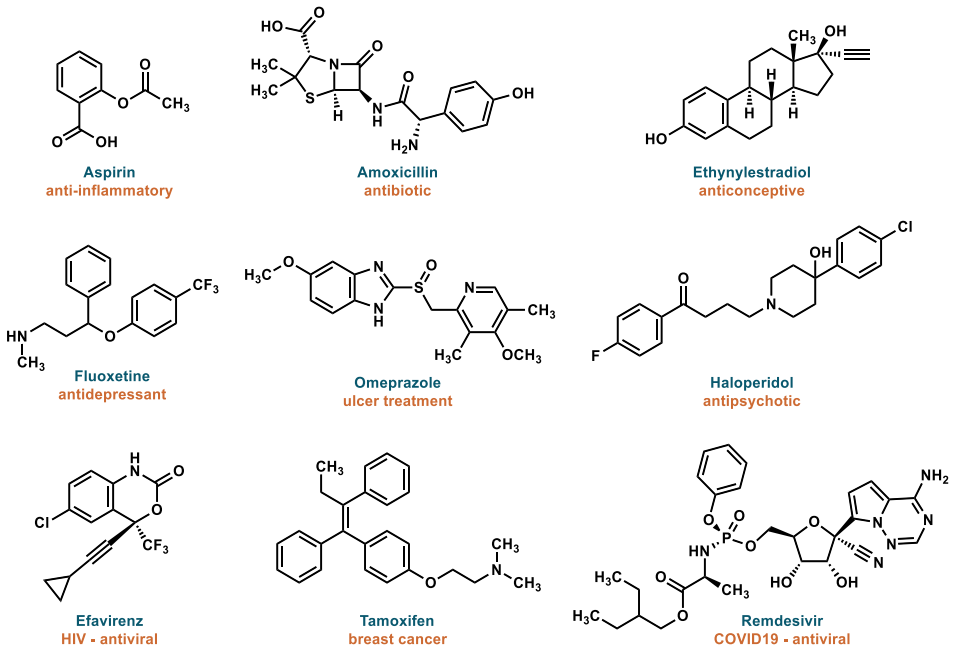

Figure 1.1. Selection of small molecule drugs which have played a major role in the progress of medicine.

[1] Nicolau, K.; Montagnon, T. *Molecules that changed the world.* Wiley-VCH Verlag GmbH, 2008.
[2] Beck, H.; Härter, M.; Haß, B.; Schmeck, C.; Baerfacker, L. *Drug Discov. Today* **2022**, *27*, 1560.
[3] Mullard, A. *Nat. Rev. Drug Discov.* **2023**, *22*, 83.

1.1.1 Chemical Space

The existence of stable organic molecules is governed by the rules of chemical bonding.[4] If we consider this affirmation, the most suitable drug for a given disease it already exists virtually. Therefore, the identification of that specific molecule and its synthetic accessibility are the two crucial factors that separate us from the ideal drug therapeutic. The identification of biological targets and putative drugs is out of the scope of this introduction.

Undoubtedly, the number of possible organic molecules allowed by the chemistry rules is infinite.[5,6] In fact, the chemical community has referred to this concept as *chemical space* to empathize on the cosmological proportions.[7] As a reference, it is estimated that combining up to 30 carbon atoms with different arrangements of nitrogen, oxygen, and sulfur atoms the resulting number of possible molecules would be 10^{63}.[8] To put this in perspective, there are not enough atoms in the universe to synthetize every single molecule.[5]

Of course, the magnitude of this landscape is reduced when we take into consideration that not all the molecules are going to be suitable drug candidates.[7,9] This spatial delimitation is caused by the drug-likeness and it is estimated to be ~10^{33} (Figure 1.2).[10] Specifically, this term refers to the different molecular properties and descriptors that can discriminate between drugs and non-drugs for such features as oral absorption, aqueous solubility, and permeability.[11]

---

[4] Anslyn, E. V.; Dougherty, D. A. Modern Physical Organic Chemistry. University Science Books, 2006.
[5] Clayden, J.; Greeves, N.; Warren, S. Organic Chemistry. Oxford University Press, 2012.
[6] Reymond, J-L. *Acc. Chem. Res.* **2015**, *48*, 722
[7] Lipinski, C.; Hopkins, A. *Nature* **2004**, 7019, 855.
[8] Bohacek, R. S.; McMartin, C.; Guida, W. C. *Med. Res. Rev.* **1996**, *16*, 3.
[9] Dobson, C. M. *Nature*, **2004**, *432*, 824.
[10] Polishchuk, P.G.; Madzhidov, T. I.; Varnek, A. *J. Comput. Aided Mol. Des.* **2013**, *27*, 675.
[11] Keller, T. H., Pichota, A.; Yin, Z. *Curr. Opin. Chem. Biol.* **2006**, *10*, 357.

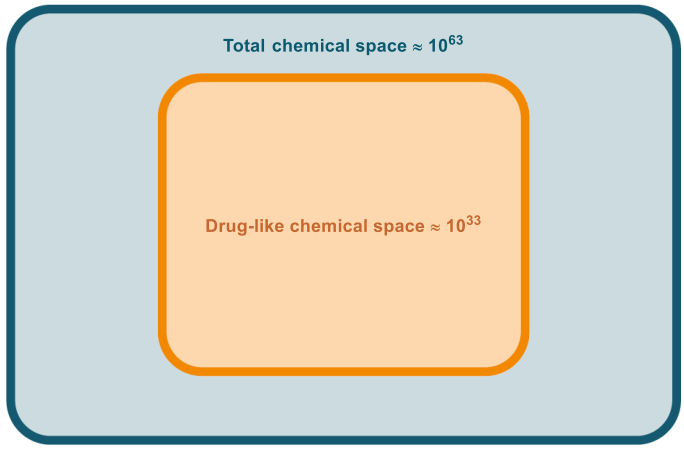

Figure 1.2. Representation of total chemical space and drug-like chemical space.

For practical reasons, the medicinal chemistry community has set some rules of thumb to serve as guidance for the classification of drug-like molecules. The most recognized standards were established by Lipinski in 1997 in his famous rule of 5.[12] After analyzing the Derwent World Drug Index he concluded that 90% of the orally absorbed drugs had the following features:

- Less than 5 hydrogen-bond donor atoms
- Less than 10 hydrogen-bond acceptors
- Molecular weight inferior to 500 daltons
- Lipophilicity values (log*P*) less than 5.

Importantly, each biological target has its own discrete space in the continuous chemical space (Figure 1.3).[7]

[12] Lipinski, C. A.; Lombardo, F.; Dominy, B. W.; Feeney, P. J. *Adv. Drug Delivery Rev.* **1997**, *23*, 3.

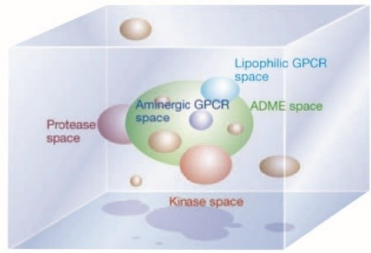

Figure 1.3. Representation of the discrete areas of chemical space with specific affinity for biological molecules, in the total chemical space. Figure extracted from ref. 7.

Even the high repercussion of these guidelines in the design of new drugs, there is not an absolute consensus about the rules that define drug-like compounds,[13] in fact, there are numerous drugs that do not meet this criteria (beyond rule of 5 drugs).[14] Also, there is controversy in this topic as some medicinal chemists point out that by over-limiting the drug-like chemical space, many opportunities could be missed.[15,16]

1.1.2 Chemical space is further limited by organic chemistry

Having set the boundaries of the drug-like molecules within the frame of the continuum chemical space, the state of the art of organic chemistry further restricts the access of this portion of desired drugs.[17]

Importantly, the availability of reagents and robust methodology delimits the drug-like chemical space.[18] Also, taking into consideration practical aspects of safety, number of synthetic steps, and cost we can even restrict

[13] DeGoey, D. A.; Chen, H.-J.; Cox, P. B.; Wendt, M. D. *J. Med. Chem.* **2017**, *61*, 2636.
[14] Caron, G.; Digiesi, V.; Solaro, S.; Ermondi, G. *Drug Discov. Today* **2020**, *25*, 621.
[15] Tomberg, A.; Boström, J. *Drug Discov. Today*, **2020**, *25*, 2174.
[16] Hartung, I. V.; Huck, B. R.; Crespo, A. *Nat. Rev. Chem.*, **2023**, *7*, 3.
[17] Zabolotna, Y.; Volochnyuk, D. M.; Ryabukhin, S. V.; Horvath, D.; Gavrilenko, K. S.; Marcou, G.; Moroz, Y. S.; Oksiuta, O.; Varnek, A. *J. Chem. Inf. Model*. **2022**, *62*, 2171
[18] Grygorenko, O. O.; Volochnyuk, D. M.; Ryabukhin, S. V.; Judd, D. B. *Chem. Eur. J.* **2019**, *26*, 1196.

further the drug-like space that is accessible for process chemistry and therefore for the whole society (Figure 1.4).[19]

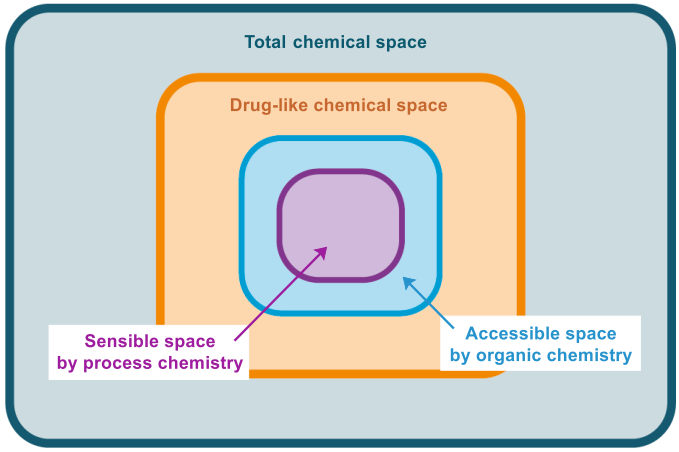

Figure 1.4. Representation of the limitations of the total chemical space by drug-likeness, organic chemistry, and process chemistry.

From the discovery point of view, the main toolbox of reactions medicinal chemists use in drug discovery surprisingly did not change from 1984 to 2014.[20] Although this analysis could be outdated, as modern methodologies as photochemistry, electrochemistry, and other methods were not implemented a decade ago, it offers a perspective of the interplay of organic chemistry and drug discovery.[21,22]

Specifically, this analysis shows how the most common reactions used in 1984 are still used in 2014, with the exceptions of few reactions as the Suzuki-Miyaura coupling, or the Buchwald-Hartwig cross-couplings.[20]

During this period, the emergence of palladium catalyzed reactions opened the opportunity to access a wide area of the chemical space comprising C_{sp^2}-C_{sp^2} linkages.[23] This had an implication on the number of

[19] Gaich, T.; Baran, P. S. *J. Org. Chem.* **2010**, *75*, 4657.
[20] Brown, D. G.; Bostgröm, J. *J. Med. Chem.* **2016**, *59*, 4443.
[21] Fernández, D. F.; González-Esguevillas, M.; Keess, S.; Schäfer, F.; Mohr, J.; Shavnya, A.; Knauber, T.; Blakemore, D. C.; MacMillan, D. W. *Org. Lett.* **2023**, in press, 10.1021/acs.orglett.3c00994.
[22] Boström, J.; Brown, D. G.; Young, R. J.; Keserü, G. M. *Nat. Rev. Drug Discov.* **2018**, *17*, 709.
[23] Buskes, M. J.; Blanco, M.-J. *Molecules* **2020**, *25*, 3493.

biaryl fragments registered in an AstraZeneca database increased upon the discovery of the Suzuki-Miyaura cross coupling (Figure 1.5, A). Indeed, the development of certain drugs such as Losartan, Azilsartan, and Irbesartan were fostered by this discovery (Figure 1.5, B).[20]

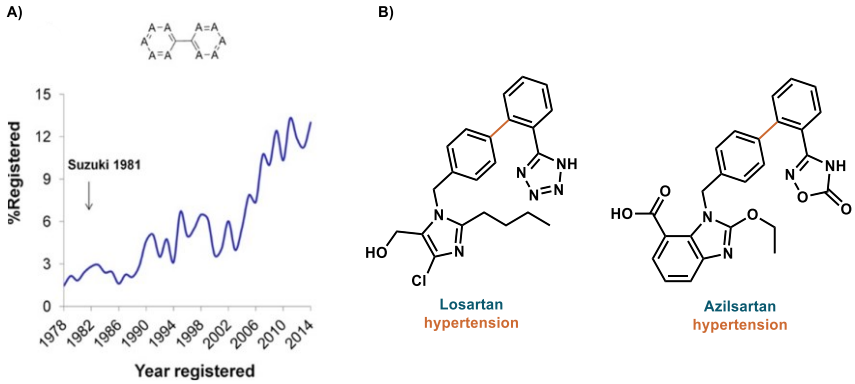

Figure 1.5. A) Percentage of biphenyl fragments registered in the AstraZeneca collection over time. Figure extracted from ref. 20. B) Losartan and Azilsartan hypertension drugs.

When analyzing the occupancy of chemical space of these biaryl compounds it was found that the drugs containing these motifs tended to have a linear shape or, to a minor extent, disk-like, contrary to sphere-like.[20] Consequently, it revealed that the chemical space was being overexplored in the linear region. In fact, since the implementation of the Pd-mediated cross-couplings most of the pharmaceutical compounds have been clustered in these shapes leaving more tridimensional molecules out of the studies.[24] This is not necessarily bad or good for the pharmaceutical industry by itself, but this overpopulation of certain chemical regions can be directly linked as a consequence of the available methodologies, leaving potential successful candidates out of sight.[20]

Another issue of methodology-derived space exploration is the case of molecular obesity.[25] This term refers to tendency to build potency into

[24] Sauer, W. H. B.; Schwarz, M. K. *J. Chem. Inf. Comput. Sci.* **2003**, *43*, 987.
[25] Hann, M. M. *Med. Chem. Commun.* **2011**, *2*, 349.

molecules by the inappropriate use of lipophilicity in early drug discovery phases. In the midterm, this has a detrimental effect in advanced drug discovery phases as the reduction of aqueous solubility.[25] A potential problem medicinal chemists face is that most of the organic methodologies published tend to exemplify the scope using apolar functionalities.[26]

Remarkably, despite the advances in organic chemistry and biology, the rate of drugs approved remains constant over the years.[27] Despite this is also associated with safety and regulatory concerns, the truth is that drug discovery campaigns are increasingly more expensive over the years, meaning that it is more difficult to find new drugs.[28] Importantly, some authors point out that this might be due to the unexploration of other chemical spaces.[29]

1.2 The interplay of organic methodologies and reagents with solutions

Undoubtedly, the development of chemical methodologies is crucial for the discovery of new chemical spaces, and thus for contributing in the search of pharmaceutical better solutions.[26,30]

To depict this, we can refer to the case of the development of NS3/4a protease inhibitors for the treatment of hepatitis C virus (HCV).[31] Specifically, when the crystal structure of this protease was disclosed, it was pointed out

[26] Blakemore, D. C.; Castro, L.; Churcher, I.; Rees, D. C.; Thomas, A. W.; Wilson, D. M.; Wood, A. *Nat. Chem.* **2018**, *10*, 383.
[27] Kalra, B. S.; Batta, A.; Khirasaria, R. *Fam. Med. Prim.* **2020**, *9*, 105.
[28] Angelis, A.; Polyakov, R.; Wouters, O. J.; Torreele, E.; McKee, M. *BMJ* **2023**, 380:e071710.
[29] Reymond, J.-L.; van Deursen, R.; Blum, L. C.; Ruddigkeit, L. *Med. Chem. Commun.* **2010**, *1*, 30.
[30] Campos, K. R.; Coleman, P. J.; Alvarez, J. C.; Dreher, S. D.; Garbaccio, R. M.; Terrett, N. K.; Tillyer, R. D.; Truppo, M. D.; Parmee, E. R. *Science* **2019**, 363, east0805.
[31] Rosenquist, Å.; Samuelsson, B.; Johansson, P.-O.; Cummings, M. D.; Lenz, O.; Raboisson, P.; Simmen, K.; Vendeville, S.; de Kock, H.; Nilsson, M.; Horvath, A.; Kalmeijer, R.; de la Rosa, G.; Beumont-Mauviel, M. *J. Med. Chem.* **2014**, *57*, 1673.

the intrinsic challenge in the design of inhibitors because the active site of the enzyme had a shallow and opened binding site, and it presented genotypic and mutational diversity.[32] By using molecular modelling, it was concluded that large macrocyclic structures could successfully adapt to the binding site to promote potent inhibition by minimizing entropic costs.[33] This is because the active site is surrounded by a flat and featureless protein surface, which implies that the inhibitor has to be large in surface and adaptable to have sufficient binding affinity.[32]

From the organic chemistry point of view, the formation of macrocycles has been a longstanding challenge due to the difficulty of linking two ends distant in space.[34] Over the years different solutions have been disclosed for this problematic as the use of high dilution conditions and various types of condensations.[34] Nonetheless, these methods usually relied on the chemistry of carbonyl-derived functionalities.[34] A major breakthrough was achieved with the development of the ring closing metathesis, as it allowed the disconnection of unfunctionalized C_{sp^3}-C_{sp^3} by metathesis followed by hydrogenation.[35] This reaction was transformative for macrocyclic construction, and specially for the preparation of the NS3/4a protease inhibitors, as it allowed efficient assembly of complex structures to explore their bioactivity properties (Figure 1.6).[36] This is an example where organic synthesis allowed the preparation new structures located in a previously inaccessible chemical space.

---

[32] Kim, J. L.; Morgenstern, K. A.; Lin, C.; Fox, T.; Dwyer, M. D.; Landro, J. A.; Chambers, S. P.; Markland, W.; Lepre, C. A.; O'Malley, E. T.; Harbeson, S. L.; Rice, C. M.; Murcko, M. A.; Caron, P. R.; Thomson, J. A. *Cell* **1996**, *87*, 343.

[33] Tsantrizos, Y. S.; Bolger, G.; Bonneau, P.; Cameron, D. R.; Goudreau, N.; Kukolj, G.; LaPlante, S. R.; Llinàs-Brunet, M.; Nar, H.; Lamarre, D. *Angew. Chem. Int. Ed.* **2003**, *42*, 1356.

[34] Martí-Centelles, V.; Pandey, M. D.; Burguete, M. I.; Luis, S. V. *Chem. Rev.* **2015**, *115*, 8736.

[35] Hoveyda, A. H.; Zhugralin, A. R. *Nature* **2007**, *450*, 243.

[36] Llinàs-Brunet, M.; Bailey, M. D.; Bolger, G.; Brochu, C.; Faucher, A.-M.; Ferland, J. M.; Garneau, M.; Ghiro, E.; Gorys, V.; Grand-Maître, C.; Halmos, T.; Lapeyre-Paquette, N.; Liard, F.; Poirier, M.; Rhéaume, M.; Tsantrizos, Y. S.; Lamarre, D. *J. Med. Chem.* **2004**, *47*, 1605.

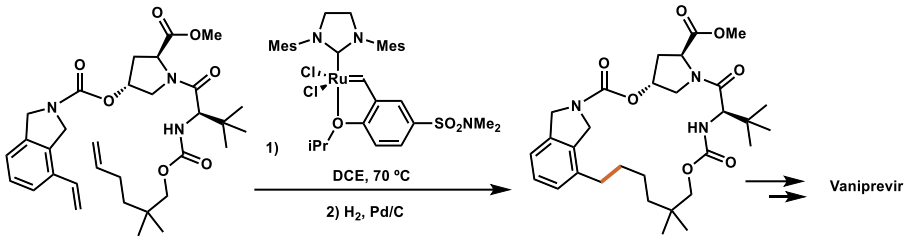

Figure 1.6. Cross metathesis and hydrogenation steps as enabling transformations for the preparation of Vaniprevir.

In the following subsections some recent examples of organic methodologies and reagents will be presented to illustrate its interplay with improved pharmaceutical solutions.

1.2.1 New structures for Csp^3-enriched molecules: escape from flatland

As presented in the previous section, the emergence of Csp^2-Csp^2 couplings in the 90s has benefited the disclosure of new drugs by easing the preparation of molecules with greater unsaturation.[23] However, these advances have also biased the exploration of chemical space by omitting more tridimensional structures.[20] In 2009, researchers from the Wyeth Company published a study on the importance of considering sp^3-rich molecules in drug design.[37] In this study, the authors proposed a descriptor to measure the complexity of molecules as the fraction of sp^3 carbons compared to the total amount of carbon atoms (Fsp^3). The presence of more sp^3 carbons, and chiral centers, was found to be correlated with higher clinical success ratio. The main premise was that greater saturation would imply greater complexity, and thus access to more chemical space. Remarkably, it was found that aqueous solubility was also improved by having a higher sp^3 fraction.[37] This is in line with the previously discussed problematic of molecular obesity linked to the overexploitation of traditional synthetic methods.[25] This study deeply influenced the endeavors of synthetic groups in the last decade. For instance,

[37] Lovering, F.; Bikker, J.; Humblet, C. *J. Med. Chem.* **2009**, *52*, 6752.

the number of publications about spirocycles as enriched sp^3 structures has constantly increased over time (Figure 1.7).

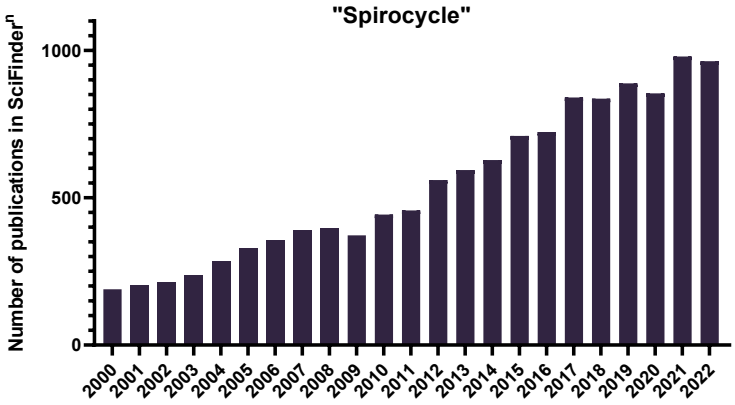

Figure 1.7. Number of hits when searching for "spirocycle" in publications since 2000 in the SciFinder^n database.

1.2.2 C–H and late-stage functionalization

From the medicinal chemistry point of view, the direct modification of a bioactive molecule into another related scaffold is considered attractive.[38,39] In fragment-based drug discovery (FBDD), this strategy allows to derivatize an advanced intermediate to multiple analogs without having to restart the synthesis for each target.[18] A plethora of methodologies have been developed to this end.[40] However, the regiochemical functionalization of complex structures in a predictable fashion is regarded as a challenge.[26] In this introduction, two sulfur-based strategies (sulfinate salts and organic thianthrenium compounds) have been selected to illustrate how organic chemistry has found solutions for the divergent synthesis of complex molecules.

---

[38] Guillemard, L.; Kaplaneris, N.; Ackermann, L.; Johansson, M. *J. Nat. Chem. Rev.* **2021**, *5*, 522.

[39] Zhang, L.; Ritter, T. *J. Am. Chem. Soc.* **2022**, *144*, 2399.

[40] Cernak, T.; Dykstra, K. D.; Tyagarajan, S.; Vachal, P.; Krska, S. W. *Chem. Soc. Rev.* **2016**, *45*, 546.

Radicals are reactive intermediates with tremendous potential for organic chemistry.[41] Importantly, their fleeting nature is not in conflict with their compatibility with densely decorated structures, with polar and unprotected motifs, and the presence of protic polar solvents. Traditionally, carboxylic acids have been used as radical precursors for the C–H functionalization of heterocycles, in the so-called Minisci reaction.[42] However, the harsh conditions to form the radical intermediates motivated the search for milder solutions. In this scenario, sulfinate salts presented a better alternative to this end. Pioneered by Langlois in 1991,[43] these reagents experienced a renaissance in 2011 by Baran,[44] who developed a series of sulfinates and radical protocols for the introduction of alkyl and fluoroalkyl substituents in complex organic molecules (Figure 1.8). Also, they offered a rationale on the prediction and modification of the regioselectivity of the transformations.[45] Overall, this transformation allowed the formation of C–C bonds in very mild conditions.

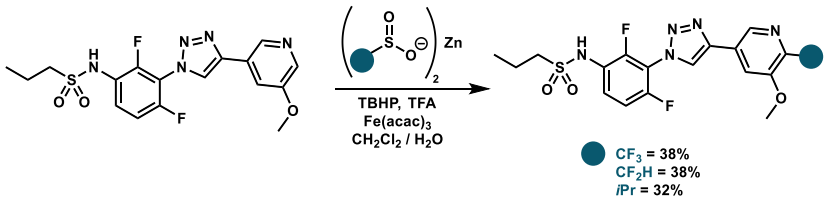

Figure 1.8. Late-stage functionalization of a drug-like molecule using sulfinates.[46]

In another approximation for the diversification of complex structures, the group of Ritter disclosed a methodology for the C–H late-stage installation of thianthrenium groups to serve as reactive handles, with perfect and

[41] Yan, M.; Lo J. C.; Edwards, J. T.; Baran, P. S. *J. Am. Chem. Soc.* **2016**, *138*, 12692.
[42] Duncton, M. A. *Med. Chem. Commun.* **2011**, *2*, 1135.
[43] Langlois, B. R.; Laurent, E.; Roidot, N. *Tetrahedron Lett.* **1991**, *32*, 7525.
[44] Ji, Y.; Brueckl, T.; Baxter, R.D.; Fujiwara, Y.; Seiple, I.B.; Su, S.; Blackmond, D.G.; Baran, P.S. *Proc. Natl. Acad. Sci. U.S.A.*, **2011**, *108*, 14411.
[45] O'Hara, F.; Blackmond, D. G.; Baran, P. S. *J. Am. Chem. Soc.* **2013**, *135*, 12122.
[46] Kuttruff, C. A.; Haile, M.; Kraml, J.; Tautermann, C. S. *ChemMedChem* **2018**, *13*, 983.

predictable regioselectivity.[47] The reaction resulted compatible with numerous unprotected functionalities. Importantly, the thianthrenium handle is very suitable for its further derivatization. Specifically, a wide array of reactivities can be employed to further functionalize the modified molecule in an orthogonal fashion.[47] For instance, borylation, phosphonylation, cyanation, halogenation, and cross-coupling products, can be achieved from the same precursor (Figure 1.9).

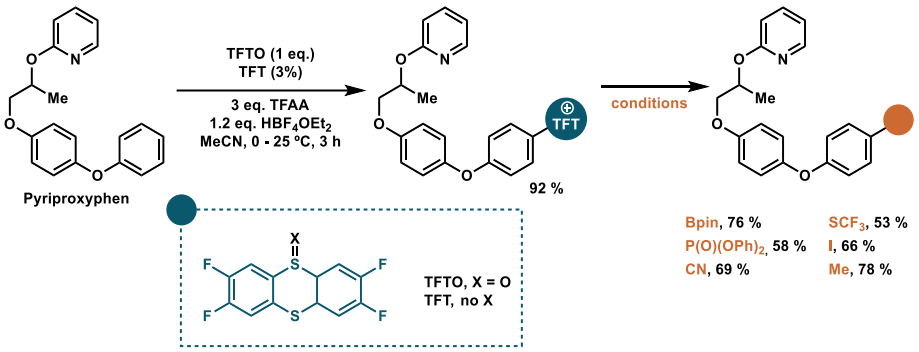

Figure 1.9. Late stage thianthrenilation of pyriproxyphen and subsequent derivatizations.[47]

1.2.3 Moonshot synthesis: molecular editing

The idea of controlled insertion, deletion, or exchange of atoms in advanced structures is a revolutionary concept that breaks the stablished rules of retrosynthesis.[40] This concept is known as molecular editing, and it is an emerging field that promises to change drug discovery by enabling the access of multiple and diverse structures of advanced intermediates.[48] Noteworthy, some already stablished reactions remind to this molecular editing strategy. For instance, Baeyer-Villiger oxidation, Beckmann rearrangement, or Curtius

[47] Berger, F.; Plutschack, M. B.; Riegger, J.; Yu, W.; Speicher, S.; Ho, M.; Frank, N.; Ritter, T. *Nature* **2019**, *567*, 223.
[48] Peplow, M. *Nature,* **2023**, *618*, 21.

rearrangement are reactions that allow for the insertion of atoms in defined scaffolds.[5]

Although molecular editing is still in its infancy, there are some recent publications which encourage to think that in the future these strategies will change the way of building molecules. To illustrate this, a selection of three recent publications has been chosen from the literature (Figure 1.10) involving (A) atom deletions, (B) atom replacements, and (C) atom insertions.[49,50,51]

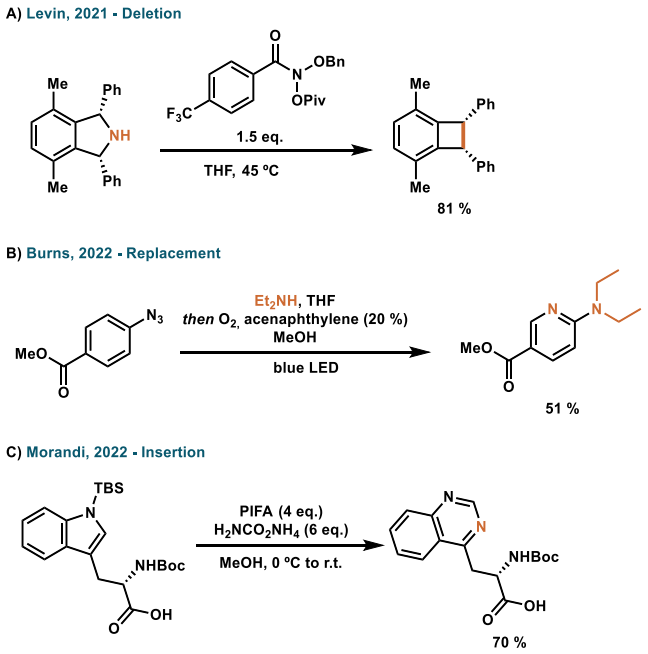

Figure 1.10. Selection of recent molecular editing methodologies.[49,50,51]

[49] Patel, S. C.; Burns, N. Z. *J. Am. Chem. Soc.* **2022**, *144*, 17797.

[50] Kennedy, S. H.; Dherange, B. D.; Berger, K. J.; Levin, M. D. *Nature* **2021**, *593*, 223.

[51] Reisenbauer, J. C.; Green, O.; Franchino, A.; Finkelstein, P.; Morandi, B. *Science* **2022**, *377*, 1104.

1.3 New opportunities for fluorine and sulfur

Sulfur and fluorine are commonly found in the chemical composition of active pharmaceutical ingredients (APIs).[52,53] To put this into perspective, in 2021, approximately 33% of the top 200 small molecule pharmaceuticals based on retail sales contained at least one sulfur atom, while approximately 25% of them contained a minimum of one fluorine atom.[54] It is important to note that these percentages have shown a consistent increase over the years.[55,53]

Sulfur exhibits a larger atomic volume, more diffuse orbitals, and lower electronegativity compared to oxygen.[56] Importantly, sulfur is an exceptionally versatile element due to its ability to expand its valence shell, allowing for the formation of multiple covalent bonds.[56] This property is fostered by its wide range of oxidation states and substitution possibilities. In the field of medicinal chemistry, the sulfonamide functionality is the most extensively utilized sulfur motif, followed by β-lactam structures, thioethers, and thiazoles.[53]

Compared to sulfur, fluorine is considered a less versatile element since it primarily forms single bonds with carbon (S–F bonds are also significant but less in number compared to C–F bonds). While fluorine is very rare in biomolecules, it has been widely adopted in medicinal chemistry due to the unique pharmacokinetic properties it imparts to parent molecules.[57] The most found fluorinated motifs in active pharmaceutical ingredients are aromatic fluorides (Csp^2–F) and trifluoromethyl groups (CF_3) corresponding to 83% of the total fragments.[53]

Remarkably, although sulfur and fluorine motifs are currently part of the medicinal chemistry toolbox, their full potential for expanding the chemical

---

[52] Mustafa, M.; Winum, J.-Y. *Expert Opin. Drug Deliv.* **2022**, *17*, 501.
[53] Ilardi, E. A.; Vitaku, E.; Njardarson, J. T. *J. Med. Chem.* **2013**, *57*, 2832.
[54] McGrath, N. A.; Brichacek, M.; Njardarson, J. T. *J. Chem. Ed.* **2010**, *87*, 1348. (updated versions)
[55] Inoue, M.; Sumii, Y.; Shibata, N. *ACS Omega* **2020**, *5*, 10633.
[56] Oae, S. *Organic Sulfur Chemistry;* CRC Press, 2018.
[57] Gillis, E. P.; Eastman, K. J.; Hill, M. D.; Donnelly, D. J.; Meanwell, N. A. *J. Med. Chem.* **2015**, *58*, 8315.

space is still to be unleashed. The synthetic chemistry community is actively directing its efforts towards developing new methodologies and reagents that can enable the synthesis of unusual functional groups bearing fluorine and sulfur atoms.[58,59] These new motifs represent opportunities for the development of finely tuned active pharmaceutical ingredients.

1.3.1 Sulfur-based emerging motifs

As outlined before, despite the prevalence of sulfur pharmacophores in active pharmaceutical ingredients, medicinal chemists have neglected some functionalities.[58,60] The main reason behind this fact is that the access to those motifs has been hampered by the lack of synthetic methodologies.[58,60] This family of neglected sulfur motifs are compiled in Figure 1.11.

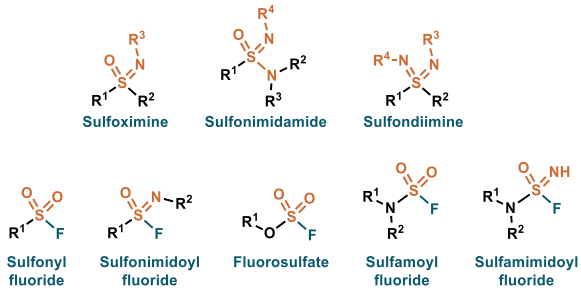

Figure 1.11. Selection of neglected sulfur-based functionalities.

These functionalities are now being revisited as they present interesting features as larger 3D-volume, stereogenic sulfur centers, increased polarity, and multiple derivatization points arising from the different substitution possibilities.[59]

---

[58] Tilby, M. J.; Willis, M. C. *Expert Opin. Drug Discov.* **2021**, *16*, 1227.

[59] Ma, J.-A.; Cahard, D. *Emerging Fluorinated Motifs: Synthesis, Properties and Applications*, Wiley-VCH Verlag GmbH & Co. KGaA: Weinheim, Germany, 2020.

[60] Lücking, U. *Org. Chem. Front.* **2019**, *6*, 1319.

For instance, sulfoximines and sulfondiimines can be gauged as aza analogs of sulfones. Importantly, the substitution of an oxygen atom by nitrogen has several implications in the physicochemical properties of the motif as the raise of an asymmetric center, the presence of a nucleophilic/basic nitrogen, and the acidification of adjacent positions (Figure 1.12).[60,61]

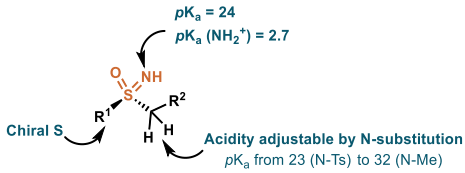

Figure 1.12. Features of sulfoximine functional group.

As a matter of example of the use of emerging sulfur motifs, medicinal chemists at Bayer discovered a potential inhibitor of a cyclin-dependent kinase (CDK) for oncological treatment (ZK 304709).[62] Despite its promising preclinical profile, the drug candidate faced solubility issues, which led to limited absorption of the compound. Additionally, it was found that the inhibitor exhibited unintended accumulation in erythrocytes due to off-target activity against carbonic anhydrases (CAs) associated with the sulfonamide functionality.[62]

To address this problem, a sulfoximine analog was synthesized, which selectively targeted CDK (Figure 1.13). After refining this analog, a final candidate named roniciclib was identified (Figure 1.13).[63] Importantly, this drug demonstrated over 20 times the aqueous solubility of the initial candidate, enabling a 50-fold reduction in the required therapeutic dose.[60]

---

[61] Mäder, P.; Kattner, L. *J. Med. Chem.* **2020**, *63*, 14243.

[62] Scholz, A.; Wagner, K.; Welzel, M.; Remlinger, F.; Wiedenmann, B.; Siemeister, G.; Rosewicz, S.; Detjen, K. M. *Cancer Chemother. Pharmacol.* **2008**, *58*, 261.

[63] Siemeister, G.; Lücking, U.; Wengner, A. M.; Lienau, P.; Steinke, W.; Schatz, C.; Mumberg, D.; Ziegelbauer, K. *Mol. Cancer Ther.* **2012**, *11*, 2265.

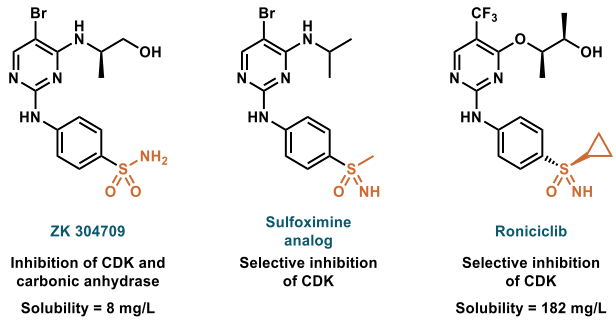

Figure 1.13. Different CDK inhibitor candidates.

In a different context, the emerging S(VI)–F motifs Figure 1.11 are seen as promising covalent inhibitors.[64] Specifically, these reactive groups are known as warheads as they can covalently bind to specific aminoacids.[65] Traditionally, most of the covalent drug discovery has targeted cysteine residues due to the unique nucleophilicity of the thiol.[65] However, cysteines are not usually found in protein binding sites making it challenging to successfully develop targeted covalent therapies.[65]

The outset of this chemistry was pioneered by the group of Sharpless who demonstrated how these S(VI)–F groups present an increased stability compared to S(VI)–Cl, and can undergo nucleophilic substitution in the so called SuFEx reactions (Sulfur(VI) Fluorine Exchange).[66] These chemical features make these groups ideal for covalent targeting of nucleophilic residues as lysine, tyrosine, and histidine.[64] Moreover, due to the versatile nature of the sulfur atom, the electrophilic properties of the covalent warheads can be tuned to balance their reactivity and the hydrolytic stability.[67] For instance, sulfuryl fluorides (RSO_2F) present higher reactivity compared to fluorosulfates ($ROSO_2F$) or sulfamoyl fluorides (R_2NSO_2F) at the expense of lower water tolerance.[67]

---

[64] Huang, H.; Jones, L. H. *Expert Opin. Drug Discov.* **2023**, 1.
[65] Gehringer, M.; Laufer, S. A. *J. Med. Chem.* **2019**, *62*, 5673.
[66] Dong, J.; Krasnova, L.; Finn, M. G.; Sharpless, K. B. *Angew. Chem. Int. Ed.* **2014**, *53*, 9430.
[67] Gilbert, K. E.; Vuorinen, A.; Aatkar, A.; Pogány, P.; Pettinger, J.; Grant, E. K.; Kirkpatrick, J. M.; Rittinger, K.; House, D.; Burley, G. A.; Bush, J. T. *ACS Chem. Biol.* **2023**, *18*, 285.

1.3.2 Fluorine-based emerging motifs

The last decade has witnessed a growing interest in the development of new fluorinated fragments.[59] The search for more chemical space and opportunities for intellectual property (IP) protection have encouraged the synthetic community to explore (or re-explore) reagents and methodologies to install fluorinated motifs different from –F and –CF_3.[68]

The combination of fluorine with heteroatoms is a promising field to expand the known chemical space. Nonetheless, special care should be taken into account when designing these motifs to avoid safety issues in its application to pharmaceutical ingredients.[69] Despite the great strength of the C–F bond (BDE = 130 Kcal/mol) in determined topologies, there is a risk of decomposition via defluorination.[76] The consequent fluoride release to the body or decomposition byproducts can result in toxicity.[69] In Figure 1.13 some examples can be gauged illustrating this problematic as (1) *in vivo* demethylation and subsequent formation of a Michael acceptor, (2) decomposition in aqueous media of a difluoromethyl group, and (3) biological *N*-dealkylation and oxidation to produce toxic fluoroacetic acid.

For these reasons, a joined understanding of physical organic chemistry and molecular properties should encompass the development of new fluorinated motifs to provide better and safer solutions.

[68] Kirsch, P. *Modern fluoroorganic chemistry: Synthesis, reactivity, applications*; Wiley-VCH, Verlag GmbH & Co. KGaA: Weinheim, Germany, 2013.
[69] Pan, Y. *ACS Med. Chem. Lett.* **2019**, *10*, 1016.

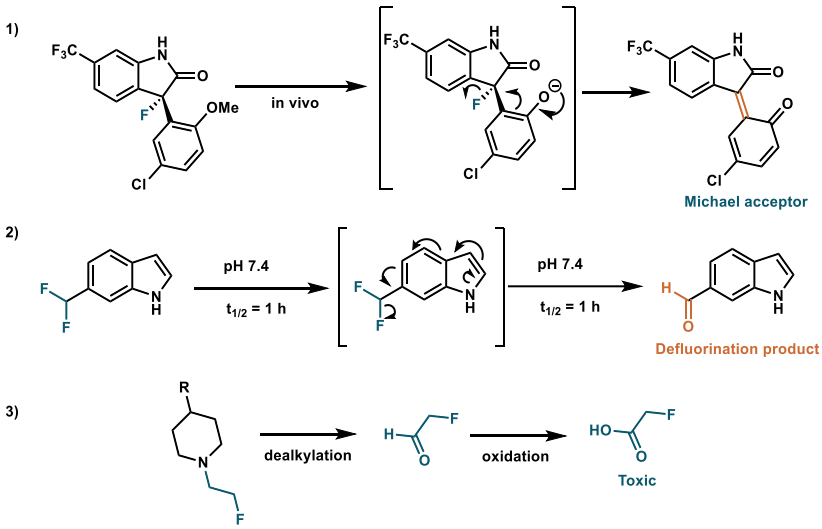

Figure 1.13. Examples of decomposition reactions of fluorinated motifs.

Of special interest are the fragments arisen from the combination of fluoroalkyl chains with other heteroatoms.[59] The electronic nature of the small electron–withdrawing atom imparts great influence in the neighboring groups.[68] This has a profound impact in some molecular properties as the lipophilicity, acidity, and isosterism of a given compound.[70] Importantly, these effects are context-dependent and should be evaluated individually. A summary of different fluorinated emerging motifs can be found in Figure 1.14.

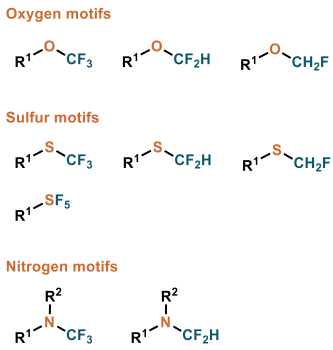

Figure 1.14. Selection of emerging fluorinated motifs.

[70] Meanwell, N. A. *J. Med. Chem.* **2018**, *61*, 5822.

Altogether, the merge of chalcogens and fluoroalkyl fragments have become an important player in this arena.[71] For instance, fluoroalkyl ethers have been used to enhance metabolic stability and increase lipophilicity compared to the non-fluorinated counterparts.[72] Additionally, the presence of terminal CF_2H presents hydrogen bonding acidity allowing for complementary interactions.[73] In a similar manner, thiofluoroalkylethers also offer alike properties to OR_F but with an increased effect in the lipophilicity.[74] In a totally different association of sulfur and fluorine, the pentafluorosulfanyl group (R-SF_5) has gained momentum as a suitable replacement of CF_3 moieties.[75] Finally, N-R_F represents a family of motifs that compromises the basicity of the amines, however the scarcity of methodologies has hampered its implementation in the medicinal chemistry toolbox.[76] A more detailed overview of the preparation and properties of these motifs will be developed in the subsequent chapters.

[71] Toulgoat, F.; Liger, F.; Billard, T. Chemistry of OCF_3, SCF_3, and $SeCF_3$ Functional Groups, In *Organofluorine Chemistry*; John Wiley & Sons, 2021, 49–97.
[72] Ghiazza, C.; Billard, T.; Dickson, C.; Tlili, A.; Gampe, C. M. *ChemMedChem* **2019**, *14*, 1586.
[73] Zafrani, Y.; Yeffet, D.; Sod-Moriah, G.; Berliner, A.; Amir, D.; Marciano, D.; Gershonov, E.; Saphier, S. J. *Med. Chem.* **2017**, *60*, 797.
[74] Hansch, C.; Leo, A.; Taft, R. W. *Chem. Rev.* **1991**, 91, 165.
[75] Savoie, P. R.; Welch, J. T. *Chem. Rev.* **2015**, *115*, 1130.
[76] Schiesser, S.; Chepliaka, H.; Kollback, J.; Quennesson, T.; Czechtizky, W.; Cox, R. J. *J. Med. Chem.* **2020**, *63*, 13076.

CHAPTER II

General Objectives

UNIVERSITAT ROVIRA I VIRGILI
REAGENTS AND METHODOLOGIES FOR THE INTRODUCTION OF THIOFLUOROALKYL AND FLUOROSULFUR MOTIFS
Miguel Bernús Pérez

2.1 General Objectives

The primary objective of this thesis is to provide methodologies and reagents for introducing thiofluoroalkyl and fluorosulfur motifs. An additional emphasis has been placed on developing chemical solutions that utilize simple, affordable, and readily accessible reagents, thereby enhancing the applicability of the research. Each experimental chapter has his own set of goals:

Chapter III: Evaluation of medicinal chemistry properties of thiofluoroalkyl fragments.

This chapter pursues finding relationships between the structure of thiofluoroalkyl fragments and its influence in lipophilicity and acidity. To accomplish this, 2-R_F-subsituted pyridines were chosen as the scaffolds to study. The specific objectives are the following:

- Preparation of a family of 2-SR_F and 2-SO_2R_F substituted pyridines comprising (i) methyl and ethyl fragments, and (ii) different fluorination degree and topology.
- Experimentally measure the log*P* value of the 2-SR_F and 2-SO_2R_F substituted pyridines.
- Experimentally measure the *p*K_a value of the 2-SR_F substituted pyridines.
- Draw relations between the fluorination degree and the measured properties.

Chapter IV: Development of electrophilic thiopolifluoroalkylating reagents.

This chapter is focused on the development of two electrophilic reagents for the introduction of -SCF_2CF_2H, and -SCF_2CF_3 fragments into organic structures. The specific objectives are the following:

- Design of the electrophilic reagent scaffolds, and its multigram preparation.
- Assessment of a survey of nucleophiles with the electrophilic reagents.
- Assessment of the application of the reagents in natural products and advanced drugs.
- Derivatization of the installed SR_F handles to access other functional groups or further decorated structures.

Chapter V: A Modular Flow Platform for SuFEx ligation.

This chapter aims to develop a modular flow platform for the installation of -SO_2F handles in phenols and amino functionalities, covering the modification of small molecules, peptides, and proteins. The specific objectives are the following:

- Design of a flow platform to generate on demand and safely dose gaseous SO_2F_2.
- Design of different reaction modules to perform SuFEx ligations (Sulfur(VI) Fluorine Exchange) in phenol and amino derivatives.
- Assessment of the scope of the transformation with small molecules.
- Development of telescoped transformations of the -SO_2F handle in small molecule substrates.
- Optimization of the system for the reaction with peptides and proteins at tyrosine residues.

CHAPTER III

Evaluation of physicochemical properties of thiofluoroalkyl fragments

UNIVERSITAT ROVIRA I VIRGILI
REAGENTS AND METHODOLOGIES FOR THE INTRODUCTION OF THIOFLUOROALKYL AND FLUOROSULFUR MOTIFS
Miguel Bernús Pérez

3.1 Introduction

3.1.1 Thiofluoroalkyl motifs in medicinal chemistry

In recent years, the pharmaceutical and agrochemical industries have begun to show interest in new fluorine-containing organic motifs that provide an alternative to the typical CF_3 substituent.[1] The uptake of structure-activity relationship (SAR) analyses and the growing advances in drug discovery[2] have expediated the discovery and implementation of new molecular fragments. The fine-tuning of physicochemical properties of active ingredients can result in the success or failure of a candidate, therefore the study of such new fragments is imperative. In this context, thiofluoroalkyl motifs occupy a privileged position,[3] which is exemplified in the large number of marketed products that contain such fragments (Figure 3.1).[3,4]

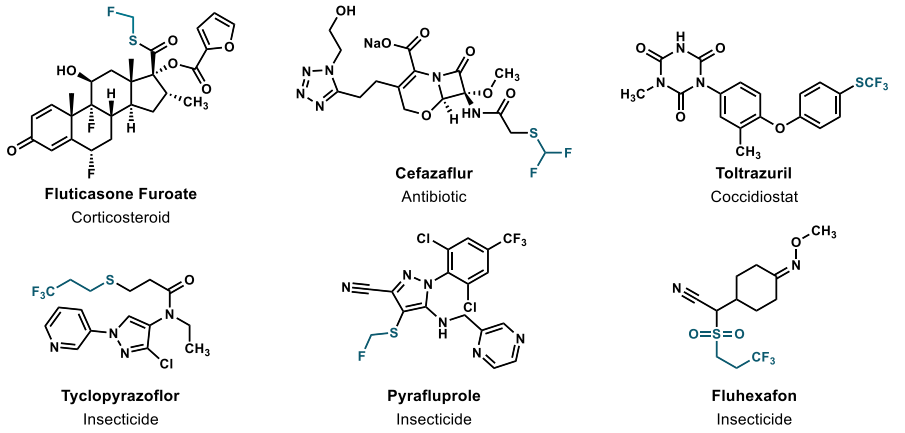

[1] (a) Mei, H.; Han, J.; Fustero, S.; Medio-Simon, M.; Sedgwick, D. M.; Santi, C.; Ruzziconi, R.; Soloshonok, V. A. *Chem. - Eur. J.* **2019**, *25*, 840. (b) Zhou, Y.; Wang, J.; Gu, Z.; Wang, S.; Zhu, W.; Acena, J. L.; Soloshonok, V. A.; Izawa, K.; Liu, H. *Chem. Rev.* **2016**, *116*, 422. (c) Fujiwara, T.; O'Hagan, D. *J. Fluor. Chemistry* **2014**, *167*, 16.

[2] Campos, K.; Coleman, P.; Alvarez, J.; Dreher, S.; Garbaccio, R.; Terrett, N.; Tillyer, R.; Truppo, M.; Parmee, E. *Science* **2019**, *363*, 6424. - and references therein.

[3] Ilardi, E. A.; Vitaku, E.; Njardarson, J. T. *J. Med. Chem.* **2014**, *57*, 2832.

[4] Mcgrath, N. A.; Brichacek, M.; Njardarson, J. T. *J. Chem. Ed.* **2010**, *87*, 1348.

Figure 3.1. Selection of thiofluoroalkyl-containing active ingredients in pharmaceutical and agrochemical formulations.

The appendage of fluoroalkyl chains to sulfur results in unique properties.[5] The marked electronegative nature of the fluorine atoms, combined with the high electronic density of the sulfur, renders these fragments highly lipophilic.[6,7] Due to their unique properties, thiofluoroalkyl chains present new avenues for the development of bioactive compounds.

Table 3.1. Hansch parameters (π) and Hammett para-substituent constants (σ_p) for different substituents.

Substituent	π[8]	σ_p[9]
$-CH_3$	0.56	-0.17
$-SCH_3$	0.61	0.00
$-CF_3$	0.88	0.54
$-SCF_3$	1.44	0.50
$-SCF_2H$	0.68	0.37

The lipophilicity of alkyl chains can be quantified by their experimentally measured 'Hansch parameters' (given by π), allowing comparison between different substituents (Table 3.1). A general trend that is apparent is that replacement of C-H bonds with C-F bonds results in greater lipophilicity ($\pi_{(CH3)}$ = 0.56 in contrast with $\pi_{(CF3)}$ = 0.88), the SCF_3 group being the most lipophilic in Table 3.1 ($\pi_{(SCF3)}$ = 1.44). Alkyl chains that branch from a chalcogen atom display larger π values than their carbon counterparts, but do not exhibit significantly different electronics ($\sigma_{p(CF3)}$ = 0.54 compared with $\sigma_{p(SCF3)}$ = 0.50). In medicinal chemistry, these attributes

[5] Ni, C.; Hu, M.; Hu, J. *Chem. Rev.* **2014**, *115*, 765.
[6] Smart, B. E. *Fluor. Chem.* **2001**, *109*, 3.
[7] Yagupol'skii, L. M.; Ilchenko, A. Y.; Kondratenko, N. V. *Russ. Chem. Rev.* **1974**, *43*, 32.
[8] (a) Fujita, T.; Iwasa, J.; Hansch, C. *J. Am. Chem. Soc.* **1964**, *86*, 5175. (b) Rico, I.; Wakselhan, C. *Tetrahedron Lett.* **1981**, *22*, 323.
[9] Hansch, C.; Leo, A.; Taft, R. W. *Chem. Rev.* **1991**, *91*, 165.

are useful as they can lead to greater metabolic stability and enhanced membrane permeability, thus increasing the bioavailability of the compound.[10]

In addition to these general features, there are certain thiofluoroalkyl motifs with distinctive properties. For example, the thiodifluoromethyl group (-SCF_2H) displays weak hydrogen bond donor abilities,[11] while the (mono)fluoromethylthio group (-SCH_2F) is often used as a bioisosteric replacement for CH_3 and CH_2OH fragments.[12]

Considering the benefits mentioned above, thiofluoroalkyl groups have been implemented in the toolbox of medicinal chemists to help design new active ingredients with specific pharmacokinetic properties.[3]

3.1.2 Lipophilicity in medicinal chemistry

Lipophilicity is defined as a compounds ability to interact favorably with non-polar materials, which can manifest itself in greater solubility with oils and lipids. This chemical property can be measured by quantifying its distribution between water and a hydrophobic medium, with n-octanol being the standard lipophilic medium of choice for such measurement (Figure 3.2).[13] The descriptor used for this metric is log*P*, which is appropriate for compounds that are nonionizable, whereas ionizable compounds such as acids and bases are better evaluated by determining their log*D* at a given pH. The phenomenon of lipophilicity arises from the interplay of several factors, including the intermolecular interactions such as hydrogen bonding and van der Waals forces, the molecule's polarity, and

[10] Lipinski, C. A.; Lombardo, F.; Dominy, B. W.; Feeney, P. J. *Adv. Drug Delivery Rev.* **1997**, *23*, 3.
[11] Zafrani, Y.; Yeffet, D.; Sod-Moriah, G.; Berliner, A.; Amir, D.; Marciano, D.; Gershonov, E.; Saphier, S. J. *Med. Chem.* **2017**, *60*, 797.
[12] Meanwell, N. A. J. *Med. Chem.* **2018**, *61*, 5822.
[13] Wenlock, M. C.; Potter, T.; Barton, P.; Austin, R. P. J. *Biomol. Screening* **2011**, *16*, 348.

any ionic or electrostatic interactions. As such, lipophilicity is governed by the key structural features of a compound.[14]

$$\log P = \log\left(\frac{[\text{compound}]_{\text{octanol}}}{[\text{compound}]_{\text{water}}}\right) \qquad \begin{array}{l} \log P > 1 \Rightarrow \text{lipophilic} \\ \log P < 1 \Rightarrow \text{hydrophilic} \end{array}$$

Figure 3.2. Log*P* mathematical description as the ratio of concentrations of a given compound between octanol and water.

The log*P* parameter is fundamental in drug design. In fact, during the drug discovery process, bioactivity and lipophilicity are simultaneously optimized.[15] The reason behind this is that lipophilicity has an impact on all the individual ADMET parameters (absorption, distribution, metabolism, elimination, and toxicology), making this metric indispensable for finding successful drug-like candidates. [16]

In a biological setting, lipophilicity is crucial to the ability of a compound to partition between the inside and outside of the phospholipid membranes of cells. As a simplified model, a cell's membrane can be regarded as a lipid barrier encapsulating an aqueous medium. Therefore, a pharmaceutical drug must be able to permeate these membranes to access the site of action.[17] In this context, Lipinski suggested that the optimal log*P* value of a drug candidate should be less than 5.[18] However, more recent studies situate the desired lipophilic range between 1 and 3.[15]

Typically, experimental log*P* measurements are tedious and time-consuming, therefore several direct and indirect analytical methods have

[14] Johnson, T. W.; Gallego, R. A.; Edwards, M. P. J. *Med. Chem.* **2018**, *61*, 6401.
[15] Arnott, J. A.; Planey, S. L. *Expert Opin. Drug Discov.* **2012**, *7*, 863.
[16] Miller, R. R.; Madeira, M.; Wood, H. B.; Geissler, W. M.; Raab, C. E.; Martin, I. J. *J. Med. Chem.* **2020**, *63*, 12156.
[17] Wang, Z.; Felstead, H.; Troup, R. I.; Linclau, B.; Williamson, P. *Angew. Chem. Int. Ed.* **2023**, e202301077.
[18] Lipinski, C. A.; Lombardo, F.; Dominy, B. W.; Feeney, P. J. *Adv. Drug Deliv. Rev.* **1997**, *23*, 3.

been developed for this purpose.[19] A convenient solution is the use of computational methods to predict the log*P* value (clog*P*).[20] This is a useful tool for the screening of thousands of compounds, as the available models mostly rely on fragment-log*P* relationships, which do not require a high computational cost. However, given the complexity of the factors influencing lipophilicity, these calculations often possess a non-negligible degree of error.[14] This is especially true when fragments that are not parametrized in the model are evaluated.[20]

3.1.2.1 Fluorination as a tool for modulation of lipophilicity

Fluorination is a frequently utilized strategy to tune the biological and physical properties of drug candidates.[21] Carbon-fluorine bonds infer hydrophobic properties compared with carbon-hydrogen bonds, so the replacement of a hydrogen atom with a fluorine atom usually results in an increase in lipophilicity and therefore log*P*.[6] However, this approach does not always result in greater lipophilicity as the pattern of fluorination across a molecule can infer drastically different properties. In fact, the introduction of fluorine can simultaneously induce competing effects: increase of the hydrophobic surface (increase in log*P*) and the introduction of dipole moments (decrease in log*P*).[22]

For instance, in pioneering work by Müller, it was demonstrated that a simple geometrical analysis proved to be useful to calculate the dipolar moment induced by the introduction of fluorine in alkyl chains and its

[19] Andrés, A.; Rosés, M.; Ràfols, C.; Bosch, E.; Espinosa, S.; Segarra, V.; Huerta, J. M. *Eur. J. Pharm. Sci.* **2015**, *76*, 181.
[20] Jia, Q.; Ni, Y.; Liu, Z.; Gu, X.; Cui, Z.; Fan, M.; Zhu, Q.; Wang, Y.; Ma, J. *J. Chem. Inf. Model*. **2022**, 62, 4928.
[21] Gillis, E. P.; Eastman, K. J.; Hill, M. D.; Donnelly, D. J.; Meanwell, N. A. *J. Med. Chem.* **2015**, *58*, 315.
[22] Jeffries, B.; Wang, Z.; Graton, J.; Holland, S. D.; Brind, T.; Greenwood, R. D.; Le Questel, J.-Y.; Scott, J. S.; Chiarparin, E.; Linclau, B. *J. Med. Chem.* **2018**, *61*, 10602.

influence in the log*P* (Figure 3.3, A).[23] Similarly, Linclau demonstrated how the fluorination of the internal positions of alkyl alcohols did not lead to an increase in lipophilicity, provided the terminal position remained nonfluorinated (Figure 3.3, B).[22]

Regarding thiofluoroalkyl motifs, O'Hagan explored the effect of the difluorination of α-S thioethers. Surprisingly, -SCF_2CH_3 structures showed a decrease in lipophilicity in comparison to their -SCH_2CH_3 counterparts (Figure 3.3, C).[24] This was rationalized by the equilibrium of rotamers with different dipolar moments. The groups of Saphier and Gershonov described how the electronic nature of R-SCF_2H fragments affected its hydrogen-bond capability and thus its lipophilicity (Figure 3.3, D).[25]

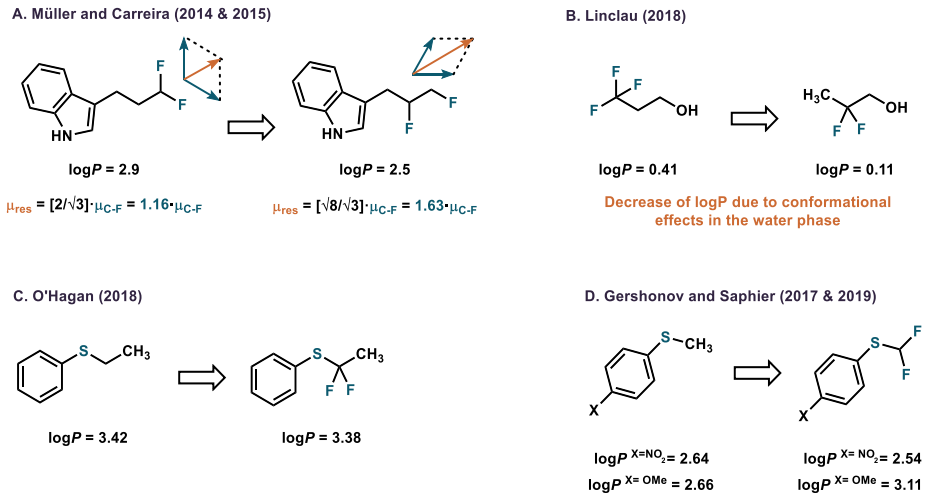

Figure 3.3. Examples of log*P* modulation by the introduction of fluorine atoms.[22,23,24,25]

[23] (a) Müller, K. *Chimia* **2014**, *68*, 356. (b) Huchet, Q. A.; Kuhn, B.; Wagner, B.; Kratochwil, N. A.; Fischer, H.; Kansy, M.; Zimmerli, D.; Carreira, E. M.; Müller, K. *J. Med. Chem.* **2015**, *58*, 9041.

[24] Tomita, R.; Al-Maharik, N.; Rodil, A.; Bühl, M.; O'Hagan, D.; *Org. Biomol. Chem.* **2018**, *16*, 1113.

[25] Zafrani, Y.; Sod-Moriah, G.; Yeffet, D.; Berliner, A.; Amir, D.; Marciano, D.; Elias, S.; Katalan, S.; Ashkenazi, N.; Madmon, M.; Gershonov, E.; Saphier, S. *J. Med. Chem.* **2019**, *62*, 5628.

3.1.3 Acid-base properties in medicinal chemistry

Ionization constants are key metrics that influence the charge state of a given compound. In the physiologically relevant pH range (pH from 1 to 8), several functionalities are susceptible to ionization. In the basic region, we find functional groups such as carboxylic acids, phenols, sulfonamides, and some nitrogen heterocycles susceptible to be deprotonated. On the other hand, common acid-sensitive functionalities include heterocyclic nitrogen atoms, aliphatic amines, guanidines, and anilines.[26]

The most notorious impact of the charge state of a compound is on its lipophilicity.[26] In the previous section, it has been described how omnipresent this parameter is in drug design due to its profound effect on ADMET properties. The ionization of a molecule increases its polarity because of the new intermolecular interactions that arise from the charges. This effect is illustrated in Figure 3.4.[27]

[26] Manallack, D. T.; Prankerd, R. J.; Yuriev, E.; Oprea, T. I.; Chalmers, D. K. *Chem. Soc. Rev.* **2013**, *42*, 485.

[27] Adapted from: Bhal, K. S. *Lipophilicity Descriptors: Understanding When to Use LogP & LogD*, Advanced Chemistry Development, www.acdlabs.com (03/04/2023).

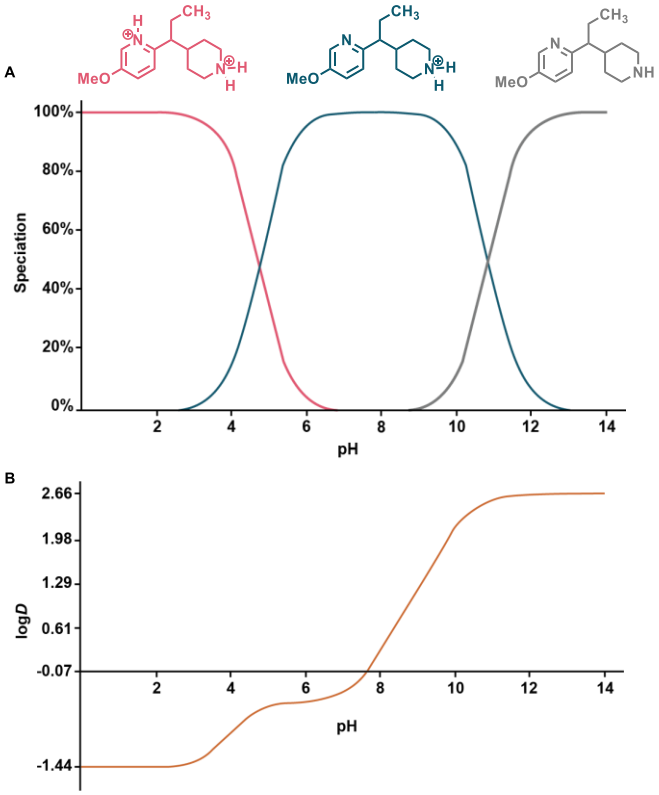

Figure 3.4. Speciation diagram of 5-Methoxy-2-(1-piperidin-4-ylpropyl)pyridine at different pH values (A), and its relation with the log*D* of the compound (B).

In this example, the variation of pH from 1 to 14, results in the speciation of 5-methoxy-2-(1-piperidin-4-ylpropyl)pyridine between three different compounds: a dicationic, a monocationic, and a neutral state (Figure 3.4, A). Consequently, the log*D* (log*P* at a given pH) changes by more than four units in this range of pH (Figure 3.4, B). Importantly, all of these acid-base equilibria are governed by the pK_a of the basic sites, which indeed is a consequence of the molecular structure of the compound.

This interplay between pK_a and log*D* has an impact on the pharmacokinetic properties of a compound. More precisely, absorption, permeability, and bioavailability are greatly influenced by polarity.[22]

The ionization of a drug candidate has many other implications in addition to those related to its lipophilicity. For instance, the presence of formal charges in a molecule creates ionic, dipolar, ion-dipole, and hydrogen-bonding interactions which might be crucial for the activity of a drug. Moreover, the formulation of an active pharmaceutical ingredient (API) is subjected to the acid-base properties of the given compound. Solubility, complexation, and chemical stability are all influenced by the ionization of a molecule.[26]

3.1.3.1 Fluorination as a tool for modulating the basicity of amines

The fluorine atom is the most electronegative across the whole periodic table. When incorporated onto an alkyl chain close to an ionizable functional group, it withdraws electronic density from the functionality by inductive effects. This has a strong effect next to acidic groups, such as carboxylic acids, leading to increased acidity. The converse is true when the fluorine atom is close to basic functionalities such as amines, leading to decreased basicity (Figure 3.5).[28]

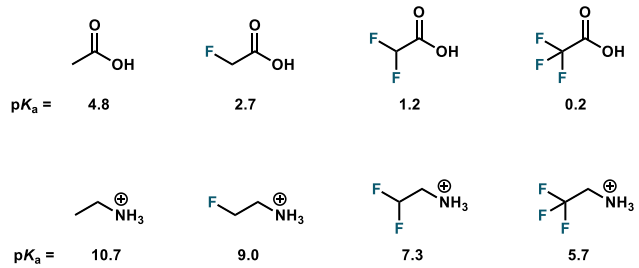

Figure 3.5. Effect of fluorination in the p*Ka* of acetic acid and ethylammonium derivatives.

Tuning the acid-base properties of a drug candidate by the introduction of fluorine is a common strategy in medicinal chemistry.[12] In particular, this is useful for modulating the basicity of amines without significantly altering

[28] Woszinska, J.; Kluger, R. *J. Org. Chem.* **2008**, *73*, 4753.

the polarity of the whole molecule. Moreover, the effects upon fluorination can be predicted by the number of fluorine atoms and the connectivity to the basic nitrogen.[12] For example, the group of Stein reported the rational design of a potent μ opioid agonist to serve as a painkiller.[29] In their hypothesis, the damaged tissues responsible for the pain had a lower pH than the non-damaged ones. Thus, by replacing a hydrogen atom for a fluorine atom in the 3-position of the piperidine, the basicity was reduced enough to avoid protonation at physiological pH (Figure 3.6). This manifested a preferential binding of the fluorinated analog over the non-fluorinated compound to the μ opioid receptors in damaged tissue.[29]

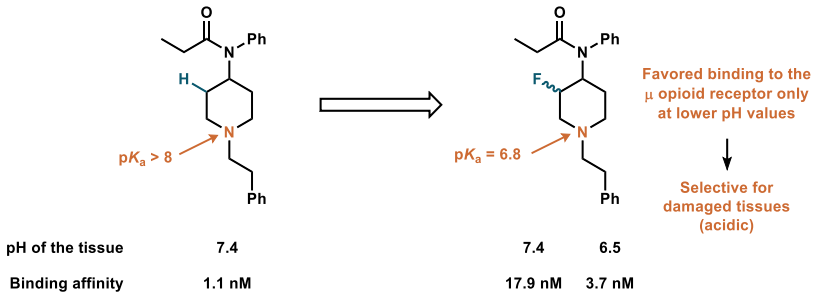

Figure 3.6. μ Opioid agonists developed by Stein *et al.*, and its binding affinity-pH dependence.

3.2 Target of the project

As discussed, sulfur- and fluorine-containing motifs are key players in the design of new fragments in drug discovery. Importantly, thiofluoroalkyl chains have gained momentum in recent years as lipophilic modulators.[3] However, there is a lack of quantitative knowledge for the supposed interplay of structure and lipophilicity in these motifs. The aim of this chapter was to perform a systematic study of the influence of the degree of fluorination and topology on methyl and ethyl thiofluoroalkyl (SR_F)

[29] Spahn, V.; Del Vecchio, G.; Labuz, D.; Rodriguez-Gaztelumendi, A.; Massaly, N.; Temp, J.; Durmaz, V.; Sabri, P.; Reidelbach, M.; Machelska, H.; Weber, M.; Stein, C. *Science* **2017**, *355*, 966.

fragments, and sulfonyl fluoroalkyl chains (SO_2R_F), on key physicochemical properties such as the pK_a and log$P$ of a model substrate.

3.3 Results and discussion

3.3.1 Selection of the model substrate

From the outset of the project, we decided to select 2-(thioalkyl)pyridines (2-SR_F) as the model system. The motivation for this choice was underpinned by the fact that pyridines are the most common aromatic heterocycles found in FDA-approved drugs.[30] In addition, substitution in the second position of the heterocycle would have a greater impact on its basicity due to the close connectivity between the nitrogen and the SR_F fragment. Finally, we were aware that 2-pyridyl thioethers are scaffolds present in various biologically active molecules.[31]

3.3.2 Synthesis of 2-SR_F-pyridines

To constrain the possible combinations of fluoroalkyl chains, we decided to focus on methyl- and ethyl-fluorinated (R_F) fragments with the most accessible fluorination patterns (Figure 3.7). Importantly, as the project goal was focused on the investigation of the physicochemical properties influenced by the SR_F fragments, the synthetic routes to access pyridine derivates were not optimized, and rapid substrate obtention was prioritized.

[30] Vitaku, E.; Smith, D. T.; Njardarson, J. T. *J. Med. Chem.* **2014**, *57*, 10257.

[31] Binepal, G.; Mabanglo, M. F.; Goodreid, J. D.; Leung, E.; Barghash, M. M.; Wong, K. S.; Lin, F.; Cossette, M.; Bansagi, J.; Song, B.; Balasco Serrao, V. H.; Pai, E. F.; Batey, R. A.; Gray-Owen, S. D.; Houry, W. A. *ACS Infect. Dis.* **2020**, *6*, 3224.

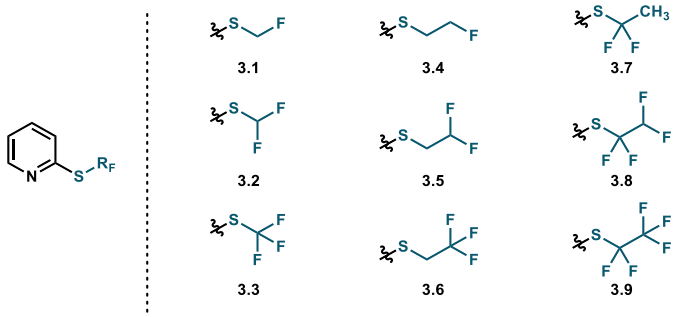

Figure 3.7. Family of 2-SR_F pyridines considered in this study.

Starting with SCH_3 derived fragments, we prepared all the fluorinated derivates by using commercially available 2-mercaptopyridine in one step (Scheme 3.1). The monofluorothiomethyl pyridine **3.1** could be obtained in excellent yield (98%) by reacting the aromatic thiol with gaseous bromofluoromethane (Scheme 3.1, A). Using potassium bromodifluoroacetate as difluorocarbene precursor, we could access pyridine **3.2** in 50% yield (Scheme 3.1, B). Finally, the SCF_3 analog **3.3** was obtained in 37% yield using potassium triflinate under radical oxidative conditions (Scheme 3.1, C).

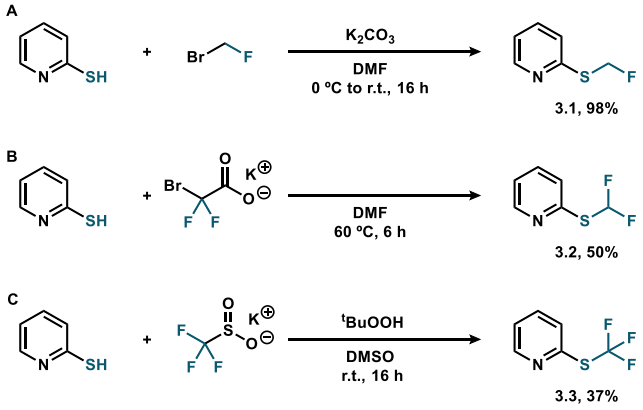

Scheme 3.1. Synthesis of fluorinated 2-thiomehtyl substituted pyridines.

For the synthesis of the ethyl derivatives, different approaches for the installation of the fluoroalkyl chain were pursued. For instance, terminal

thiomonofluoro- **3.4**, thiodifluoro- **3.5**, and thiotrifluoroethyl **3.6** pyridines were accessed by reaction of 2-pyridyl thiol with the corresponding alkyl tosylates in good yields (66-83%) through a simple S_N2 reaction (Scheme 3.2, A). Similarly, we obtained 2-tetrafluoroethylthiopyridine **3.8** in 75% yield using *ex situ* generated tetrafluoroethylene as an electrophilic source of fluoroalkyl chain (Scheme 3.2, B). For the perfluorinated analog **3.9** (44%), potassium pentafluoropropionate was subjected to thermal decarboxylation to form a perfluoroethyl anion that reacted with electrophilic 2-pyridyl disulfide (Scheme 3.2, C). Lastly, internal thiodifluoroethyl pyridine **3.7** was prepared in a four-step sequence (Scheme 3.2, D). 2-Pyridyl thiol was reacted with ethylbromodifluoroacetate to give pyridine **3.10** (70%), which was then reduced using sodium borohydride to render intermediate **3.11** (74%), both transformations were achieved in good yield. Next, the alcohol from **3.11** was successfully transformed to thioxoester **3.12** (81%). Finally, pyridine **3.12** was subjected to Barton-McCombie deoxygenation conditions to afford targeted pyridine **3.7** in a low 12% yield.

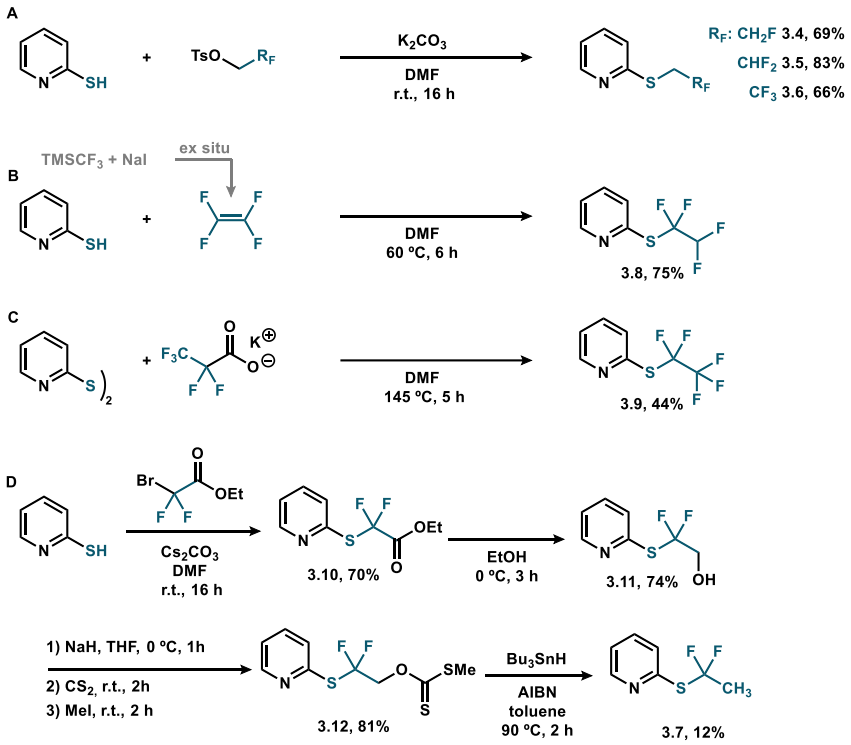

Scheme 3.2. Synthesis of fluorinated 2-thioehtyl substituted pyridines.

Remarkably, the synthesis of pyridine **3.7** proved challenging, as up to six different strategies were pursued without success (see Scheme 3.3). Initial attempts were based on the seminal report by O'Hagan[24] using TIPS-EBX reagent (Scheme 3.3, A.1). However, the 2-thio-alkynyl substituted pyridine intermediate (**int-1**) was never observed, and only decomposition products were obtained. Other strategies to obtain **int-1** by nucleophilic alkynylation (Scheme 3.3, A.1 and A.2) were also unsuccessful. Additionally, attempts to methylate pyridine **3.2** were futile, resulting in only decomposition products when THF was used as a solvent, or byproduct **3.13** when DMF was used (Scheme 3.3, B). Finally, electrophilic sources of the fluoroalkyl fragment were used to alkylate 2-pyridyl thiol (Schemes 3.3, C and D), but only starting material was recovered after multiple attempts.

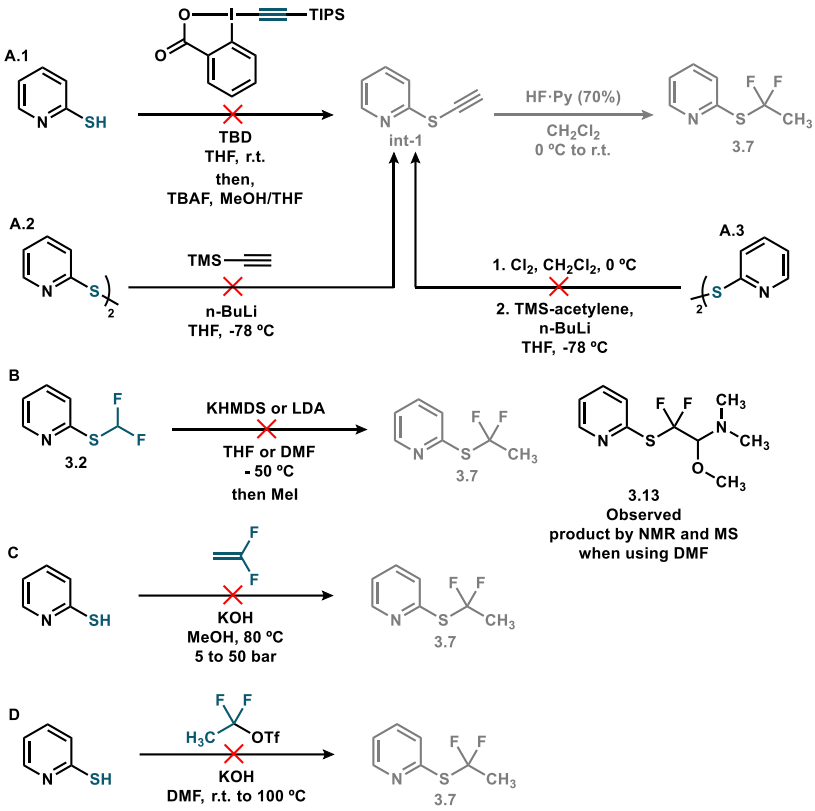

Scheme 3.3. Synthetic attempts towards the preparation of pyridine **3.7**.

3.3.3 Synthesis of 2-SO_2R_F-pyridines

The preparation of the fluorinated pyridyl sulfones was achieved by oxidation of the corresponding thioethers. Sulfones **3.1o** to **3.9o** can be synthesized with excellent yields (78-99%) using molybdenum or ruthenium catalysis, and either hydrogen peroxide or sodium periodate as terminal oxidants (Scheme 3.4).

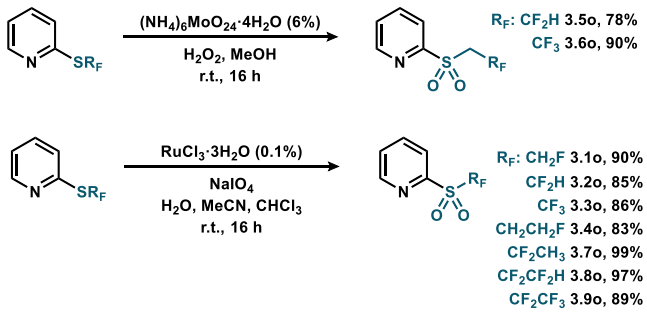

Scheme 3.4. Synthesis of 2-SO_2R_F pyridines from the oxidation of the 2-SR_F counterparts.

3.3.4 Synthesis of nonfluorinated pyridines

For the sake of comparison, the methyl and ethyl congeners were prepared from reported procedures (Scheme 3.5). 2-(Methylthio)pyridine **3.15** was purchased directly from a commercial supplier.

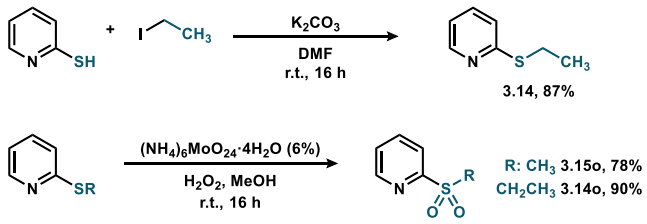

Scheme 3.5. Synthesis of 2-thioethyl pyridine, and oxidation of 2-SAlkyl ones.

3.3.5 Measurement of lipophilicity

To experimentally measure the log*P* values of the fluorinated pyridines, we resorted to a ^{19}F NMR method developed by Linclau (Figure 3.8).[32] This approach is based on a variation of the traditional "shake-flask method" in which a sample is partitioned into octanol and water together with a fluorinated internal standard of known lipophilicity. Then, the relative integration of the ^{19}F NMR signals of the product and the internal standard in each phase can provide the log*P* value of the compound of interest.

[32] Linclau, B.; Wang, Z.; Compain, G.; Paumelle, V.; Fontenelle, C. Q.; Wells, N.; Weymouth-Wilson, A. *Angew. Chem. Int. Ed.* **2016**, *55*, 674.

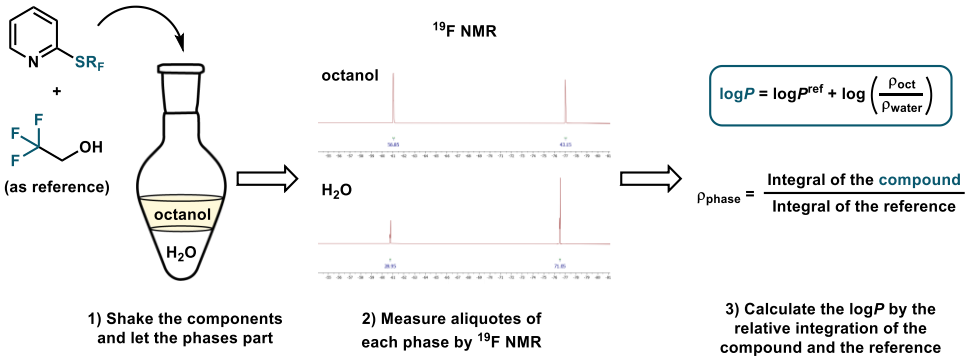

Figure 3.8. Linclau's method for the determination of log*P* of fluorinated compounds using ^{19}F NMR.

For the non-fluorinated analogs, log*P* was determined by the usual "shake-flask method" using HPLC-UV to quantify the compound in the aqueous phase before and after partitioning.[19] As SR_F are electron-withdrawing motifs, we did not find any difference in log*P* using water or a 7.4-pH buffer provided that the pyridines were not protonated in a neutral medium.

Unfortunately, 2-SCH_2F (**3.1**) and 2-SCH_2CH_2F (**3.4**) pyridines were unstable under aqueous conditions, as decomposition was observed during the log*P* measurements. Probably, the assistance of sulfur aided the leaving of the fluoride and the subsequent addition of water (Scheme 3.6).

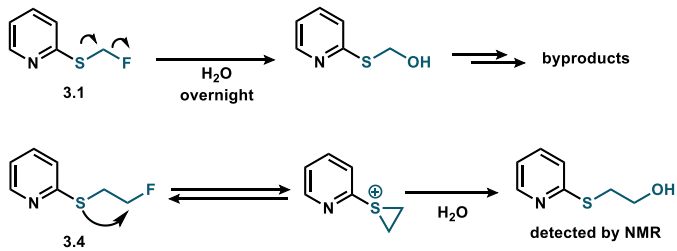

Scheme 3.6. Plausible reactions responsible for the decomposition in water of **3.1** and **3.4**.

Our initial hypothesis was that the degree of fluorination and length of the alkyl chain would increase the lipophilicity of the molecule due to the concomitant increase in the hydrophobic volume. Also, increasing the oxidation state of the sulfur center by changing the thioether to a sulfonyl group would decrease the lipophilicity of the compound, as sulfones are more polar than thioethers.

Analyzing the SR_F log*P* series (Figure 3.9) we find that indeed in the methyl fragments, the corresponding SCF_2H (**3.2**), and SCF_3 (**3.3**) pyridines are gradually more lipophilic than the nonfluorinated SCH_3 (**3.15**). However, measurement of the log*P* of the ethyl derivatives shows that there is not a simple accumulative correlation between degree of fluorination and lipophilicity. Firstly, the internally difluorinated S-CF_2CH_3 pyridine (**3.7**) has a lower log*P* value than the fully alkyl one (SCH_2CH_3, **3.14**). This decrease in lipophilicity is consistent with the observations of O'Hagan in phenyl scaffolds.[24]

Surprisingly, 2-SCH_2CF_2H (**3.5**), and 2-SCF_2CF_2H (**3.8**) substituted pyridines had the same lipophilicity profile as the non-fluorinated ethyl group (**3.14**). These results suggest that the particular fluorination topology in these fragments does not affect the lipophilicity, implying that here the fluorine atoms are acting as lipophilic isosteres to the hydrogens.

Finally, analyzing the terminally perfluorinated fragments SCH_2CF_3 (**3.6**) and perfluorinated fragment SCF_2CF_3 (**3.9**), increased log*P* values are observed relative to the other ethyl fragments. This observation is in line with Linclau's studies on terminal fluorination of alkyl chains.[22] However, these fragments present a similar log*P* value where the internal fluorines in SCF_2CF_3 (**3.9**) do not spike up its lipophilicity value.

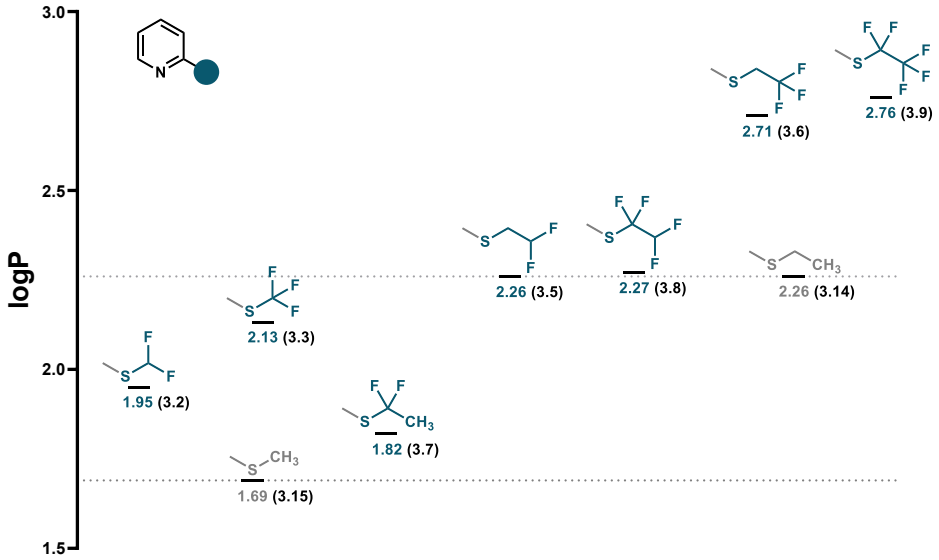

Figure 3.9. Experimental log*P* values for the 2-SR$_F$ substituted pyridines.

When studying the results of the 2-sulfonyl fluoroalkyl pyridines (Figure 3.10), an increase in log*P* is observed with increasing degree of fluorination. This is unsurprising, as all the oxidized fragments exhibit reduced lipophilicity compared to the thiofluoroalkyl fragments.

However, there are some interesting tendencies to highlight. Firstly, the terminally monofluorinated SO_2-CH_2CH_2F fragment (**3.4o**) presents a greater affinity for water than the nonfluorinated SO_2-CH_2CH_3 (**3.15o**). In addition, the internally difluorinated SO_2-CF_2CH_3 (**3.7o**) exhibits greater lipophilicity than the terminally difluorinated SO_2-CH_2CF_2H pyridine (**3.5o**). This phenomenon is in contrast to 2-pyridyl thioether, in which the opposite trend is observed (see Figure 3.9). Interestingly, comparing the methyl and ethyl series, the introduction of a CH_2 α-to-sulfur results in a decreased log*P*, even though the chain length is increased (see SO_2CF_2H (**3.2o**, 0.55) *vs.* $SO_2CH_2CF_2H$ (**3.5o**, 0.31), and SO_2CF_3 (**3.3o**, 1.43) *vs.* $SO_2CH_2CF_3$ (**3.6o**, 0.81)).

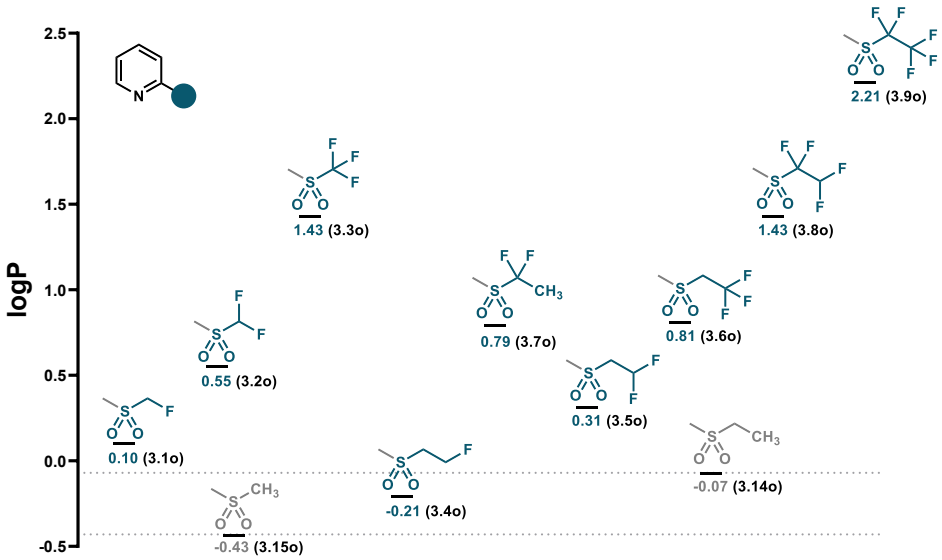

Figure 3.10. Measured log*P* values for 2-SO_2R_F pyridines.

Having considered the effect of the fluorination pattern and the sulfur oxidation state on lipophilicity, we were devoted to understanding the underlying factors responsible for these trends. To do so, we initiated a collaboration with Prof. Jordi Carbó and Dr. Maria Besora from the quantum chemistry group at the Rovira and Virgili University. The idea was to develop a model to predict log*P* values of 2-SR_F and 2-SO_2R_F substituted pyridines. At the same time, this would provide information to explain the experimental observations and link them with the structural features of the compounds.

The workflow used for this computational study is based on a statistical approach (Figure 3.11). First, the experimental log*P* values of 12 2-substituted pyridines were fed to a Python algorithm together with more than 200 molecular descriptors (topological or DFT-derived from the optimization of the 2-substituted pyridines), which were normalized to the unit. This algorithm was able to combine both inputs to generate over 24 000 multilinear regression models predicting the log*P*. After examining the

correlation between the experimental values and the predicted ones, the model with the highest r^2 was selected as the optimal (Figure 3.12, A).

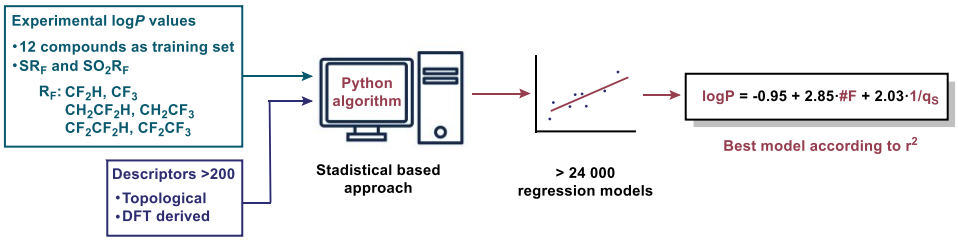

Figure 3.11. Computational workflow for the obtention of a descriptor-based model of log*P*.

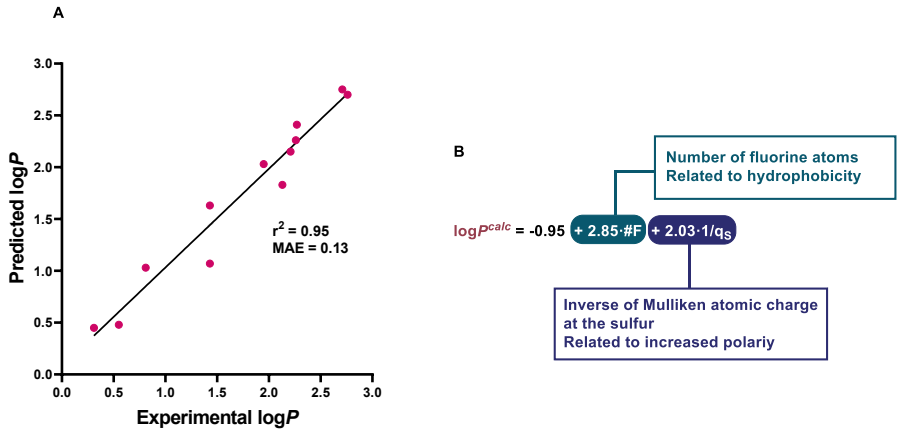

Figure 3.12. Correlation between the experimental log*P* and the predicted ones (A), and mathematical model for the prediction of log*P* values of the 2-SR_F substituted pyridines (B).

Examining the equation of the best model for the prediction of log*P*, two mathematical terms can be distinguished (Figure 3.12, B). The first is related to the number of fluorine atoms in the molecule. As the coefficient multiplied by this descriptor is positive, the increase in the number of F atoms results in an increase in the lipophilicity. This is consistent with the higher hydrophobic surface created in the molecule by fluorination. The

second term is related to the Mulliken atomic charge at the sulfur atom. This descriptor is dividing the coefficient, reflecting that the higher the atomic charge on sulfur, the lower the lipophilicity of the molecule. Indeed, by the introduction of fluorine atoms, the sulfur atom loses electronic density, polarizing the whole molecule. Finally, we observe that both coefficients multiplying the descriptors have a similar value (2.85 and 2.03). This implies that subtle differences in the fluorination pattern can lead to significant changes in lipophilicity.

The descriptors used in the model are normalized for the sake of comparison. This means that in applying the mathematical formula we should divide the descriptor value by the maximum value used in the model. For instance, if the number of fluorine atoms considered is 3, we should use 0.6 (3/5) as 5 is the highest fluorination degree in an ethyl fragment. Similarly, the considered Mulliken charge at the sulfur atom should be divided by the highest one (+1.18) which corresponds to the 2-$SO_2CF_2CF_3$ pyridine (**3.9o**).

In summary, this study corroborated the dual nature of fluorination in lipophilicity. On the one hand, the presence of more fluorine atoms leads to a larger hydrophobic surface area, resulting in an increase in log*P*. However, on the other hand, fluorination can also induce greater dipole moments, thereby increasing the overall polarity of the molecule and leading to a decrease in log*P*. Significantly, this delicate balance is governed by the specific disposition of the fluorine atoms in the molecule.

Based on our previous findings, we extracted chemical information from the statistical model that aided in our understanding of our experimental observations. For instance, 2-SCF_2CH_3 pyridine (**3.7**) had a lower log*P* value compared to the non-fluorinated counterpart (**3.14**) (see figure 3.9). This can be explained because fluorination adjacent to sulfur polarizes the chalcogen, inducing a dipole moment which is responsible for the decrease in lipophilicity.

It is worth noting that 2-SCH_2CF_2H (**3.5**), 2-SCF_2CF_2H (**3.8**), and 2-SCH_2CH_3 (**3.14**) substituted pyridines display a similar effect, with almost identical log*P* values (Figure 3.13). In this scenario, an interplay of factors is responsible for this behavior. First, the presence of terminal -CF_2H could be accountable for the polarization of the S-center resulting in a decrease in the lipophilicity of the molecule. In the second term, fluorination of the α-to-the-S position induces an even greater polarization of the S center, increasing the polarity of the pyridine. Importantly, this polarization counteracts the increase in the hydrophobic surface, which does not dramatically affect the log*P* value. This same analysis can be translated to 2-SCH_2CF_3 (**3.6**) and 2-SCF_2CF_3 (**3.9**) substituted pyridines, where the lipophilicity value is already higher due to the presence of the terminal CF_3 group.

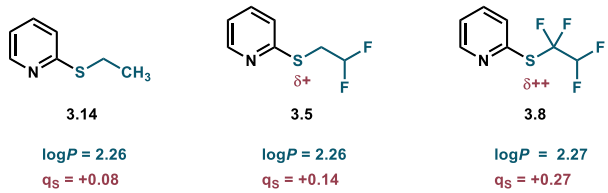

Figure 3.13. Comparison of experimental log*P* values and Mulliken charges at the sulfur atom of pyridines **3.14**, **3.5**, and **3.8**.

Examining the 2-SO_2R_F series, we can justify the difference in trends compared with the 2-SR_F substituted pyridines. When the sulfur center is oxidized, the chalcogen is less polarizable; therefore the effect of introducing fluorine is diminished (Figure 3.14). Consequently, the main factor governing the log*P* is the fluorination degree of the molecule. This analysis is consistent with the experimental values obtained and with our mathematical model.

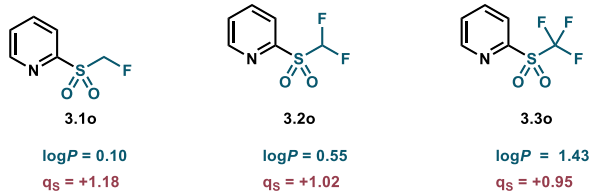

Figure 3.14. Comparison of experimental log*P* values and Mulliken charges at the sulfur atom, of pyridines **3.1o**, **3.2o**, and **3.3o**.

The regression model is useful not only for explaining the underlying factors of structure and lipophilicity, but also for predicting other 2-SR_F or 2-SO_2R_F motifs. For example, this allowed for obtention of log*P* values of 2-SCH_2F (**3.1**) and 2-SCH_2CH_2F (**3.4**) substituted pyridines (Figure 3.15) which could not be experimentally determined due to their decomposition in water (see Scheme 3.6).

2-SCH_2F-Pyridine (**3.1**) log*P* value was found to be in between the 2-SCF_2H (**3.2**) and 2-SCF_3 (**3.3**) analogs (Figure 3.9). Interestingly, 2-SCH_2CH_2F (**3.4**) had a greater polarity than 2-SCH_2CH_3 (**3.14**) substituted pyridine. These trends can also be explained by the balance of polarization and the hydrophobic surface induced by fluorination.

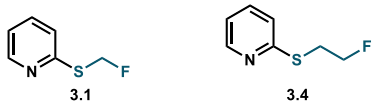

Figure 3.15. Calculated log*P* values for pyridines **3.1** and **3.4**.

3.3.6 p*K*a measurement

To experimentally measure the p*K*a values of the pyridine derivatives, a ^{19}F NMR method developed by Leito was followed (see figure 3.16).[33] This procedure involves preparing a series of NMR samples with the compound of interest at different pH values, with an external standard (KF in D_2O)

[33] Parman, E.; Toom, L.; Selberg, S.; Leito, I. *J. Phys. Org. Chem.* **2019**, *32*, e3940.

inserted into the NMR tube. Next, the samples are measured, and the chemical shifts plotted against their respective pH. The specific chemical shift is related to the equilibrium between the neutral compound and its protonated form. Therefore, by taking the second derivative of the sigmoidal curve, the inflection point can be obtained which corresponds to the pK_a value of the compound. For the nonfluorinated analogs, pK_a was determined by an analogous method using ^{1}H NMR, and 2,2,2-trifluoroethanol as internal standard.[34]

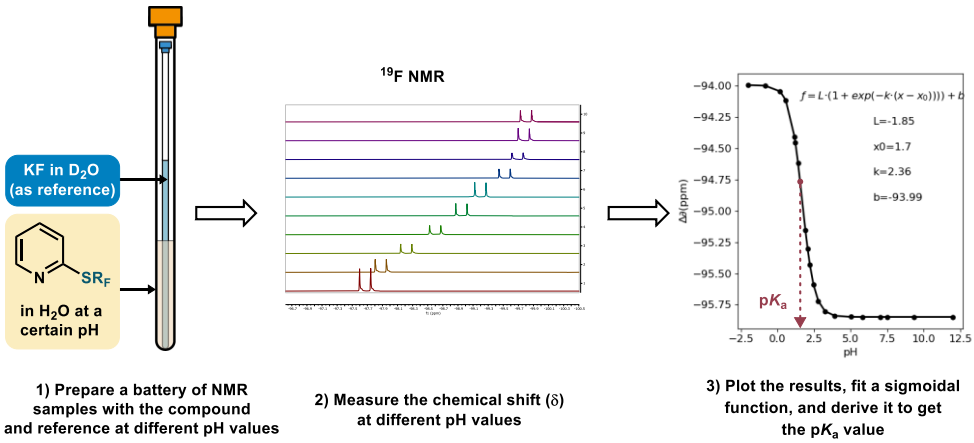

Figure 3.16. Leito's method for the determination of pK_a of fluorinated compounds using ^{19}F NMR.

The results of these measurements are presented in Figure 3.17. The measurement of 2-SO_2R_F pyridines were not performed as the basicity of these compounds is practically nonexistent due to the strong electron-withdrawing effects of the fluoroalkyl sulfone substitution.

[34] Gift, A. D.; Stewart, A. M.; Bokashanga, P. K. *J. Chem. Educ.* **2012**, *89*, 1458.

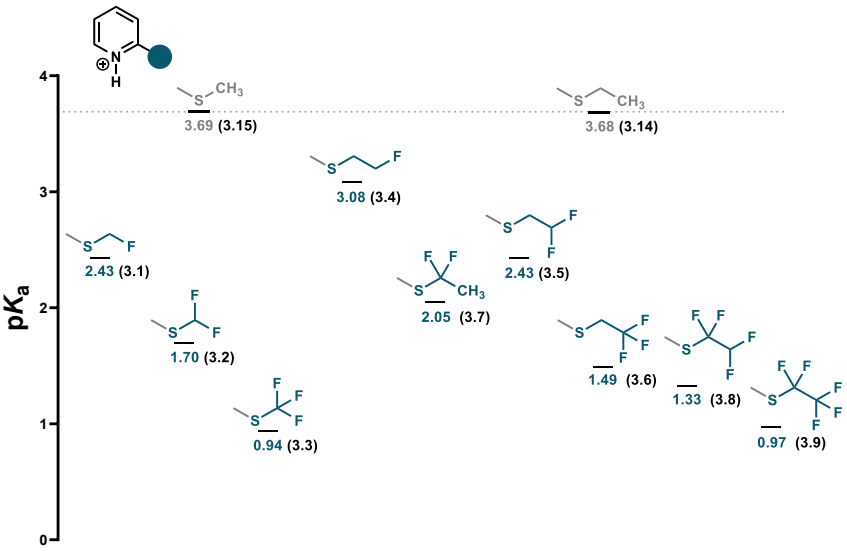

Figure 3.17. Measured pK_a values for 2-SR_F pyridines.

Unsurprisingly, the pK_a values of the 2-SR_F pyridines are lower than the non-fluorinated SCH_3 and SCH_2CH_3 ones, due to the electron withdrawing properties of the SR_F groups. Overall, the pK_a values are influenced by inductive effects related to the degree of fluorination and the connectivity to the basic nitrogen. Thus, α-to-S fluorination has a greater impact on basicity compared to the fluorination of terminal positions. Examining Figure 3.17, we see how these trends are maintained through all the motifs following the previous reasoning.

3.3.7 Isosteric relationships of SR_F compounds

Using experimental measurements and computed values for log*P* and pK_a, we have demonstrated that the topology of the fluorinated SR_F and SO_2R_F fragments can significantly affect the physicochemical properties of the linked pyridines. Importantly, by analyzing simultaneously lipophilicity and acidity, we have identified some non-obvious patterns which might be useful for the design of active pharmaceutical ingredients (APIs).

For example, the acid-base properties of the pyridine nitrogen adjacent to the S-CH_2CH_3 fragment could be altered by introducing fluorine atoms, such as in SCH_2CF_2H or SCF_2CF_2H, without compromising the overall molecule's lipophilicity. This could have interesting implications, such as blocking the metabolic oxidation of the sulfur center, as fluorinated molecules are more difficult to oxidize.[3] Additionally, if decreased log*P* values are desired in SR_F-containing fragments, selection of SCF_2CH_3 may be beneficial, which would also decrease the overall electron density of the linked molecule.

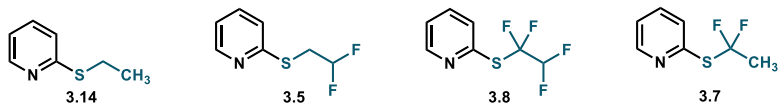

Figure 3.18. Comparison of log*P* and pK_a values of **3.14**, **3.5**, **3.8**, and **3.7** pyridines.

3.4 Conclusions

In this chapter, a detailed study of the lipophilicity and acid properties of 2-SR_F and 2-SO_2R_F compounds has been presented. By using ^{19}F NMR as an analytical method, we experimentally determined the log*P* and pK_a values of a wide array of 2-substituted pyridines. In addition, computational modeling was applied to gain insight into the structure-properties relationship, which helped to reason the experimental observations. This model was also used to predict the log*P* values of other 2-SR_F pyridines.

The results presented in this chapter offer a description of the influence of fluorination topology in SR_F fragments and reflected the dual effect of this element affecting the balance in polarity. Conclusions distilled from these observations may be extrapolated to other systems containing these motifs.

By studying the methyl and ethyl fragments, we found that by changing the oxidation state of the sulfur atom and the fluorination pattern, there is a

small-step gradient from lower log*P* values to higher ones. Furthermore, when combined with acidity information (pK_a values), we find some complementary physicochemical properties along the SR_F family.

Finally, we provided evidence to demonstrate that the influence of fluorination is highly context-dependent and should not be overlooked. We expect our findings to be useful for the synthetic community, especially the medicinal chemistry one, to fine-tune the physicochemical properties of new active pharmaceutical ingredients.

3.5 Experimental section

General Remarks. Proton (^{1}H NMR), carbon (^{13}C{^{1}H}) NMR), and fluorine (^{19}F NMR) nuclear magnetic resonance spectra were recorded on a Varian Mercury spectrometer or a Bruker Avance Ultrashield (400 MHz for ^{1}H), (100.6 MHz for ^{13}C{^{1}H}), and (376.5 MHz for ^{19}F). Spectra were fully assigned using COSY, HSQC, HMBC, and NOESY. All chemical shifts are quoted on the δ scale in parts per million (ppm) using the residual solvent as internal standard (^{1}H NMR: $CDCl_3$ = 7.26, CD_3OD = 3.31 and (^{13}C{^{1}H} NMR): $CDCl_3$ = 77.16, CD_3OD = 49.0). Coupling constants (*J*) are reported in Hz with the following splitting abbreviations: s = singlet, d = doublet, t = triplet, q = quartet, and app = apparent. Infrared (IR) spectra were recorded on a FTIR–ATR spectrophotometer. Absorption maxima (ν_{max}) are reported in wavenumbers (cm^{-1}). High-resolution mass spectra (HRMS) were recorded on an LC–MS system (UHPLC 1290 Infinity II Series coupled to a qTOF/MS 6550 Series, both Agilent Technologies (Agilent Technologies). For the ionization, an ESI operating on positive or negative ionization or an APCI operating on positive or negative ionization was used. Water and methanol with 0.05% formic acid were used as mobile phases. The quadrupole time of flight mass spectrometer (qTOF) operated in high resolution MS scan mode between 100–1000 *m*/*z*. For GC–HRMS mass determination the compounds were directly analyzed by gas chromatography coupled to high-resolution

mass spectrometry (7200 GC–qTOF from Agilent technologies). For ionization, electron impact ionization was used. The chromatographic column was a 5HP–MS from Agilent and carried gas was He. The quadrupole time of flight mass spectrometer (qTOF) operated in high resolution MS scan mode between 100–600 *m*/*z*. Nominal and exact *m*/*z* values are reported in Daltons. Thin layer chromatography (TLC) was carried out using commercial backed sheets coated with 60 Å F_{254} silica gel. Visualization of the silica plates was achieved using a UV lamp (λ_{max} = 254 nm), 6% H_2SO_4 in EtOH, cerium molybdate, and/or potassium permanganate staining solutions. Flash column chromatography was carried out using silica gel 60 Å CC (230–400 mesh). Mobile phases are reported in relative composition (*e.g.*, 1:1 EtOAc/hexane v/v). All reactions using anhydrous conditions were performed using oven-dried apparatus under an atmosphere of argon. Brine refers to a saturated solution of sodium chloride. Anhydrous sodium sulfate (Na_2SO_4) was used as drying agent after reaction work-up, as indicated. All reagents were purchased from Sigma Aldrich, Cymit, Carbosynth, Apollo Scientific, Fluorochem and Manchester Organics chemical companies. Fluoroethyl tosylates were prepared according to reported procedures.[35]

3.5.1 Preparation of 2-SR_F and 2-SO_2R_F pyridines

General procedure for the introduction of CH_2R_F motifs (GP-1)

A round-bottom flask, equipped with a magnetic stir bar, was charged with 2-mercaptopyridine (1 equiv) and potassium carbonate (1.2 equiv). The flask was then evacuated and backfilled with argon three times. Subsequently, anhydrous DMF (1 M) was added using a syringe, and the

[35] (a) Wu, J.-Q.; Zhang, S.-S.; Gao, H.; Qi, Z.; Zhou, C.-J.; Ji, W.-W.; Liu, Y.; Chen, Y.; Li, Q.; Li, X.; Wang, H. *J. Am. Chem. Soc.* **2017**, *139*, 3537. (b) Kuduk, S. D.; Reger T. S.; Roecker, A. J.; Kuduk, S. D.; Reger, T. S.; Roecker, A. J. Diazepane orexin receptor antagonists. WO2015095111A1, 2015. (c) Axer, A.; Hermann, S.; Kehr, G.; Clases, D.; Karst, U.; Fischer-Riepe, L.; Roth, J.; Fobker, M.; Schäfers, M.; Gilmour, R.; Faust, A. *ChemMedChem* **2018**, *13*, 241.

mixture was sparged with argon for 15 min. Next, the corresponding fluoroalkyl tosylate (1 equiv) was added, and the reaction mixture was stirred overnight at room temperature. Then, the mixture was diluted with diethyl ether, washed with brine, and dried over Na_2SO_4. Upon filtration, the organic layer was concentrated under reduced pressure, and purified by column chromatography.

General procedure for the oxidation of SR_F motifs with Mo-catalyst (GP-2)

To a solution of pyridine-SR_F (1.0 equiv.) in MeOH (0.2 M) was added ammonium molybdate tetrahydrate (from 5 to 10%), and hydrogen peroxide (30% (w/w) in water, from 3 to 6 equiv). The reaction was then left stirring overnight at room temperature. Next, the reaction was quenched with water, extracted with Et_2O, and washed with brine. The combined organic fractions were dried with Na_2SO_4, filtered, and evaporated under reduced pressure. Upon filtration, the organic layer was concentrated under reduced pressure, and purified (if needed) by column chromatography to render the oxidized products.

General procedure for the oxidation of SR_F motifs with Ru-catalyst (GP-3)

To a solution of pyridine-SR_F (1.0 equiv.) in H_2O (1 mL), CH_3CN (0.5 mL), and $CHCl_3$ (0.5 mL) was added ruthenium(III) chloride trihydrate, and sodium periodate at 0 °C. The reaction was then left stirring overnight at room temperature. Next, the reaction was quenched with water, extracted with dichloromethane, and washed with brine. The combined organic fractions were dried with Na_2SO_4, filtered, and evaporated under reduced pressure. Upon filtration, the organic layer was concentrated under reduced pressure, and purified (if needed) by column chromatography to render the oxidized products.

3.5.2 Characterization data of 2-SR_F and 2-SO_2R_F pyridines

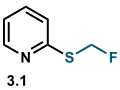
3.1

2-((Fluoromethyl)thio)pyridine (3.1). A 10 mL round-bottom flask, equipped with a magnetic stir bar, was charged with 2-mercaptopyridine (556 mg, 5 mmol, 1.0 equiv) and potassium carbonate (830 mg, 6 mmol, 1.2 equiv). The flask was then evacuated and backfilled with argon three times. Subsequently, anhydrous DMF (5 mL, 1 M) was added using a syringe. Then, bromofluoromethane (~850 mg, 7.5 mmol, 1.5 equiv) was bubbled to the reaction mixture at 0 °C, and the reaction was stirred overnight at room temperature with a water bath. The crude was diluted with diethyl ether, washed with brine, and dried over Na_2SO_4. Upon filtration, the organic layer was concentrated under reduced pressure to afford pure **3.1** as a yellow oil (1.00 g, 98%).

^{1}H NMR ($CDCl_3$, 400 MHz): δ = 8.51 (ddd, *J* = 4.9, 1.8, 0.9 Hz, 1H), 7.58 (td, *J* = 7.8, 1.9 Hz, 1H), 7.28 (dt, *J* = 8.0, 0.9 Hz, 1H), 7.10 (ddd, *J* = 7.4, 4.9, 1.0 Hz, 1H), 6.15 (d, *J* = 51.7 Hz, 2H); **^{13}C NMR ($CDCl_3$, 100.6 MHz):** δ = 155.3, 149.9, 136.9, 122.9 (d, J = 1.9 Hz), 121.1, 83.5 (d, *J* = 215.9 Hz).; **^{19}F NMR ($CDCl_3$, 376.5 MHz):** δ = –187.53 (t, *J* = 51.7 Hz, 1F); **HRMS (ESI+)** for $(M+H)^+$ $C_6H_7FNS^+$ (m/z): calc. 144.0278; found 144.0278.

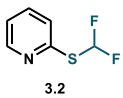
3.2

2-((Difluoromethyl)thio)pyridine *(3.2)*. A 50 mL round-bottom flask, equipped with a magnetic stir bar, was charged with dried potassium bromodifluoroacetate (7.93 g, 37.2 mmol, 2.0 equiv), 2-mercaptopyridine (2.07 g, 18.6 mmol, 1.0 equiv) and potassium carbonate (3.86 g, 27.9 mmol, 1.5 equiv). The flask was then evacuated and backfilled with argon three times. Subsequently, anhydrous DMF (11 mL, 1.7 M) was added using a syringe. Then, the reaction mixture was stirred for 6 h at 60 °C. The mixture was diluted with diethyl ether, washed with brine, and dried over Na_2SO_4. Upon filtration, the organic layer was concentrated under reduced pressure and purified by flash column chromatography

(SiO_2, 1:9 Ethyl acetate/hexane) to afford **3.2** as a pale-yellow oil (1.51 g, 50%).

^{1}H NMR ($CDCl_3$, 400 MHz): δ = 8.48 (d, *J* = 4.8, 1H), 7.68 (t, *J* = 56.2 Hz, 1H), 7.59 (t, *J* = 7.7 Hz, 1H), 7.25 (d, *J* = 7.9, 1H), 7.13 (dd, *J* = 7.4, 4.9 Hz, 1H); **^{13}C NMR ($CDCl_3$, 100.6 MHz):** δ = 153.2, 150.1, 137.1, 124.3, 121.7, 121.4 (t, *J* = 270.9 Hz); **^{19}F NMR ($CDCl_3$, 376.5 MHz):** δ = –96.28 (d, *J* = 56.1 Hz, 2F); **HRMS (ESI+)** for $(M+H)^+$ $C_6H_6F_2NS^+$ (m/z): calc. 162.0184; found 162.0188.

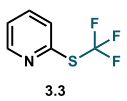

3.3

2-((Trifluoromethyl)thio)pyridine (3.3). In a 250 mL round-bottom flask, equipped with a magnetic stir bar, 2-mercaptopyridine (1 g, 9.0 mmol, 1.0 equiv) and potassium trifluoromethanesulfinate (2.8 g, 18.0 mmol, 2.0 equiv) were added and dissolved in DMSO (90 mL, 0.1 M). Then, the solution was cooled at 0 °C and *tert*-butyl hydroperoxide (70% (w/w) in water, 3.8 mL, 27.0 mmol, 3.0 equiv) was added dropwise. The mixture was stirred overnight at room temperature. To the reaction mixture water was added and it was extracted with CH_2Cl_2. The combined organic layers were washed with brine, dried over Na_2SO_4, filtered and concentrated under reduced pressure. The organic residue was purified by flash column chromatography (SiO_2, 2:8 Ethyl acetate/hexane) to afford **2a** as a pale-yellow oil (597 mg, 37%).

^{1}H NMR ($CDCl_3$, 400 MHz): δ 8.56 (d, *J* = 4.9 Hz, 1H), 7.66 (t, *J* = 7.7 Hz, 1H), 7.52 (d, *J* = 7.9 Hz, 1H), 7.25 (dd, *J* = 7.5, 4.8 Hz, 1H); **^{13}C NMR ($CDCl_3$, 100.6 MHz):** δ = 150.7, 149.4, 137.7, 129.4 (q, *J* = 307.6 Hz), 128.2, 123.8; **^{19}F NMR ($CDCl_3$, 376.5 MHz):** δ –40.21 (s, 3F); **HRMS (ESI+)** for $(M+H)^+$ $C_6H_5F_3NS^+$ (m/z): calc. 180.0089; found 180.0092.

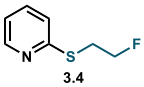

3.4

2-((2-Fluoroethyl)thio)pyridine (3.4). Following the general procedure **GP-1**, starting from K_2CO_3 (1.05 g, 7.6 mmol), 2-mercaptopyridine (707 mg, 6.4 mmol), 2-fluoroethyl tosylate (1.39 g, 6.4 mmol) and DMF (6.4 mL); the pyridine derivative **3.4** (703 mg, 69%) was

obtained as a pale-yellow oil after purification by flash column chromatography (SiO_2, 1:9 Ethyl acetate/hexane).

^{1}H NMR ($CDCl_3$, 400 MHz): δ = 8.39 (d, *J* = 4.6 Hz, 1H), 7.46 (t, *J* = 7.6 Hz, 1H), 7.17 (d, *J* = 8.0 Hz, 1H), 6.98 (dd, *J* = 7.4, 5.0 Hz, 1H), 4.62 (dt, *J* = 47.1, 6.5 Hz, 2H), 3.50 (dt, *J* = 18.7, 6.6 Hz, 2H); **^{13}C NMR ($CDCl_3$, 100.6 MHz):** δ = 157.3, 149.4, 136.0, 122.3, 119.7, 82.1 (d, *J* = 170.5 Hz), 29.2 (d, *J* = 21.8 Hz); **^{19}F NMR ($CDCl_3$, 376.5 MHz):** δ = –212.23 (tt, *J* = 47.1, 18.6 Hz, 1F); **HRMS (ESI+)** for $(M+H)^+$ $C_7H_9FNS^+$ (m/z): calc. 158.0434; found 158.0438.

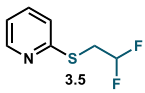

2-((2,2-Difluoroethyl)thio)pyridine (3.5). Following the general procedure **GP-1**, starting from K_2CO_3 (946 mg, 6.8 mmol), 2-mercaptopyridine (634 mg, 5.7 mmol), 2,2-difluoroethyl tosylate (1.35 g, 5.7 mmol) and DMF (5.7 mL); the pyridine derivative **3.5** (844 mg, 83%) was obtained as a black oil after purification by flash column chromatography (SiO_2, 1:9 Ethyl acetate/hexane).

^{1}H NMR ($CDCl_3$, 400 MHz): δ = 8.40 (d, *J* = 4.7 Hz, 1H), 7.49 (t, *J* = 7.8 Hz, 1H), 7.19 (d, *J* = 8.1 Hz, 1H), 7.01 (dd, *J* = 7.4, 4.9 Hz, 1H), 6.00 (tt, *J* = 57.1, 4.6 Hz, 1H), 3.58 (td, *J* = 15.0, 4.6 Hz, 2H); **^{13}C NMR ($CDCl_3$, 100.6 MHz):** δ = 156.3, 149.5, 136.3, 122.2, 120.1, 115.2 (t, *J* = 241.7 Hz); **^{19}F NMR ($CDCl_3$, 376.5 MHz):** δ = –115.18 (dt, *J* = 57.2, 15.5 Hz, 2F); **HRMS (ESI+)** for $(M+H)^+$ $C_7H_8F_2NS^+$ (m/z): calc. 176.0340; found 176.0342.

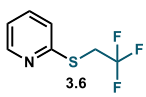

2-((2,2,2-Trifluoroethyl)thio)pyridine (3.6). Following the general procedure **GP-1**, starting from K_2CO_3 (859 mg, 6.2 mmol), 2-mercaptopyridine (575 mg, 5.2 mmol), 2,2,2-trifluoroethyl tosylate (1.32 g, 5.2 mmol) and DMF (5.2 mL); the pyridine derivative **3.6** (672 mg, 66%) was obtained as a pale yellow oil after purification by flash column chromatography (SiO_2, 1:9 Ethyl acetate/hexane).

^{1}H NMR ($CDCl_3$, 400 MHz): δ = 8.43 (d, *J* = 4.9 Hz, 1H), 7.51 (t, *J* = 7.8 Hz, 1H), 7.22 (d, *J* = 7.9 Hz, 1H), 7.04 (dd, *J* = 7.4, 5.0 Hz, 1H), 4.03 (q, *J* = 9.9 Hz,

2H); **^{13}C NMR ($CDCl_3$, 100.6 MHz):** δ = 154.6, 149.4, 136.5, 125.5 (q, *J* = 275.8 Hz), 122.4, 120.5, 30.97 (q, *J* = 33.6 Hz); **^{19}F NMR ($CDCl_3$, 376.5 MHz):** δ = –66.65 (t, *J* = 10.2 Hz, 3F); **HRMS (ESI+)** for $(M+H)^+$ $C_7H_7F_3NS^+$ (m/z): calc. 194.0246; found 194.0251.

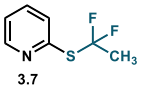
3.7

2-((1,1-Difluoroethyl)thio)pyridine (3.7). A 5 mL round-bottom flask, equipped with a magnetic stir bar, was charged with *O*-(2,2-difluoro-2-(pyridin-2-ylthio)ethyl) *S*-methyl carbonodithioate **3.12**, (400 mg, 1.42 mmol, 1.0 equiv), tributyltin hydride (575 μL, 2.13 mmol, 1.5 equiv), and azobisisobutyronitrile (AIBN) (35 mg, 0.21 mmol, 0.15 equiv). The flask was rapidly evacuated and backfilled with argon three times. Subsequently, anhydrous toluene (3 mL, 0.47 M) was added using a syringe. Then, the reaction mixture was heated to 90 °C, and left stirring 2 h. The mixture was then concentrated under reduced pressure and purified using preparative chromatography (SiO_2, 3:7 Et_2O/pentane) to afford **3.7** as a pale-yellow oil (30 mg, 12%).

^{1}H NMR (CD_2Cl_2, 400 MHz): δ = 8.68–8.49 (m, 1H), 7.69 (td, *J* = 7.7, 1.9 Hz, 1H), 7.59 (d, *J* = 8.0 Hz, 1H), 7.26 (ddd, *J* = 7.5, 4.8, 1.1 Hz, 1H), 2.08 (t, *J* = 17.3 Hz, 3H); **^{13}C NMR (CD_2Cl_2, 100.6 MHz):** δ = 152.8, 150.6, 137.5, 129.3 (t, *J* = 275.7 Hz), 128.2, 123.2, 27.0 (t, *J* = 25.5 Hz); **^{19}F NMR (CD_2Cl_2, 376.5 MHz):** δ = –65.6 (q, *J* = 17.2 Hz).

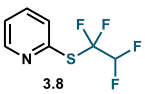
3.8

2-((1,1,2,2-Tetrafluoroethyl)thio)pyridine (3.8). A 50 mL round-bottom flask, equipped with a magnetic stir bar, was charged with potassium hydroxide (1.32 g, 23.5 mmol, 5.0 equiv) and 2-mercaptopyridine (526 mg, 4.7 mmol, 1.0 equiv). The flask was then evacuated and backfilled with argon three times. Subsequently, anhydrous acetonitrile (12 mL, 0.4 M) was added using a syringe. Then, a current of tetrafluoroethylene was bubbled into the solution for 15 min and the mixture was stirred overnight at room temperature. The mixture was then acidified with HCl, diluted with diethyl ether, washed with brine, and

dried over Na_2SO_4. Upon filtration, the organic layer was concentrated under reduced pressure and purified by flash column chromatography (SiO_2, 1:9 Ethyl acetate/hexane) to afford **3.8** as a pale-yellow oil (759 mg, 75%).

^{1}H NMR ($CDCl_3$, 400 MHz): δ = 8.55 (d, J = 4.6 Hz, 1H), 7.68 (t, J = 7.6 Hz, 1H), 7.51 (d, J = 7.9 Hz, 1H), 7.30–7.22 (m, 1H), 6.33 (tt, J = 53.8, 4.6 Hz, 1H); **^{13}C NMR ($CDCl_3$, 100.6 MHz):** δ = 150.5, 149.7 (t, J = 4.1 Hz), 137.5, 128.2, 123.5, 122.5 (tt, J = 286.6, 28.5 Hz), 109.5 (tt, J = 253.9, 34.6 Hz); **^{19}F NMR ($CDCl_3$, 376.5 MHz):** δ = –93.65 (m, 2F), –134.75 (dt, J = 53.8, 9.7 Hz, 2F); **HRMS (ESI+)** for $(M+H)^+$ $C_7H_6F_4NS^+$ (m/z): calc. 212.0152; found 212.0155.

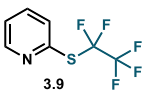

3.9

2-((Perfluoroethyl)thio)pyridine (3.9). A 25 mL round-bottom flask, equipped with a magnetic stir bar, was charged with dried potassium perfluoroacetate (1.01 g, 5.3 mmol, 1.2 equiv) and 2,2′-dipyridyldisulfide (0.87 g, 4.4 mmol, 1.0 equiv). The flask was then evacuated and backfilled with argon three times. Subsequently, anhydrous DMF (11 mL, 0.4 M) was added using a syringe. Then, the reaction mixture was stirred for 5 h at 145 °C. The mixture was diluted with diethyl ether, washed with brine and dried over Na_2SO_4. Upon filtration, the organic layer was concentrated under reduced pressure and purified by flash column chromatography (SiO_2, 1:9 Ethyl acetate/hexane) to afford **3.9** as a yellow oil (672 mg, 44%).

^{1}H NMR ($CDCl_3$, 400 MHz): δ = 8.63 (d, J = 4.8 Hz, 1H), 7.73 (t, J = 7.7 Hz, 1H), 7.65 (d, J = 7.9 Hz, 1H), 7.39–7.31 (m, 1H); **^{13}C NMR ($CDCl_3$, 100.6 MHz):** δ = 150.9, 147.6 (t, J = 2.9 Hz), 137.6, 130.8, 124.5, 120.6 (tq, J = 289.6, 41.0 Hz), 118.5 (qt, J = 286.5, 36.4 Hz); **^{19}F NMR ($CDCl_3$, 376.5 MHz):** δ = –82.86 (t, J = 3.5 Hz, 3F), –90.66 (m, 2F); **HRMS (ESI+)** for $(M+H)^+$ $C_7H_5F_5NS^+$ (m/z): calc. 230.0057; found 230.0064.

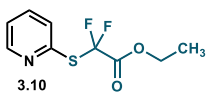

3.10

Ethyl 2,2-difluoro-2-(pyridin-2-ylthio)acetate (3.10). A 100 mL round-bottom flask, equipped with a magnetic stir bar, was charged with 2-mercaptopyridine (1.67 g, 15 mmol, 1.0 equiv) and cesium carbonate (9.77 g, 30 mmol, 2.0 equiv). The flask was then evacuated and backfilled with argon three times. Subsequently, anhydrous DMF (50 mL, 0.3 M) was added using a syringe, and the mixture was sparged with argon for 15 min. Next, ethyl bromodifluoroacetate (2.89 mL, 22.5 mmol, 1.5 equiv) was added and the reaction mixture was stirred overnight at room temperature. Then, the mixture was diluted with diethyl ether, extracted with brine several times, and dried over Na_2SO_4. Upon filtration, the organic layer was concentrated under reduced pressure, and purified by column chromatography (SiO_2, 1:9 ethyl acetate/hexane) to afford **3.10** as a yellow oil (2.45 g, 70%).

^{1}H NMR ($CDCl_3$, 400 MHz): δ = 8.51 (ddd, *J* = 4.9, 1.9, 0.9 Hz, 1H), 7.66 (td, *J* = 7.7, 1.9 Hz, 1H), 7.50 (dd, *J* = 7.9, 1.0 Hz, 1H), 7.37–7.19 (m, 1H), 4.32 (q, *J* = 7.1 Hz, 2H), 1.28 (td, *J* = 7.2, 0.8 Hz, 3H).; **^{13}C NMR ($CDCl_3$, 100.6 MHz):** δ = 161.8 (t, *J* = 31.7 Hz), 151.1, 150.3, 137.4, 127.6, 123.3, 123.2, 119.0 (t, *J* = 286.1 Hz), 63.8, 13.9; **^{19}F NMR ($CDCl_3$, 376.5 MHz):** δ = –82.3. (s, 1F).; **HRMS (ESI+)** for $(M+Na)^+$ $C_9H_9F_2NNaO_2S^+$ (m/z): calc. 256.0214; found 256.0212.

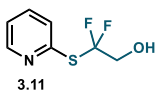

3.11

2,2-Difluoro-2-(pyridin-2-ylthio)ethan-1-ol (3.11). A 50 mL round-bottom flask, equipped with a magnetic stir bar, was charged with ethyl 2,2-difluoro-2-(pyridin-2-ylthio)acetate **3.10,** (2.45 g, 10.5 mmol, 1.0 equiv). The flask was then evacuated and backfilled with argon three times. Subsequently, anhydrous ethanol (25 mL, 0.42 M) was added using a syringe. Next, sodium borohydride (776 mg, 20.5 mmol, 2.0 equiv) was added at 0 °C, and the reaction mixture was stirred for 3 h in an ice bath. Then, the mixture was diluted with dichloromethane, extracted with brine, and dried over Na_2SO_4. Upon filtration, the organic layer was concentrated under reduced pressure, and purified by column

chromatography (SiO_2, from 5:95 to 20:80 ethyl acetate/hexane) to afford **3.11** as a yellow solid (1.49 g, 74%).

^{1}H NMR ($CDCl_3$, 400 MHz): δ = 8.54 (ddd, *J* = 4.9, 2.0, 0.9 Hz, 1H), 7.71 (td, *J* = 7.7, 1.9 Hz, 1H), 7.59 (dt, *J* = 7.9, 1.3 Hz, 1H), 7.30 (ddd, *J* = 7.5, 4.9, 1.3 Hz, 1H), 4.84 (bs, 1H), 3.98 (t, *J* = 12.1 Hz, 2H).; **^{13}C NMR ($CDCl_3$, 100.6 MHz):** δ = 151.0 (t, *J* = 4.6 Hz), 150.1, 138.0, 129.7 (t, *J* = 282.6 Hz), 129.2, 123.6, 65.4 (t, *J* = 31.2 Hz); **^{19}F NMR ($CDCl_3$, 376.5 MHz):** δ = –80.23 (t, *J* = 11.9 Hz); **HRMS (ESI+)** for $(M+H)^+$ $C_7H_8F_2NOS^+$ (m/z): calc. 192.0289; found 192.0287.

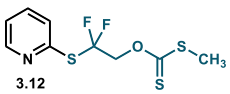

3.12

***O*-(2,2-Difluoro-2-(pyridin-2-ylthio)ethyl) *S*-methyl carbonodithioate (3.12).** A 10 mL round-bottom flask, equipped with a magnetic stir bar, was charged with 2,2-difluoro-2-(pyridin-2-ylthio)ethan-1-ol **3.11,** (382 mg, 2 mmol, 1.0 equiv). The flask was then evacuated and backfilled with argon three times. Subsequently, anhydrous THF (5 mL, 0.40 M) was added using a syringe. Next, sodium hydride 60% in weight (200 mg, 5 mmol, 2.5 equiv) was added at 0 °C, and the reaction mixture was stirred 1 h at room temperature. Then, the mixture was cooled down at 0 °C, and carbon disulfide (604 μL, 10 mmol, 5.0 equiv) was added with a syringe, and the mixture was left stirring for 2 h at room temperature. Next, the mixture was cooled down at 0 °C, and methyl iodide (250 μL, 4 mmol, 2.0 equiv) was added with a syringe, and left stirring for 2 h at room temperature. Then, the reaction was quenched with $NH_4Cl_{(aq)}$, diluted with dichloromethane, washed with brine, and dried over Na_2SO_4. Upon filtration, the organic layer was concentrated under reduced pressure, and purified by column chromatography (SiO_2, 1:9 ethyl acetate/hexane) to afford **3.12** as a red oil (453 mg, 81%).

^{1}H NMR ($CDCl_3$, 400 MHz): δ = 8.58 (dd, *J* = 4.8, 1.1 Hz, 1H), 7.67 (td, *J* = 7.7, 1.9 Hz, 1H), 7.55 (d, *J* = 7.9 Hz, 1H), 7.40–7.22 (m, 1H), 5.18 (t, *J* = 12.5 Hz, 2H), 2.59 (s, 3H).; **^{13}C NMR ($CDCl_3$, 100.6 MHz):** δ = 214.8, 151.1 (t, *J* = 3.9 Hz), 150.6, 137.5, 128.4, 127.5 (t, *J* = 281.7 Hz), 123.4, 72.2 (t, *J* = 29.5 Hz), 19.4;

^{19}F NMR ($CDCl_3$, 376.5 MHz): δ = –80.15 (t, J = 12.6 Hz); **HRMS (ESI+)** for $(M+H)^+$ $C_9H_{10}F_2NOS_3^+$ (m/z): calc. 281.9887; found 281.9882.

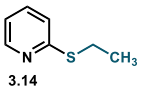
3.14

2-(Ethylthio)pyridine (3.14). A 25 mL round-bottom flask, equipped with a magnetic stir bar, was charged with 2-mercaptopyridine (700 mg, 6.3 mmol, 1.0 equiv) and potassium carbonate (1.04 g, 7.6 mmol, 1.2 equiv). The flask was then evacuated and backfilled with argon three times. Subsequently, anhydrous DMF (7 mL, 0.9 M) was added using a syringe, and the mixture was sparged with argon for 15 min. Next, ethyl iodide (0.5 mL, 6.3 mmol, 1.0 equiv) was added and the reaction mixture was stirred overnight at room temperature. Next, the crude was diluted with diethyl ether, washed with brine, and dried over Na_2SO_4. Upon filtration, the organic layer was concentrated under reduced pressure to afford pure **3.14** as a colorless oil (763 mg, 87%). The spectroscopic data are in agreement with those reported in the literature.[36]

^{1}H NMR ($CDCl_3$, 400 MHz): δ = 8.41 (ddd, *J* = 5.0, 1.9, 1.0 Hz, 1H), 7.48–7.41 (m, 1H), 7.14 (dt, *J* = 8.1, 1.0 Hz, 1H), 6.98–6.90 (m, 1H), 3.15 (q, *J* = 7.4 Hz, 2H), 1.36 (t, *J* = 7.4 Hz, 3H); **^{13}C NMR ($CDCl_3$, 100.6 MHz):** δ = 159.5, 149.5, 135.9, 122.2, 119.3, 24.5, 14.7.

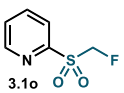
3.1o

2-((Fluoromethyl)sulfonyl)pyridine (3.1o). Following the general procedure **GP-3,** starting from pyridine **3.1** (143 mg, 1 mmol), $RuCl_3{\cdot}3H_2O$ (2 mg) and $NaIO_4$ (535 mg, 2.5 mmol); the pyridine derivative **3.1o** (158 mg, 90%) was obtained as a pale-yellow solid. The spectroscopic data are in agreement with those reported in the literature.[37]

^{1}H NMR ($CDCl_3$, 400 MHz): δ = 8.78 (ddd, *J* = 4.7, 1.6, 0.9 Hz, 1H), 8.15 (dt, *J* = 7.8, 1.0 Hz, 1H), 8.02 (td, *J* = 7.8, 1.7 Hz, 1H), 7.62 (ddd, *J* = 7.7, 4.7, 1.1 Hz, 1H),

[36] Heinz, B.; Balkenhohl, M.; Knochel, P. *Synthesis* **2019**, 4452.
[37] Zhao, Y.; Gao, B.; Hu, J. *J. Am. Chem. Soc.* **2012**, *134*, 5790.

5.52 (d, *J* = 46.9 Hz, 2H).; **^{13}C NMR ($CDCl_3$, 100.6 MHz):** δ = 154.1, 150.6, 138.5, 128.3, 123.7, 88.7 (d, J = 219.0 Hz); **^{19}F NMR ($CDCl_3$, 376.5 MHz):** δ = –213.6 (t, *J* = 46.9 Hz).

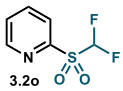
3.2o

2-((Difluoromethyl)sulfonyl)pyridine (3.2o). Following the general procedure **GP-3,** starting from pyridine **3.2** (300 mg, 1.9 mmol), $RuCl_3{\cdot}3H_2O$ (1 mg) and $NaIO_4$ (995 mg, 4.7 mmol); the pyridine derivative **3.2o** (316 mg, 85%) was obtained as a white solid after purification by flash column chromatography (SiO_2, 4:6 Ethyl acetate/hexane).

^{1}H NMR ($CDCl_3$, 400 MHz): δ = 8.82 (d, J = 4.4 Hz, 1H), 8.15 (d, J = 7.9 Hz, 1H), 8.04 (t, J = 7.8 Hz, 1H), 7.71–7.64 (m, 1H), 6.62 (t, J = 53.4 Hz, 1H); **^{13}C NMR ($CDCl_3$, 100.6 MHz):** δ = 152.7, 151.0, 138.7, 128.9, 125.1, 114.0 (t, J = 286.3 Hz); **^{19}F NMR ($CDCl_3$, 376.5 MHz):** δ = –124.45 (d, J = 53.6 Hz, 2F); **HRMS (ESI+)** for $(M+H)^+$ $C_6H_6F_2NO_2S^+$ (m/z): calc. 194.0082; found 194.0088.

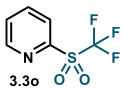
3.3o

2-((Trifluoromethyl)sulfonyl)pyridine (3.3o). Following the general procedure **GP-3**, pyridine **3.3** (300 mg, 1.7 mmol), $RuCl_3{\cdot}3H_2O$ (1 mg) and $NaIO_4$ (920 mg, 4.3 mmol); the pyridine derivative **3.3o** (304 mg, 86%) was obtained as a white solid after purification by flash column chromatography (SiO_2, 4:6 Ethyl acetate/hexane).

^{1}H NMR ($CDCl_3$, 400 MHz): δ = 8.90 (d, J = 4.5 Hz, 1H), 8.23 (d, J = 7.9 Hz, 1H), 8.08 (t, J = 7.8 Hz, 1H), 7.73 (dd, J = 7.8, 4.7 Hz, 1H); **^{13}C NMR ($CDCl_3$, 100.6 MHz):** δ = 151.4, 138.7, 129.5, 126.3, 119.8 (q, J = 326.9 Hz); **$CDCl_3$, 100.6 MHz):** δ =; **^{19}F NMR ($CDCl_3$, 376.5 MHz):** δ –75.60 (s, 3F); **HRMS (ESI+)** for $(M+H)^+$ $C_6H_5F_3NO_2S^+$ (m/z): calc. 211.9988; found 211.9986.

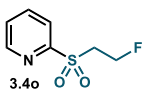
3.4o

2-((2-Fluoroethyl)sulfonyl)pyridine (3.4o). Following the general procedure **GP-3**, starting from pyridine **3.4** (300 mg, 1.9 mmol), $RuCl_3{\cdot}3H_2O$ (1 mg) and $NaIO_4$ (1.02 g, 4.8 mmol); the

pyridine derivative **3.4o** (309 mg, 83%) was obtained as a yellow solid after purification by flash column chromatography (SiO_2, 4:6 Ethyl acetate/hexane).

^{1}H NMR ($CDCl_3$, 400 MHz): δ = 8.74 (d, J = 4.7 Hz, 1H), 8.09 (d, J = 7.8 Hz, 1H), 7.97 (t, J = 7.8 Hz, 1H), 7.56 (dd, J = 7.7, 4.7 Hz, 1H), 4.85 (dt, J = 46.4, 5.7 Hz, 2H), 3.82 (dt, J = 21.9, 5.7 Hz, 2H); **^{13}C NMR ($CDCl_3$, 100.6 MHz):** δ = 157.4, 150.2, 138.3, 127.6, 122.0, 77.0 (d, J = 172.7 Hz), 52.5 (d, J = 21.8 Hz); **^{19}F NMR ($CDCl_3$, 376.5 MHz):** δ = –221.35 (tt, J = 46.5, 21.9 Hz, 1F); **HRMS (ESI+)** for $(M+H)^+$ $C_7H_9FNO_2S^+$ (m/z): calc. 190.0333; found 190.0341.

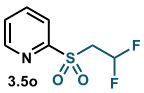

2-((2,2-Difluoroethyl)sulfonyl)pyridine (3.5o). Following the general procedure **GP-2**, starting from pyridine **3.5** (300 mg, 1.7 mmol), ammonium molybdate tetrahydrate (105 mg, 0.09 mmol), H_2O_2 (525 μL, 5.1 mmol) and MeOH (5.2 mL); the pyridine derivative **3.5o** (308 mg, 78%) was obtained as a white solid after purification by flash column chromatography (SiO_2, 4:6 Ethyl acetate/hexane).

***R**f*: (4:6 Ethyl acetate/hexane): 0.33; **^{1}H NMR ($CDCl_3$, 400 MHz):** δ = 8.76 (d, J = 4.6 Hz, 1H), 8.08 (d, J = 7.9 Hz, 1H), 7.99 (t, J = 7.8 Hz, 1H), 7.59 (dd, J = 7.7, 4.7 Hz, 1H), 6.26 (tt, J = 54.8, 4.6 Hz, 1H), 4.00 (td, J = 13.6, 4.6 Hz, 2H); **^{13}C NMR ($CDCl_3$, 100.6 MHz):** δ = 156.8, 150.4, 138.5, 128.0, 122.0, 111.7 (t, J = 243.6 Hz), 55.0 (t, J = 25.1 Hz); **^{19}F NMR ($CDCl_3$, 376.5 MHz):** δ = –115.11 (dt, J = 55.0, 13.7 Hz, 2F); **HRMS (ESI+)** for $(M+H)^+$ $C_7H_8F_2NO_2S^+$ (m/z): calc. 208.0238; found 208.0247.

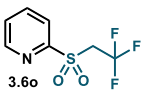

2-((2,2,2-Trifluoroethyl)sulfonyl)pyridine (3.6o). Following the general procedure **GP-2**, starting from pyridine **3.6** (300 mg, 1.6 mmol), ammonium molybdate tetrahydrate (96 mg, 0.08 mmol), H_2O_2 (476 μL, 4.7 mmol) and MeOH (5.2 mL); the pyridine derivative **3.6o** (329 mg, 90%) was obtained as a white solid after purification by flash column chromatography (SiO_2, 4:6 Ethyl acetate/hexane).

^{1}H NMR ($CDCl_3$, 400 MHz): δ = 8.76 (d, J = 4.4 Hz, 1H), 8.12 (d, J = 7.9 Hz, 1H), 8.01 (t, J = 7.8 Hz, 1H), 7.65–7.57 (m, 1H), 4.31 (qt, J = 9.0, 1.1, 2H); **^{13}C NMR ($CDCl_3$, 100.6 MHz):** δ = 156.3, 150.4, 138.6, 128.2, 122.2, 121.2 (q, J = 276.9 Hz), 53.4 (q, J = 31.8 Hz); **^{19}F NMR ($CDCl_3$, 376.5 MHz):** δ = –61.11 (t, J = 9.0 Hz, 3F); **HRMS (ESI+)** for $(M+H)^+$ $C_7H_7F_3NO_2S^+$ (m/z): calc. 226.0144; found 226.0159.

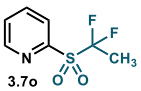

3.7o

2-((1,1-Difluoroethyl)sulfonyl)pyridine (3.7o). Following the general procedure **GP-3,** starting from pyridine **3.7** (15 mg, 0.09 mmol), $RuCl_3{\cdot}3H_2O$ (0.3 mg) and $NaIO_4$ (45.8 mg, 0.214 mmol); the pyridine derivative **3.7o** was obtained as a yellow solid after workup (18 mg, 99%).

^{1}H NMR ($CDCl_3$, 400 MHz): δ = 9.00–8.75 (m, 1H), 8.18 (d, *J* = 7.9 Hz, 1H), 8.04 (td, *J* = 7.8, 1.7 Hz, 1H), 7.67 (ddd, *J* = 7.7, 4.7, 1.1 Hz, 1H), 2.12 (t, *J* = 18.7 Hz, 3H); **^{13}C NMR ($CDCl_3$, 100.6 MHz):** δ = 152.3, 151.1, 138.4, 128.8, 126.5, 124.7 (t, *J* = 284.7 Hz), 17.7 (t, *J* = 21.5 Hz).; **^{19}F NMR ($CDCl_3$, 376.5 MHz):** δ = –95.6 (q, *J* = 18.6 Hz).

3.8o

2-((1,1,2,2-Tetrafluoroethyl)sulfonyl)pyridine (3.8o). Following the general procedure **GP-3**, starting from pyridine **3.8** (300 mg, 1.4 mmol), $RuCl_3{\cdot}3H_2O$ (1 mg) and $NaIO_4$ (760 mg, 3.5 mmol); the pyridine derivative **3.8o** (339 mg, 97%) was obtained as a white solid after purification by flash column chromatography (SiO_2, 4:6 Ethyl acetate/hexane).

^{1}H NMR ($CDCl_3$, 400 MHz): δ = 8.90–8.84 (m, 1H), 8.19 (d, J = 7.8 Hz, 1H), 8.08 (t, J = 7.6 Hz, 1H), 7.76–7.68 (m, 1H), 6.39 (tt, J = 52.1, 5.8 Hz, 1H); **^{13}C NMR ($CDCl_3$, 100.6 MHz):** δ = 151.8, 151.2, 138.9, 129.6, 126.3, 115.1 (tt, J = 298.2, 27.0 Hz), 107.8 (tt, J = 256.3, 28.3 Hz); **^{19}F NMR ($CDCl_3$, 376.5 MHz):** δ = –119.20 (m, 2F), –135.01 (dt, J = 52.1, 8.3 Hz, 2F); **HRMS (ESI+)** for $(M+H)^+$ $C_7H_6F_4NO_2S^+$ (m/z): calc. 244.0050; found 244.0055.

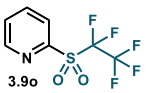

2-((Perfluoroethyl)sulfonyl)pyridine (3.9o). Following the general procedure **GP-3**, starting from pyridine **3.9** (300 mg, 1.3 mmol), $RuCl_3 \cdot 3H_2O$ (1 mg) and $NaIO_4$ (700 mg, 3.3 mmol); the pyridine derivative **3.9o** (308 mg, 89%) was obtained as a white solid after purification by flash column chromatography (SiO_2, 4:6 Ethyl acetate/hexane).

^{1}H NMR ($CDCl_3$, 400 MHz): δ = 8.90 (d, J = 4.8 Hz, 1H), 8.22 (d, J = 7.9 Hz, 1H), 8.09 (t, J = 7.8 Hz, 1H), 7.77–7.70 (m, 1H); **^{13}C NMR ($CDCl_3$, 100.6 MHz):** δ = 151.6, 151.4, 138.7, 129.6, 126.8, 116.0 (m), 113.1 (m); **^{19}F NMR ($CDCl_3$, 376.5 MHz):** δ = –78.08 (s, 3F), –114.80 (s, 2F); **HRMS (ESI+)** for $(M+H)^+$ $C_7H_5F_5NO_2S^+$ (m/z): calc. 261.9956; found 261.9962.

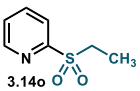

2-(Ethylsulfonyl)pyridine (3.14o). Following the general procedure **GP-2**, starting from pyridine **3.14** (250 mg, 1.8 mmol), ammonium molybdate tetrahydrate (111 mg, 0.09 mmol), H_2O_2 (551 μL, 4.7 mmol) and MeOH (9 mL); the pyridine derivative **3.14o** (277 mg, 90%) was obtained as a yellowish solid after workup. The spectroscopic data are in agreement with those reported in the literature.[38]

^{1}H NMR ($CDCl_3$, 400 MHz): δ = 8.85–8.69 (m, 1H), 8.08 (d, *J* = 7.8 Hz, 1H), 7.96 (td, *J* = 7.8, 1.6 Hz, 1H), 7.55 (dd, *J* = 7.1, 4.9 Hz, 1H), 3.41 (q, *J* = 7.5 Hz, 2H), 1.28 (t, *J* = 7.5 Hz, 3H).; **^{13}C NMR ($CDCl_3$, 100.6 MHz):** δ = 156.5, 150.3, 138.2, 127.5, 122.4, 46.4, 6.8.

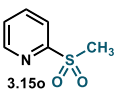

2-(Methylsulfonyl)pyridine (3.15o). Following the general procedure **GP-2**, starting from pyridine **3.15** (225 mg, 1.8 mmol), ammonium molybdate tetrahydrate (111 mg, 0.09 mmol), H_2O_2 (551 μL, 4.7 mmol) and MeOH (9 mL); the pyridine derivative **3.15o** (221 mg, 78%) was obtained as a yellowish solid after workup. The spectroscopic data are in agreement with those reported in the literature.[39]

[38] Von Wolff, N.; Char, J.; Frogneux, X.; Cantat, T. *Angew. Chem. Int. Ed.* **2017**, *56*, 5616.

^{1}H NMR ($CDCl_3$, 400 MHz): δ = 8.72 (ddd, *J* = 4.7, 1.5, 0.9 Hz, 1H), 8.07 (dt, *J* = 7.9, 1.0 Hz, 1H), 7.96 (td, *J* = 7.8, 1.7 Hz, 1H), 7.55 (ddd, *J* = 7.6, 4.7, 1.2 Hz, 1H), 3.21 (s, 3H); **^{13}C NMR ($CDCl_3$, 100.6 MHz):** δ = 157.9, 150.1, 138.4, 127.5, 121.1, 40.1.

3.5.3 General procedure for log*P* determination using ^{19}F NMR

A protocol developed by the group of Linclau[Error! Bookmark not defined.] was f ollowed for the determination of the log*P* values of the 2-substituted pyridines. The 4-step process was replicated three times for each compound:

1) Partitioning: to a 10 mL pear-shaped flask was added 2 mL of 1-octanol, 2-substituted pyridine (1–10 mg), trifluoroethanol (5 μl), and 2 mL of phosphate buffer (pH = 7.4). The resulting mixture was stirred at 25 °C for 2 h controlling the temperature by an immersion cooler, then it was left to stand at 25°C overnight to enable complete phase separation.

2) Sample preparation: using a 1 mL disposable syringe an aliquot of 0.6 mL was carefully taken from the aqueous or the 1-octanol phase. Next, the needle was carefully wiped with a dry tissue and the aliquot was placed into an NMR tube, followed by addition of 0.1 mL acetone-d_6. The NMR tubes were sealed using a rubber septum stopper and shaken to obtain a homogenous solution for NMR measurement. When taking an aliquot of the lower water phase, to avoid the contamination of the syringe with the upper octanol phase, 0.05 mL of air was taken into syringe before putting the needle into the solution, and while immersing it through the upper octanol layer, the air was gently pushed out. Upon reaching the water phase, all air bubbles are pushed out of the syringe, the aliquot taken, and the needle quickly removed from the solution. Then a small amount of water phase was discarded (to ensure all traces of octanol are out of the needle, leaving 0.6 mL sample in the syringe.

---

[39] Laudadio, G.; Straathof, N. J.; Lanting, M. D.; Knoops, B.; Hessel, V.; Noël, T. *Green Chem.* **2017**, *19*, 4061.

3) NMR measurement: fluorine ($^{19}F\{1H\}$ NMR) nuclear magnetic resonance spectra were recorded on a Varian Mercury spectrometer or a Bruker Avance Ultrashield (376.5 MHz for ^{19}F NMR). Parameters used in the determination of lipophilicities were obtained from the experiments carried out by Linclau and co-workers.[Error! Bookmark not defined.] First, the sealed tube was i nserted to the NMR spectrometer and following automatic locking and gradient shimming, a simple ^{19}F spectrum was recorded on the non-spinning sample to assess the required spectral width (SW) and frequency offset point (O1P). The O1P is centered between the two diagnostic F signals and the spectral width (SW) is left at 200 ppm (it can be reduced if better S/N ratio is required). Then, the 90° pulse was measured with the automated pulsecal routine obtaining a power (PW) of 16 μ s. The measured 90° pulse, SW and O1P were transferred into the inversion-recovery experiment. For practical purposes it is recommended to use a D1 of 30 sec for the octanol sample and of 60 sec for the water sample as pulse delay, given the D1 value should be greater than 5*T1 for quantitative integration. The number of transients (NS) is selected or each sample to afford a suitable signal to noise ratio (SNR should be > 250).

4) Data processing: data were processed using Mestre Nova NMR software. The obtained FID file was reprocessed using following conditions: WFunction (LB = 2, Exponential), Zero Filling (increasing points from 65536 to 262144) and then Fourier transform, followed by phasing with mouse and auto baseline correction. The integration ratio was obtained by manual integration.

3.5.4 General procedure for log*P* determination using HPLC-UV

A protocol described by the group of Ràfols[19] was followed for the determination of the log*P* values of the non-fluorinated pyridines. The 4-step process was replicated three times for each compound:

1) Stock solution preparation: in a 12 ml vial 15 mg of the pyridine was charged. Then, 6 mL of phosphate buffer pH = 7.4 was added, and the mixture was vigorously shaken for 2 h. An aliquot of this stock solution was measured by HPLC-UV.

2) Partitioning: three partitioning experiments were carried out for each compound. To prepare an experiment, in a vial containing a magnetic stir bar, a known amount of the stock solution was introduced followed by another known amount of 1-octanol. Next, the biphasic mixture was stirred for 2 h and left to stand overnight to allow phase partition. For the selection of the different volume ratios, it was followed Ràfols[19] recommendations, although 1:1, 10:1, and 1:10 octanol:stock solution were usually employed.

3) Sample preparation and measurement: to prepare the sample, 0.1 ml of the aqueous phase was taken and introduced in a 2 mL vial, following the precautions described in the previous section. The samples were then analyzed with the same HPLC-UV method than the stock solution. The log*P* value was obtaining by comparing the initial amount of pyridine in the aqueous phase before and after partitioning, taking into consideration the volume rates.[19]

3.5.5 General procedure for *p*K_a determination using NMR

A protocol developed by the group of Leito[Error! Bookmark not defined.] was f ollowed for the determination of the log*P* values of fluorinated 2-substituted pyridines using ^{19}F NMR. For the non-fluorinated ones, a similar protocol developed by the group of Gift[Error! Bookmark not defined.] using ^{1}H NMR was followed.

1) Aqueous solutions: 11 aqueous stock solutions (10 mL) different *p*K_a (from –1 to 12) were prepared using HCl, NaOH, Na_2CO_3, and MiliQ water.

2) Sample preparation: in an NMR tube, a small amount of the pyridine of interest was introduced (~1 mg), followed by 0.5 mL of a given pH aqueous solution. Next, the tube was caped and shaken vigorously, and the

pH of the resulting solution was measured inside the tube with a pH-meter with an NMR-tube probe. This procedure was repeated for all the aqueous solutions to have a battery of NMR tubes at different pH values. If needed, additional solutions were prepared to ensure a continuum in the pH values.

3) Sample measurement: for ^{19}F NMR measurements, a 3 mm NMR tube containing a solution of 8 mg of KF in 1 mL of D_2O was inserted into the NMR tube of interest to serve as external standard. Next a standard ^{19}F NMR experiment was recorded to determine the chemical shifts of the external standard and the sample of interest. For the ^{1}H method, the same protocol was applied changing the external standard for 5 μL of trifluoroethanol instead of KF. The battery of NMR samples at different pH values were all measured.

4) Data processing: using MestreNova NMR software, the chemical shifts of the pyridines were determined. For ^{19}F NMR experiments, the KF reference was set to –125.00 ppm, and the closest ^{19}F signal of the pyridine was chosen for the chemical shift determination. For ^{1}H NMR experiments, the trifluoroethanol reference (CF_3CH_2OH) was set to 3.14 ppm, and the methyl signals of the nonfluorinated pyridines were chosen for the chemical shift determination. Next, the selected signal for each pyridine was plotted against the respective pH value of the measured solution. Using Prism GraphPad software, a sigmoidal curve was adjusted and the second derivate was performed to obtain the pK_a value of the given pyridine.

CHAPTER IV

DEVELOPMENT OF ELECTROPHILIC THIOPOLIFLUOROALKYLATING REAGENTS

UNIVERSITAT ROVIRA I VIRGILI
REAGENTS AND METHODOLOGIES FOR THE INTRODUCTION OF THIOFLUOROALKYL AND FLUOROSULFUR MOTIFS
Miguel Bernús Pérez

4.1 Introduction

In the previous chapter of this thesis (Chapter III: Evaluation of physicochemical properties of thiofluoroalkyl fragments), SR_F motifs were identified as useful fragments for tuning the lipophilic and acid-base properties of organic molecules. However, the synthetic methods required to access these compounds were not explained in detail. This introduction aims to provide an overview of the methodologies and reagents covered in the literature for forging or installing these thiofluoroalkyl motifs.

4.1.1. The preparation of SR_F compounds

Across the family of thiofluoroalkyl (SR_F) fragments, the thiotrifluoromethyl substituent has received substantially greater attention compared with thiodifluoromethyl and thio(mono)fluoromethyl groups (Figure 4.1).[1,2,3]

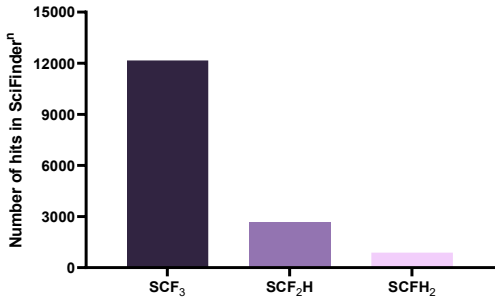

Figure 4.1. Number of total hits of trifluromethylthiolation, difluromethylthiolation, and fluoromethylthiolation in the SciFinder^n database (March 2023).[1]

[1] SciFinder^n Database, March 2023. Total hits correspond to all document type in the database.
[2] Xu, X.-H.; Matsuzaki, K.; Shibata, N. *Chem. Rev.* **2014**, *115*, 731.
[3] Toulgoat, F.; Alazet, S.; Billard, T. *Eur. J. Org. Chem.* **2014**, *12*, 2415.

Consequently, there is a large library of methods for the preparation of SCF_3-containing compounds that, in most cases, can be translated into their lower-fluorinated counterparts.[4,5] To have a panoramic view of the available methods, we can classify them according to the disconnections applied to prepare the most general -SCF_3 motif (Figure 4.2).

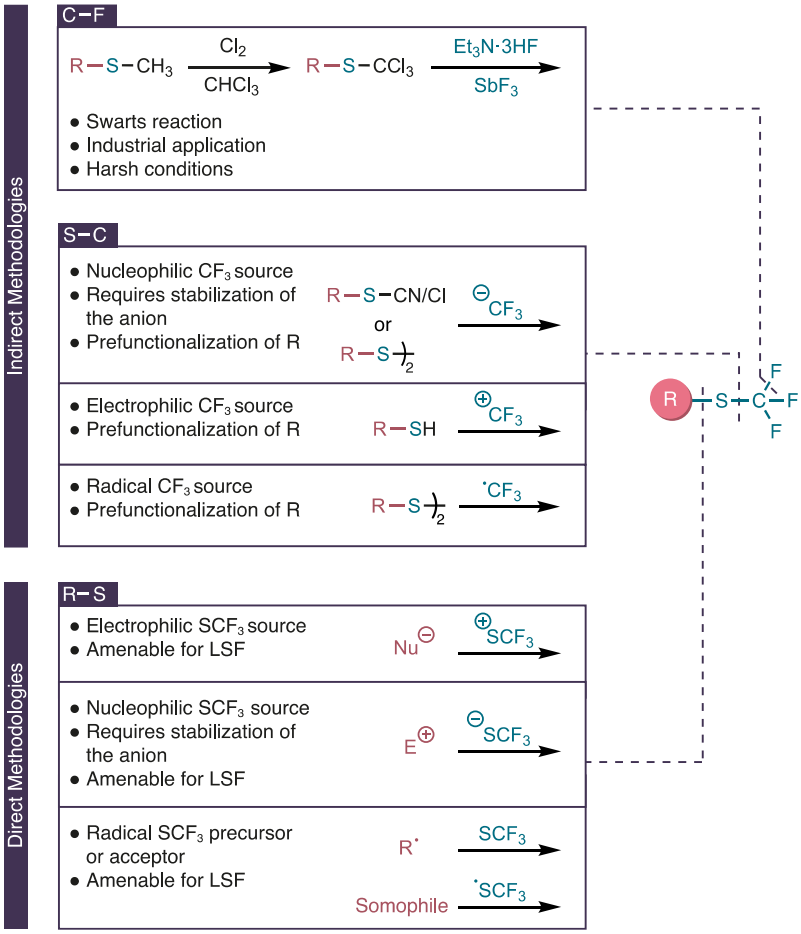

Figure 4.2. Possible disconnections to construct SCF_3-substituted molecules and the methodology available for each transformation.

[4] Xu, X.-H.; Matsuzaki, K.; Shibata, N. *Chem. Rev.* **2014**, *115*, 731.

[5] Xiao, X.; Zheng, Z.-T.; Li, T.; Zheng, J.-L.; Tao, T.; Chen, L.-M.; Gu, J.-Y.; Yao, X.; Lin, J.-H.; Xiao, J.-C. *Synthesis* **2019**, *52*, 197.

4.1.2 Indirect methods for the preparation of SR_F compounds

4.1.2.1 C-F bond-forming methodologies

Considering the disconnection of the C–F bond (Figure 4.2, upper panel), only methods based on chlorination and subsequent nucleophilic displacement by the fluoride anion are encountered. Focusing on the second step, the reaction usually involves heating a mixture of a trichloromethyl sulfide with anhydrous HF or SbF_3.[6] As a result of the reaction setup and the use of corrosive HF, this methodology is restricted to industrial use.[7] Moreover, the harsh conditions are not compatible with most functional groups, which limits this reaction to simple arene substrates.[8] Regarding other fluoroalkyl chains, their preparation is restricted to the number of chlorine atoms of the starting precursor.[6]

4.1.2.2 S-CF_3 bond-forming methodologies

On the other hand, the forgery of the S–CF_3 bond presents a wider variety of methodologies compared to the previous formation of the C–F bond (Figure 4.2, middle panel). Intrinsically, this disconnection is more interesting because it enables the functionalization of sulfur groups with different fluoroalkyl chains provided the adequate precursors are available. However, this methodology is limited by the requirement for previous installation of a sulfur handle in the parent molecule.

The reactions for the formation of S–R_F bonds can be classified in three categories depending on the nature of the source of CF_3: electrophilic, nucleophilic, and radical (Figure 4.3).

---

[6] V. N. Boiko, *Beilstein J. Org. Chem.* **2010**, *6*, 880.

[7] F. Leroux, P. Jeschke, M. Schlosser, *Chem. Rev.* **2005**, *105*, 827.

[8] E. A. Nodiff, S. Lipschutz, P. N. Craig, M. Gordon, *J. Org. Chem.* **1960**, *25*, 60.

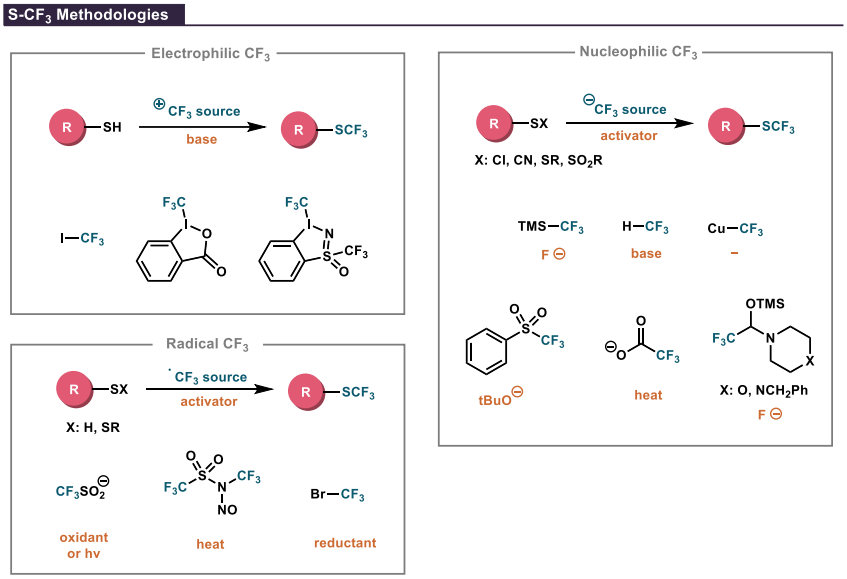

Figure 4.3. Reported methodologies for the trifluoromethylation of sulfur handles.

Under basic conditions, thiolate anions can perform nucleophilic substitutions in CF_3-electrophilic reagents such as trifluoromethyl iodide[9] or hypervalent iodine Togni reagents (Figure 4.3, upper left panel).[10] The main problem with these reactions is that most of the small iodopolyfluoroalkyl chains are ozone depleting gases, and that there are not many *Togni-like* reagents for the incorporation of different fluoroalkyl chains more than CF_3.

Reversing the polarity of the transformation, we encounter the nucleophilic strategies. In this case the sulfur handle must be electrophilic, for which umpolung starting materials such as sulfenyl halides, sulfenyl cyanates, and disulfides can be used (Figure 4.3, right panel). As the nucleophilic partner, trifluoromethyl anions can be generated in situ in solution or stabilized as organometallic complexes.[11] Regarding the *in situ generated* species, Prakash reagent ($TMSCF_3$) is one of the most widely used.

---

[9] Harsányi, A.; Dorkó, É.; Csapó, Á.; Bakó, T.; Peltz, C.; Rábai, J. *J. Fluor. Chem.* **2011**, *132*, 1241.

[10] (a) Kieltsch, I.; Eisenberger, P.; Togni, A. *Angew. Chem. Int. Ed.* **2007**, *46*, 754. (b) Kalim, J.; Duhail, T.; Le, T.-N.; Vanthuyne, N.; Anselmi, E.; Togni, A.; Magnier, E. *Chem. Sci.* **2019**, *10*, 10516.

[11] Langlois, B. R.; Billard, T. *Synthesis* **2003**, *2*, 185.

Its activation by a fluoride salt releases the CF_3 anion into the reaction medium to perform a nucleophilic substitution at the sulfur atom.[12] This strategy has also been used with similar reagents reported by Langlois.[13] On the same line, fluoroform can be deprotonated under basic conditions to yield the desired nucleophile.[14] Other strategies regard extrusion of the CF_3 anion as leaving group[15] or its formation by decarboxylation of metal salts.[16] On the other hand, stable 'ligandless' $CuCF_3$ organometallic species can be used directly as a nucleophile.[17] Although nucleophilic methods are more abundant, precursors of different fluoroalkyl anions are scarce or not compatible with the reported procedures.[18]

Finally, the trifluoromethylation of sulfur handles can be approached by radical means (Figure 4.3, lower left panel). In this sense, the Langlois reagent (CF_3SO_2Na) can provide CF_3 radicals in the presence of suitable oxidants or UV irradiation.[19] Those radicals can engage several reaction manifolds to forge new S–CF_3 bonds. In 1986, Umemoto reported a CF_3 radical precursor reagent that could trigger the same transformations by thermal activation.[20] Trifluoromethyl bromide can also be a radical precursor by using suitable reductant reagents.[21]

---

[12] (a) Movchun, V. N.; Kolomeitsev, A. A.; Yagupolskii, Y. L. *J. Fluor. Chem.* **1995**, *70*, 255. (b) Billard, T.; Langlois, B. R. *Tetrahedron Lett.* **1996**, *37*, 6865. (c) Billard, T.; Large, S.; Langlois, B. R. *Tetrahedron Lett.* **1997**, *38* (1), 65.

[13] Blond, G.; Billard, T.; Langlois, B. *Tetrahedron Letters* **2001**, *42*, 2473.

[14] (a) Russell, J.; Roques, N. *Tetrahedron* **1998**, *54*, 13771. (b) Large, S.; Roques, N.; Langlois, B. R. *J. Org. Chem.* **2000**, *65*, 8848.

[15] Prakash, G. K. S.; Hu, J.; Olah, G. A. *Org. Lett.* **2003**, *5*, 3253.

[16] Quiclet-Sire, B.; Saicic, R. N.; Zard, S. Z. *Tetrahedron Lett.* **1996**, *37*, 9057.

[17] Potash, S.; Rozen, S. *J. Fluor. Chem.* **2014**, *168*, 173.

[18] In our laboratory we have tried CuC_2F_5 as nucleophile against R-SCN compounds without success.

[19] (a) Billard, T.; Roques, N.; Langlois, B. R. *J. Org. Chem.* **1999**, *64*, 3813. (b) Pooput, C.; Dolbier, W. R.; Médebielle, M. *J. Org. Chem.* **2006**, *71*, 3564.

[20] Umemoto, T.; Ando, A. *Bull. Chem. Soc. Jpn.* **1986**, *59*, 447.

[21] (a) Wakselman, C.; Tordeux, M.; Clavel, J.-L.; Langlois, B. *J. Chem. Soc., Chem. Commun.* **1991**, *15*, 9. (b) Koshechko, V.; Kiprianova, L.; Fileleeva, L. *Tetrahedron Lett.* **1992**, *33*, 6677.

In general, there is a broad range of protocols to construct the S–CF_3 bond. However, most of them rely on low-boiling-point or sensitive reagents, which need external activators. Most importantly, this strategy is not compatible with divergent synthesis, as the parent molecule must bear a preinstalled sulfur handle.

4.1.3 Direct methods for the preparation of SR_F compounds

In contrast to indirect strategies, the straightforward introduction of thiofluoroalkyl motifs has gained momentum over the past 10 years (Figure 4.4).[1]

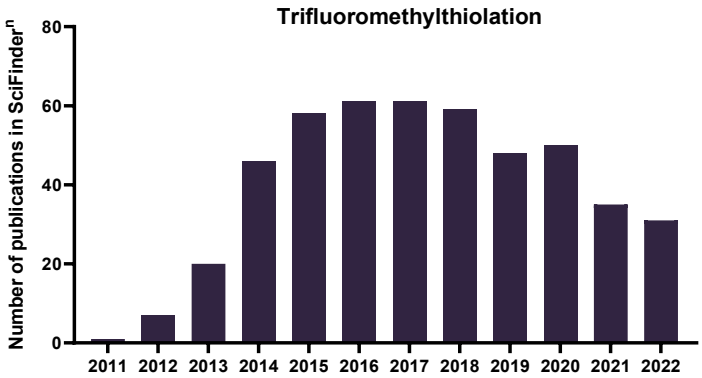

Figure 4.4. Number of hits of "trifluromethylthiolation" publications since 2011 in the SciFinder^n database.[1]

The blooming of new protocols responds to the need for more convenient strategies to install thiofluoroalkyl motifs. In this direction, these protocols are more appealing to chemists and outstrip indirect methods for different reasons.

First, most of the methodologies offer the desired transformations under mild conditions. Most importantly, the chemical community has created an extensive toolbox of reagents, additives, and catalysts that can practically introduce thiofluoroalkyl motifs in multiple architectures. These protocols can functionalize carbon-reacting centers but also heteroatoms such as

nitrogen, sulfur, or oxygen, among others covering most of the chemical space.[22]

This is crucial as most of the developed methodologies are compatible with late-stage functionalization (LSF) of complex organic structures. This becomes helpful for the discovery of new active ingredients in diverse-oriented synthesis (DOS) and other derivatization protocols where a library of compounds must be made from an elaborated parent molecule.

4.1.3.1 Thiofluoroalkylating reagents

The sources of thiofluoroalkyl motifs are the key elements of the direct SRF-installing protocols. At first sight, the fluoroalkyl thiols could be seen as potential reagents. However, these species are not stable under basic conditions. For example, trifluoromethylthiol decomposes upon deprotonation to form difluorothiophosgene, which is an extremely reactive compound (Scheme 4.1).[23]

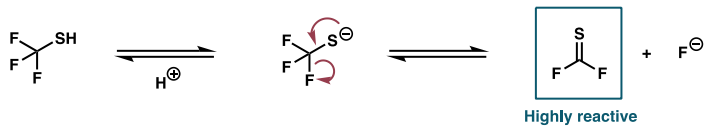

Scheme 4.1. Decomposition of trifluoromethylthiol by α-fluoride elimination.

In addition, the high acidity of the RFS–H bond facilitates this equilibrium. It must be pointed out that the thiol and the byproduct formed are not only unpleasantly smelly, but also display acute toxicity.[24] There are limited reports in which thiols are employed as reagents in thiofluoroalkylation,

[22] (a) Liu,H.; Hangming, G.; Shen, Q. Reagents for the Direct Trifluoromethylthiolation. In *Emerging Fluorinated Motifs: Synthesis, Properties and Applications*, 1st edition; Ma, J.-A.; Cahard, D.; Wiley-VCH Verlag GmbH & Co. KGaA: Weinheim, Germany, 2020; pp 309-341. (b) Besset, T.; Poisson, T. Extension to the SCF_2H, SCH_2F, and SCF_2R Motifs (R = $PO(OEt)_2$, CO_2R, Rf). In *Emerging Fluorinated Motifs: Synthesis, Properties and Applications*, 1st edition; Ma, J.-A.; Cahard, D.; Wiley-VCH Verlag GmbH & Co. KGaA: Weinheim, Germany, 2020; pp 449-475.

[23] Haszeldine, R. N.; Kidd, J. M. *J. Chem. Soc.*, **1955**, *0*, 3871.

[24] Stump, E. C.; *Chem. Eng. News* **1967**, *45*, 44.

which rely on harsh radical means to perform thiol-ene additions.[25] However, these protocols install both the H and the SR_F in the final molecule and require strong UV irradiation.

To overcome these intrinsic issues associated with thiols, two strategies have been adopted: umpolung of the sulfur atom, and stabilization of the thiolate anion. Both approaches minimize of the electronic density at the sulfur and thus inhibit α-fluoride elimination. These solutions have been implemented in numerous reagents of different nature.

The first reagents employed following these strategies were F_3CSCl, F_3CSSCF_3, and $Hg(SCF_3)_2$ (Figure 4.5).

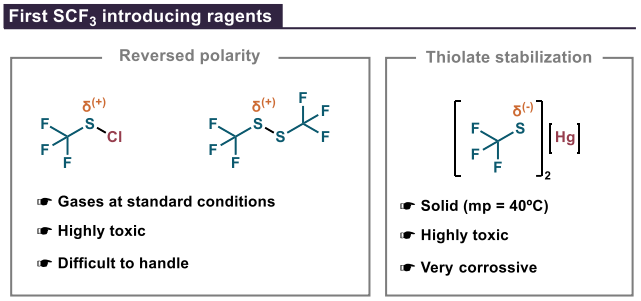

Figure 4.5. First disclosed thiotrifluoromethylating reagents.

These compounds represent the first generation of thiotrifluoromethylating reagents. Although they show good reactivity, their toxicity and difficult handling are drawbacks which have restricted their application.[26] Surprisingly, $Hg(SCF_3)_2$ was used as transmetallating agent from 1959 up to 1975 when the direct synthesis of the most benign $CuSCF_3$ was disclosed.[27] On the other hand, F_3CSCl was used almost exclusively from 1960 until 2009. From that year on, this chemistry experienced a *Renaissance*

[25] Harris, J. F.; Stacey, F. W. *J. Am. Chem. Soc.* **1961**, *83*, 840.
[26] Man, E. H.; Coffman, D. D.: Muetterties, E. L. *J. Am. Chem. Soc.* **1959**, *81*, 3575.
[27] Yagupolskii, L. M.; Kondratenko, N. V.; Sambur, V. P. *Synthesis* **1975**, *11*, 721.

as the endeavors of many research groups focused on the development of better reagents for the introduction of thiofluoroalkyl chains.[3]

The classification of these *new* reagents is often found according to their reactivity in electrophilic, nucleophilic, and radical categories. Nevertheless, this can be misleading, since some reagents behave as an SR_F source in multiple and complementary reaction manifolds.[28] For this reason, in this introduction, a classification with regard to its chemical structure is chosen. Despite advances in recent years, most thiotrifluoromethylating agents serve to introduce the SCF_3 moiety (Figure 3.6),[29] followed in number by SCF_2H[30]

---

[28] Glenadel, Q.; Bordy, M.; Alazet, S.; Tlili, A.; Billard, T. *Asian J. Org. Chem.* **2016**, *5*, 428.

[29] (a) Haas, A.; Möller, G. *Chem. Ber.*, **1996**, *129*, 1383. (b) Munavalli, S.; Rohrbaugh, D. K.; Rossman, D. I.; Berg, F. J.; Wagner, G. W.; Durst, H. D. *Synth. Commun.* **2000**, *30*, 2847. (c) Xu, C.; Ma, B.; Shen, Q. *Angew. Chem. Int. Ed.* **2014**, *53*, 9316. (d) Ferry Aurélien; Billard, T.; Langlois, B. R.; Bacqué Eric. *J. Org. Chem.* **2008**, *73*, 9362. (e) Ferry, A.; Billard, T.; Langlois, B. R.; Bacqué, E. *Angew. Chem., Int. Ed.* **2009**, *48*, 8551. (f) Bonazaba Milandou, L. J. C.; Carreyre, H.; Alazet, S.; Greco, G.; Martin-Mingot, A.; Nkounkou Loumpangou, C.; Ouamba, J.-M.; Bouazza, F.; Billard, T.; Thibaudeau, S. *Angew. Chem. Int. Ed.* **2017**, *56*, 169. (g) Alazet, S.; Zimmer, L.; Billard, T. *Chem. Eur. J.* **2014**, *20*, 8589. (h) Zhang, P.; Li, M.; Xue, X.-S.; Xu, C.; Zhao, Q.; Liu, Y.; Wang, H.; Guo, Y.; Lu, L.; Shen, Q. *J. Org. Chem.* **2016**, *81*, 7486. (i) Zhang, H.; Leng, X.; Wan, X.; Shen, Q. *Org. Chem. Front.* **2017**, *4*, 1051. (j) Haas, A.; Oh, D. Y. *Chem. Ber.* **1969**, *102*, 77. (k) Haas, A.; Lieb, M.; Zhang, Y. *J. Fluor. Chem.* **1985**, *29*, 297. (l) Shao, X.; Wang, X.; Yang, T.; Lu, L.; Shen, Q. *Angew. Chem. Int. Ed.* **2013**, *52*, 3457. Structure revision: Vinogradova, E. V.; Müller, P.; Buchwald, S. L. *Angew. Chem. Int. Ed.* **2014**, *53*, 3125. (m) Shao, X.; Xu, C.; Lu, L.; Shen, Q. *J. Org. Chem.* **2015**, *80*, 3012. (n) Yang, Y.-D.; Azuma, A.; Tokunaga, E.; Yamasaki, M.; Shiro, M.; Shibata, N. *J. Am. Chem. Soc.* **2013**, *135*, 8782. (o) Huang, Z.; Okuyama, K.; Wang, C.; Tokunaga, E.; Li, X.; Shibata, N. *ChemistryOpen* **2016**, *5* (3), 188. (p) Li, H.; Shan, C.; Tung, C.-H.; Xu, Z. *Chem. Sci.* **2017**, *8*, 2610. (q) Jiang, L.; Qian, J.; Yi, W.; Lu, G.; Cai, C.; Zhang, W. *Angew. Chem., Int. Ed.* **2015**, *54*, 14965. (r) Chachignon, H.; Maeno, M.; Kondo, H.; Shibata, N.; Cahard, D. *Org. Lett.* **2016**, *18*, 2467. (s) Yagupolskii, L. M.; Kondratenko, N. V.; Sambur, V. P. *Synthesis* **1975**, *11*, 721. (t) Emeléus, H. J; MacDuffie, D. E. *J. Chem. Soc.* **1961**, 2597. (u) Tyrra, W.; Naumann, D.; Hoge, B.; Yagupolskii, Y. L. *J. Fluor. Chem* **2003**, *119*, 101. (v) Dix, S.; Jakob, M.; Hopkinson, M. N. *Chem. Eur. J.* **2019**, *25*, 7635. (w) Yang, X.-G.; Zheng, K.; Zhang, C. *Org. Lett.* **2020**, *22*, 2026. (x) Wang, D.; Carlton, C. G.; Tayu, M.; McDouall, J. J.; Perry, G. J.; Procter, D. J. *Angew. Chem. Int. Ed.* **2020**, *59*, 15918.

[30] (a) Zhu, D.; Gu, Y.; Lu, L.; Shen, Q. *J. Am. Chem. Soc.* **2015**, *137*, 10547. (b) Ismalaj, E.; Le Bars, D.; Billard, T. *Angew. Chem. Int. Ed.* **2016**, *55*, 4790. (c) Shen, F.; Zhang, P.; Lu, L.; Shen, Q. *Org. Lett.* **2017**, *19*, 1032. (d) Xiong, H.-Y.; Bayle, A.; Pannecoucke, X.; Besset, T. *Angew. Chem. Int. Ed.* **2016**, *55*, 13490. (e) Arimori, S.; Matsubara, O.; Takada, M.; Shiro, M.; Shibata, N. R. *Soc. Open Sci.* **2016**, *3*, 160102. (f) Wu, J.; Gu, Y.; Leng, X.; Shen, Q. *Angew. Chem. Int. Ed.* **2015**, *54*, 7648. (g) Zhu, D.; Shao, X.; Hong, X.; Lu, L.; Shen, Q. *Angew. Chem. Int. Ed.* **2016**, *55*, 15807. (h) Zheng, J.; Wang, L.; Lin, J.-H.; Xiao, J.-C.; Liang, S. H. *Angew. Chem. Int. Ed.* **2015**, *54*, 13236. (i) Huang, Z.; Matsubara, O.; Jia, S.; Tokunaga, E.; Shibata, N. *Org. Lett.* **2017**, *19*, 934. (j) Jiang, L.; Yi, W.; Liu, Q. *Adv. Synth. Catal.* **2016**, *358*, 3700. (k)

and some derivatives (Figure 3.7), and by SCH_2F[31] (Figure 3.8). In general terms, this chemistry has been mainly disclosed by the efforts of Billard, Shibata, and Shen[32] laboratories.

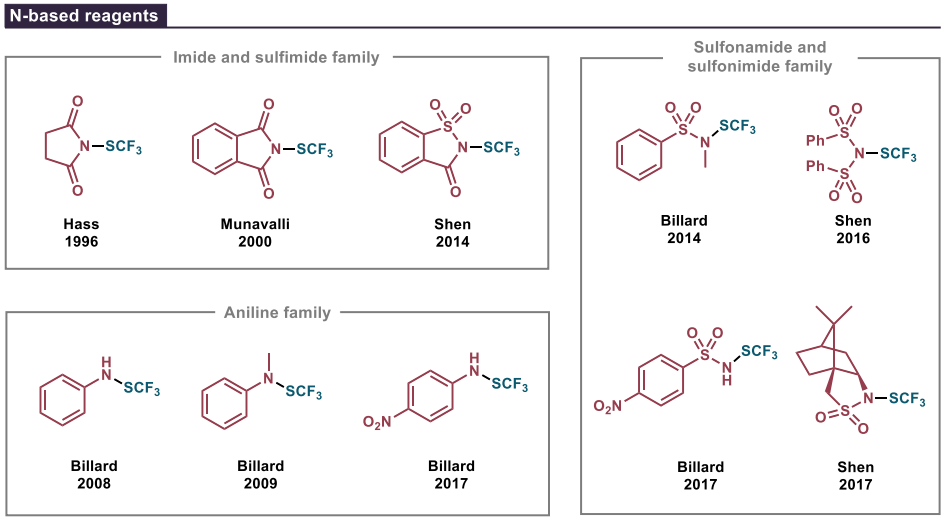

Jiang, L.; Yan, Q.; Wang, R.; Ding, T.; Yi, W.; Zhang, W. *Chem. Eur. J.* **2018**, *24*, 18749. (l) Tironi, M.; Hopkinson, M. N. *Eur. J. Org. Chem.* **2022**, *2022*, ejoc.202101557.

[31] (a) Zhao, Q.; Lu, L.; Shen, Q. *Angew. Chem. Int. Ed.* **2017**, *56*, 11575. (b) Liu, F.; Jiang, L.; Qiu, H.; Yi, W. *Org. Lett.* **2018**, *20*, 6270. (c) Zhang, H.; Shen, Q. *Tetrahedron*, **2021**, *101*, 132508.

[32] Shen, Q. *J. Org. Chem.* **2023**, 88, 3359.

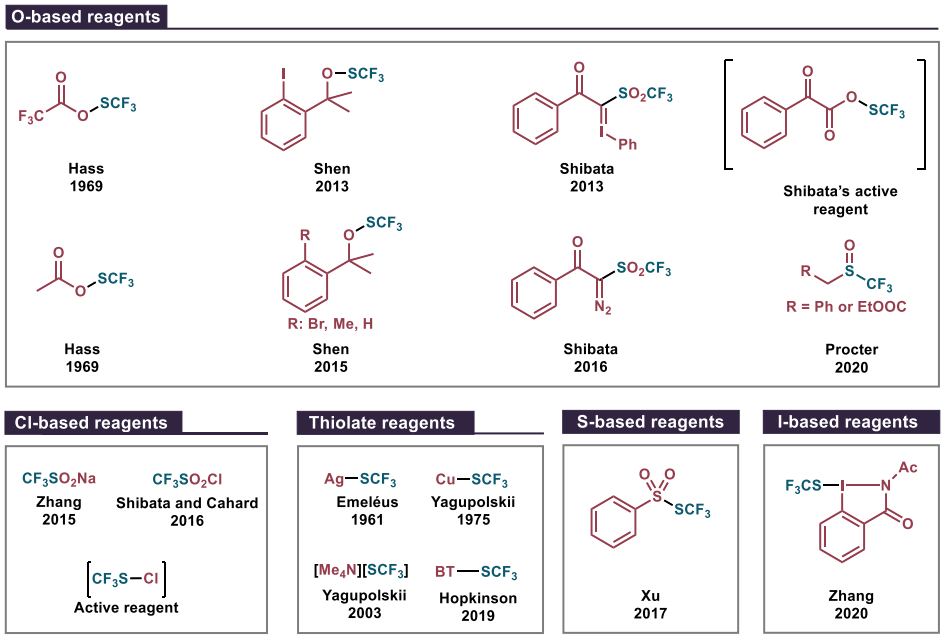

Figure 4.6. Compilation of thiotrifluoromethylating reagents. BT = benzothiazolium.

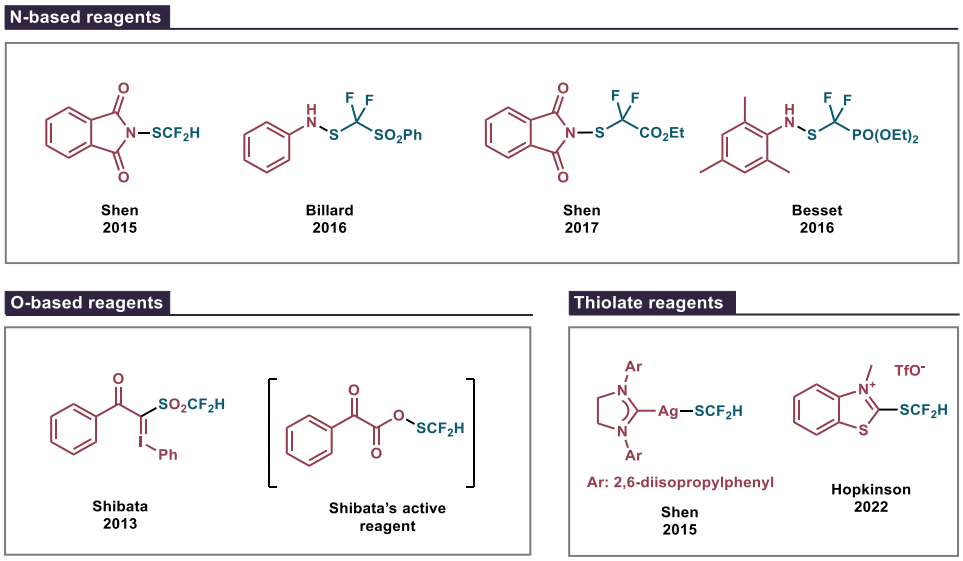

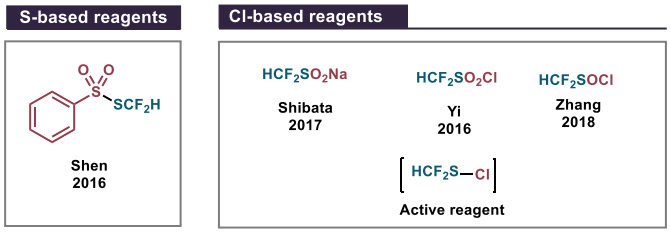

Figure 4.7. Compilation of thiodifluoromethylating and related SCF_2R reagents.[30]

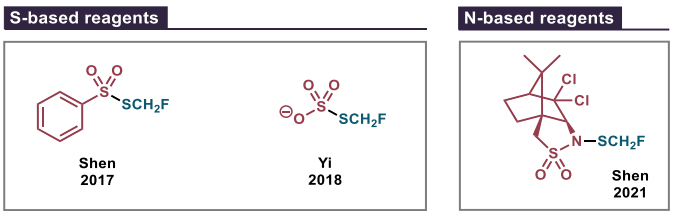

Figure 4.8. Compilation of thiomonofluoromethylating reagents.[31]

Taking into account the general trends, nitrogen-based reagents arguably are the most used scaffolds in the design of SR_F reagents. Evidence for this is the great number of reagents that bear the *N*-SR_F linkage in the form of derivates of anilines, imides, sulfimindes, sulfonimides, and sulfonamides (see Figures 4.6, 4.7, and 4.8). In the second term, oxygen-based reagents also represent an important family followed by sulfur-based and organometallic reagents. It must be noted that there are some thiofluoroalkylating agents that are not active by themselves because they need the use of another species to achieve its activation.[29q] This is also the case of the chlorine-based and Shibata oxygen-based reagents family.[29n] Moreover, there are some protocols where the use of a cocktail of reagents generates some of the active species previously described by forging all the bonds involved in the R–SR_F moieties.[33] These methodologies have not been considered in the classification because of clarity purposes.

[33] For exaplmes see: (a) Zheng, J.; Wang, L.; Lin, J. H.; Xiao, J. C.; Liang, S. H. *Angew. Chem. Int. Ed.* **2015**, *54*, 13236. (b) Chen, C.; Xie, Y.; Chu, L.; Wang, R.-W.; Zhang, X.; Qing, F.-L. *Angew. Chem. Int. Ed.* **2012**, *51*, 2492.

4.1.3.2 Electrophilic Methodologies

Electrophilic protocols for the introduction of SR_F motifs outnumber any other methodology.[22] Their polar nature relies on nucleophilic partners performing substitution reactions in electrophilic reagents (Figure 4.9).

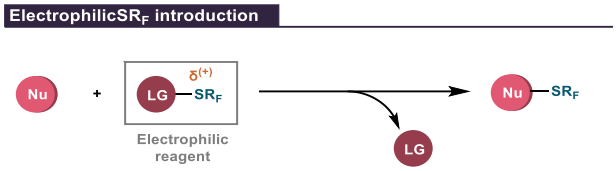

Figure 4.9. General reaction for the electrophilic introduction of thiofluoroalkyl motifs.

Specifically, nitrogen, oxygen, hypervalent iodine, and chlorine-based reagents can behave as electrophilic counterparts (Figures 4.6 and 4.7). Its design capitalizes on the attachment of a good leaving group to the SR_F fragment, thus inverting the natural polarity of the sulfur atom. In this regard, the better leaving group, the more reactive the reagent will be. With this premise in hand, the Cheng group investigated the relative reactivity of most of the reagents experimentally and computationally.[34] The results of these studies place every reagent on an electrophilic scale that can be paired with a nucleophilic one to predict reaction outcomes. Indeed, this represents a useful tool for pairing nucleophiles with adequate electrophilic SR_F reagents.[35]

With the numerous reagents available in the literature, a wide variety of nucleophilic partners have been shown to be suitable for thiotrifluoromethylation (Figure 4.10).[22]

[34] (a) Zhang, J.; Yang, J.-D.; Zheng, H.; Xue, X.-S.; Mayr, H.; Cheng, J.-P. *Angew. Chem. Int. Ed.* **2018**, *57*, 12690. (b) Li, M.; Guo, J.; Xue, X.-S.; Cheng, J.-P. *Org. Lett.* **2016**, *18*, 264.

[35] Yang, Y.; Saffon-Merceron, N.; Vantourout, J. C.; Tlili, A. *Chem. Sci.* **2023**, *14*, 3893.

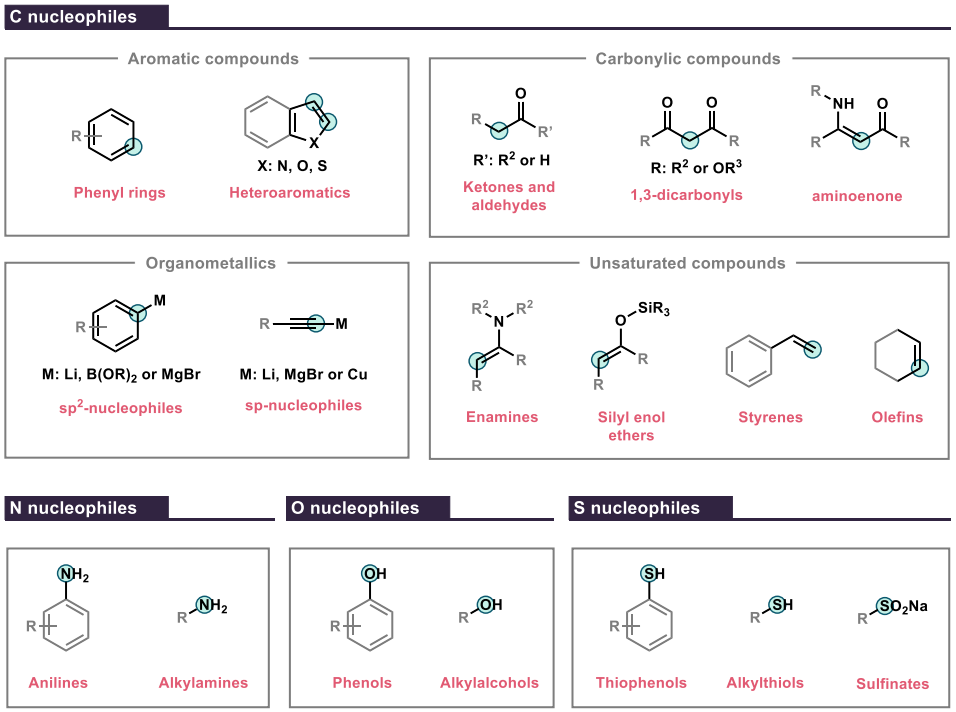

Figure 4.10. Nucleophiles amenable to electrophilic thiofluoroalkylation. The highlighted positions correspond to the reacting points of the molecule.[22]

Forging C–SR_F bonds is by far the most common transformation related to these methodologies. Electron-rich (hetero)aromatic compounds, and organometallic species can serve directly as nucleophilic partners.[36] When the nucleophiles are not strong enough to react with the electrophilic reagents, suitable activators can be used to enhance their nucleophilicity. The use of bases or Lewis or Brønsted acids, enables the reaction of alkenes, enamines, silyl enol ethers and various carbonylic compounds.[22] In this context, asymmetric transformations for the thiofluoroalkylation of carbonylic

[36] (a) Yi, W.; Song, Z.; Liu, J.; Mumtaz, Y.; Zhang, W. Trifluoromethylthiolation of Aromatic and Heteroaromatic Compounds. In *Emerging Fluorinated Motifs: Synthesis, Properties and Applications*, 1st edition; Ma, J.-A.; Cahard, D.; Wiley-VCH Verlag GmbH & Co. KGaA: Weinheim, Germany, 2020; pp 373-401.

compounds are found in the literature either by the use of chiral reagents[29i] or by the aid of chiral auxiliaries or catalysts.[37]

In contrast, the modification of heteroatom-based nucleophiles (N, O, and S) is not as explored as the C-partners. This is because the reaction products are very reactive since the new bond formed by X–SR_F is weak and sometimes compromises product stability. Nonetheless, aromatic, and aliphatic amines, alcohols, and thiols can be functionalized by the same means.[31]

The intrinsic reactivity of electrophilic reagents can also be enhanced by the use of suitable additives. Two strategies can be adopted: one relies on the use of Lewis or Brønsted acids, while the other uses nucleophilic catalysts (Figure 4.11).

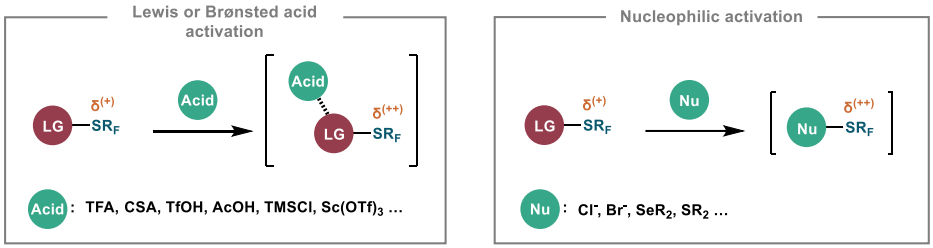

Figure 4.11. Activation of SR_F reagents by external means.

The first strategy capitalizes on the coordination of an acid with a basic site on the leaving group scaffold of the reagent, usually a carbonyl or a nitrogen linchpin. This new linkage polarizes the reactive bond, making the reagent more electrophilic (Figure 4.11, left panel).

However, the use of suitable nucleophiles can *in situ* generate more reacting species by withdrawing more electron density on the sulfur (Figure 4.11, right panel). This nucleophilic activation can be used in a catalytic fashion as the activator is released again to the medium after the reaction.

[37] Sicignano, M.; Rodríguez, R. I.; Capaccio, V.; Borello, F.; Cano, R.; Riccardis, F. D.; Bernardi, L.; Díaz-Tendero, S.; Sala, G. D.; Alemán, J. *Org. Biomol. Chem.* **2020**, *18*, 2914. (and references therein).

Glorius and co-workers used this last activation mode to functionalize substituted furans (Figure 4.12).[38]

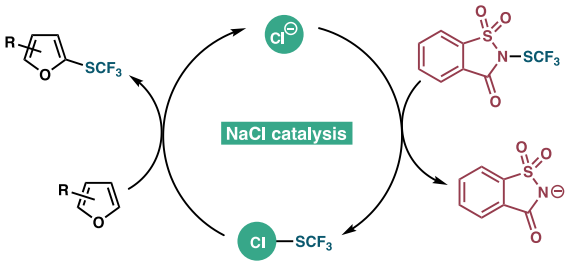

Figure 4.12. Proposed catalytic cycle for NaCl-catalyzed trifluoromethylthiolation of furans.[38]

Furans proved unreactive towards the SCF_3-saccharin reagent. Nevertheless, the use of a catalytic amount of inexpensive NaCl allowed the *in situ* formation of the more reactive CF_3SCl species that could react with furan derivates. Upon transfer of the SCF_3 unit, the chloride anion is released and can engage the cycle again by a nucleophilic attack to the saccharin reagent.[38]

4.1.3.3 Nucleophilic methodologies

Nucleophilic methodologies exploit the synthetic potential of thiolate anions to install SR_F moieties. Despite not being as numerous as the electrophilic methods, they present complementary reactivity, which expands the diversity of substrates amenable to modification. These methods rely on nucleophilic substitution or metal catalyzed reactions (Figure 4.13).

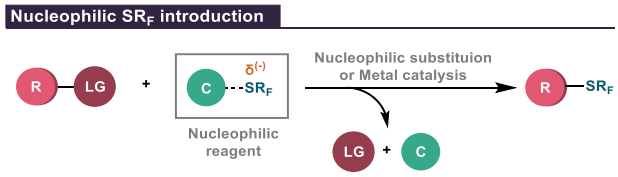

Figure 4.13. General reaction for the nucleophilic introduction of thiofluoroalkyl motifs. C represents a stabilizing moiety for the thiolate anion.

[38] Glorius, F.; Ernst, J.; Rakers, L. *Synthesis* **2016**, *49*, 260.

As mentioned above (see Scheme 4.1), thiofluoroalkyl anions suffer from decomposition by α-defluorination.[23] For this reason, these species require the use of a stabilizing moiety capable of diminishing the electronic density on the sulfur atom, such as a metal or a large countercation. In this sense, the most common reagents for thiofluoroalkylation are copper and silver complexes, cesium salts, and quaternary ammonium salts. Noticeably, nitrogen-based reagents (Figures 4.6, and 4.7), which are used as electrophilic reagents, can be converted into sources of nucleophilic thiofluoroalkyl anions by treatment with Bu_4NI (Scheme 4.2).[28]

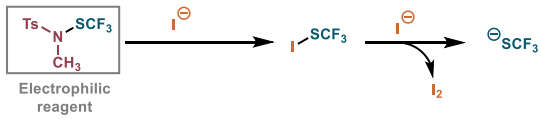

Scheme 4.2. Bu_4NI-mediated generation of SCF_3 anions from electrophilic reagents. [28]

Considering these nucleophilic strategies, numerous substrates have been shown to be successful reaction partners (Figure 4.14).

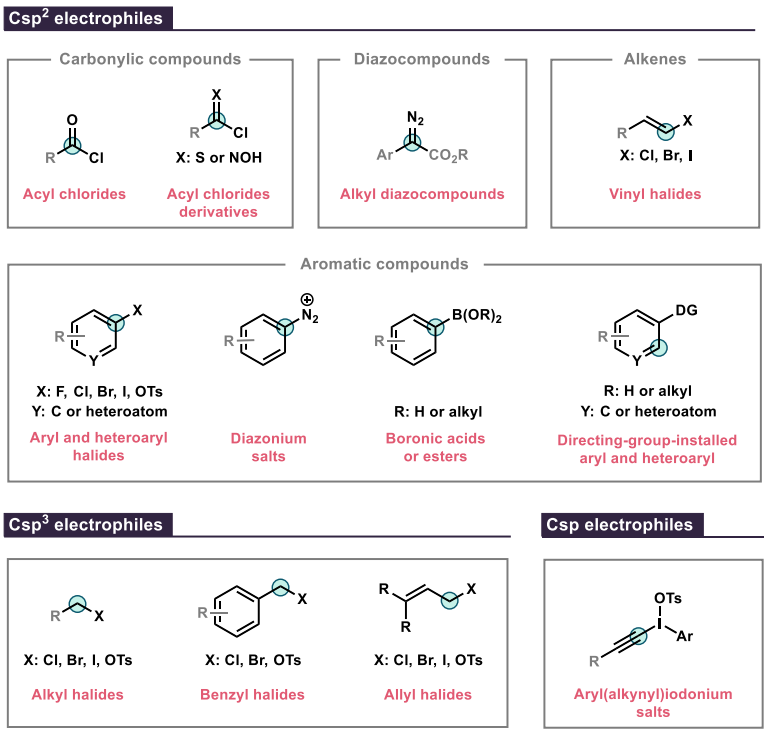

Figure 4.14. Substrates that are amenable to nucleophilic thiofluoroalkylation. The highlighted positions correspond to the reacting points of the molecule.

Strong electrophiles such as acyl chlorides, hypervalent iodine compounds, alkyl benzyl or allyl halides readily react with SCF_3 salts. On the other hand, modification of vinyl and aryl compounds is normally performed with the assistance of a metal catalyst involving the usual oxidative addition, transmetallation, and reductive elimination steps. However, C–H activation methodologies and aryne-type reactivity have also been exploited for the installation of SR_F motifs in aromatic substates.[22]

4.1.3.4 Radical methodologies

Radical reactions to introduce SR_F fragments complement the palette of substrates amenable to modification. In this regard, two modes of reactivity

can be exploited (Figure 4.15).[39] Typically, for these reactions *N*-SRF based reagents or metallic salts are employed.

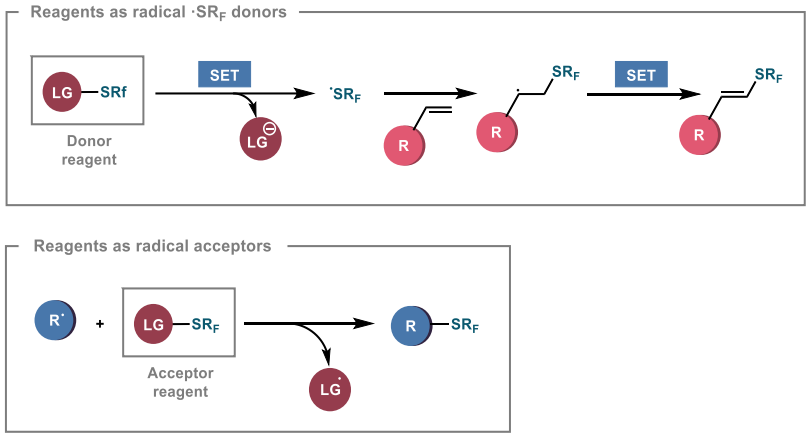

Figure 4.15. Reactivity modes for the radical incorporation of SRF fragments. SET = single-electron transfer.

The first reactivity mode (Figure 4.15, top panel) usually employs an external photocatalyst (or alternatively a chemical reductant) to induce single-electron reduction of an SRF donor reagent. The reduced species can then undergo mesolytic cleavage to render an SRF radical which can engage further transformations. Some selected reactions that follow this approach include the functionalization of styrenes,[40] the carbotrifluoromethylthiolation of alkenes,[41] and the ring expansion of cyclic alcohols.[42]

The second mode relies on the independent formation of a radical species that can then react with an adequate SRF reagent acting as somophile to forge the S–C bond. For example, photoredox catalysis allowed the use of carboxylic acids as radical precursors to install SCF_3 motifs.[43] Alternatively, HAT (hydrogen atom transfer) strategies allowed radical formation directly from

[39] Ghiazza, C.; Billard, T.; Tlili, A. *Chem. Eur. J.* **2019**, *25*, 6482.
[40] Honeker, R.; Garza-Sanchez, R. A.; Hopkinson, M. N.; Glorius, F. *Chem. Eur. J.* **2016**, *22*, 4395.
[41] Dagousset, G.; Simon, C.; Anselmi, E.; Tuccio, B.; Billard, T.; Magnier, E. *Chem. Eur. J.* **2017**, *23*, 4282.
[42] Xu, B.; Wang, D.; Hu, Y.; Shen, Q. Org. *Chem. Front.* **2018**, *5*, 1462.
[43] Hu, F.; Shao, X.; Zhu, D.; Lu, L.; Shen, Q. *Angew. Chem. Int. Ed.* **2014**, *53*, 6105.

aldehydes or unactivated Csp^3–H bonds to deliver trifluoromethylthioesters[44] and SCF_3 ethers,[45] respectively.

4.2 Target of the project

As discussed in the introduction of this chapter, the reagents reported in the literature cover only the chemical space corresponding to the SCF_3 and, to some extent, SCF_2H and SCH_2F. In view of the interesting physicochemical properties induced by SCF_2CF_2H and SCF_2CF_3 motifs disclosed in Chapter III, we wondered if we could develop effective reagents to directly introduce these SR_F into a wide variety of chemical structures.

4.3 Results and discussion

4.3.1 Reagent design

We began this project by reasoning that of the putative SR_F reagents, *N*-based scaffolds (see Section 4.1.3.1) could serve as ideal reagents for three main reasons: (i) accessible preparation, (ii) they have widely explored reactivity in polar and radical manifolds, and (iii) presumable stability.

First, we envisaged the preparation of the reagents from the reaction of N–Cl compounds with fluoroalkyl thiolate salts (Scheme 4.3). Initial attempts failed to deliver the targeted reagent, and only traces or defluorination products were observed. Presumably, the propensity of longer polyfluoroalkylthiolates to α-fluoride elimination hampers the formation of the S–Cl bond.

[44] Ye, Z.; Lei, Z.; Ye, X.; Zhou, L.; Wang, Y.; Yuan, Z.; Gao, F.; Britton, R. *J. Org. Chem.* **2022**, *87*, 765.
[45] Mukherjee, S.; Maji, B.; Tlahuext-Aca, A.; Glorius, F. *J. Am. Chem. Soc.* **2016**, *138*, 16200.

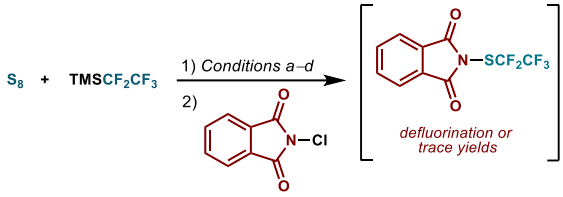

(*a*) CsF, THF. (*b*) Me_4NF, monoglyme or diglyme or THF. (*c*) KF, CuBr or CuI, DMF. (*d*) AgF, DMF.

Scheme 4.3. Initial attempts towards the preparation of the electrophilic reagents using *in situ* generated polifluoroalkylthiolates.

Alternatively, we sought another strategy to prepare the reagents avoiding the formation of an R_FS^- intermediate at any point of the synthesis (Scheme 3.2). In general terms, the controlled chlorination of a benzyl polyfluoroalkyl thioether (**1a**/**b**) could deliver an umpoled sulflinyl chloride (**2a**/**b**). In the second step, this intermediate reacted with a *N*-salt to afford the final reagent.

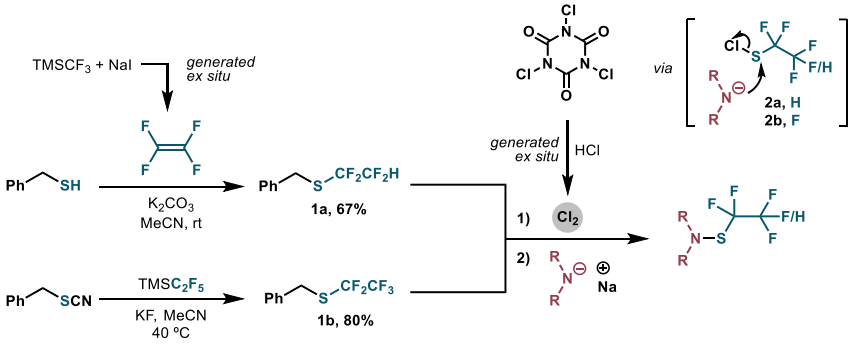

Scheme 4.4. Umpolung route for the preparation of the N-based reagents.

Key thioether **1a** was obtained from the reaction of benzyl mercaptan with *ex situ* generated tetrafluoroethylene in 67% yield. More than 15 g could be obtained after distillation of a single batch, demonstrating the potential scalability of the transformation. For the pentafluoroethyl motif, thioether **1b** was obtained in 80% yield (>27 g) starting from the already electrophilic benzyl thiocyanate and using $TMSC_2F_5$ as perfluoroalkyl anion source.

Overall, this strategy appeared useful for the installation of different N-based scaffolds that can be easily prepared from commercially available

materials. Moreover, the use of *ex situ* generated chlorine gas allows for a clean and fast conversion of thioethers to sulfinyl chlorides. On top of this, no special equipment is needed for the generation of the reactive gases.

4.3.2 Leaving group selection

We continued our study of the leaving group by preparing up to seven different *N*-based SCF_2CF_2H reagents to evaluate which one was best. Using a GAR (green-amber-red) analysis, Table 4.1 summarizes the performance of the different reagents in terms of stability upon storage, ease of purification, yield obtained, availability of the precursors and reactivity, and reaction compatibility. The reactivity parameter was evaluated by reacting the reagents with 1*H*-Indole and checking the conversion by ^{19}F NMR. All of the reagents were obtained as free-flowing solids.

Table 4.1. GAR analysis (green-amber-red) of electrophilic reagents **1–9**. See experimental section for more information.

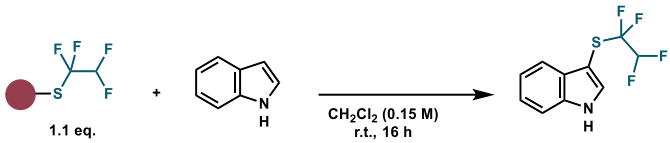

Entry	Scaffold	Stability	Ease of purification	Yield	Commercial availability	Reactivity/ compatibility
1	3 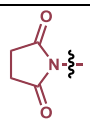					
2	4 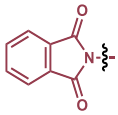					
3	5 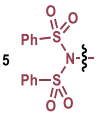					
4	6 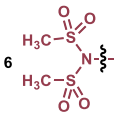					
5	7 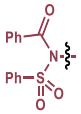					
6	8a 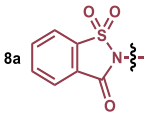					
7	9 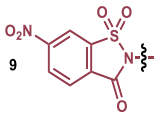					

After analysis of all factors, saccharin **8a** was chosen as the best scaffold due to its superior performance in all the indicators. Succinimide **3** and phthalimide **4** presented limited reactivity and were difficult to purify.

Bisphenylsulfonamide **5** exhibited moderate stability, while bismethyl analogue **6** was discarded as the scaffold was not commercially available and the CH_3 protons could be incompatible with strongly basic conditions. Compound **7** was also discarded as it required column chromatography for its isolation. Finally, the more reactive 5-nitro-saccharin **9** presented severe stability issues that led us to discard this scaffold.

4.3.3 Saccharin as scaffold of choice

Saccharin based reagents for the incorporation of SCF_2CF_2H **8a** and SC_2F_5 **8b** motifs (Figure 4.16) could be obtained on multigram scale in a single batch operation in 99% and 96% yield respectively, following the previous synthetic procedure (Scheme 4.4).

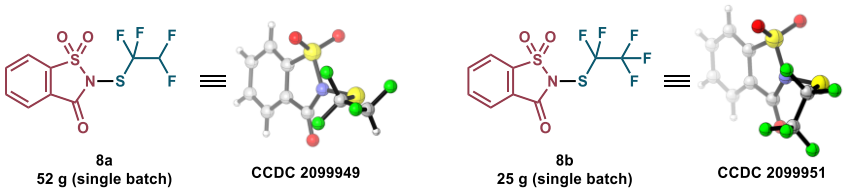

Figure 4.16. X-ray structure of the optimal saccharin-based reagents.

Once the two reagents were in hand, we decided to assess their stability in the solid state and in solution. Thermogravimetric analysis (TGA) of the reagents presented a 5% weight decomposition at 209 °C for **8a** and 179 °C for **8b**. Furthermore, calorimetric studies (DSC) of **8a** and **8b** showed no exotherm up to 250 °C (see supplementary information), meaning that their thermal decomposition was nonexplosive. These analyses demonstrate the safe use of the reagents in a wide range of temperatures.

The stability test of reagent **8a** in solution was performed by measuring its concentration by ^{19}F NMR for more than a week. This assay was carried out at room temperature and at 50 °C using different solvents (Figure 3.17).

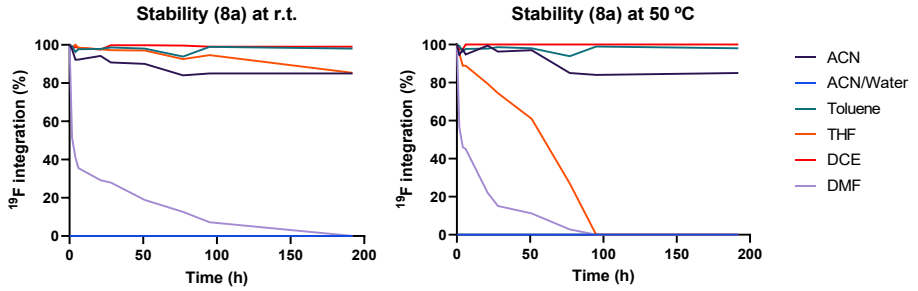

Figure 4.17. Stability of reagent **8a** in solution with different solvents at room temperature (left plot), and 50 °C (right plot). The integration was referenced to a fixed amount of 1,4-difluorobenzene used as the internal standard.

As depicted in Figure 4.17, reagent **8a** is completely stable in nonpolar solvents such as 1,2-dichloroethane and toluene, both at room temperature and 50 °C. On the other hand, coordinating polar solvents such as acetonitrile and tetrahydrofuran compromise its stability. The highly polar solvents dimethylformamide and water were shown to lead to rapid decomposition. This might be due to the nucleophilic nature of those solvents. Higher temperature speeds up the rate of decomposition when using the incompatible solvents (Figure 4.17, right plot).

Finally, during our studies no decomposition was observed after storage in the freezer (–20 °C) for more than 2 years.

4.3.4 Structural analysis of reagents

Analysis of the ^{19}F NMR spectra of saccharin-based reagents **8a** and **8b** revealed an anomalous multiplicity pattern. More specifically, the α-to the S fluorines (-S**C**$\mathbf{F_2}$CF_2H/F) appeared as a broad complex signal where a geminal $^2J_{F\text{-}F}$ coupling constant of about 230 Hz could be measured. These observations indicated that the internal fluorine atoms exhibited diastereotopicity. Interestingly, all the studied reagents containing the (RSO_2)(RCO)N- moiety displayed this unusual multiplicity pattern (**7**, **8**, and **9**).

VT-NMR experiments of reagents **8a** and **8b** were carried out to confirm the existence of a preferential conformation responsible for NMR splitting (Figure 4.18).

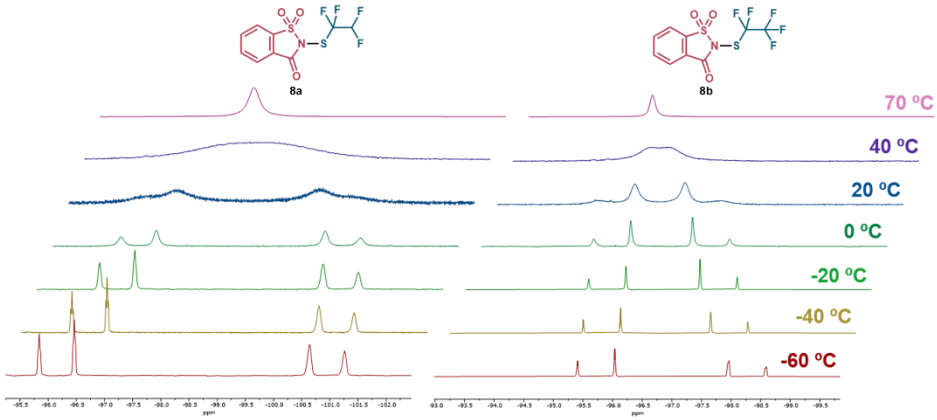

Figure 4.18. VT-NMR experiments for reagents **8a** and **8b**. Samples were dissolved in toluene.

By recording the ^{19}F NMR at low temperatures, the set of signals are resolved to reveal two doublets of triplets (dt, J = 234.3, 8.7 Hz) for reagent **8a**, and two doublets of quadruplets (dq, J = 236.3, 3.5 Hz) for reagent **8b** (Figure 4.18). Moreover, heating above room temperature produces the coalescence of signals. Next, we measured the ^{19}F NMR spectra in different solvents for reagent **8a** (Figure 4.19).

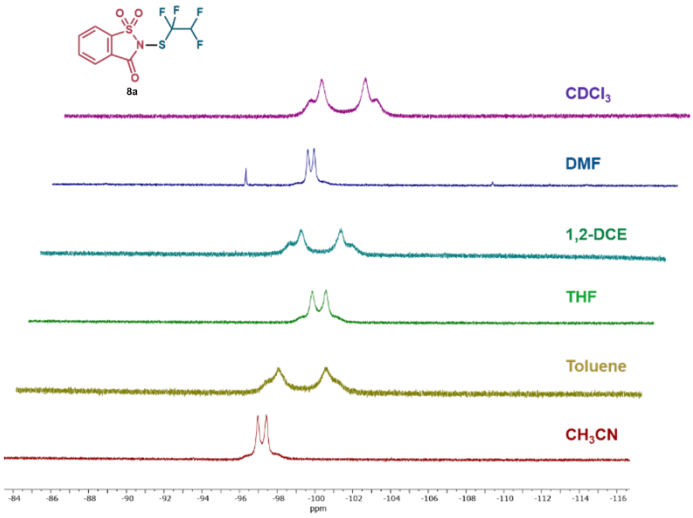

Figure 4.19. ^{19}F NMR close-up of reagent **8a** at room temperature in different solvents.

Interestingly, the signals changed significantly depending on the sample solvent used, indicating that the conformation of the fluorine atoms (Saccharin-S**CF**$_2$CF$_2$H) is affected by the interactions with the solvent.

To gain more insight into these structural nuisances, X-ray analysis of the crystal structure of saccharin reagent **8a** and phthalimide reagent **4** was performed (Figure 4.20).

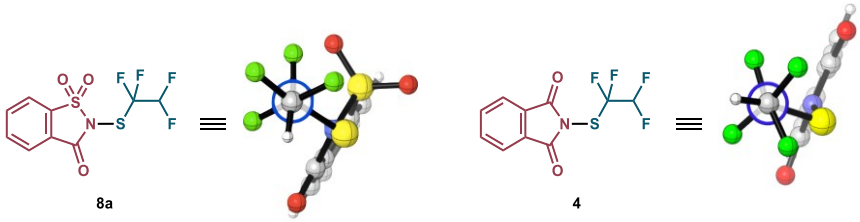

Figure 4.20. X-ray structure of the saccharin-based **8a** and phthalimide-based **4a**. Orientation of the molecules chosen to mimic the Newman projections.

Interestingly, the internal F atoms (Saccharin-S**CF**$_2$CF$_2$H) adopt a gauche conformation in reagent **8a** that could be responsible for the ^{19}F NMR

observations (Figure 4.20, left)[46]. However, in reagent **4**, which displays the expected ^{19}F NMR splitting pattern (triple doublet and doublet of triplets), a typical staggered conformation is observed (Figure 4.20, right). Based on these observations, we concluded that the -SO_2- moiety in the saccharin reagent **8a** has an influence on the conformational behavior of the -S**C**$F_2$$CF_2$H fragment.

On the other hand, analysis of the X-ray structure of saccharin-based -SCF_2CF_3 reagent **8b** revealed the co-crystallization of two conformers (Figure 4.21, A). In this case, the gauche effect cannot be invoked to justify the anomalous multiplicity splitting (Figure 4.18) as the terminal carbon is perfluorinated and cannot give the usual $\sigma_{C\text{-}H} \rightarrow \sigma^*_{C\text{-}F}$ interactions.

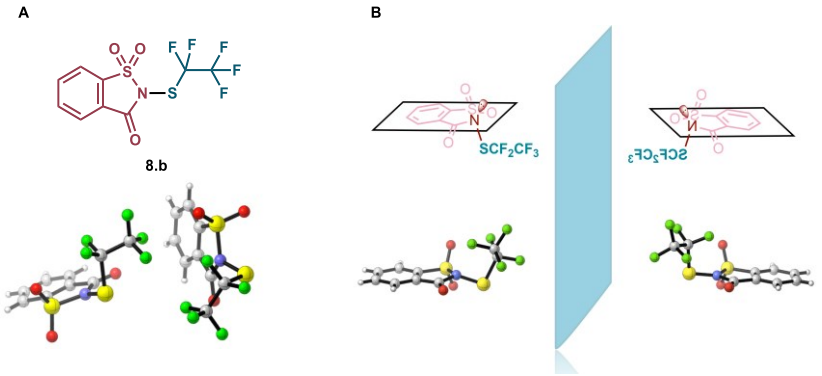

Figure 4.21. A) X-ray structures found in the crystal of reagent **8b**; B) Confrontation of X-ray structures by a plane of symmetry.

If we oppose both X-ray structures of reagent **8b** by a plane of symmetry (Figure 4.21, B), we see how the -SCF_2CF_3 fragment is either on one side or on the other respect to the plane of the aromatic ring of the reagent. The observed diasteropicity arises from the different chemical environment of the internal -S**C**$F_2$$CF_3$ fluorine atoms. This indicates that the rotation of the S-C bond is not very fast which could explain the observations in the VT-NMR experiments

[46] Thiehoff, C.; Ret, P. Y.; Gilmour, R. *Isr. J. Chem.* **2017**, *57*, 92.

(Figure 4.18). Finally, the crystallization of two conformers suggests that the energy between the structures might be very similar.

Computational studies are currently being carried out to help to understand the structural peculiarities of this family of reagents.

4.3.5 Small molecule scope

Once the reagents were shown to be stable, we wanted to demonstrate their applicability with different nucleophilic partners. We began our studies selecting indole as the model nucleophile and reacted with reagent **8a** in different solvents (Scheme 4.5).

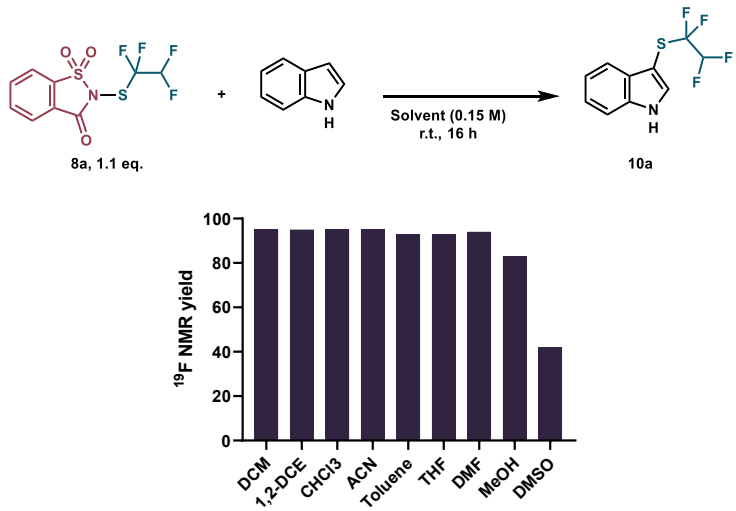

Scheme 4.5. SCF_2CF_2H functionalization of N-*H* indole using different solvents.

As demonstrated in Scheme 4.5, the functionalization of N-*H* indole proceeds in excellent yield in a wide variety of solvents. Reduced yields are observed only when highly polar solvents are used (methanol and dimethylsulfoxide). We next evaluated the scope of the reaction with respect to the indole component by varying the substituents on the benzene ring and on nitrogen (Scheme 4.6).

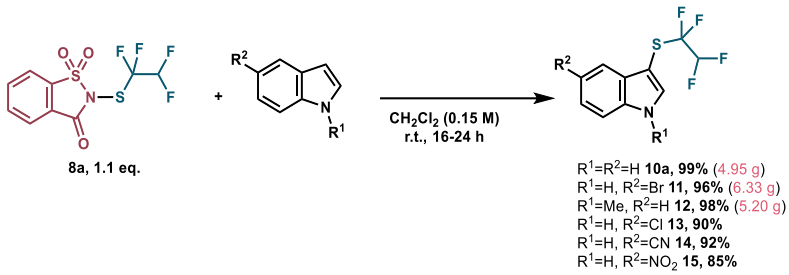

Scheme 4.6. Scope of different 5-substituted indoles with reagent **8a**.

The scalability of the transformation was assessed simultaneously by performing the reaction with 20 mmol of the indole partners. Gratifyingly, *N*-H indole **10a**, 5-bromo indole **11** and *N*-methyl indole **12** could be functionalized at the 3-position in excellent yields. Remarkably, no column chromatography was needed to isolate the pure compounds on a gram scale. Instead, the by-product saccharine can be easily removed by precipitation or washed out of organic solution by a basic aqueous work-up.

Finally, we assessed the transformation with less nucleophilic indoles to afford products bearing 5-chloro **13**, 5-cyano **14** and 5-nitro **15** substitution. In these cases, only a minor decrease of the reaction yield was observed (all >85%).

We next investigated the scope of nucleophiles that could be modified using both **8a** and **8b** reagents (scheme 4.7)

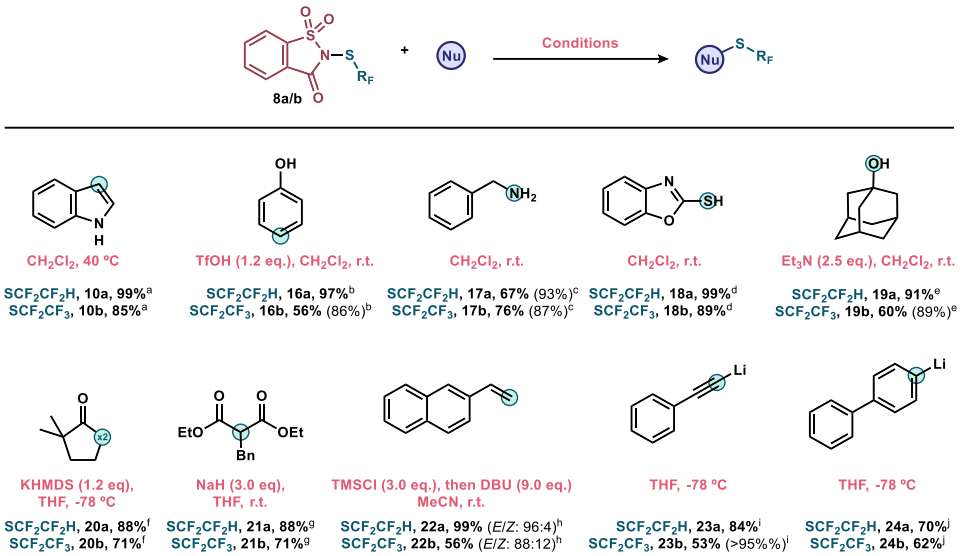

Scheme 4.7. Survey of representative nucleophiles. [a]N-H indole (1.0 eq.), **8a/b** (1.1 eq.), 40 °C, CH_2Cl_2. [b]phenol (1.0 eq.), **8a/b** (1.2 eq.), TfOH (1.0 eq), r.t., CH_2Cl_2. [c]benzylamine (1.0 eq.), **8a/b** (1.1 eq.), rt, CH_2Cl_2. [d]2-mercaptobenzoxazole (1.0 eq.), **8a/b** (1.1 eq.), rt, CH_2Cl_2. [e]adamantol (1.0 eq.), **8a/b** (1.3 eq.), Et_3N (2.5 eq.), r.t., CH_2Cl_2. [f]2,2-dimethylcyclopentan-1-one (1.0 eq.), KHMDS (1.2), then **8a/b** (2.5 eq.), -78 °C, THF. [g]diethyl 2-benzylmalonate (1.0 eq.), NaH (3 eq.), then **8a/b** (1.7 eq.), r.t., THF. [h]2-vinylnaphthalene (1.0 eq.), TMSCl (3 eq.), **8a/b** (2.2 eq.), then DBU (6 eq), r.t., ACN. [i]phenylacetylene (1.0 eq.), ^{n}BuLi (1.1 eq.), then **8a/b** (1.2 eq.), -78 °C, THF. [i]4-bromo-1,1′-biphenyl (1.0 eq.), ^{n}BuLi (1.1 eq.), then **8a/b** (1.2 eq.), -78 °C, THF. Isolated yields given. Yields in parentheses were determined by ^{19}F NMR using 1,4-difluorobenzene as internal standard.

Starting with activated arenes, we observed that by heating N-*H* indole at 40 °C in the dichloromethane, product **10a** could be obtained with excellent yield after 1h, and **10b** in 24 h. Reaction with phenol required the addition of triflic acid as promoter to afford **16a** (97%), and **16b** (56%). Next, we tested the suitability of other nucleophiles to afford *N*–, *O*–, and *S*–SR_F bonds. Therefore, the reaction with benzylamine gave the desired products **17a** (93%) and **17b** (87%) after 1 h at room temperature, while the reaction with 2-mercaptobenzoxazole immediately provided disulfides **18a** (99%) and **18b** (89%). Unlike phenol, which required an acid to activate the electrophilic

reagent, preliminary results with alcoholic nucleophiles indicate the need for an exogenous base (*e.g.*, Et_3N) to deprotonate the hydroxyl moiety and deliver the desired products. Therefore, adamantol derivatives **19a** (91%) and **19b** (89%) were obtained after 1 h at room temperature, using Et_3N as a base. Then, we directed our focus to the formation of C–SR_F bonds. Reactions with the preformed enolate of 2,2-dimethylcyclopentanone afforded the double substitution products **20a** (53%) and **20a** (38%). Attempts to selectively obtain the monosubstituted ketone were unsuccessful because of the increased reactivity of the monosubstituted intermediate. Treatment of diethyl benzylmalonate with sodium hydride (NaH) and subsequent reaction with **8a/b** afforded **21a** and **21b** in 88% and 71% yield, respectively. Alkenes are also suitable nucleophiles as demonstrated with 2-vinylnaphthalene, using an addition/elimination sequence that afforded *E*/*Z* mixtures (up to 96:4) of vinylic SCF_2CF_2H **22a** (99%) and SCF_2CF_3 **22b** (56%). Whilst treatment of phenylacetylene with **8a** in the presence of CuBr failed to deliver the desired product, reaction of the alkyne with *n*-BuLi and subsequent reaction with **8a/b** rendered **23a** (84%) and **23b** (>95%). Similarly, generation of the organolithium intermediate from 4-bromobiphenyl by lithium-bromine exchange afforded **24a** (70%) and **24b** (62%) after subsequent reaction with **8a/b**.

4.3.6 Scope of natural products and commercial drugs

Having demonstrated the versatility of reagents **8a** and **8b** with model nucleophiles, our objective was to evaluate their efficiency with more complex substrates such as natural products and pharmaceutical drugs (Scheme 4.8).

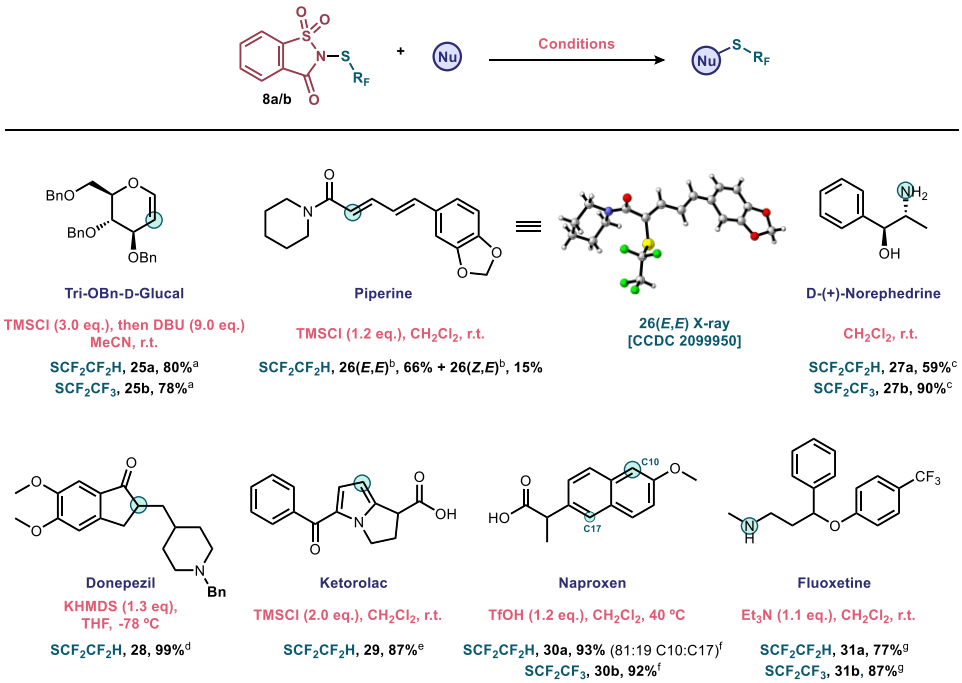

Scheme 4.8. Functionalization of natural products and pharmaceuticals. [a](i) tri-O-Benzyl-D-glucal (1.0 eq.), 3 Å MS, TMSCl (3 eq.), **8a/b** (2.2 eq.); (ii) DBU (6 eq.), MeCN, r.t. [b]Piperine (1.0 eq.), **8a** (2.2 eq.), TMSCl (1.2 eq.), CH_2Cl_2, r.t.. [c](1*S*,2*R*)-(+)-Norephedrine (1.0 eq.), **8a/b** (3 eq.), CH_2Cl_2, r.t.. [d](i) Donepezil (1.0 eq.), KHMDS (1.3 eq.); (ii) **8a** (1.3 eq.), THF, –78 °C. [e]Ketorolac (1.0 eq.), **8a** (2.0 eq.), TMSCl (2 eq.), CH_2Cl_2, r.t.. [f]rac-Naproxen (1.0 eq.), **8a/b** (1.5 eq.), TfOH (1.2 eq.), $CHCl_3$, 40 °C (for **30a**) or 70 °C (for **30b**). [g]Fluoxetine (1.0 eq.), **8a/b** (1.5 eq.), Et_3N (1.1 eq.), CH_2Cl_2, r.t..

First, following Ye's protocol for the trifluoromethyl thiolation of glycals,[47] benzyl-protected D-glucal could react in a two-step sequence to afford **25a** (80%) and **25b** (78%). Similarly, the use of trimethylsilyl chloride (TMSCl) as a promoter enabled the modification of piperine (black pepper alkaloid) to product **26** as a separable mixture of *E*/*Z*-isomers **26*E*,*E*** (66%) and **26*E*,*Z*** (15%), resulting from the modification of the conjugated diene system as determined by NMR and X-ray (for the *E*-isomer) analysis. Next, (+)-Norephedrine was chemoselectively *N*-modified to **27a** (59%) and **27b** (90%)

[47] Yu, Y.; Xiong, D.; Ye, X. *Org. Biomol. Chem.* **2016**, *14*, 6403.

under mild reaction conditions without competitive *O*-substitution. Donepezil, a drug used in the treatment of Alzheimer's disease, was reacted with potassium bis(trimethylsilyl)amide (KHMDS) to generate the enolate that subsequently reacted with **8a** to afford **28** in an excellent 99% yield. Reaction of **8a** with ketorolac, an anti-inflammatory agent, afforded **29** (87%) with the exclusive modification of the pyrrole moiety, thus demonstrating the compatibility of our reagent **8a** with carboxylic acids. When naproxen was reacted with **8a** and triflic acid as promoter, **30a** (93%) was obtained as an 81:19 mixture of C10/C17 regioisomers. In contrast, reaction with **8b** afforded **20b** (92%) as the sole C10-isomer. Finally, the secondary amine of fluoxetine (Prozac™) also reacted successfully to deliver **31a,b** in 77% and 87% yield, respectively.

4.3.7 Derivatization of final SR_F substituted products

The synthesized SR_F compounds are potentially reactive handles to access other functional groups or more elaborated structures. To prove this point, a series of derivatization reactions were conducted.

To begin with, we considered the -SCF_2CF_2H fragment as a potential oxidizable point (Scheme 4.9). Indeed, treatment of indole **10a** under catalytic oxidative conditions delivered the corresponding sulfone **33** in excellent yield.

Difluoromethylene fragments are known to be acidic,[48] for this reason we envisioned that the -SCF_2CF_2H motif could serve as a bridge unit to further derivatize its terminal position. Starting from *N*-Boc protected indole **32** and using KHDMS as base, we could deprotonate the -CF_2H to further quench it with benzophenone forging a new C–C bond (Scheme 4.9). Finally, subsequent Boc-deprotection with TFA delivered indole **34** in good yield (76%).

[48] Sessler, C. D.; Rahm, M.; Becker, S.; Goldberg, J. M.; Wang, F.; Lippard, S. J. *J. Am. Chem. Soc.* **2017**, *139*, 9325.

Next, we demonstrated the compatibility of the installed fluoroalkylthioether with Pd-catalyzed transformations. Suzuki coupling between (4-phenoxyphenyl)boronic acid and **10a** to give indole **35** in 90% yield.

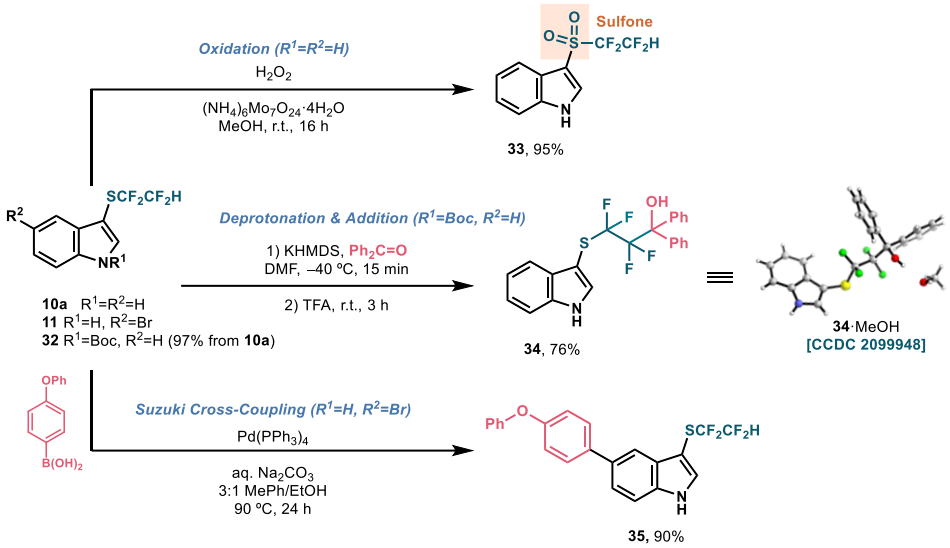

Scheme 4.9. Derivatizations of 3-SCF_2CF_2H-substituted indole.

Lastly, we turned our attention to *N*-SR_F linkages as potential candidates for oxidation. Specifically, we could modify sulfenamides **31a/b** to their corresponding sulfonamides **36a** (56%) and **36b** (75%) by applying the same molybdenum catalyzed oxidative conditions as for the sulfone **33** (Scheme 4.9). This transformation allows a new disconnection for the preparation of fluoroalkyl sulfonamides.

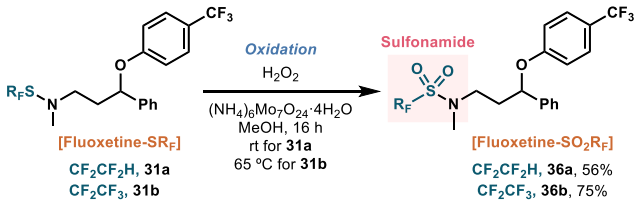

Scheme 4.10. Oxidation of fluoxetine derivatives **31a** and **31b**.

4.4 Conclusions

In summary, two new reagents for the direct introduction of SCF_2CF_2H and SCF_2CF_3 motifs have been disclosed. These electrophilic agents are synthesized in three steps from simple and readily available starting materials and can be obtained on a multigram scale. After a careful evaluation of the leaving group, saccharin was selected as the optimal scaffold to transfer the SR_F motifs.

Electrophilic introduction has proven successful in a range of different nucleophiles, including amines, alcohols, thiols, electron-rich (hetero)aromatics, phenols, ketones, 1,3-diesters, and alkenes as well as organolithium alkyne and arene derivatives. The robustness of the transformation, including its operational and purification simplicity, has been further demonstrated with a variety of complex structures, including blockbuster drugs and natural products. Multigram scale reactions, product derivatization to sulfones, sulfonamides, functionalization of SCF_2CF_2H as well as orthogonal metal-mediated reactions, have also been demonstrated.

We expect our findings will provide new opportunities in drug and agrochemical discovery process by expanding the toolbox of reagents for the introduction of new fluorinated motifs into natural products and active ingredients.

4.5 Experimental section

General Remarks. Proton (^1H NMR), carbon ($^{13}C\{^1H\}$) NMR), and fluorine (^{19}F NMR) nuclear magnetic resonance spectra were recorded on a Varian Mercury spectrometer or a Bruker Avance Ultrashield (400 MHz for ^1H), (100.6 MHz for $^{13}C\{^1H\}$), and (376.5 MHz for ^{19}F). Spectra were fully assigned using COSY, HSQC, HMBC, and NOESY. All chemical shifts are quoted on the δ scale in parts per million (ppm) using the residual solvent as internal

standard (^{1}H NMR: $CDCl_3$ = 7.26, CD_3OD = 3.31 and ($^{13}C\{^1H\}$ NMR): $CDCl_3$ = 77.16, CD_3OD = 49.0). Coupling constants (*J*) are reported in Hz with the following splitting abbreviations: s = singlet, d = doublet, t = triplet, q = quartet, and app = apparent. Infrared (IR) spectra were recorded on a FTIR–ATR spectrophotometer. Absorption maxima (ν_{max}) are reported in wavenumbers (cm^{-1}). High-resolution mass spectra (HRMS) were recorded on an LC–MS system (UHPLC 1290 Infinity II Series coupled to a qTOF/MS 6550 Series, both Agilent Technologies (Agilent Technologies). For the ionization, an ESI operating on positive or negative ionization or an APCI operating on positive or negative ionization was used. Water and methanol with 0.05% formic acid were used as mobile phases. The quadrupole time of flight mass spectrometer (qTOF) operated in high resolution MS scan mode between 100–1000 *m*/*z*. For GC–HRMS mass determination the compounds were directly analyzed by gas chromatography coupled to high-resolution mass spectrometry (7200 GC–qTOF from Agilent technologies). For ionization, electron impact ionization was used. The chromatographic column was a 5HP–MS from Agilent and carried gas was He. The quadrupole time of flight mass spectrometer (qTOF) operated in high resolution MS scan mode between 100–600 *m*/*z*. Nominal and exact *m*/*z* values are reported in Daltons. Thin layer chromatography (TLC) was carried out using commercial backed sheets coated with 60 Å F_{254} silica gel. Visualization of the silica plates was achieved using a UV lamp (λ_{max} = 254 nm), 6% H_2SO_4 in EtOH, cerium molybdate, and/or potassium permanganate staining solutions. Flash column chromatography was carried out using silica gel 60 Å CC (230–400 mesh). Mobile phases are reported in relative composition (*e.g.*, 1:1 EtOAc/hexane v/v). All reactions using anhydrous conditions were performed using oven-dried apparatus under an atmosphere of argon. Brine refers to a saturated solution of sodium chloride. Anhydrous sodium sulfate (Na_2SO_4) was used as drying agent after reaction work-up, as indicated. All reagents were purchased from Sigma Aldrich, Cymit, Carbosynth, Apollo Scientific, Fluorochem and Manchester Organics chemical companies. A sample of the

product was charged in an HRMS vial and was dissolved using a minimal amount of THF. The HRMS vial was fitted inside a bigger vial containing pentane and the latter was capped and left unperturbed overnight. Slow vapor diffusion caused growing of crystals that showed good quality for single crystal X-ray diffraction analysis. X-ray figures in the article were rendered with CyLview software.

4.5.1 Characterization data

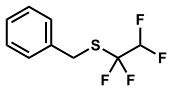

Benzyl(1,1,2,2-tetrafluoroethyl)sulfane (**1a**). A 250 mL round-bottom flask (reaction flask A), equipped with a magnetic stir bar was charged with potassium hydroxide (90%, 1.68 g, 30 mmol). The flask was then evacuated and backfilled with argon three times. Subsequently, anhydrous and deoxygenated MeCN (100 mL) was added followed by benzyl mercaptan (11.7 mL, 100 mmol) and an argon balloon was attached through the rubber septa using a needle. Then, a second flask (reaction flask B) containing NaI (2.25 g, 15 mmol) in anhydrous and deoxygenated THF (100 mL) was attached to a reflux condenser connected to a Teflon (PTFE) tube and the outlet was immersed in the solution of reaction flask A. Then, reaction flask B was heated to 70 °C with an aluminum heating block and $TMSCF_3$ was added (4 x 11 mL, 74.4 mmol, every 30 min) while bubbling was observed in reaction flask A. If overpressure was observed by dilation of the balloon connected to flask A, this was detached, emptied, and connected again to liberate excess of pressure. When bubbling stopped after additions of $TMSCF_3$, the reaction mixture was stirred at room temperature for further 3 h. Then, the reaction mixture was concentrated in a rotary evaporator without heating, the crude redissolved in Et_2O and washed with 10% aqueous KOH and brine. The organic phase was dried with Na_2SO_4, filtered, and concentrated under gentle vacuum in a rotary evaporator without heating. The product was distilled under reduced pressure to afford **1a** (15.1 g, 67%) as a colorless liquid.

***R**f* (hexane): 0.26; **^{1}H NMR ($CDCl_3$, 400 MHz):** δ 7.48–7.31 (m, 5H), 5.80 (tt, *J* = 53.9, 3.3 Hz, 1H), 4.19 (s, 2H); **$^{13}C\{^1H\}$ NMR ($CDCl_3$, 100.6 MHz):** δ 135.5, 129.2, 129.0, 128.1, 123.8 (tt, *J* = 283.4, 30.1 Hz), 109.9 (tt, *J* = 252.8, 38.2 Hz), 32.4 (t, *J* = 4.0 Hz); **^{19}F NMR ($CDCl_3$, 376.5 MHz):** δ –92.03 (td, *J* = 9.0, 3.2 Hz, 2F), –132.00 (dt, *J* = 54.0, 9.0 Hz, 2F); **FTIR–ATR** (neat) ν in cm^{-1}: 1496, 1455, 1383, 1212, 1105, 990, 808, 768, 697, 663, 636, 551; **HRMS (APCI$^-$)** for $(M–H)^-$ $C_9H_7F_4S^-$ (*m*/*z*): calc. 223.0210; found 223.0201.

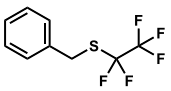

Benzyl(perfluoroethyl)sulfane (**1b**). A flask containing dry KF (8.3 g, 142.4 mmol) and benzylthiocyanate (32.0 g, 213.6 mmol) was evacuated and backfilled with argon three times followed by sequential addition of anhydrous MeCN (110 mL). Then, the mixture was cooled down to 0 °C and $TMSCF_2CF_3$ (25 mL, 142.4 mmol) was added with a syringe. The mixture was stirred under argon at 40 °C with an aluminum heating block for 48 h. Next, the reaction mixture was cooled down to room temperature and diluted with Et_2O. The organic phase was washed with brine and dried over Na_2SO_4. After filtration, the solvent was removed under reduced pressure and the residue was purified by distillation under reduced pressure to afford **1b** (27.59 g, 80%) as a colorless liquid.

***R**f* (hexane): 0.44; **^{1}H NMR ($CDCl_3$, 400 MHz):** δ 7.37–7.28 (m, 5H), 4.16 (s, 2H); **$^{13}C\{^1H\}$ NMR ($CDCl_3$, 100.6 MHz):** δ 134.81, 129.3, 1291, 128.3, 119.0 (qt, *J* = 284.2, 35.8 Hz), 121.7 (tt, *J* = 288.1, 40.3 Hz), 33.1 (t, *J* = 3.9 Hz); ^{19}F NMR ($CDCl_3$, 376.5 MHz): δ –83.4 (t, *J* = 3.7 Hz, 3F), –92.4 (q, *J* = 3.7 Hz, 2F); **FTIR–ATR** (neat) ν in cm^{-1}: 1496, 1455, 1099, 1030, 774, 766, 755, 695, 480, 465. After extensive analyses with different spectrometric techniques the molecular peak could not be found; only fragmentation can be described by **HRMS (TOF EI)** for $(Bn)^+$ $C_7H_7^+$ (*m*/*z*): calc. 91.0542; found 91.0543.

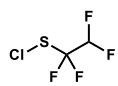

1,1,2,2-Tetrafluoroethyl hypochlorothioite (**2a**). To a solution of benzyl thioether **1a** (43.07 g, 192 mmol) in $CHCl_3$ (100 mL) was bubbled an excess of chlorine gas (27.2 g, 384 mmol) at 0 °C. The reaction

mixture was stirred at room temperature and the conversion monitored by ^{19}F NMR. After completion of the reaction, the mixture was distilled to collect the desired 1,1,2,2-tetrafluoroethyl hypochlorothioite **2a** as a yellowish solution in $CHCl_3$ (115 mL, 1.59 M, 96%). To determine the concentration of **2a** in $CHCl_3$, 0.5 mL of the distilled fraction was transferred to an NMR tube followed by addition of 1,4-difluorobenzene (DFB, 20 μL, internal standard) and the concentration was analyzed by quantitative ^{19}F NMR.

^{19}F NMR ($CHCl_3$, 376.5 MHz): δ –97.40 (m, 2F), –133.90 (dt, *J* = 53.6, 8.3 Hz, 2F). DFB referenced to –119.70 ppm.

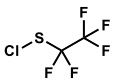

Perfluoroethyl hypochlorothioite (**2b**). To a solution of benzyl thioether **1b** (26.85 g, 110.9 mmol) in CH_2Cl_2 (110 mL) was bubbled an excess of chlorine gas (4.7 g, 332.6 mmol) at 0 °C. The reaction mixture was stirred at room temperature and the conversion monitored by ^{19}F NMR. After completion of the reaction, the mixture was distilled to collect the desired perfluoroethyl hypochlorothioite **2b** as a solution yellowish in CH_2Cl_2 (71 mL, 1.13 M, 72%). To determine the concentration of **2b** in CH_2Cl_2, 0.5 mL of the distilled fraction was transferred to an NMR tube followed by addition of 1,3-bis(trifluoromethyl)benzene (BTB, 20 μL, internal standard) and the concentration was analyzed by quantitative ^{19}F NMR.

^{19}F NMR (CH_2Cl_2, 376.5 MHz): δ –81.46 (t, *J* = 2.6 Hz, 3F), –97.50 (m, 2F). BTB referenced to –62.90 ppm.

1-((1,1,2,2-Tetrafluoroethyl)thio)pyrrolidine-2,5-dione (**3**). A round-bottom flask, equipped with a magnetic stir bar, was charged with potassium succinimide salt (206 mg, 1.5 mmol). Subsequently, $CHCl_3$ (5 mL) was added using a syringe. Then, the mixture was cooled down to 0 °C and a 1.59 M solution of 1,1,2,2-tetrafluoroethyl hypochlorothioite **2a** in $CHCl_3$ was added (0.63 mL, 1 mmol). The mixture was stirred at room temperature for 1 h. The reaction mixture was filtered through Celite®, concentrated under reduced pressure, and purified by flash column

chromatography (1:1 EtOAc/hexane) to afford **3** (203 mg, 88%) as a white solid.

***R**f* (2:3 EtOAc/hexane): 0.28; **m.p:** 61–63 °C; **^{1}H NMR ($CDCl_3$, 400 MHz):** δ 5.96 (tt, *J* = 53.2, 3.8 Hz, 1H), 2.92 (s, 4H); **$^{13}C\{^1H\}$ NMR ($CDCl_3$, 100.6 MHz):** δ 175.1, 120.8 (tt, *J* = 291.9, 30.0 Hz), 109.5 (tt, *J* = 253.8, 35.7 Hz), 28.6; **^{19}F NMR ($CDCl_3$, 376.5 MHz):** δ –98.1 (td, *J* = 8.9, 3.8 Hz, 2F), –132.8 (dt, *J* = 53.2, 8.9 Hz, 2F); **FTIR–ATR** (neat) ν in cm^{-1}: 1717, 1299, 1217, 1115, 1001, 812, 656, 621, 547, 462, 438; **HRMS (TOF ES$^+$)** for $(M+H)^+$ $C_6H_6F_4NO_2S^+$ (*m*/*z*): calc. 232.0050; found 232.0057.

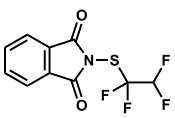

2-((1,1,2,2-Tetrafluoroethyl)thio)isoindoline-1,3-dione (**4**). A round-bottom flask, equipped with a magnetic stir bar, was charged with potassium phthalimide salt (278 mg, 1.5 mmol). Subsequently, $CHCl_3$ (1.6 mL) was added using a syringe. Then, the mixture was cooled down to 0 °C and a 1.59 M solution of 1,1,2,2-tetrafluoroethyl hypochlorothioite **2a** in $CHCl_3$ was added (0.63 ml, 1 mmol). The mixture was stirred at room temperature for 1 h. The reaction mixture was filtered through Celite®, concentrated under reduced pressure, and purified by flash column chromatography (1:9 EtOAc/hexane) to afford **4** (170 mg, 60%) as a white solid.

***R**f* (1:9 EtOAc/hexane): 0.14; **m.p**: 78–80 °C; **^{1}H NMR ($CDCl_3$, 400 MHz):** δ 8.01–7.93 (m, 2H), 7.89–7.81 (m, 2H), 5.98 (tt, *J* = 53.2, 3.8 Hz, 1H); **$^{13}C\{^1H\}$ NMR ($CDCl_3$, 100.6 MHz):** δ 166.4, 135.4, 131.6, 124.7, 120.9 (tt, *J* = 291.5, 30.2 Hz), 109.43 (tt, *J* = 253.8, 35.8 Hz); **^{19}F NMR ($CDCl_3$, 376.5 MHz):** δ –98.96 (td, *J* = 8.8, 3.8 Hz, 2F), –132.98 (dt, *J* = 53.2, 8.8 Hz, 2F); **FTIR–ATR** (neat) ν in cm^{-1}: 1747, 1719, 1281, 1100, 1038, 868, 714, 689, 626, 526, 402; **HRMS (TOF ES$^+$)** for $(M+H)^+$ $C_{10}H_6F_4NO_2S^+$ (*m*/*z*): calc. 280.0050; found 280.0056.

***N*-(Phenylsulfonyl)-*N*-((1,1,2,2-tetrafluoroethyl)thio)benzenesulfonamide**

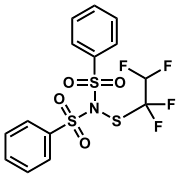

(**5**). A round-bottom flask, equipped with a magnetic stir bar, was charged with silver *N*-(phenylsulfonyl)benzenesulfonamide salt (404 mg, 1.5 mmol). Subsequently, $CHCl_3$ (1.6 mL) was added using a syringe. Then, the mixture was cooled down to 0 °C and a 1.59 M solution of 1,1,2,2-tetrafluoroethyl hypochlorothioite **2a** in $CHCl_3$ was added (0.63 mL, 1 mmol). The mixture was stirred at room temperature for 1 h. The reaction mixture was filtered through a sintered funnel and concentrated under reduced pressure to afford **5** (386 mg, 90%) as a white solid.

***R**f* (1:4 EtOAc/hexane): decomposes; **m.p**: 123–125 °C; **^{1}H NMR ($CDCl_3$, 400 MHz):** δ 8.02–7.96 (m, 4H), 7.70–7.62 (m, 2H), 7.57–7.48 (m, 4H), 6.18 (tt, *J* = 53.0, 4.7 Hz, 1H); **^{13}C{^{1}H} NMR ($CDCl_3$, 100.6 MHz):** δ 137.5, 135.0, 129.2, 129.0, 120.0 (tt, *J* = 296.4, 29.0 Hz), 109.0 (tt, *J* = 253.1, 34.2 Hz); **^{19}F NMR ($CDCl_3$, 376.5 MHz):** δ –99.29 (td, *J* = 10.1, 4.7 Hz, 2F), –135.08 (dt, *J* = 53.0, 10.1 Hz, 2F); **FTIR–ATR** (neat) ν in cm^{-1}: 1362, 1151, 1082, 863, 755, 723, 684, 575, 539, 466; **HRMS (APCI$^+$)** for $(M)^{+\cdot}$ $C_{14}H_{11}F_4NO_4S_3^{+\cdot}$ (*m*/*z*): calc. 428.9786; found 428.9786.

***N*-(methylsulfonyl)-*N*-((1,1,2,2-tetrafluoroethyl)thio)methanesulfonamide**

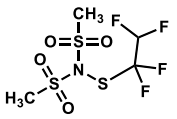

(**6**). A round-bottom flask, equipped with a magnetic stir bar, was charged with potassium *N*-(methylsulfonyl)methanesulfonamide salt (1.06 g, 5.02 mmol). Subsequently, $CHCl_3$ (8 mL) was added using a syringe. Then, the mixture was cooled down to 0 °C and a 1.59 M solution of 1,1,2,2-tetrafluoroethyl hypochlorothioite **2a** in $CHCl_3$ was added (2.26 mL, 3.6 mmol). The mixture was stirred at room temperature for 2 h. The reaction mixture was filtered through a sintered funnel and concentrated under reduced pressure to afford **7a** (1.1 g, 87%) as a white solid.

***R**f* (3:7 EtOAc/hexane): decomposes; **m.p**: 41–43 °C; **^{1}H NMR ($CDCl_3$, 400 MHz):** δ 6.12 (tt, *J* = 52.9, 4.1 Hz, 1H), 3.39 (s, 6H); **^{13}C{^{1}H} NMR ($CDCl_3$, 100.6 MHz):** δ 120.6 (tt, *J* = 293.6, 29.8 Hz), 109.1 (tt, *J* = 253.3, 34.9 Hz), 43.2; **^{19}F NMR**

($CDCl_3$, 376.5 MHz): δ –98.7 (td, *J* = 9.2, 4.1 Hz, 2F), –134.0 (dt, *J* = 52.9, 9.2 Hz, 2F); **FTIR–ATR** (neat) ν in cm^{-1}: 1353, 1161, 1118, 996, 961, 909, 794, 755, 526, 500, 472, 429; **HRMS (TOF EI)** for $(M)^{+\cdot}$ $C_4H_7F_4NO_4S_3^{+\cdot}$ (*m*/*z*): calc. 304.9468; found 304.9458.

***N*-(Phenylsulfonyl)-*N*-((1,1,2,2-tetrafluoroethyl)thio)benzamide** (**7**). A

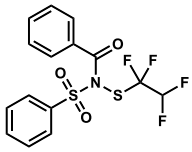

round-bottom flask, equipped with a magnetic stir bar, was charged with potassium *N*–(phenylsulfonyl)benzamide salt (790 mg, 2.64 mmol). Subsequently, $CHCl_3$ (5 mL) was added using a syringe. Then, the mixture was cooled down to 0 °C and a 1.59 M solution of 1,1,2,2-tetrafluoroethyl hypochlorothioite **2a** in $CHCl_3$ (1.25 mL, 2 mmol) was added. The mixture was stirred at room temperature for 1 h. The reaction mixture was filtered through a sintered funnel and concentrated under reduced pressure to afford **7** (605 mg, 77%) as a white solid.

R_f (1:4 EtOAc/hexane): decomposes; **m.p**: 47–49 °C; **^{1}H NMR ($CDCl_3$, 400 MHz):** δ 8.13–8.08 (m, 2H), 7.70–7.60 (m, 3H), 7.60–7.52 (m, 3H), 7.46–7.40 (m, 2H), 5.89 (tt, *J* = 53.1, 3.6 Hz, 1H); **^{13}C{^{1}H} NMR ($CDCl_3$, 100.6 MHz):** δ 171.7, 137.0, 134.8, 133.3, 131.9, 129.5, 129.4, 129.1, 128.6, 121.2 (tt, *J* = 293.7, 30.4 Hz), 109.0 (tt, *J* = 253.6, 36.0 Hz); **^{19}F NMR ($CDCl_3$, 376.5 MHz):** δ –94.81 (d, *J* = 234.3 Hz, 1F), –98.94 (d, *J* = 234.3 Hz, 1F), –133.65 (m, 2F); **FTIR–ATR** (neat) ν in cm^{-1}: 1716, 1360, 1170, 1101, 1053, 1024, 562, 545; **HRMS (TOF ES$^+$)** for $(M+H)^+$ $C_{15}H_{12}F_4NO_3S_2^+$ (*m*/*z*): calc. 394.0189; found 394.0192.

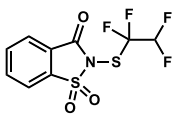

2-((1,1,2,2-Tetrafluoroethyl)thio)benzo[d]isothiazol-3(2H)-one 1,1-dioxide (**8a**). A round-bottom flask, equipped with a magnetic stir bar, was charged with potassium saccharin salt (46.17 g, 209 mmol). Subsequently, $CHCl_3$ (100 mL) was added using a syringe. Then, the mixture was cooled down to 0 °C and a 1.59 M solution of 1,1,2,2-tetrafluoroethyl hypochlorothioite **2a** in $CHCl_3$ was added (105 mL, 167 mmol). The mixture was stirred at room temperature for 1 h. The reaction

mixture was filtered through a sintered funnel and concentrated under reduced pressure to afford **8a** (52 g, 99%) as a white solid.

***R**f* (1:4 EtOAc/hexane): decomposes; m.p: 75–78 °C; **^{1}H NMR ($CDCl_3$, 400 MHz):** δ 8.17 (d, *J* = 7.7 Hz, 1H), 8.05–7.96 (m, 2H), 7.96–7.89 (m, 1H), 6.12 (tt, *J* = 52.8, 4.3 Hz, 1H); **^{13}C{^{1}H} NMR ($CDCl_3$, 100.6 MHz):** δ 158.9, 137.8, 136.5, 135.1, 126.5, 126.2, 120.3 (tt, *J* = 294.3, 30.1), 120.0, 109.2 (tt, *J* = 253.9, 34.6 Hz); **^{19}F NMR ($CDCl_3$, 376.5 MHz):** δ –96.9 (bd, *J* = 225.0 Hz, 1F), –99.8 (bd, *J* = 225.0 Hz, 1F), –133.9 (m, 2F); **FTIR–ATR** (neat) ν in cm^{-1}: 1761, 1338, 1214, 1099, 978, 936, 806, 746, 668, 592, 528, 500; **HRMS (TOF ESI$^+$)** for $(M+H)^+$ $C_9H_5F_4NO_3S_2^+$ (*m*/*z*): calc. 315.9720; found 315.9727.

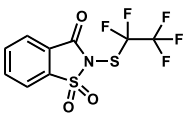

2-((Perfluoroethyl)thio)benzo[d]isothiazol-3(2H)-one 1,1-dioxide (**8b**). *A* round-bottom flask, equipped with a magnetic stir bar, was charged with potassium saccharin salt (20.32 g, 91.83 mmol). Subsequently, the flask was cooled down to 0 °C and a 1.13 M solution of perfluoroethyl hypochlorothioite **2b** in CH_2Cl_2 was added (71 mL, 79.85 mmol). The mixture was stirred at room temperature for 1 h. The reaction mixture was filtered through a sintered funnel and concentrated under reduced pressure to afford **8b** (25.55 g, 96%) as a white solid.

***R**f* (1:4 EtOAc/hexane): decomposes; **m.p**: 68–70 °C; **^{1}H NMR ($CDCl_3$, 400 MHz):** δ 8.18 (d, *J* = 7.7 Hz, 1H), 8.05–7.98 (m, 2H), 7.96–7.89 (m, 1H); **^{13}C{^{1}H} NMR ($CDCl_3$, 100.6 MHz):** δ 158.5, 138.0, 136.5, 135.1, 126.6, 126.1, 122.1, 118.2 (tq, *J* = 41.8, 299.5 Hz), 118.1 (qt, *J* = 286.7, 35.3 Hz); **^{19}F NMR ($CDCl_3$, 376.5 MHz):** δ –82.4 (t, *J* = 3.0 Hz, 3F), –95.36 (m, 2F); **FTIR–ATR** (neat) ν in cm^{-1}: 1764, 1351, 1194, 1096, 930, 749, 671, 590, 576, 529, 499, 414; **HRMS (APCI$^+$)** for $(M+H)^+$ $C_9H_5F_5NO_3S_2^+$ (*m*/*z*): calc. 333.9626; found 333.9619.

6-Nitro-2-((1,1,2,2-tetrafluoroethyl)thio)benzo[*d*]isothiazol-3(2*H*)-one 1,1-dioxide (**9**). A round-bottom flask, equipped with a magnetic stir bar, was charged with potassium 6-nitrobenzo[*d*]isothiazol-3(2*H*)-one-1,1-dioxide salt (703

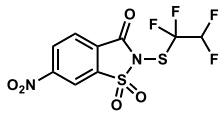

mg, 2.64 mmol). Subsequently, $CHCl_3$ (5 mL) was added using a syringe. Then, the mixture was cooled down to 0 °C and a 1.59 M solution of 1,1,2,2-tetrafluoroethyl hypochlorothioite **2a** in $CHCl_3$ was added (1.25 mL, 2 mmol). The mixture was stirred at room temperature for 1 h. The reaction mixture was filtered through a sintered funnel concentrated under reduced pressure to afford **9** (186 mg, 26%) as a yellowish solid.

***R**f* (1:4 EtOAc/hexane): decomposes; **m.p**: 70–72 °C (decomposes); **^{1}H NMR ($CDCl_3$, 400 MHz):** δ 8.87 (d, *J* = 1.9 Hz, 1H), 8.76 (dd, *J* = 8.4, 1.9 Hz, 1H), 8.41 (d, *J* = 8.4 Hz, 1H), 6.10 (tt, *J* = 53.0, 3.8 Hz, 1H); **^{13}C{^{1}H} NMR ($CDCl_3$, 100.6 MHz):** δ 157.2, 152.4, 139.2, 130.6, 130.0, 128.3, 120.5 (m), 118.2, 109.2 (tt, *J* = 254.1, 35.1 Hz); **^{19}F NMR ($CDCl_3$, 376.5 MHz):** δ –96.60 (m, 2F), –133.18 (d, *J* = 53.0 Hz, 2F); **HRMS** could not be obtained due to instability of the final product.

3-((1,1,2,2-Tetrafluoroethyl)thio)-1H-indole (**10a**). An 8 mL reaction vial, equipped with a magnetic stir bar, was charged with 1*H*-indole (35 mg, 0.3 mmol). The flask was then evacuated and backfilled with argon three times. Subsequently, anhydrous CH_2Cl_2 (1.5 mL) was added using a syringe. Then, reagent **8a** (104 mg, 0.33 mmol) was added to the flask and the mixture was stirred at 40 °C with an aluminum heating block for 1 h. The reaction mixture was diluted with CH_2Cl_2, washed with saturated aqueous $NaHCO_3$, and dried over $MgSO_4$. Upon filtration, the organic layer was concentrated under reduced pressure and purified by flash column chromatography (1:4 EtOAc/hexane) to afford **10a** (71 mg, 95%) as a brownish solid.

***R**f* (1:4 EtOAc/hexane): 0.39; **m.p**: 48 °C; **^{1}H NMR** ($CDCl_3$, 400 MHz): δ 8.44 (bs, 1H), 7.88–7.81 (m, 1H), 7.50 (d, *J* = 2.7 Hz, 1H), 7.47–7.39 (m, 1H), 7.36–7.28 (m, 2H), 5.75 (tt, *J* = 53.7, 4.0 Hz, 1H); **^{13}C{^{1}H} NMR** ($CDCl_3$, 100.6 MHz): δ 136.1, 133.3, 129.9, 123.6, 122.2 (tt, *J* = 284.4, 28.5 Hz), 121.8, 119.4, 111.9, 109.4 (tt, *J* = 252.8, 36.8 Hz), 94.4 (t, *J* = 3.9 Hz); **^{19}F NMR** ($CDCl_3$, 376.5 MHz): δ –94.4 (td, *J*

= 9.8, 4.0 Hz, 2F), –133.7 (dt, *J* = 53.7, 9.8 Hz, 2F); **FTIR–ATR** (neat) ν in cm^{-1}: 3383, 1376, 1095, 1070, 759, 750, 676, 651, 618, 584, 536, 426; **HRMS** ($APCI^+$) for $(M+H)^+$ $C_{10}H_8F_4NS^+$ (*m*/*z*): calc. 250.0308; found 250.0302.

Large-Scale Preparation of 10a. To a solution of 1*H*-indole (2.34 g, 20 mmol) in CH_2Cl_2 (20 mL) was added reagent **8a** (6.93 g, 22 mmol) under vigorous stirring at 0 °C. The reaction mixture was gradually warmed to room temperature and stirred for 16 h. Then, EtOAc (150 mL) was added and the organic phase was washed with saturated aqueous Na_2CO_3 (4 x 20 mL). The combined organic fractions were dried with Na_2SO_4, filtered, and the solvent evaporated under reduced pressure to afford **10a** (4.95 g, 99%) as a brownish solid.

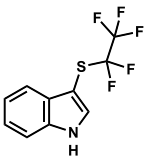

3-((Perfluoroethyl)thio)-1H-indole (**11b**). To a round bottom flask containing 1*H*-indole (18 mg, 0.15 mmol) was sequentially added anhydrous CH_2Cl_2 (0.6 mL) and reagent **8b** (55 mg, 0.17 mmol) under argon. The mixture was stirred at 40 °C with an aluminum heating block for 24 h. The solvent was then removed under reduced pressure and the residue was purified by column chromatography (1:4 EtOAc/hexane) to afford **11b** (34 mg, 85%) as a yellowish solid.

***R**f* (1:4 EtOAc/hexane): 0.22; **m.p**: 62 °C; **^{1}H NMR ($CDCl_3$, 400 MHz):** δ 8.50 (bs, 1H), 7.85–7.78 (m, 1H), 7.53 (d, *J* = 2.8 Hz, 1H), 7.46–7.40 (m, 1H), 7.34–7.27 (m, 2H); **^{13}C{^{1}H} NMR ($CDCl_3$, 100.6 MHz):** δ 136.1, 133.5, 130.0, 123.6, 121.8, 124.5–118.0 (m), 119.5, 117.4 (m), 111.8, 94.0 (t, *J* = 3.7 Hz); **^{19}F NMR ($CDCl_3$, 376.5 MHz):** δ –82.47 (t, *J* = 3.4 Hz, 3F), –93.13 (q, *J* = 3.4 Hz, 2F); **FTIR–ATR** (neat) ν in cm^{-1}: 3380, 1316, 1194, 1092, 958, 746, 555, 533, 426; **HRMS ($APCI^+$)** for $(M+H)^+$ $C_{10}H_7F_5NS^+$ (*m*/*z*): calc. 268.0214; found 268.0205.

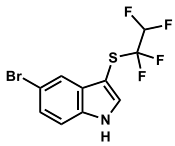

5-Bromo-3-((1,1,2,2-tetrafluoroethyl)thio)-1*H*-indole (**11**). To a solution of 5-bromoindole (3.92 g, 20 mmol) in CH_2Cl_2 (20 mL) was added reagent **8a** (6.93 g, 22 mmol) under vigorous stirring at 0 °C. The reaction mixture was gradually warmed to room temperature and stirred for 16 h. Then, EtOAc (150 mL) was added and the organic phase was washed with saturated aqueous Na_2CO_3 (4 x 20 mL). The combined organic fractions were dried with Na_2SO_4, filtered, and the solvent evaporated under reduced pressure to afford **11** (6.33g, 96%) as a brownish solid.

***R**f* (3:7 EtOAc/hexane): 0.31; **m.p**: 50 °C; **^{1}H NMR ($CDCl_3$, 400 MHz):** δ 8.48 (s, 1H), 7.95 (bs, 1H), 7.45 (d, *J* = 2.8 Hz, 1H), 7.35 (dd, *J* = 8.6, 1.9 Hz, 1H), 7.22 (d, *J* = 8.7 Hz, 1H), 5.82 (tt, *J* = 53.7, 3.7 Hz, 1H); **^{13}C{^{1}H} NMR ($CDCl_3$, 100.6 MHz):** δ 134.8, 134.3, 131.7, 126.6, 122.1, 122.1 (tt, *J* = 285.5, 30.0 Hz), 115.3, 113.3, 109.4 (tt, *J* = 252.8, 37.2 Hz), 94.1 (t, *J* = 4.0 Hz); **^{19}F NMR ($CDCl_3$, 376.5 MHz):** δ –93.47 (td, *J* = 9.4, 3.7 Hz, 2F), –133.05 (dt, *J* = 53.7, 9.4 Hz, 2F); **FTIR–ATR** (neat) ν in cm^{-1}: 3853, 3470, 2321, 1457, 1208, 1103, 994, 799, 585, 513; **HRMS (APCI$^+$)** for $(M+H)^+$ $C_{10}H_7BrF_4NS^+$ (*m*/z): calc. 327.9413; found 327.9403.

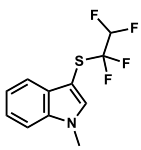

1-Methyl-3-((1,1,2,2-tetrafluoroethyl)thio)-1*H*-indole (**12**). To a solution of 1-methyl-1*H*-indole (2.62 g, 20 mmol) in CH_2Cl_2 (20 mL) was added reagent **8a** (6.93 g, 22 mmol) under vigorous stirring at 0 °C. The reaction mixture was gradually warmed to room temperature and stirred for 16 h. Then, EtOAc (150 mL) was added and the organic phase was washed with saturated aqueous Na_2CO_3 (4 x 20 mL). The combined organic fractions were dried with Na_2SO_4, filtered and the solvent evaporated under reduced pressure to afford **12** (5.20 g, 98%) as a brownish solid.

***R**f* (1:9 EtOAc/hexane): 0.31; **^{1}H NMR ($CDCl_3$, 400 MHz):** δ 7.84 (bd, *J* = 7.4 Hz, 1H), 7.42–7.29 (m, 4H), 5.76 (tt, *J* = 53.6, 4.1 Hz, 1H), 3.82 (s, 3H); **^{13}C{^{1}H} NMR ($CDCl_3$, 100.6 MHz):** δ 137.4, 137.3, 130.7, 123.0, 122.1 (tt, *J* = 283.9, 28.1 Hz), 121.4, 119.4, 110.1, 109.33 (tt, *J* = 252.6, 36.5 Hz), 91.8 (t, *J* = 3.9 Hz); **^{19}F NMR**

(CDCl$_3$, 376.5 MHz): δ –94.99 (td, *J* = 10.0, 4.1 Hz, 2F), –133.96 (dt, *J* = 53.6, 10.0 Hz, 2F); **FTIR–ATR** (neat) ν in cm^{-1}: 1512, 1210, 1103, 1080, 996, 972, 812, 741, 543, 426; **HRMS (APCI$^+$)** for (M+H)$^+$ $C_{11}H_{10}F_4NS^+$ (*m*/*z*): calc. 264.0465; found 264.0459.

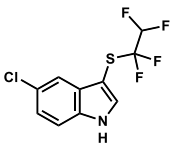

5-Chloro-3-((1,1,2,2-tetrafluoroethyl)thio)-1*H*-indole (**13**). To a solution of 5-chloroindole (45.5 mg, 0.3 mmol) in CH_2Cl_2 (1.5 mL) was added reagent **8a** (104 mg, 0.33 mmol) under vigorous stirring at 0 °C. The reaction mixture was gradually warmed to room temperature and stirred for 16 h. Then, EtOAc (50 mL) was added and the organic phase was washed with saturated aqueous Na_2CO_3 (4 x 10 mL). The combined organic fractions were dried with Na_2SO_4, filtered, and the solvent evaporated under reduced pressure to afford **13** (77 mg, 90%) as a brownish solid.

***R**$_f$* (1:4 EtOAc/hexane): 0.25; **m.p**: 66–67 °C; **^{1}H NMR (CDCl$_3$, 400 MHz):** δ 8.59 (bs, 1H), 7.77 (bd, *J* = 1.8 Hz, 1H), 7.53 (d, *J* = 2.8 Hz, 1H), 7.33 (dd, *J* = 8.6, 0.4 Hz, 1H), 7.24 (d, *J* = 8.7 Hz, 2 Hz, 1H), 5.76 (tt, *J* = 53.7, 3.7 Hz, 1H); **^{13}C{^{1}H} NMR (CDCl$_3$, 100.6 MHz):** δ 134.5, 134.5, 131.2, 127.8, 124.1, 122.1 (tt, *J* = 284.3, 29.0 Hz), 119.1, 113.0, 109.4 (tt, *J* = 252.8, 37.1 Hz), 94.3 (t, *J* = 3.8 Hz); **^{19}F NMR (CDCl$_3$, 376.5 MHz):** δ –93.53 (td, *J* = 9.2, 3.5 Hz, 2F), –133.08 (dt, *J* = 53.5, 9.2 Hz, 2F); **FTIR–ATR** (neat) ν in cm^{-1}: 3471, 3438, 1461, 1407, 1381, 1210, 1105, 1010, 994, 892, 801, 590, 493; **HRMS (APCI$^+$)** for (M+H)$^+$ $C_{10}H_7ClF_4NS^+$ (*m*/*z*): calc. 283.9918; found 283.9896.

3-((1,1,2,2-Tetrafluoroethyl)thio)-1*H*-indole-5-carbonitrile (**14**). To a solution of 1*H*-indole-5-carbonitrile (43 mg, 0.3 mmol) in CH_2Cl_2 (1.5 mL) was added reagent **8a** (104 mg, 0.33 mmol) under vigorous stirring at 0 °C. The reaction mixture was gradually warmed to room temperature and stirred for 16 h. Then, EtOAc (50 mL) was added and the organic phase was washed with saturated aqueous Na_2CO_3 (4 x 10 mL). The combined organic fractions were dried with Na_2SO_4, filtered,

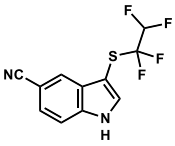

and the solvent evaporated under reduced pressure to afford **14** (76 mg, 92%) as a white solid.

***R**f* (1:4 EtOAc/hexane): 0.10; **m.p**: 130–131 °C; **^{1}H NMR ($CDCl_3$, 400 MHz):** δ 9.44 (bs, 1H), 8.15 (s, 1H), 7.70 (bs, 1H), 7.57 (d, *J* = 8.2, 1H), 7.52 (d, *J* = 8.2 Hz, 1H), 5.79 (bt, *J* = 53.7, 1H); **^{13}C{^{1}H} NMR ($CDCl_3$, 100.6 MHz):** δ 138.2, 135.7, 130.1, 126.2, 125.3, 122.1 (tt, *J* = 284.6, 29.6 Hz), 120.4, 113.2, 109.5 (tt, *J* = 253.0, 37.8 Hz), 104.6, 95.5 (t, *J* = 4.0 Hz); **^{19}F NMR ($CDCl_3$, 376.5 MHz):** δ –92.56 (bt, *J* = 8.3 Hz, 2F), –132.55 (dt, *J* = 53.8, 8.3 Hz, 2F); **FTIR–ATR** (neat) ν in cm^{-1}: 3280, 2227, 1618, 1471, 1418, 1381, 1341, 1242, 1213, 1107, 1011, 995, 811, 675, 637; **HRMS (APCI$^+$)** for $(M+H)^+$ $C_{11}H_6F_4N_2S^+$ (*m*/*z*): calc. 275.0261; found 275.0281.

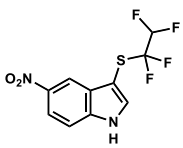

5-Nitro-3-((1,1,2,2-tetrafluoroethyl)thio)-1*H*-indole (**15**). To a solution of 5-nitro-1*H*-indole (49 mg, 0.3 mmol) in CH_2Cl_2 (1.5 mL) was added reagent **8a** (104 mg, 0.33 mmol) under vigorous stirring at 0 °C. The reaction mixture was gradually warmed to room temperature and stirred for 24 h. Then, EtOAc (50 mL) was added and the organic phase was washed with saturated aqueous Na_2CO_3 (4 x 10 mL). The combined organic fractions were dried with Na_2SO_4, filtered, and the solvent evaporated under reduced pressure to afford **15** (75 mg, 85%) as a yellow solid.

***R**f* (4:6 EtOAc/hexane): 0.29; **m.p**: 147–149 °C; **^{1}H NMR (CD_3CN, 400 MHz):** δ 10.37 (bs, 1H), 8.50 (d, *J* = 2.1, 1H), 8.07 (bs, *J* = 9.0, 2.3 Hz, 1H), 7.80 (s, 1H), 7.59 (dd, *J* = 9.0, 0.5 Hz, 1H), 6.09 (tt, *J* = 53.0, 3.9, 1H); **^{13}C{^{1}H} NMR ($CDCl_3$, 100.6 MHz):** δ 143.9, 140.5, 139.0, 130.4, 123.2 (tt, *J* = 283.1, 28.7 Hz), 119.1, 116.4, 113.9, 110.6 (tt, *J* = 250.7, 36.3 Hz), 95.8 (t, *J* = 3.9 Hz); **^{19}F NMR ($CDCl_3$, 376.5 MHz):** δ –94.50 (td, *J* = 9.5, 3.9, Hz, 2F), –134.80 (dt, *J* = 53.6, 9.3 Hz, 2F); **FTIR–ATR** (neat) ν in cm^{-1}: 3316, 1518, 1325, 1304, 1213, 1078, 992, 835, 816, 738; **HRMS (APCI$^+$)** for $(M+H)^+$ $C_{11}H_6F_4N_2S^+$ (*m*/*z*): calc. 295.0159; found 295.0186.

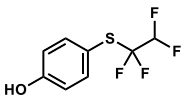

4-((1,1,2,2-Tetrafluoroethyl)thio)phenol (**16a**). A 5 mL round-bottom flask, equipped with a magnetic stir bar, was charged with phenol (28 mg, 0.3 mmol). The flask was then evacuated and backfilled with argon three times. Subsequently, anhydrous CH_2Cl_2 (3 mL) was added using a syringe followed by trifluoromethanesulfonic acid (32 μL, 0.36 mmol). Then, reagent **8a** (114 mg, 0.36 mmol) was quickly added to the flask. The mixture was stirred at room temperature for 16 h. The reaction mixture was diluted with Et_2O, washed with saturated aqueous $NaHCO_3$ and dried over $MgSO_4$. Upon filtration, the organic layer was concentrated under reduced pressure and purified by flash column chromatography (1:9 EtOAc/hexane) to afford **16a** (66 mg, 97%) as a yellowish semisolid.

***R**f* (1:9 EtOAc/hexane): 0.14; **^{1}H NMR ($CDCl_3$, 400 MHz):** δ 7.51 (d, *J* = 8.6 Hz, 2H), 6.85 (d, *J* = 8.6 Hz, 2H), 5.75 (tt, *J* = 53.8, 3.5 Hz, 1H), 5.23 (s, 1H); **^{13}C{^{1}H} NMR ($CDCl_3$, 100.6 MHz):** δ 158.0, 139.2, 122.4 (tt, *J* = 283.9, 29.2 Hz), 116.6, 109.6 (tt, *J* = 252.9, 37.6 Hz); **^{19}F NMR ($CDCl_3$, 376.5 MHz):** δ –92.74 (td, *J* = 9.2, 3.4 Hz, 2F), –132.58 (dt, *J* = 53.8, 9.5 Hz, 2F); **FTIR–ATR** (neat) ν in cm^{-1}: 3370, 1586, 1496, 1212, 1113, 996, 833, 524; **HRMS (TOF ES$^-$)** for $(M–H)^-$ $C_8H_5F_4OS^-$ (*m*/z): calc. 225.0003; found 225.0004.

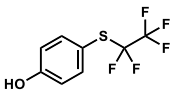

4-((Perfluoroethyl)thio)phenol (**16b**). A 5 mL round-bottom flask, equipped with a magnetic stir bar, was charged with phenol (28 mg, 0.3 mmol). The flask was then evacuated and backfilled with argon three times. Subsequently, anhydrous CH_2Cl_2 (3 mL) was added using a syringe followed by trifluoromethanesulfonic acid (32 μL, 0.36 mmol). Then, reagent **8b** (120 mg, 0.36 mmol) was quickly added to the flask. The mixture was stirred at room temperature for 16 h. The reaction mixture was diluted with Et_2O, washed with saturated aqueous $NaHCO_3$, and dried over $MgSO_4$. Upon filtration, the organic layer was concentrated under reduced pressure and purified by flash column chromatography (1:9 EtOAc/hexane) to afford **16b** (41 mg, 56%) as a colorless syrup.

***R**f* (1:4 EtOAc/Hexane): 0.29; **^{1}H NMR ($CDCl_3$, 400 MHz):** δ 7.51 (m, 2H), 6.87 (m, 2H), 5.40 (s, 1H); **$^{13}C\{^1H\}$ NMR ($CDCl_3$, 100.6 MHz):** δ 158.3, 139.4, 120.4 (m), 119.9 (m), 116.7; **^{19}F NMR ($CDCl_3$, 376.5 MHz):** δ –82.4 (t, *J* = 3.6 Hz, 3F), –92.8 (q, *J* = 3.6 Hz, 2F); **FTIR–ATR** (neat) ν in cm^{-1}: 3286, 1584, 1495, 1433, 1334, 1195, 1088, 960, 831, 749, 523; **HRMS (TOF ESI$^-$)** for $(M–H)^-$ $C_8H_4F_5OS^-$ (*m*/*z*): calc. 242.9909; found 242.9913.

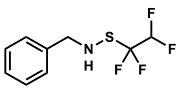

***N*-Benzyl-*S*-(1,1,2,2-tetrafluoroethyl)thiohydroxylamine** (**17a**). A 10 mL round-bottom flask, equipped with a magnetic stir bar, was charged with benzylamine (33 μL, 0.3 mmol). The flask was then evacuated and backfilled with argon three times. Subsequently, anhydrous CH_2Cl_2 (6 mL) was added using a syringe. Then, reagent **8a** (99 mg, 0.32 mmol) was quickly added to the flask. The mixture was stirred at room temperature for 1 h. The reaction mixture was concentrated under reduced pressure and purified by flash column chromatography (pentane) to afford **17a** (48 mg, 67%) as a yellowish liquid.

***R**f* (pentane): 0.15; **^{1}H NMR (CD_2Cl_2, 400 MHz):** δ 7.59–7.17 (m, 5H), 5.98 (tt, *J* = 53.7, 4.0 Hz, 1H), 4.19 (d, *J* = 5.6 Hz, 2H), 3.12 (bs, 1H); **$^{13}C\{^1H\}$ NMR (CD_2Cl_2, 100.6 MHz):** δ 139.2, 129.2, 128.7, 128.4, 123.8 (tt, *J* = 286.0, 29.1 Hz), 110.1 (tt, *J* = 251.2, 37.0 Hz), 58.5; **^{19}F NMR (CD_2Cl_2, 376.5 MHz):** δ –103.0 (td, *J* = 8.5, 3.8 Hz, 2F), –135.1 (dt, *J* = 53.9, 8.7 Hz, 2F); **FTIR–ATR** (neat) ν in cm^{-1}: 3356, 1214, 1108, 1003, 814, 699; **HRMS (APCI$^+$)** for $(M+H)^+$ $C_9H_{10}F_4NS^+$ (*m*/*z*): calc. 240.0465; found 240.0462.

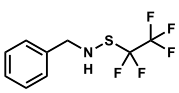

***N*-Benzyl-*S*-(perfluoroethyl)thiohydroxylamine** (**17b**). A 10 mL round-bottom flask, equipped with a magnetic stir bar, was charged with benzylamine (22 μL, 0.2 mmol). The flask was then evacuated and backfilled with argon three times. Subsequently, anhydrous CH_2Cl_2 (6 mL) was added using a syringe. Then, reagent **8b** (70 mg, 0.21 mmol) was quickly added to the flask. The mixture was stirred at room temperature for 1 h. The reaction mixture was concentrated under reduced

pressure and purified by flash column chromatography (pentane) to afford **17b** (39 mg, 76%) as a colorless oil.

***R**f* (pentane): 0.35; **^{1}H NMR (CD_2Cl_2, 400 MHz):** δ 7.46–7.26 (m, 5H), 4.24 (d, *J* = 5.4 Hz, 2H), 3.19 (bs, 1H); **^{13}C{^{1}H} NMR (CD_2Cl_2, 100.6 MHz):** δ 139.1, 129.2, 128.8, 128.5, 121.3 (tq, *J* = 289.7, 39.8 Hz), 119.6 (qt, *J* = 286.2, 37.3 Hz), 58.4; **^{19}F NMR (CD_2Cl_2, 376.5 MHz):** δ –82.77 (t, *J* = 3.1 Hz, 3F), –102.53 (q, *J* = 2.6 Hz, 2F); **FTIR–ATR** (neat) ν in cm^{-1}: 3853, 3744, 2924, 2372, 2320, 1653, 1558, 1541, 1457; **HRMS (APCI$^-$)** for $(M–H)^-$ $C_9H_7F_5NS^-$ (*m*/*z*): calc. 256.0225; found 256.0216.

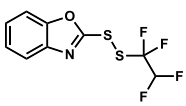

2-((1,1,2,2-Tetrafluoroethyl)disulfaneyl)benzo[*d*]oxazole (**18a**). A 10 mL round-bottom flask, equipped with a magnetic stir bar, was charged with 2-mercaptobenzoxazole (48 mg, 0.3 mmol). The flask was then evacuated and backfilled with argon three times. Subsequently, anhydrous CH_2Cl_2 (2 mL) and anhydrous MeCN (2 mL) were added using a syringe. Then, the mixture was cooled down to 0 °C and reagent **8a** (104 mg, 0.33 mmol) was quickly added to the flask. The mixture was stirred at room temperature for 5 min. The reaction mixture was diluted with EtOAc, washed with saturated aqueous $NaHCO_3$, and dried over $MgSO_4$. Upon filtration, the organic layer was concentrated under reduced pressure and the organic residue was redissolved in pentane, extracted, and concentrated again under reduced pressure to afford **18a** as a yellow oil (85 mg, 99%).

***R**f* (1:9 EtOAc/hexane): 0.33; **^{1}H NMR ($CDCl_3$, 400 MHz):** δ 7.74–7.68 (m, 1H), 7.56–7.50 (m, 1H), 7.39–7.33 (m, 2H), 6.11 (tt, *J* = 53.2, 3.5 Hz, 1H); **^{13}C{^{1}H} NMR ($CDCl_3$, 100.6 MHz):** δ 159.6, 152.6, 141.8, 125.9, 125.2, 121.3 (t, *J* = 290.5, 30.0 Hz), 120.1, 110.7, 109.2 (t, *J* = 253.7, 36.1 Hz); **^{19}F NMR ($CDCl_3$, 376.5 MHz):** δ –95.02 (td, *J* = 8.6, 3.6 Hz, 2F), –132.96 (dt, *J* = 53.3, 8.6 Hz, 2F); **FTIR–ATR** (neat) ν in cm^{-1}: 1499, 1450, 1237, 1218, 1125, 1096, 1079, 984, 803, 757, 744; **HRMS (APCI$^-$)** for $(M–H)^-$ $C_9H_4F_4NOS_2^-$ (*m*/*z*): calc. 281.9676; found 281.9673.

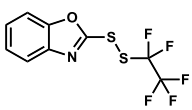

2-((Perfluoroethyl)disulfaneyl)benzo[*d*]oxazole (**18b**). A 10 mL round-bottom flask, equipped with a magnetic stir bar, was charged with 2-mercaptobenzoxazole (48 mg, 0.3 mmol). The flask was then evacuated and backfilled with argon three times. Subsequently, anhydrous CH_2Cl_2 (2 mL) and anhydrous MeCN (2 mL) were added using a syringe. Then, the mixture was cooled down to 0 °C and reagent **8b** (107 mg, 0.32 mmol) was quickly added to the flask. The mixture was stirred at room temperature for 5 min. The reaction mixture was diluted with EtOAc, washed with saturated aqueous $NaHCO_3$ and dried over $MgSO_4$. Upon filtration, the organic layer was concentrated under reduced pressure and the organic residue was redissolved in pentane, extracted, and concentrated again under reduced pressure to **18b** (81 mg, 89%) as a white-off solid.

***R**f* decomposes; m.p: 71–73 °C (decomposes); **^{1}H NMR ($CDCl_3$, 400 MHz):** δ 7.74–7.68 (m, 1H), 7.57–7.51 (m, 1H), 7.40–7.32 (m, 2H); **^{13}C{^{1}H} NMR ($CDCl_3$, 100.6 MHz):** δ 158.8, 152.6, 141.9, 125.9, 125.3, 120.28 (tq, 118.0, *J* = 295.8, 41.1 Hz), 118.4 (qt, *J* = 287.0, 36.0 Hz), 110.8; **^{19}F** NMR ($CDCl_3$, 376.5 MHz): δ –82.27 (t, *J* = 3.0 Hz, 3F), –94.91 (q, *J* = 2.9 Hz, 2F); **FTIR–ATR** (neat) ν in cm^{-1}: 1500, 1449, 1232, 1127, 1092, 801, 745; **HRMS (APCI$^-$)** for $(M–H)^-$ $C_9H_3F_5NOS_2^-$ (*m*/*z*): calc. 299.9582; found 299.9575.

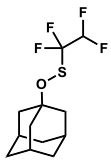

(Adamantan-1-yloxy)(1,1,2,2-tetrafluoroethyl)sulfane (**19a**). A 10 mL round-bottom flask, equipped with a magnetic stir bar, was charged with 1-adamantol (46 mg, 0.3 mmol). The flask was then evacuated and backfilled with argon three times. Subsequently, anhydrous CH_2Cl_2 (6 mL) was added using a syringe followed by triethylamine (104 μL, 0.75 mmol). Then, reagent **8a** (123 mg, 0.39 mmol) was quickly added to the flask. The mixture was stirred at room temperature for 20 min. The reaction mixture was concentrated under reduced pressure and purified by flash column chromatography (pentane) to afford **19a** (78 mg, 91%) as a colorless oil.

***R**f* (pentane): 0.26; **^{1}H NMR (CDCl$_3$, 400 MHz):** δ 5.99 (tt, *J* = 53.5, 4.3 Hz, 1H), 2.23 (bs, 3H), 1.80 (m, 6H), 1.61 (m, 6H); **^{13}C{^{1}H} NMR (CDCl$_3$, 100.6 MHz):** δ 123.3 (tt, *J* = 286.6, 28.2 Hz), 109.17 (tt, *J* = 252.9, 35.6 Hz), 82.6, 41.6, 35.9, 31.4; **^{19}F NMR (CDCl$_3$, 376.5 MHz):** δ –103.9 (td, *J* = 9.9, 4.3 Hz, 2F), –135.1 (dt, *J* = 53.5, 9.9 Hz, 2F); **FTIR–ATR** (neat) ν in cm^{-1}: 2913, 2855, 1214, 1118, 1000, 892, 819; **HRMS (APCI$^-$)** for $(M–H)^-$ $C_{12}H_{15}F_4OS^-$ (*m*/*z*): calc. 283.0785; found 283.0780.

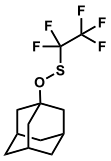

(Adamantan-1-yloxy)(perfluoroethyl)sulfane (**19b**). A 10 mL round-bottom flask, equipped with a magnetic stir bar, was charged with 1-adamantol (46 mg, 0.3 mmol). The flask was then evacuated and backfilled with argon three times. Subsequently, anhydrous CH_2Cl_2 (6 mL) was added using a syringe followed by triethylamine (104 μL, 0.75 mmol). Then, reagent **8b** (130 mg, 0.39 mmol) was quickly added to the flask. The mixture was stirred at room temperature for 10 min. The reaction mixture was concentrated under reduced pressure and purified by flash column chromatography (pentane) to afford **19b** (54 mg, 60%) as a colorless oil.

***R**f* (pentane): 0.66; **^{1}H NMR (CDCl$_3$, 400 MHz):** δ 2.24 (bs, 3H), 1.81 (m, 6H), 1.69–1.54 (m, 6H); **^{13}C{^{1}H} NMR (CDCl$_3$, 100.6 MHz):** δ 121.1 (m), 118.9 (qt, *J* = 286.8, 36.8 Hz), 83.2, 41.6, 35.9, 31.5; **^{19}F NMR** ($CDCl_3$, 376.5 MHz): δ –81.9 (t, *J* = 3.6 Hz, 3F), –102.5 (q, *J* = 3.6 Hz, 2F); **FTIR–ATR** (neat) ν in cm^{-1}: 3853, 3649, 2923, 2852, 1699, 1653, 1558, 1541, 1507, 1457, 1035. After extensive analyses with different spectrometric techniques the molecular peak could not be found; only fragmentation can be described by **HRMS (TOF EI)** for $(Adamantyl)^+$ $C_{10}H_{15}^+$ (*m*/*z*): calc. 135.1168; found 135.1169; $(pentafluoroethyl)^+$ $C_2F_5^+$ (*m*/*z*): calc. 118.9915; found 118.9910; $SC_2F_4^+$ (*m*/*z*): calc. 131.9651; found 131.9645.

2,2-Dimethyl-5,5-bis((1,1,2,2-tetrafluoroethyl)thio)cyclopentan-1-one (**20a**).

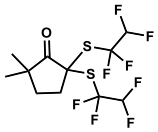

A 0.35 M stock solution of 2,2-dimethylcyclopentan-1-one potassium enolate was prepared using the following procedure: a 5 mL round-bottom flask, equipped with a magnetic stir bar, was charged with 2,2-dimethylcyclopentan-1-one (113 μL, 0.9 mmol). The flask was then evacuated and backfilled with argon three times. Subsequently, anhydrous THF (1.5 mL) was added using a syringe and the mixture was cooled down to –78 °C. Next, a solution of potassium bis(trimethylsilyl)amide (1.0 M in toluene, 1.1 mL, 1.1 mmol) was added dropwise. The mixture was stirred at –78 °C for 30 min. Then, to a 5 mL round-bottom flask, equipped with a magnetic stir bar, was charged with reagent **8a** (237 mg, 0.75 mmol). The flask was then evacuated and backfilled with argon three times. Subsequently, anhydrous THF (2 mL) was added using a syringe. The mixture was cooled down to –78 °C and then, the previously prepared enolate solution (0.86 mL, 0.35 M, 0.3 mmol) was added using a syringe. Then, the mixture was left to stir at room temperature for 3 h. The reaction mixture was diluted with Et_2O, washed with saturated aqueous NH_4Cl and dried over $MgSO_4$. Upon filtration, the organic layer was concentrated under reduced pressure and purified by flash column chromatography (hexane) to afford **20a** (60 mg, 53%) as a colorless liquid.

***R**f* (1:9 EtOAc/hexane): 0.31; **^{1}H NMR (CD_2Cl_2, 400 MHz):** δ 5.99 (tdd, *J* = 53.4, 5.1, 2.8 Hz, 2H), 2.64 (t, *J* = 6.8 Hz, 2H), 2.08 (t, *J* = 6.8 Hz, 2H), 1.23 (s, 6H); **^{13}C{^{1}H} NMR (CD_2Cl_2, 100.6 MHz):** δ 210.7, 127.1–120.4 (m), 112.4–106.5 (m), 65.3, 44.6, 37.8, 35.1, 26.8; **^{19}F** NMR (CD_2Cl_2, 376.5 MHz): δ –88.02 (dt, *J* = 234.5, 8.3 Hz), –89.89 (ddd, *J* = 234.5, 14.2, 9.2 Hz), –132.4 (m), –134.50 (ddt, *J* = 295.2, 53.5, 9.2 Hz); **FTIR–ATR** (neat) ν in cm^{-1}: 2975, 1743, 1461, 1382, 1208, 1113, 984, 877, 812, 634, 553; **HRMS (APCI$^+$)** for $(M+H)^+$ $C_{11}H_{13}F_8OS_2^+$ (*m*/z): calc. 377.0275; found 377.0268.

2,2-Dimethyl-5,5-bis((perfluoroethyl)thio)cyclopentan-1-one (**20b**). A 0.35 M stock solution of 2,2-dimethylcyclopentan-1-one potassium enolate was prepared using the following procedure: a 5 mL round-bottom flask, equipped with a magnetic stir bar, was charged with 2,2-dimethylcyclopentan-1-one (113 μL, 0.9 mmol). The flask was then evacuated and backfilled with argon three times. Subsequently, anhydrous THF (1.5 mL) was added using a syringe and the mixture was cooled down to –78 °C. Next, a solution of potassium bis(trimethylsilyl)amide (1.0 M in toluene, 1.1 mL, 1.1 mmol) was added dropwise. The mixture was stirred at –78 °C for 30 min. Then, to a 5 mL round-bottom flask, equipped with a magnetic stir bar, was charged with reagent **8b** (250 mg, 0.75 mmol). The flask was then evacuated and backfilled with argon three times. Subsequently, anhydrous THF (2 mL) was added using a syringe. The mixture was cooled down to –78 °C and then, the previously prepared enolate solution (0.86 mL, 0.35 M, 0.3 mmol) was added using a syringe. Then, the mixture was left to stir at room temperature for 3 h. The reaction mixture was diluted with Et_2O, washed with saturated aqueous NH_4Cl and dried over $MgSO_4$. Upon filtration, the organic layer was concentrated under reduced pressure and purified by flash column chromatography (hexane) to afford **20b** (47 mg, 38%) as a colorless liquid.

***R**f* (1:9 EtOAc/hexane): 0.47; **^{1}H NMR (CD_2Cl_2, 400 MHz):** δ 2.71 (t, *J* = 6.8 Hz, 2H), 2.13 (t, *J* = 6.8 Hz, 2H), 1.29 (s, 6H); **^{13}C{^{1}H} NMR (CD_2Cl_2, 100.6 MHz):** δ 210.7, 127.1–120.4 (m), 112.4–106.5 (m), 65.3, 44.6, 37.8, 35.1, 26.8; **^{19}F NMR (CD_2Cl_2, 376.5 MHz):** δ –88.02 (dt, *J* = 234.5, 8.3 Hz), –89.89 (ddd, *J* = 234.5, 14.2, 9.2 Hz), –132.4 (m), –134.50 (ddt, *J* = 295.2, 53.5, 9.2 Hz); **FTIR–ATR** (neat) ν in cm^{-1}: 1751, 1328, 1212, 1099, 953, 751; **HRMS (APCI$^+$)** for $(M+H)^+$ $C_{11}H_{11}F_{10}OS_2^+$ (*m*/z): calc. 413.0086; found 413.0085.

Diethyl 2-benzyl-2-((1,1,2,2-tetrafluoroethyl)thio)malonate (**21a**). A 5 mL round-bottom flask, equipped with a magnetic stir bar, was charged with NaH (60% in mineral oil, 9 mg, 0.23 mmol). The flask was then evacuated and backfilled with argon three times. Subsequently, anhydrous THF (1.5 mL) was added using a syringe followed by diethyl 2-benzylmalonate (35.5 μL, 0.15 mmol) and the mixture was stirred at room temperature for 15 min. Then, reagent **8a** (118 mg, 0.38 mmol) was quickly added to the flask and the mixture was stirred at room temperature for 15 min. The reaction mixture was diluted with Et_2O, washed with aqueous NH_4Cl, and dried over $MgSO_4$. Upon filtration, the organic layer was concentrated under reduced pressure and purified by flash column chromatography (1:9 EtOAc/hexane) to afford **21a** (51 mg, 88%) as a colorless oil.

***R**f* (1:9 EtOAc/hexane): 0.26; **^{1}H NMR ($CDCl_3$, 400 MHz):** δ 7.30–7.18 (m, 5H), 5.80 (tt, *J* = 53.7, 3.5 Hz, 1H), 4.29–4.15 (m, 4H), 3.64 (s, 2H), 1.23 (t, *J* = 7.1 Hz, 6H); **^{13}C{^{1}H} NMR ($CDCl_3$, 100.6 MHz):** δ 167.2, 134.1, 130.7, 128.3, 127.8, 124.06 (tt, *J* = 287.4 , 29.3 Hz), 109.47 (tt, *J* = 254.4, 36.4 Hz), 64.7, 63.2, 41.3, 13.9,; **^{19}F NMR ($CDCl_3$, 376.5 MHz):** δ –88.79 (td, *J* = 8.9, 3.5 Hz, 2F), –132.48 (dt, *J* = 53.7, 8.9 Hz, 2F); **FTIR**–ATR (neat) ν in cm^{-1}: 2985, 1260, 1224, 1114, 990, 860, 810, 701; **HRMS (APCI$^+$)** for $(M+H)^+$ $C_{16}H_{19}F_4O_4S^+$ (*m*/*z*): calc. 383.0935; found 383.0922.

Diethyl 2-benzyl-2-((perfluoroethyl)thio)malonate (**21b**). A 5 mL round-bottom flask, equipped with a magnetic stir bar, was charged with NaH (60% in mineral oil, 22 mg, 0.9 mmol). The flask was then evacuated and backfilled with argon three times. Subsequently, anhydrous THF (3 mL) was added using a syringe followed by diethyl 2-benzylmalonate (71 μL, 0.3 mmol) and the mixture was stirred at room temperature for 15 min. Then, reagent **8b** (170 mg, 0.51 mmol) was quickly added to the flask and the mixture was stirred at room temperature for 15 min. The reaction mixture was diluted with Et_2O, washed with

saturated aqueous NH_4Cl, and dried over $MgSO_4$. Upon filtration, the organic layer was concentrated under reduced pressure and purified by flash column chromatography (9:0.5 EtOAc/hexane) to afford **21b** (112 mg, 93%) as a yellowish oil.

***R**f* (1:9 EtOAc/hexane): 0.35; **^{1}H NMR ($CDCl_3$, 400 MHz):** δ 7.34–7.19 (m, 5H), 4.32–4.18 (m, 4H), 3.68 (s, 2H), 1.26 (t, *J* = 7.2 Hz, 6H); **^{13}C{^{1}H} NMR ($CDCl_3$, 100.6 MHz):** δ 166.7, 134.0, 130.7, 128.4, 127.8, 122.1 (tq, *J* = 292.3, 40.9), 118.2 (qt, *J* = 286.8, 34.9 Hz), 65.3, 63.3, 41.2 (d, *J* = 1.9 Hz), 13.8; **^{19}F NMR ($CDCl_3$, 376.5 MHz):** δ –83.44 (t, *J* = 3.5 Hz, 3F), –88.59 (q, *J* = 3.5 Hz, 2F); **FTIR–ATR** (neat) ν in cm^{-1}: 1739, 1311, 1259, 1217, 1095, 1083, 959, 750, 701; **HRMS (APCI$^+$)** for $(M+H)^+$ $C_{16}H_{18}F_5O_4S^+$ (*m*/*z*): calc. 401.0840; found 401.0828.

(*E*/*Z*)-(2-(Naphthalen-2-yl)vinyl)(1,1,2,2-tetrafluoroethyl)sulfane (**22a**). A 25 mL round-bottom flask, equipped with a magnetic stir bar, was charged with 2-vinylnaphthalene (46 mg, 0.3 mmol). The flask was then evacuated and backfilled with argon three times. Subsequently, anhydrous MeCN (9 mL) was added using a syringe followed by trimethylsilyl chloride (114 μL, 0.9 mmol). Then, reagent **8a** (104 mg, 0.33 mmol) was quickly added to the flask. The mixture was stirred at room temperature for 5 h. Next, 1,8-diazabicyclo[5.4.0]undec-7-ene (DBU, 269 μL, 1.8 mmol) was added and the mixture was left to stir at room temperature for 16 h. Then, the reaction mixture was concentrated under reduced pressure and purified by flash column chromatography (hexane) to afford **22a** (85 mg, 99%) as a white solid as an inseparable 96:4 *E*/*Z* mixture.

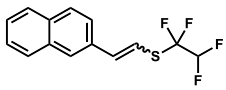

***R**f* (hexane): 0.24; **m.p**: 48–50 °C; **FTIR–ATR** (neat) ν in cm^{-1}: 2320, 1699, 1653, 1558, 1541, 1507, 1457, 1105; **HRMS (TOF EI)** for $(M)^{+\cdot}$ $C_{14}H_{10}F_4S^{+\cdot}$ (*m*/*z*): calc. 286.0434; found 286.0435. ***E*-isomer: ^{1}H NMR ($CDCl_3$, 400 MHz):** δ 7.87–7.79 (m, 3H), 7.76 (d, *J* = 0.7 Hz, 1H), 7.57 (dt, *J* = 6.7, 3.3 Hz, 1H), 7.53–7.45 (m, 2H), 7.16 (d, *J* = 15.4 Hz, 1H), 6.86 (d, *J* = 15.3 Hz, 1H), 5.92 (tt, *J* = 53.8, 3.2 Hz, 1H); **^{13}C{^{1}H} NMR ($CDCl_3$, 100.6 MHz):** δ 141.0, 133.6, 133.5, 132.9, 128.8, 128.4,

127.9, 127.5, 126.8, 126.8, 123.2, 122.7 (tt, *J* = 284.4, 30.0 Hz), 111.5 (t, *J* = 5.0 Hz), 109.8 (tt, *J* = 253.1, 38.3 Hz); **^{19}F NMR ($CDCl_3$, 376.5 MHz):** δ –92.94 (td, *J* = 8.9, 2.8 Hz, 2F), –132.08 (dt, *J* = 54.0, 8.9 Hz, 2F). Selected signals for the ***Z*-isomer: ^{1}H NMR ($CDCl_3$, 400 MHz):** δ 6.98 (d, *J* = 10.5 Hz, 1H), 6.53 (d, *J* = 10.6 Hz, 1H); **^{19}F NMR ($CDCl_3$, 376.5 MHz):** δ –93.93 (td, *J* = 8.4, 2.8 Hz, 2F), 131.9–132.1 (m, 2H).

(*E*/*Z*)-(2-(Naphthalen-2-yl)vinyl)(perfluoroethyl)sulfane (**22b**). A 25 mL

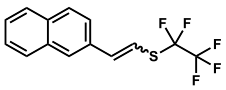

round-bottom flask, equipped with a magnetic stir bar, was charged with 2-vinylnaphthalene (46 mg, 0.3 mmol). The flask was then evacuated and backfilled with argon three times. Subsequently, anhydrous MeCN (9 mL) was added using a syringe followed by trimethylsilyl chloride (228 μL, 1.8 mmol). Then, reagent **8b** (220 mg, 0.66 mmol) was quickly added to the flask. The mixture was stirred at 65 °C for 16 h. Next, 1,8-diazabicyclo[5.4.0]undec-7-ene (DBU, 269 μL, 1.8 mmol) was added and the mixture was left to stir at room temperature for 16 h. Then, the reaction mixture was concentrated under reduced pressure and purified by flash column chromatography (hexane) to afford **22b** (51 mg, 56%) as a white solid as an inseparable 88:12 *E*/*Z* mixture.

***R**f* (hexane): 0.50; **m.p**: 46–48 °C; **FTIR–ATR** (neat) ν in cm^{-1}: 1507, 1338, 1202, 1092, 947, 862, 819, 795, 748, 624, 479; **HRMS** (APCI$^+$) for $(M)^{+\cdot}$ $C_{14}H_9F_5S^{+\cdot}$ (*m*/*z*): calc. 304.0340; found 304.0334. ***E*-isomer: ^{1}H NMR ($CDCl_3$, 400 MHz):** δ 7.89–7.80 (m, 3H), 7.77 (s, 1H), 7.57 (dd, *J* = 8.6, 1.7 Hz, 1H), 7.54–7.48 (m, 2H), 7.20 (d, *J* = 15.3 Hz, 1H), 6.82 (d, *J* = 15.3 Hz, 1H); **^{13}C{^{1}H} NMR ($CDCl_3$, 100.6 MHz):** δ 142.4, 133.8, 133.5, 132.6, 128.8, 128.5, 127.9, 127.8, 127.0, 126.9, 123.2, 120.3 (tq, *J* = 288.8, 40.7 Hz), 118.9 (qt, *J* = 286.3, 37.2 Hz), 110.6 (t, *J* = 5.0 Hz); **^{19}F NMR ($CDCl_3$, 376.5 MHz):** δ –82.98 (t, *J* = 3.3 Hz, 2F), –93.76 (q, *J* = 3.7 Hz, 2F). Selected signals for the ***Z*-isomer: ^{1}H NMR ($CDCl_3$, 400 MHz):** δ 7.02 (d, *J* = 10.5 Hz, 1H), 6.48 (d, *J* = 10.5 Hz, 1H); **^{19}F NMR ($CDCl_3$, 376.5 MHz):** δ –83.24 (t, *J* = 3.3 Hz, 2F), –94.69 (q, *J* = 3.6 Hz, 2F).

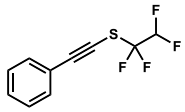

(Phenylethynyl)(1,1,2,2-tetrafluoroethyl)sulfane (**23a**). A 0.42 M stock solution of lithium phenylacetylide was prepared using the following procedure: a 5 mL round-bottom flask, equipped with a magnetic stir bar, was charged with phenylacetylene (102 mg, 1.0 mmol). The flask was then evacuated and backfilled with argon three times. Subsequently, anhydrous THF (2 mL) was added using a syringe and the mixture was cooled down to –78 °C. Next, a titrated solution of *n*-BuLi (2.88 M in hexanes, 0.38 mL, 1.1 mmol) was added dropwise. The mixture was stirred at –78 °C for 30 min. To a 5 mL round-bottom flask, equipped with a magnetic stir bar, reagent **8a** (114 mg, 0.36 mmol) was charged. The flask was then evacuated and backfilled with argon three times. Subsequently, anhydrous THF (2.2 mL) was added using a syringe and the mixture was cooled down to –78 °C. Then, the previously prepared solution of lithium phenylacetylide (0.72 mL, 0.3 mmol) was added dropwise to the reaction flask. The reaction mixture was stirred at –78 °C for 15 min and then left to warm up to room temperature. Finally, the crude was cooled down to 0 °C and first quenched with H_2O (5 mL) and secondly with saturated aqueous NH_4Cl (5 mL). The mixture is transferred to an extraction funnel and the organic layer is separated and dried over $MgSO_4$. Upon filtration, the organic layer was concentrated under reduced pressure and purified by flash column chromatography (pentane) to afford **23a** (59 mg, 84%) as a colorless liquid.

***R**f* (hexane): 0.40; **^{1}H NMR ($CDCl_3$, 400 MHz):** δ 7.50–7.45 (m, 2H), 7.40–7.30 (m, 3H), 6.05 (tt, *J* = 53.4, 3.8 Hz, 1H); **^{13}C{^{1}H} NMR ($CDCl_3$, 100.6 MHz):** δ 132.2, 129.7, 128.5, 121.6, 121.4 (tt, *J* = 290.1, 29.5 Hz), 108.9 (tt, *J* = 254.0, 35.8 Hz), 99.8, 66.9 (s, *J* = 6.6 Hz); **^{19}F** NMR ($CDCl_3$, 376.5 MHz): δ –95.12 (td, *J* = 8.9, 3.8 Hz, 2F), –133.50 (dt, *J* = 53.4, 9.0 Hz, 2F); **FTIR**–ATR (neat) ν in cm^{-1}: 2923, 1653, 1558, 1541, 1457, 465; **HRMS (APCI$^+$)** for $(M)^{+\cdot}$ $C_{10}H_6F_4S^{+\cdot}$ (*m*/*z*): calc. 234.0126; found 234.0116.

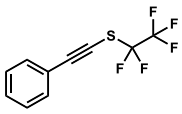

(Perfluoroethyl)(phenylethynyl)sulfane (**23b**). A 0.41 M stock solution of lithium phenylacetylide was prepared using the following procedure: a 5 mL round-bottom flask, equipped with a magnetic stir bar, was charged with phenylacetylene (102 mg, 1.0 mmol). The flask was then evacuated and backfilled with argon three times. Subsequently, anhydrous THF (2 mL) was added using a syringe and the mixture was cooled down to –78 °C. Next, a titrated solution of *n*-BuLi (2.58 M in hexanes, 0.43 mL, 1.1 mmol) was added dropwise. The mixture was stirred at –78 °C for 30 min. To a 5 mL round-bottom flask, equipped with a magnetic stir bar, reagent **8b** (120 mg, 0.36 mmol) was charged. The flask was then evacuated and backfilled with argon three times. Subsequently, anhydrous THF (2 mL) was added using a syringe and the mixture was cooled down to –78 °C. Then, the previously prepared solution of lithium phenylacetylide (0.73 mL, 0.3 mmol) was added dropwise to the reaction flask. The reaction mixture was stirred at –78 °C for 15 min and then left to warm up to room temperature. Finally, the crude was cooled down to 0 °C and first quenched with H_2O (5 mL) and secondly with saturated aqueous NH_4Cl (5 mL). The mixture is transferred to an extraction funnel and the organic layer is separated and dried over $MgSO_4$. Upon filtration, the organic layer was concentrated under reduced pressure and purified by flash column chromatography (pentane) to afford **23b** (40 mg, 53%) as a yellowish semisolid.

***R**f* (hexane): 0.61; **^{1}H NMR ($CDCl_3$, 400 MHz):** δ 7.57–7.47 (m, 2H), 7.45–7.32 (m, 3H); **^{13}C{^{1}H} NMR ($CDCl_3$, 100.6 MHz):** δ 132.4, 129.9, 128.6, 121.7, 119.1 (tq, *J* = 294.8, 40.0), 118.6 (qt, *J* = 287.1, 36.4 Hz), 101.0, 65.9 (t, *J* = 6.4 Hz); **^{19}F NMR ($CDCl_3$, 376.5 MHz):** δ –82.59 (t, *J* = 2.7 Hz, 3F), –94.61 (q, *J* = 2.6 Hz, 2F); **FTIR–ATR** (neat) ν in cm^{-1}: 2922, 2320, 1221, 1109, 958, 753; **HRMS (APCI$^+$)** for $(M)^{+\cdot}$ $C_{10}H_5F_5S^{+\cdot}$ (*m*/*z*): calc. 252.0032; found 252.0024.

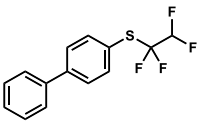

[1,1'-Biphenyl]-4-yl(1,1,2,2-tetrafluoroethyl)sulfane (**24a**). A 0.18 M stock solution of [1,1′-biphenyl]-4-yllithium was prepared using the following procedure: a 10 mL round-bottom flask, equipped with a magnetic stir bar, was charged with 4-bromo-1,1′-biphenyl (233 mg, 1.0 mmol). The flask was then evacuated and backfilled with argon three times. Subsequently, anhydrous THF (5.5 mL) was added using a syringe and the mixture was cooled down to –78 °C. Next, a titrated solution of *n*-BuLi (2.88 M in hexanes, 0.36 mL, 1.0 mmol) was added dropwise. The mixture was stirred at –78 °C for 1.5 h. To a 25 mL round-bottom flask, equipped with a magnetic stir bar, reagent **8a** (114 mg, 0.36 mmol) was charged. The flask was then evacuated and backfilled with argon three times. Subsequently, anhydrous THF (8.4 mL) was added using a syringe and the mixture was cooled down to –78 °C. Then, the previously prepared solution of [1,1′-biphenyl]-4-yllithium (1.8 mL, 0.3 mmol) was added dropwise to the reaction flask. The reaction mixture was stirred at –78 °C for 30 min and then left to warm up to room temperature. Finally, the crude was cooled down to 0 °C and first quenched with H_2O (3 mL) and secondly with saturated aqueous NH_4Cl (3 mL). The mixture is transferred to an extraction funnel and the organic layer is separated and dried over $MgSO_4$. Upon filtration, the organic layer was concentrated under reduced pressure and purified by flash column chromatography (pentane) to afford **24a** (60 mg, 70%) as a white solid.

***R**f* (pentane): 0.48; **m.p**: 42–44 °C; **^{1}H NMR ($CDCl_3$, 400 MHz):** δ 7.75–7.69 (m, 2H), 7.67–7.58 (m, 4H), 7.53–7.45 (m, 2H), 7.44–7.35 (m, 1H), 5.82 (tt, *J* = 53.8, 3.4 Hz, 1H); **^{13}C{^{1}H} NMR ($CDCl_3$, 100.6 MHz):** δ 143.68, 139.66, 137.38, 128.96, 128.12, 128.05, 127.20, 122.45 (tt, *J* = 284.9, 29.3 Hz), 122.05, 109.43 (tt, *J* = 253.2, 37.5 Hz); **^{19}F NMR ($CDCl_3$, 376.5 MHz):** δ –91.8 (td, *J* = 9.5, 2.8 Hz, 2F), –133.7 (dt, *J* = 53.8, 9.6 Hz, 2F); **FTIR–ATR** (neat) ν in cm^{-1}: 1477, 1379, 1097, 1005, 836, 760, 688, 673, 626, 473; **HRMS (APCI$^+$)** for $(M)^{+\cdot}$ $C_{14}H_{10}F_4S^{+\cdot}$ (*m*/*z*): calc. 286.0439; found 286.0427.

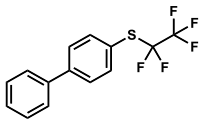

[1,1'-Biphenyl]-4-yl(perfluoroethyl)sulfane (**24b**). A 2.0 M stock solution of [1,1'-biphenyl]-4-yllithium was prepared using the following procedure: a 10 mL round-bottom flask, equipped with a magnetic stir bar, was charged with 4-bromo-1,1'-biphenyl (233 mg, 1.0 mmol). The flask was then evacuated and backfilled with argon three times. Subsequently, anhydrous THF (5.5 mL) was added using a syringe and the mixture was cooled down to –78 °C. Next, a titrated solution of *n*-BuLi (2.58 M in hexanes, 0.39 mL, 1.0 mmol) was added dropwise. The mixture was stirred at –78 °C for 1.5 h. To a 25 mL round-bottom flask, equipped with a magnetic stir bar, reagent **8b** (160 mg, 0.48 mmol) was charged. The flask was then evacuated and backfilled with argon three times. Subsequently, anhydrous THF (8 mL) was added using a syringe and the mixture was cooled down to –78 °C. Then, the previously prepared solution of [1,1'-biphenyl]-4-yllithium (0.2 mL, 0.4 mmol) was added dropwise to the reaction flask. The reaction mixture was stirred at –78 °C for 30 min and then left to warm up to room temperature. Finally, the crude was cooled down to 0 °C and first quenched with H_2O (3 mL) and secondly with saturated aqueous NH_4Cl (3 mL). The mixture is transferred to an extraction funnel and the organic layer is separated and dried over $MgSO_4$. Upon filtration, the organic layer was concentrated under reduced pressure and purified by flash column chromatography (hexane) to afford **24b** (76 mg, 62%) as a white solid.

***R**f* (hexane): 0.55; **m.p**: 54–56 °C; **^{1}H NMR ($CDCl_3$, 400 MHz):** δ 7.72 (m, 2H), 7.67–7.56 (m, 4H), 7.52–7.45 (m, 2H), 7.44–7.36 (m, 1H). **^{13}C{^{1}H} NMR ($CDCl_3$, 100.6 MHz):** δ 144.5. 141.2, 139.9, 139.8, 138.0, 129.4, 128.6, 128.5, 127.6, 121.6 (t, *J* = 3.3 Hz), 121.1–114.5 (m); **^{19}F NMR ($CDCl_3$, 376.5 MHz):** δ –82.82 (t, *J* = 3.6 Hz, 3F), –92.15 (q, *J* = 3.6 Hz, 2F); **FTIR–ATR** (neat) ν in cm^{-1}: 2319, 1336, 1204, 1104, 1089, 970, 837, 761, 718, 690; **HRMS (APCI$^+$)** for $(M)^{+\cdot}$ $C_{14}H_9F_5S^{+\cdot}$ (*m*/*z*): calc. 304.0345; found 304.0333.

1,5-Anhydro-3,4,6-tri-*O*-benzyl-2-deoxy-2-(1,1,2,2-tetrafluoroethyl)thio-*D*-

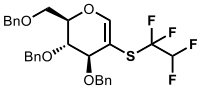

arabino-hex-1-enitol (**25a**). A 5 mL round-bottom flask, equipped with a magnetic stir bar, was charged with tri-*O*-benzyl-D-glucal (42 mg, 0.1 mmol) and 3 Å molecular sieves (300 mg, 3 g/mmol glucal). The flask was then evacuated and backfilled with argon three times. Subsequently, anhydrous MeCN (1.5 mL) and reagent **8a** (38 mg, 0.12 mmol) were added. The mixture was stirred at room temperature for 2 h. Then, trimethylsilyl chloride (38 μL, 0.3 mmol) was added and the mixture was stirred until complete consumption of the starting material as monitored by TLC (*ca.* 3.5 h). Next, 1,8-diazabicyclo(5.4.0)undec-7-ene (45 μL, 0.6 mmol) was added and the reaction mixture was left to stir at room temperature for 16 h. The reaction mixture was diluted with CH_2Cl_2, filtered through Celite® washed with H_2O, brine, and dried over $MgSO_4$. Upon filtration, the organic layer was concentrated under reduced pressure and purified by flash column chromatography (1:9 EtOAc/hexane) to afford **25a** (44 mg, 80%) as a colorless oil.

***R**f* (1:9 EtOAc/hexane): 0.19; **^{1}H NMR ($CDCl_3$, 400 MHz):** δ 7.40–7.23 (m, 15H), 6.98 (s, 1H), 5.87 (tdd, *J* = 53.7, 4.9, 2.9 Hz, 1H), 4.74 (d, *J* = 11.1 Hz, 1H), 4.66 (d, *J* = 11.6 Hz, 1H), 4.61 (d, *J* = 11.1 Hz, 1H), 4.58 (d, *J* = 11.6 Hz, 1H), 4.53 (s, 2H), 4.47–4.40 (m, 1H), 4.08 (d, *J* = 4.0 Hz, 1H), 3.91 (dd, *J* = 5.0, 4.3 Hz, 1H), 3.77 (dd, *J* = 10.7, 6.3 Hz, 1H), 3.68 (dd, *J* = 10.7, 4.2 Hz, 1H); **^{13}C{^{1}H} NMR ($CDCl_3$, 100.6 MHz):** δ 156.1, 137.8, 137.7, 137.5, 128.7, 128.6, 128.24, 128.2, 128.1, 128.0, 127.9, 127.9, 125.9–119.3 (m), 108.2 (tdd, *J* = 252.7, 38.6, 35.3 Hz), 97.0 (t, *J* = 2.9 Hz), 77.0, 76.3, 73.6, 73.4, 72.9, 67.9; **^{19}F NMR ($CDCl_3$, 376.5 MHz):** δ –92.6 (m, 1F), –95.1 (m, 1F), –133.74 (m, 2F); **FTIR–ATR** (neat) ν in cm^{-1}: 1613, 1454, 1365, 1210, 1184, 1102, 1065, 989, 914, 811, 735, 695; **HRMS (TOF ESI$^+$)** for $(M+Na)^+$ $C_{29}H_{28}F_4NaO_4S^+$ (*m*/*z*): calc. 571.1537; found 571.1540.

1,5-Anhydro-3,4,6-tri-*O*-benzyl-2-deoxy-2-(perfluoroethyl)thio-*D*-arabino-hex-1-enitol (**25b**). 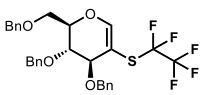 A 5 mL round-bottom flask, equipped with a magnetic stir bar, was charged with tri-*O*-benzyl-D-glucal (126 mg, 0.3 mmol) and 3 Å molecular sieves (900 mg, 3 g/mmol glucal). The flask was then evacuated and backfilled with argon three times. Subsequently, anhydrous MeCN (9 mL) and reagent **8b** (220 mg, 0.66 mmol) were added. The mixture was stirred at room temperature for 2 h. Then, trimethylsilyl chloride (228 μL, 1.8 mmol) was added and the mixture was stirred until complete consumption of the starting material as monitored by TLC (*ca.* 4 h). Next, 1,8-diazabicyclo(5.4.0)undec-7-ene (538 μL, 3.6 mmol) was added and the reaction mixture was left to stir at room temperature for 18 h. The reaction mixture was diluted with CH_2Cl_2, filtered through Celite® washed with H_2O, brine, and dried over $MgSO_4$. Upon filtration, the organic layer was concentrated under reduced pressure and purified by flash column chromatography (hexane to 5:1 EtOAc/hexane) to afford **25b** (130 mg, 78%) as a colorless oil.

***R**f* (1:4 EtOAc/hexane): 0.43; **^{1}H NMR ($CDCl_3$, 400 MHz):** δ 7.69–7.49 (m, 15H), 7.26 (s, 1H), 5.05 (d, *J* = 11.1 Hz, 1H), 4.97 (d, *J* = 11.5 Hz, 1H), 4.91 (d, *J* = 11.1 Hz, 1H), 4.85 (d, *J* = 11.5 Hz, 1H), 4.80 (s, 2H), 4.67 (dd, *J* = 10.0, 5.4 Hz, 1H), 4.40 (d, *J* = 4.6 Hz, 1H), 4.19 (dd, *J* = 5.8, 4.9 Hz, 1H), 4.07 (dd, *J* = 10.7, 5.9 Hz, 1H), 3.99 (dd, *J* = 10.7, 3.9 Hz, 1H); **^{13}C{^{1}H} NMR ($CDCl_3$, 100.6 MHz):** δ 156.6, 137.8, 137.6, 128.6, 128.5, 128.2, 128.1, 128.0, 127.9, 127.9, 127.8, 124–114 (m), 118.9 (qt, *J* = 284.8, 37.2), 97.1 (t, *J* = 2.3 Hz), 77.5, 76.5, 73.8, 73.6, 73.2, 72.2, 67.8; **^{19}F NMR ($CDCl_3$, 376.5 MHz):** δ –82.39 (t, *J* = 3.6 Hz, 3F), –92.79 (q, *J* = 3.4 Hz, 2F); **FTIR–ATR** (neat) ν in cm^{-1}: 1614, 1454, 1329, 1206, 1186, 1091, 1027, 957, 914, 748, 695; **HRMS (TOF ESI$^+$)** for $(M+Na)^+$ $C_{29}H_{27}F_5NaO_4S^+$ (*m*/*z*): calc. 589.1442; found 589.1444.

(2*E*,4*E*)-5-(Benzo[*d*][1,3]dioxol-5-yl)-1-(piperidin-1-yl)-2-((1,1,2,2-tetrafluoro-ethyl)thio)penta-2,4-dien-1-one (**26*E*,*E***) and **(2*Z*,4*E*)-5-(benzo[*d*][1,3]dioxol-5-yl)-1-(piperidin-1-yl)-5-((1,1,2,2-tetrafluoroethyl)thio)penta-2,4-dien-1-one** (**26*Z*,*E***). A 10 mL round-bottom flask, equipped with a magnetic stir bar, was charged with piperine (86 mg, 0.3 mmol). The flask was then evacuated and backfilled with argon three times. Subsequently, anhydrous CH_2Cl_2 (3 mL) was added using a syringe followed by trimethylsilyl chloride (46 μL, 0.36 mmol). Then, reagent **8a** (208 mg, 0.66 mmol) was quickly added to the flask. The mixture was stirred at room temperature for 18 h. Then, the reaction mixture was concentrated under reduced pressure and the crude purified by flash column chromatography (from CH_2Cl_2 to 1:19 CH_3OH/CH_2Cl_2) to afford **26*E*,*E*** (82 mg, 66%) as a yellow solid and **26*E*,*Z*** (19 mg, 15%) as a yellow solid.

***E*-isomer**: R_f (1:19 CH_3OH/CH_2Cl_2): 0.70; **^{1}H NMR ($CDCl_3$, 400 MHz):** δ 7.19 (dd, J = 15.4, 10.7 Hz, 1H), 7.03 (s, 1H), 7.02 (d, J = 10.7 Hz, 1H), 6.93 (dd, J = 8.1, 1.6 Hz, 1H), 6.80 (d, J = 15.4 Hz, 1H), 6.79 (d, J = 8.1 Hz, 1H), 6.06 (tt, J = 53.5, 4.2 Hz, 1H), 5.98 (s, 2H), 3.72–3.30 (m, 4H), 1.73–1.52 (m, 6H); **^{13}C{^{1}H} NMR ($CDCl_3$, 100.6 MHz):** δ 167.8, 149.0, 148.5, 145.9, 141.3, 130.5, 123.4, 122.8 (tt, J = 286.8, 28.8 Hz), 121.9, 117.3 (t, J = 2.8 Hz), 109.3 (tt, J = 253.4, 35.6 Hz), 108.7, 106.2, 101.6, 48.6 (bs), 43.7 (bs), 25.9 (bs), 24.6; **^{19}F NMR ($CDCl_3$, 376.5 MHz):** δ –91.83 (td, J = 9.8, 4.1 Hz, 2H), –133.97 (dt, J = 53.3, 9.9 Hz, 2F); **FTIR–ATR** (neat) ν in cm^{-1}: 2940, 2320, 1624, 1490, 1447, 1255, 1108, 1038, 977, 810; **HRMS (TOF ESI$^+$)** for $(M+H)^+$ $C_{19}H_{20}F_4NO_3S^+$ (m/z): calc. 418.1095; found 418.1093.

***Z*-isomer**: R_f (1:19 CH_3OH/CH_2Cl_2): 0.76; **^{1}H NMR ($CDCl_3$, 400 MHz):** δ 6.93 (d, J = 1.6 Hz, 1H), 6.93 (d, J = 11.1 Hz, 1H), 6.88 (dd, J = 8.1, 1.6 Hz, 1H), 6.78 (d, J = 8.0 Hz, 1H), 6.73 (d, J = 15.5 Hz, 1H), 6.59 (dd, J = 15.5, 11.1 Hz, 1H), 6.15 (tt, J = 53.4, 4.6 Hz, 1H), 5.99 (s, 2H), 3.69 (d, J = 5.5 Hz, 2H), 3.43–3.34 (m, 2H), 1.78–1.53 (m, 6H); **^{13}C{^{1}H} NMR ($CDCl_3$, 100.6 MHz):** δ 165.7, 149.0, 148.5,

145.8, 140.2, 130.3, 123.4, 122.8 (tt, J = 286.4, 29.2 Hz), 121.7, 117.4 (t, J = 3.0 Hz), 109.3 (tt, J = 253.3, 34.8 Hz), 108.8, 106.0, 101.6, 48.2, 43.1, 26.4, 25.7, 24.6; **^{19}F NMR ($CDCl_3$, 376.5 MHz):** δ –93.01 (bs, 2F), –134.53 (bd, J = 53.2 Hz, 2F); **FTIR–ATR** (neat) ν in cm^{-1}: 2940, 2859, 1620, 1504, 1490, 1445, 1254, 1209, 1107, 1038, 993, 972, 810; **HRMS (TOF ES$^+$)** for $(M+H)^+$ $C_{19}H_{20}F_4NO_3S^+$ (m/z): calc. 418.1095; found 418.1091.

(1*S*,2*R*)-1-Phenyl-2-(((1,1,2,2-tetrafluoroethyl)thio)amino)propan-1-ol (*D*-(+)-Norephedrine-SCF_2CF_2H, (**27a**). A 5 mL round-bottom flask, equipped with a magnetic stir bar, was charged with (*1S,2R*)-(+)-norephedrine (46 mg, 0.3 mmol). The flask was then evacuated and backfilled with argon three times. Subsequently, anhydrous CH_2Cl_2 (3 mL) was added using a syringe. Next, reagent **8a** (284 mg, 0.9 mmol) was quickly added to the flask and the mixture was stirred at room temperature for 3 h. Then, the reaction mixture was concentrated under reduced pressure and purified by flash column chromatography (1:10 MeOH/CH_2Cl_2) to afford **27a** (50 mg, 59%) as a colorless syrup.

***R**$_f$* (1:19 CH_3OH/CH_2Cl_2): 0.67; **^{1}H NMR ($CDCl_3$, 400 MHz):** δ 7.41–7.27 (m, 5H), 5.90 (tt, *J* = 53.8, 3.9 Hz, 1H), 4.87 (d, *J* = 3.9 Hz, 1H), 3.33–3.21 (m, 1H), 2.88 (bd, *J* = 4.9 Hz, 1H), 2.17 (bs, *J* = 69.3 Hz, 1H), 1.04 (d, *J* = 6.7 Hz, 3H); **^{13}C{^{1}H} NMR ($CDCl_3$, 100.6 MHz):** 140.7, 128.6, 128.0, 126.3, 122.9 (tt, *J* = 285.5, 28.0 Hz), 109.5 (tt, *J* = 250.8, 37.6 Hz), 75.4, 63.3, 14.9; **^{19}F NMR ($CDCl_3$, 376.5 MHz):** δ –102.45 (dtd, *J* = 244.7, 8.4, 4.0 Hz, 1F), –103.18 (dtd, *J* = 20.8, 8.8, 4.0 Hz, 1F), –134.74 (dt, *J* = 53.7, 8.5 Hz, 2F); **FTIR–ATR** (neat) ν in cm^{-1}: 3350, 2310, 1699, 1684, 1653, 1558, 1541, 1507, 1457, 1111, 703; **HRMS (APCI$^-$)** for $(M–H)^-$ $C_{11}H_{12}F_4NOS^-$ (*m*/*z*): calc. 282.0581; found 282.0574.

(1*S*,2*R*)-2-(((Perfluoroethyl)thio)amino)-1-phenylpropan-1-ol (***D*-(+)-Norephedrine-SCF_2CF_3**, (**27b**). A 5 mL round-bottom flask, equipped with a magnetic stir bar, was charged with *(1S,2R)*-(+)-norephedrine (46 mg, 0.3 mmol). The flask was then evacuated and

backfilled with argon three times. Subsequently, anhydrous CH_2Cl_2 (3 mL) was added using a syringe. Next, reagent **8b** (300 mg, 0.9 mmol) was quickly added to the flask and the mixture was stirred at room temperature for 3 h. Then, the reaction mixture was concentrated under reduced pressure and purified by flash column chromatography (1:10 MeOH/CH_2Cl_2) to afford **27b** (81 mg, 90%) as a colorless syrup.

***R**f* (1:19 CH_3OH/CH_2Cl_2): 0.71; **^{1}H NMR ($CDCl_3$, 400 MHz):** δ 7.42–7.28 (m, 5H), 4.84 (d, *J* = 3.9 Hz, 1H), 3.37–3.24 (m, 1H), 2.97 (d, *J* = 4.4 Hz, 1H), 2.26 (s, *J* = 37.0 Hz, 1H), 1.05 (d, *J* = 6.7 Hz, 3H); **^{13}C{^{1}H} NMR ($CDCl_3$, 100.6 MHz):** 140.5, 128.6, 128.0, 126.4, 120.3 (tq, *J* = 290.5, 38.9 Hz), 119.0 (qt, *J* = 287.4, 37.2 Hz), 75.7, 63.2, 14.7; **^{19}F NMR ($CDCl_3$, 376.5 MHz):** δ –82.56 (t, *J* = 3.1 Hz), –102.79 (dq, *J* = 245.6, 2.8 Hz), –103.52 (dq, *J* = 245.8, 2.8 Hz); **FTIR–ATR** (neat) ν in cm^{-1}: 3370, 2310, 1699, 1684, 1653, 1558, 1541, 1507, 1457, 1208; **HRMS (TOF ESI$^-$)** for $(M–H)^-$ $C_{11}H_{11}F_5NOS^-$ (*m*/*z*): calc. 300.0487; found 300.0479.

2-((1-Benzylpiperidin-4-yl)methyl)-5,6-dimethoxy-2-((1,1,2,2-tetrafluoroethyl)thio)-2,3-dihydro-1*H*-inden-1-one (**Donepezil-SCF_2CF_2H**, **28**). To a solution of donepezil (114 mg, 0.3 mmol) in anhydrous THF (1.5 mL) at –78 °C was added KHMDS (1.0 M in toluene, 0.4 mL, 0.38 mmol) and stirred at the same temperature for 1 h. Then, a solution in anhydrous THF (2 mL) of the reagent **8a** (142 mg, 0.45 mmol) was added dropwise under argon to the donepezil potassium enolate solution and the reaction mixture was stirred at –78 °C for 1 h. Next, water was added to the reaction mixture (5 mL) and the product was extracted successively with CH_2Cl_2 (3 x 20 mL). The combined organic fractions were dried with Na_2SO_4, filtered, and evaporated under reduced pressure. The organic crude was purified by flash column chromatography (from CH_2Cl_2 to 1:19 CH_3OH/CH_2Cl_2) to afford **28** (152 mg, 99%) as a brown syrup.

***R**f* (1:19 CH_3OH/CH_2Cl_2): 0.35; **^{1}H NMR ($CDCl_3$, 400 MHz):** δ 7.34–7.20 (m, 5H), 7.20 (s, 1H), 6.83 (s, 1H), 5.76 (tt, J = 53.8, 3.8 Hz, 1H), 3.98 (s, 3H), 3.92 (s,

3H), 3.57 (d, J = 17.8 Hz, 1H), 3.47 (s, 2H), 3.42 (d, J = 17.9 Hz, 1H), 2.81 (bd, J = 8.9 Hz, 2H), 2.07–1.86 (m, 3H), 1.82 (dd, J = 14.4, 7.1 Hz, 1H), 1.68–1.46 (m, 3H), 1.42–1.21 (m, 2H); **$^{13}C\{^1H\}$ NMR ($CDCl_3$, 100.6 MHz):** 201.1, 156.6, 150.1, 145.8, 138.3, 129.3, 128.2, 127.0, 126.8, 124.3 (tt, J = 287.1, 29.4 Hz), 109.4 (tt, J = 253.8, 36.2 Hz), 107.1, 105.2, 63.4, 60.0, 56.4, 56.2, 53.6, 53.5, 44.7, 41.8, 33.8, 33.3, 33.0; **^{19}F NMR ($CDCl_3$, 376.5 MHz):** δ –87.07 (m, 2F), –132.39 (ddt, J = 294.9, 54.0, 10.0 Hz, 1F), –133.29 (ddt, J = 294.9, 54.2, 10.0 Hz, 1F); **FTIR–ATR (neat)** ν in cm^{-1}: 1701, 1592, 1504, 1457, 1311, 1271, 1115, 742; **HRMS (TOF ES$^+$)** for $(M+H)^+$ $C_{26}H_{30}F_4NO_3S^+$ (m/z): calc. 512.1877; found 512.1878.

5-Benzoyl-7-((1,1,2,2-tetrafluoroethyl)thio)-2,3-dihydro-1*H*-pyrrolizine-1-carboxylic acid (**Ketorolac-SCF_2CF_2H**, **29**). A 10 mL round-bottom flask, equipped with a magnetic stir bar, was charged with ketorolac (77 mg, 0.3 mmol). The flask was then evacuated and backfilled with argon three times. Subsequently, anhydrous CH_2Cl_2 (3 mL) was added using a syringe followed by trimethylsilyl chloride (76 μL, 0.6 mmol). Then, reagent **8a** (189 mg, 0.6 mmol) was quickly added to the flask. The mixture was stirred at room temperature for 18 h. Then, the reaction mixture was concentrated under reduced pressure and the crude purified by flash column chromatography (10:1:0.1 CH_2Cl_2/MeCN/AcOH) to afford **29** (101 mg, 87%) as a purple syrup. R_f (1:19 CH_3OH/CH_2Cl_2): 0.29; **^1H NMR ($CDCl_3$, 400 MHz):** δ 10.17 (bs, 1H), 7.90–7.71 (m, 2H), 7.64–7.55 (m, 1H), 7.48 (t, *J* = 7.5 Hz, 2H), 6.99 (s, 1H), 5.79 (tt, *J* = 53.7, 3.5 Hz, 1H), 4.67–4.50 (m, 2H), 4.16 (dd, *J* = 9.0, 4.2 Hz, 1H), 3.03–2.80 (m, 2H); **$^{13}C\{^1H\}$ NMR ($CDCl_3$, 100.6 MHz):** δ 185.3, 176.67, 147.3, 138.2, 132.3, 131.4, 129.1, 128.6, 128.2, 122.1 (tt, *J* = 284.2, 29.2 Hz), 109.5 (tt, *J* = 252.9, 37.3 Hz), 95.3 (t, *J* = 4.0 Hz), 48.9, 42.2, 32.3.; **^{19}F NMR ($CDCl_3$, 376.5 MHz):** δ –92.83 (dtd, *J* = 231.8, 9.4, 3.4 Hz, 1F), –93.5 (dtd, *J* = 231.4, 9.4, 3.7 Hz, 1F), –132.9 (m, 2F); **FTIR–ATR** (neat) ν in cm^{-1}: 2934, 2375, 2320, 1716, 1633, 1457, 1393, 1258, 1213, 1110, 998, 725; **HRMS (TOF ESI$^+$)** for $(2M+Na)^+$ $C_{34}H_{26}F_8N_2NaO_6S_2^+$ (*m*/*z*): calc. 797.0997; found 797.1001.

2-(6-Methoxy-7-((1,1,2,2-tetrafluoroethyl)thio)naphthalen-2-yl)propanoic acid (**30a**). 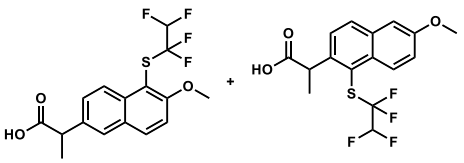 A 5 mL round-bottom flask, equipped with a magnetic stir bar, was charged with *rac*-naproxen (69.1 mg, 0.3 mmol). The flask was then evacuated and backfilled with argon three times. Subsequently, anhydrous $CHCl_3$ (3 mL) was added using a syringe followed by trifluoromethanesulfonic acid (32 μL, 0.36 mmol). Then, reagent **8a** (141.8 mg, 0.45 mmol) was quickly added to the flask. The mixture was stirred at 40 °C with an aluminum heating block for 16 h. The reaction mixture was diluted with Et_2O, washed with saturated aqueous $NaHCO_3$ and dried over $MgSO_4$. Upon filtration, the organic layer was concentrated under reduced pressure and purified by flash column chromatography (10:1:0.1 CH_2Cl_2/MeCN/AcOH) to afford **30a** (102 mg, 93%) as a purple syrup as an inseparable 81:19 C10/C17 mixture.

C10-isomer: R_f (1:19 CH_3OH/CH_2Cl_2): 0.40; **^{1}H NMR ($CDCl_3$, 400 MHz):** δ 11.0 (bs, 1H), 8.4 (d, *J* = 8.9 Hz, 1H), 7.8 (d, *J* = 9.1 Hz, 1H), 7.6 (d, *J* = 2.0 Hz, 1H), 7.5 (dd, *J* = 8.9, 2.0 Hz, 1H), 7.2 (d, *J* = 9.1 Hz, 1H), 5.7 (tt, *J* = 53.7, 4.1 Hz, 1H), 3.9 (s, 2H), 3.8 (q, *J* = 7.1 Hz, 1H), 1.5 (d, *J* = 7.1 Hz, 3H); **^{13}C{^{1}H} NMR ($CDCl_3$, 100.6 MHz):** δ 180.9, 161.0, 136.9, 135.8, 134.0, 129.5, 128.2, 126.8, 126.0, 125.1, 122.6 (tt, *J* = 287.2, 28.53 Hz), 113.4, 109.7 (tt, *J* = 253.3, 36.3 Hz), 56.9, 45.2, 18.1; **^{19}F NMR ($CDCl_3$, 376.5 MHz):** δ –92.6 (td, *J* = 10.2, 4.1 Hz, 1F), –133.1 (dt, *J* = 53.9, 10.2 Hz, 1F); **FTIR–ATR** (neat) ν in cm^{-1}: 2978, 1706, 1595, 1498, 1274, 1207, 1106, 1065, 979, 806; **HRMS (TOF ESI$^+$)** for $(M+Na)^+$ $C_{16}H_{14}F_4NaO_3S^+$ (*m*/*z*): calc. 385.0492; found 385.0474.

Selected signals for the **C17-isomer**: **^{1}H NMR ($CDCl_3$, 400 MHz):** δ 8.2 (d, *J* = 8.8 Hz, 1H), 7.8 (d, *J* = 9.1 Hz, 1H), 7.1–7.1 (m, 1H), 6.1 (tt, *J* = 53.6, 4.4 Hz, 1H), 3.9 (s, 3H). **^{19}F NMR ($CDCl_3$, 376.5 MHz):** δ –95.7 (td, *J* = 9.9, 4.4 Hz, 1F), –135.0 (dt, *J* = 53.6, 10.0 Hz, 1F).

2-(6-Methoxy-7-((1,1,2,2-tetrafluoroethyl)thio)naphthalen-2-yl)propanoic acid (**30b**). *A* 5 mL round-bottom flask, equipped with a magnetic stir bar, was charged with *rac*-naproxen (69.1 mg, 0.3 mmol). The flask was then evacuated and backfilled with argon three times. Subsequently, anhydrous $CHCl_3$ (3 mL) was added using a syringe followed by trifluoromethanesulfonic acid (32 μL, 0.36 mmol). Then, reagent **8b** (150.0 mg, 0.45 mmol) was quickly added to the flask. The mixture was stirred at 70 °C with an aluminum heating block for 16 h. The reaction mixture was diluted with Et_2O, washed with saturated aqueous $NaHCO_3$ and dried over $MgSO_4$. Upon filtration, the organic layer was concentrated under reduced pressure and purified by flash column chromatography (10:1:0.1 CH_2Cl_2/MeCN/AcOH) to afford **30b** (105 mg, 92%) as a purple syrup.

***R**f* (1:19 CH_3OH/CH_2Cl_2): 0.58; **^{1}H NMR ($CDCl_3$, 400 MHz):** δ 10.0 (bs, 1H), 8.46 (d, *J* = 8.8 Hz, 1H), 7.98 (d, *J* = 9.0 Hz, 1H), 7.73 (d, *J* = 1.9 Hz, 1H), 7.59 (dd, *J* = 8.8, 1.9 Hz, 1H), 7.33 (d, *J* = 9.0 Hz, 1H), 4.03 (s, 3H), 3.91 (q, *J* = 7.1 Hz, 1H), 1.61 (d, *J* = 7.1 Hz, 3H); **^{13}C{^{1}H} NMR ($CDCl_3$, 100.6 MHz):** δ 180.5, 161.2, 136.7, 135.6, 134.2, 129.3, 128.2, 126.7, 125.7, 120.1 (m), 117.3 (m), 113.3, 103.8, 56.8, 45.0, 18.0.; **^{19}F NMR ($CDCl_3$, 376.5 MHz):** δ –83.1 (t, *J* = 3.5 Hz, 3F), –91.1 (q, *J* = 3.5 Hz, 2F); **FTIR–ATR** (neat) ν in cm^{-1}: 2917, 1704, 1596, 1458, 1328, 1274, 1196, 1096, 951, 806, 748; **HRMS (TOF ESI$^+$)** for $(M+Na)^+$ $C_{16}H_{13}F_5NaO_3S^+$ (*m*/*z*): calc. 403.0398; found 403.0378.

***N*-Methyl-*N*-(3-phenyl-3-(4-(trifluoromethyl)phenoxy)propyl)-*S*-(1,1,2,2-tetrafluoroethyl)thiohydroxylamine** (**Fluoxetine-SCF_2CF_2H**, **31a**). A 10 mL round-bottom flask, equipped with a magnetic stir bar, was charged with fluoxetine (155 mg, 0.5 mmol). The flask was then evacuated and backfilled with argon three times. Subsequently, anhydrous CH_2Cl_2 (5 mL) was added using a syringe. Next, reagent **8a** (237 mg, 0.75 mmol) was quickly added to the flask followed by triethylamine (77 μL, 0.55 mmol). The mixture was

stirred at room temperature for 3 h. Lastly, the reaction mixture was concentrated under reduced pressure and purified by flash column chromatography (1:9 EtOAc/hexane) to afford **31a** (170 mg, 77%) as a colorless syrup.

***R**f* (1:4 EtOAc/hexane): 0.45; **^{1}H NMR ($CDCl_3$, 400 MHz):** δ 7.46 (d, J = 9.0 Hz, 2H), 7.41–7.34 (m, 4H), 7.34–7.26 (m, 1H), 6.92 (d, J = 8.6 Hz, 2H), 5.82 (tt, J = 54.1, 3.5 Hz, 1H), 5.23 (dd, J = 8.6, 4.6 Hz, 1H), 3.32–3.16 (m, 2H), 2.98 (s, 3H), 2.35–2.12 (m, 2H); **^{13}C{^{1}H} NMR ($CDCl_3$, 100.6 MHz):** 160.6 (bq, J = 1.1 Hz), 140.9, 129.0, 128.1, 126.9 (q, J = 3.8 Hz), 125.9, 125.7 (tt, J = 289.4, 30.4 Hz), 124.8 (q, J = 271.5 Hz), 123.1 (q, J = 32.7 Hz), 115.9, 109.6 (tt, J = 251.1, 38.0 Hz), 77.8, 56.9, 48.4, 37.2; **^{19}F NMR ($CDCl_3$, 376.5 MHz):** δ –61.59 (s, 3F), –97.63 (bs, 2F), –133.77 (bd, J = 54.3 Hz, 2F); **FTIR–ATR** (neat) ν in cm^{-1}: 1615, 1517, 1324, 1248, 1105, 1066, 835, 812, 701; **HRMS (APCI^{+})** for $(M+H)^+$ $C_{19}H_{19}F_7NOS^+$ (m/z): calc. 442.1070; found 442.1063.

***N*-Methyl-*S*-(perfluoroethyl)-*N*-(3-phenyl-3-(4-(trifluoromethyl)phenoxy)propyl)thiohydroxylamine (Fluoxetine-SCF_2CF_3,**

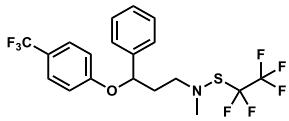

31b). A 10 mL round-bottom flask, equipped with a magnetic stir bar, was charged with fluoxetine (155 mg, 0.5 mmol). The flask was then evacuated and backfilled with argon three times. Subsequently, anhydrous CH_2Cl_2 (5 mL) was added using a syringe. Next, reagent **8b** (250 mg, 0.75 mmol) was quickly added to the flask followed by triethylamine (77 μL, 0.55 mmol). The mixture was stirred at room temperature for 3 h. Lastly, the reaction mixture was concentrated under reduced pressure and purified by flash column chromatography (1:9 EtOAc/hexane) to afford **31b** as a colorless syrup (200 mg, 87%).

***R**f* (1:4 EtOAc/hexane): 0.51; **^{1}H NMR ($CDCl_3$, 400 MHz):** δ 7.47 (d, *J* = 8.5 Hz, 2H), 7.42–7.35 (m, 4H), 7.35–7.27 (m, 1H), 6.94 (d, *J* = 8.5 Hz, 2H), 5.23 (dd, *J* = 8.6, 4.5 Hz, 1H), 3.39–3.21 (m, 2H), 3.02 (s, 3H), 2.36–2.25 (m, 1H), 2.25–2.13 (m, 1H); **^{13}C{^{1}H} NMR ($CDCl_3$, 100.6 MHz):** 160.6 (bq, *J* = 1.0 Hz), 140.8, 129.1,

128.2, 126.9 (q, *J* = 3.8 Hz), 125.9, 123.2 (q, *J* = 32.7 Hz), 123.0 (tq, *J* = 294.2, 40.0 Hz) 125.0 (q, *J* = 270.5 Hz), 115.9, 118.7 (qt, *J* = 285.4, 36.7 Hz), 77.7, 56.9, 48.2, 37.2; **^{19}F NMR ($CDCl_3$, 376.5 MHz):** δ –61.63 (s, 3F), –83.43 (s, 2F), –98.99 (bs, 2F); **FTIR–ATR** (neat) ν in cm^{-1}: 1615, 1517, 1325, 1249, 1202, 1108, 1067, 948, 835, 700; **HRMS (APCI$^+$)** for $(M+H)^+$ $C_{19}H_{18}F_8NOS^+$ (*m*/*z*): calc. 460.0976; found 460.0968.

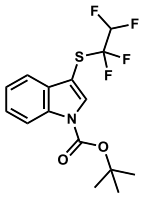

tert-Butyl 3-((1,1,2,2-tetrafluoroethyl)thio)-1*H*-indole-1-carboxylate (**32**). To a solution of indole **10a** (498 mg, 2 mmol) in CH_2Cl_2 (10 mL) was added Et_3N (557 μL, 4 mmol) and 4–(dimethylamino)pyridine (12 mg, 0.1 mmol). At room temperature, di–*tert*–butyl dicarbonate (523 mg, 2.4 mmol) was added and the reaction mixture was stirred at the same temperature for 16 h. Water was then added and the product was extracted with CH_2Cl_2 (3 x 20 mL). The combined organic fractions were dried with Na_2SO_4, filtered, and evaporated under reduced pressure. The residue was purified by flash column chromatography (1:9 EtOAc/hexane) to afford **32** (680 mg, 97%) as a white solid.

***R**f* (1:4 EtOAc/hexane): 0.51; **m.p**: 71 °C; **^{1}H NMR ($CDCl_3$, 400 MHz):** δ 8.19 (d, *J* = 8.0 Hz, 1H), 7.94 (s, 1H), 7.75 (d, *J* = 7.5 Hz, 1H), 7.44–7.34 (m, 2H), 5.78 (tt, *J* = 53.7, 3.6 Hz, 1H), 1.70 (s, 9H); **^{13}C{^{1}H} NMR ($CDCl_3$, 100.6 MHz):** δ 148.8, 135.5, 134.5, 131.6, 125.5, 123.8, 122.2 (tt, *J* = 286.0, 29.1 Hz), 119.7, 115.5, 109.4 (tt, *J* = 252.9, 37.1 Hz), 100.5 (t, *J* = 3.7 Hz), 85.2, 28.1; **^{19}F NMR ($CDCl_3$, 376.5 MHz):** δ –92.35 (td, *J* = 9.0, 3.3 Hz, 2F), –132.91 (dt, *J* = 18.5, 8.8 Hz, 2F); **FTIR–ATR** (neat) ν in cm^{-1}: 1742, 1449, 1371, 1356, 1252, 1224, 1153, 1115, 1064, 747; **HRMS (APCI$^+$)** for $(M+H)^+$ $C_{15}H_{16}F_4NO_2S^+$ (*m*/*z*): calc. 350.0832; found 350.0823.

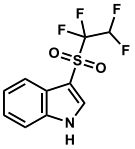

3-((1,1,2,2-Tetrafluoroethyl)sulfonyl)-1*H*-indole (**33**). To a solution of indole **10a** (249 mg, 1 mmol) in CH_3OH (5 mL) was added ammonium molybdate tetrahydrate (61 mg, 0.05 mmol). H_2O_2 (30% w/w in H_2O, 306 μL, 3 mmol) was added and the reaction mixture stirred at room temperature for 16 h. A second batch of H_2O_2 (30% w/w in H_2O, 500 μL, 4.9 mmol) was added and the reaction mixture was stirred at room temperature for 24 h. Water was added to the reaction mixture and the product was extracted successively with CH_2Cl_2 (3 x 20 mL). The combined organic fractions were dried with Na_2SO_4, filtered, and evaporated under reduced pressure to afford **33** (267 mg, 95%) as an orange solid.

***R**f* (1:4 EtOAc/hexane): 0.17; **m.p**: 92–93 °C; **^{1}H NMR ($CDCl_3$, 400 MHz):** δ 9.56 (bs, 1H), 8.00–7.89 (m, 2H), 7.57–7.44 (m, 1H), 7.41–7.28 (m, 2H), 6.30 (tt, *J* = 52.3, 5.6 Hz, 1H); **^{13}C{^{1}H} NMR ($CDCl_3$, 100.6 MHz):** δ 136.4, 135.6, 125.0, 124.5, 124.0, 119.6, 114.6 (tt, *J* = 293.6, 26.6 Hz), 113.0, 108.1 (tt, *J* = 254.7, 28.8 Hz), 105.7; **^{19}F NMR ($CDCl_3$, 376.5 MHz):** δ –120.91 (td, *J* = 8.2, 5.6 Hz, 2F), –134.56 (dt, *J* = 52.2, 8.2 Hz, 2F); **FTIR–ATR** (neat) ν in cm^{-1}: 3358, 1148, 1111, 741, 670, 608, 583, 550, 532, 487, 419; **HRMS (APCI$^+$)** for $(M+H)^+$ $C_{10}H_8F_4NO_2S^+$ (*m*/*z*): calc. 282.0206; found 282.0202.

3-((1*H*-Indole-3-yl)thio)-2,2,3,3-tetrafluoro-1,1-diphenylpropan-1-ol (**34**). To

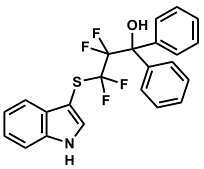

a Schlenk tube charged with indole **32a** (175 mg, 0.5 mmol) and benzophenone (182 mg, 1 mmol), was added anhydrous DMF (5 mL) under argon. The reaction mixture was cooled to –40 °C and KHMDS (1M, 1 mL) was added and the mixture stirred at the same temperature for 15 min. Et_2O (30 mL) and water (2 mL) were added at –40 °C under stirring and the organic phase was washed with saturated aqueous NH_4Cl (3 x 10 mL), dried with Na_2SO_4, filtered and the solvent evaporated. The residue was diluted with trifluoroacetic acid (5 mL) and stirred at room temperature for 3 h. The reaction crude was then concentrated under reduced pressure and the residue was diluted with Et_2O (30 mL) and washed with saturated aqueous $NaHCO_3$

(3 x 10 mL), dried with Na_2SO_4, filtered and the solvent evaporated. The residue was purified by flash column chromatography (1:9 EtOAc/hexane) to afford **34** (151 mg, 76%) as a brown solid.

***R**f* (1:4 EtOAc/hexane): 0.18; **m.p**: 112 °C; **^{1}H NMR ($CDCl_3$, 400 MHz):** δ 8.36 (s, 1H), 7.78–7.70 (m, 1H), 7.70–7.63 (m, 4H), 7.42–7.31 (m, 8H), 7.30–7.22 (m, 2H), 3.07 (s, 1H); **^{13}C{^{1}H} NMR ($CDCl_3$, 100.6 MHz):** δ 140.6, 136.1, 133.2, 130.3, 128.3, 128.1, 127.6, 125.3 (tt, *J* = 291.2, 36.0), 123.2, 121.4, 119.7, 117.8 (tt, *J* = 267.3, 30.7), 111.6, 95.5, 79.9 (t, *J* = 24.1 Hz); **^{19}F NMR ($CDCl_3$, 376.5 MHz):** δ –81.01 (t, *J* = 4.9 Hz, 2F), –109.64 (t, *J* = 4.7 Hz, 2F); **FTIR–ATR** (neat) ν in cm^{-1}: 3534, 3419, 1448, 1092, 741, 698; **HRMS (TOF ESI$^+$)** for $(M+Na)^+$ $C_{23}H_{17}F_4NNaOS^+$ (*m*/*z*): calc. 454.0859; found 454.0847.

5-(4-Phenoxyphenyl)-3-((1,1,2,2-tetrafluoroethyl)thio)-1*H*-indole (**35**). To a

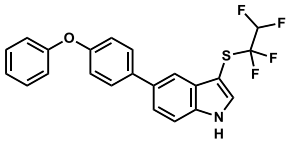

reaction vial equipped with a magnetic stir bar was added **11** (98 mg, 0.3 mmol), (4–phenoxyphenyl)boronic acid (71 mg, 0.33 mmol), $Pd(PPh_3)_4$ (35 mg, 0.03 mmol) and toluene (2 mL). Then, Na_2CO_3 (79 mg, 0.75 mmol), water (0.3 mL) and EtOH (0.6 mL) were successively added and the reaction mixture was sparged with argon for 5 min. The vial was then capped with a rubber septum and the reaction mixture stirred at 90 °C with an aluminum heating block for 24 h. After reaction completion, the reaction crude was concentrated under reduced pressure and the residue was purified by flash column chromatography (hexane to 1:4 EtOAc/hexane) to afford **35** (113 mg, 90%) as a yellowish syrup.

***R**f* (1:4 EtOAc/hexane): 0.27; **^{1}H NMR ($CDCl_3$, 400 MHz):** δ 8.54 (s, 1H), 8.02 (s, 1H), 7.69–7.62 (m, 2H), 7.56–7.51 (m, 2H), 7.47 (d, *J* = 8.5 Hz, 1H), 7.42–7.36 (m, 2H), 7.18–7.08 (m, 5H), 5.79 (tt, *J* = 53.7, 3.9 Hz, 1H); **^{13}C{^{1}H} NMR ($CDCl_3$, 100.6 MHz):** δ 157.3, 156.5, 137.0, 135.4, 134.7, 133.8, 130.4, 129.8, 128.8, 123.3, 123.1, 122.2 (tt, *J* = 284.2, 28.6 Hz), 119.2, 118.9, 117.4, 112.0, 109.53 (tt, *J* = 252.8, 36.9 Hz), 94.7 (t, *J* = 3.9 Hz); **^{19}F NMR ($CDCl_3$, 376.5 MHz):** δ –94.00 (td, *J* = 9.7, 4.0 Hz, 2F), –133.43 (dt, *J* = 53.6, 9.5 Hz, 2F); **FTIR–ATR** (neat) ν in cm^{-1}: 3409,

1489, 1470, 1235, 1107, 993, 809; **HRMS (APCI$^+$)** for $(M+H)^+$ $C_{22}H_{16}F_4NOS^+$ (*m*/*z*): calc. 418.0883; found 418.0873.

***1*,1,2,2-Tetrafluoro-*N*-methyl-*N*-(3-phenyl-3-(4-(trifluoromethyl)phenoxy)pro-pyl)ethane-1-sulfonamide (Fluoxetine-$SO_2CF_2CF_2H$, 36a)**. A 5 mL round-bottom flask, equipped with a magnetic stir bar, was charged with **31a** (132 mg, 0.3 mmol) and ammonium molybdate tetrahydrate (37 mg, 0.03 mmol). Next, CH_3OH (2 mL) was added using a syringe followed by H_2O_2 (30% w/w in H_2O, 340 μL, 3 mmol). The mixture was stirred at room temperature for 16 h. Lastly, the reaction mixture was concentrated under reduced pressure and purified by flash column chromatography (1:4 EtOAc/hexane) to afford **36a** as a colorless syrup (134 mg, 56%).

***R*$_f$** (1:4 EtOAc/hexane): 0.33; **^{1}H NMR ($CDCl_3$, 400 MHz):** δ 7.44 (d, J = 9.0 Hz, 2H), 7.39–7.27 (m, 4H), 6.89 (d, J = 8.6 Hz, 2H), 6.12 (tt, J = 52.4, 5.7 Hz, 1H), 5.24 (dd, J = 9.0, 3.7 Hz, 1H), 4.09–3-30 (bs, 2H), 3.08 (s, 3H), 2.43–2.08 (m, 2H); **^{13}C{^{1}H} NMR ($CDCl_3$, 100.6 MHz):** 160.1, 140.1, 129.2, 128.4, 127.0 (q, J = 3.7 Hz), 125.8, 124.4 (q, J = 271.5 Hz), 123.3 (q, J = 32.8 Hz), 115.9, 115.9 (tt, J = 291.6, 26.5 Hz), 107.9 (tt, J = 255.7, 30.3 Hz), 77.4, 48.3, 37.3, 35.9; **^{19}F NMR ($CDCl_3$, 376.5 MHz):** δ –61.66 (s, 1F), -119.33 (m, 2F), -135.62 (dtd, J = 52.4, 7.9, 2.1 Hz, 2F); **FTIR–ATR** (neat) ν in cm^{-1}: 1615, 1517, 1373, 1326, 1247, 1177, 1109, 1067, 837, 702, 584; **HRMS (APCI$^-$)** for $(M)^-$ $C_{19}H_{18}F_7NO_3S^-$ (m/z): calc. 473.0896; found 473.0886.

1,1,2,2,2-Pentafluoro-*N*-methyl-*N*-(3-phenyl-3-(4-(trifluoromethyl)phenoxy)pro-pyl)ethane-1-sulfonamide (Fluoxetine-$SO_2CF_2CF_3$, 36b). A 5 mL round-bottom flask, equipped with a magnetic stir bar, was charged with **31b** (138 mg, 0.3 mmol) and ammonium molybdate tetrahydrate (37 mg, 0.03 mmol). Next, CH_3OH (2 mL) was added

using a syringe followed by H_2O_2 (30% w/w in H_2O, 340 μL, 3 mmol). The mixture was stirred at 65 °C with an aluminum heating block for 16 h. As the mixture contained still starting material (observed by TLC), H_2O_2 (30% w/w in H_2O, 340 μL, 3 mmol) and ammonium molybdate tetrahydrate (37 mg, 0.03 mmol) were added again, letting the mixture stirred at 65 °C with an aluminum heating block for 16 h more. Lastly, the reaction mixture was concentrated under reduced pressure and purified by flash column chromatography (1:9 EtOAc/hexane) to afford **36b** as a colorless syrup (185 mg, 75%).

***R**f* (1:4 EtOAc/hexane): 0.43; **^{1}H NMR ($CDCl_3$, 400 MHz):** δ 7.44 (d, J = 8.6 Hz, 2H), 7.39–7.27 (m, 4H), 6.89 (d, J = 8.6 Hz, 2H), 5.24 (dd, J = 9.0, 3.7 Hz, 1H), 3.87 (bs, 1H), 3.42 (bs, 1H), 3.09 (s, 3H), 2.43–2.06 (m, 2H); **^{13}C{^{1}H} NMR ($CDCl_3$, 100.6 MHz):** 160.1, 140.0, 129.2, 128.5, 127.0 (q, J = 3.7 Hz), 125.8, 123.4 (q, J = 32.7 Hz), 124.5 (q, J = 270.2 Hz), 117.5 (tt, J = 287.6, 31.8 Hz), 115.9, 113.6 (tq, J = 295.0, 40.2 Hz), 77.4, 48.5, 37.3, 36.0; **^{19}F NMR ($CDCl_3$, 376.5 MHz):** δ –61.67 (s, 3F), –79.65 (bs, 3F), –115.92 (bs, 2F); **FTIR–ATR** (neat) ν in cm^{-1}: 1615, 1518, 1389, 1325, 1222, 1162, 1111, 1068, 836, 702, 593; **HRMS (APCI$^-$)** for $(M–H)^-$ $C_{19}H_{16}F_8NO_3S^-$ (m/z): calc. 490.0729; found 490.0723.

UNIVERSITAT ROVIRA I VIRGILI
REAGENTS AND METHODOLOGIES FOR THE INTRODUCTION OF THIOFLUOROALKYL AND FLUOROSULFUR MOTIFS
Miguel Bernús Pérez

CHAPTER V

A Modular Flow Platform for Sulfur(VI) Fluorine Exchange (SuFEx) ligation

UNIVERSITAT ROVIRA I VIRGILI
REAGENTS AND METHODOLOGIES FOR THE INTRODUCTION OF THIOFLUOROALKYL AND FLUOROSULFUR MOTIFS
Miguel Bernús Pérez

5.1 Introduction

5.1.1 Click chemistry

"Click chemistry", a term first coined by Sharpless in 2001, refers to chemical reactions, which rapidly piece together molecular fragments with exceptional efficiency. Recognized with the Nobel Prize for Chemistry in 2022,[1] the development of this field owes to its now well-defined and stringent criteria:[2]

- Reactions must be modular, broad in scope, stereospecific, and give very high yields toward the formation of a single product.
- Transformations must be highly atom economic, and only non-toxic byproducts can be generated.
- The processes must be simple under the reaction conditions (ambient temperature, and compatible with oxygen and moisture), and must use readily available starting materials and reagents. Also, the use of benign solvents (or no solvents) is required.
- Purification (if needed) must be nonchromatographic.
- Consequently, click reactions usually have a high thermodynamic driving force (>20 kcal mol^{-1}). In fact, Sharpless defined these reactions as being "as a spring-loaded for a single trajectory".[2]

The development of such highly "ideal reactions" was inspired to mimic the biochemical machinery that drive the synthesis of molecular entities under physiological conditions. More specifically, this philosophy is based on the creation of chemical complexity by linking organic building blocks through multiple heteroatomic bonds (C–X–C). For example, nature builds an

[1]In 2022 the Royal Swedish Academy of Sciences awarded Carolyn R. Bertozzi, Morten Meldal, and K. Barry Sharpless with the Chemistry Nobel prize "for the development of click chemistry and bioorthogonal chemistry".

[2] Kolb, H. C.; Finn, M. G.; Sharpless, K. B. *Angew. Chem. Int. Ed.* **2001**, *40*, 2004.

immense variety of structurally and functionally diverse proteins by modulating the order in which the 20 common amino acids are linked. The peptide bond, which serves to link amino acids together, is an example of natural click chemistry (C–N–C).[2]

The great potential of click chemistry is underpinned by the new molecular properties that can arise from joining small building blocks, and its operational simplicity would allow scientists untrained in synthetic chemistry to perform these reactions.[3] This facile access to molecular diversity is particularly sought-after in the pharmaceutical industry during the drug discovery process,[4] but click chemistry has also found application in many other fields, including material science,[5] surface chemistry,[6] and chemical biology.[7]

The most common examples of the click reaction family are cycloadditions of unsaturated species (1,3-dipolar cycloadditions and Diels-Alder-type), ring-opening reactions of strained heterocyclic electrophiles, carbonyl condensations (non-aldol reactions), additions to unsaturated C–C bonds, and perhaps the most famous examples are the copper-mediated and the strain-promoted azide-alkyne cycloaddition reactions (CuAAC and SPAAC, respectively) (Figure 5.1).[2,8]

[3] Devaraj, N. K.; Finn, M. G. *Chem. Rev.* **2021**, *121*, 6697.
[4] Thirumurugan, P.; Matosiuk, D.; Jozwiak, K. *Chem. Rev.* **2013**, *113*, 4905.
[5] Xi, W.; Scott, T. F.; Kloxin, C. J.; Bowman, C. N. *Adv. Funct. Mater.* **2014**, *24*, 2572.
[6] Nair, D. P.; Podgórski, M.; Chatani, S.; Gong, T.; Xi, W.; Fenoli, C. R.; Bowman, C. N. *Chem. Mater.* **2013**, *26*, 724.
[7] Rodríguez, D. F.; Moglie, Y.; Ramírez-Sarmiento, C. A.; Singh, S. K.; Dua, K.; Zacconi, F. C. *RSC Adv.* **2022**, *12*, 1932.
[8] Jewett, J. C.; Bertozzi, C. R. *Chem. Soc. Rev.* **2010**, *39*, 1272.

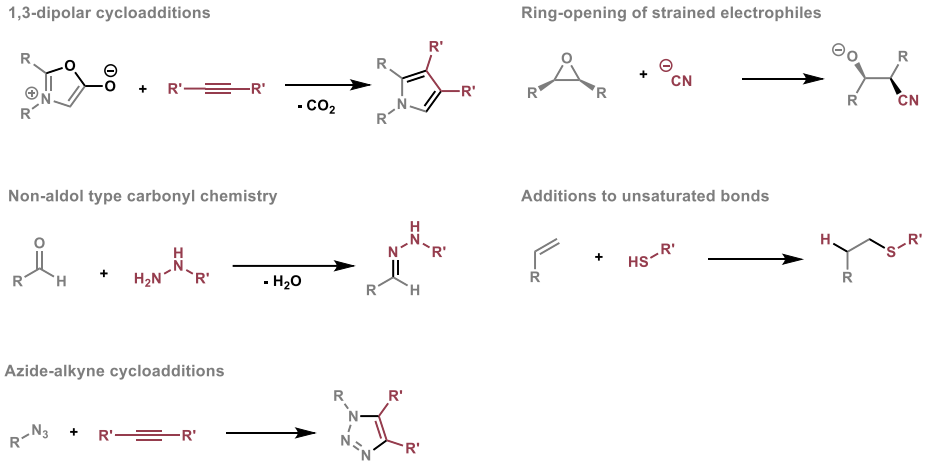

Figure 5.1. Examples of reactions of the most common click transformations.

5.1.2 Sulfur(VI) Fluorine Exchange (SuFEx) reactions

In 2014, Sharpless introduced a new family of click connective reactions based on sulfur(VI)-fluorine exchange (SuFEx).[9] This new category of transformations capitalizes on the unique thermodynamic and kinetic properties of the S^{VI}–F bond to forge new heteroatom linkages under mild conditions (Figure 5.2, A).

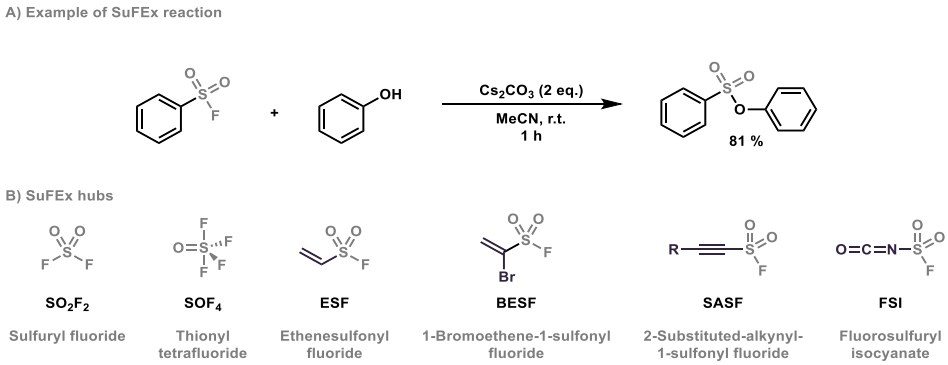

Figure 5.2. A) Example of a SuFEx reaction. B) Family of connective SuFEx hubs.

[9] Dong, J.; Krasnova, L.; Finn, M. G.; Sharpless, K. B. *Angew. Chem. Int. Ed.* **2014**, *53*, 9430.

This typology of click reactions has been exploited by the so-called "SuFEx hubs" (Figure 5.2, B).[10,11] These chemical reagents are dielectrophiles, often with two orthogonal reactive sites, enabling the stepwise click reaction with two, or even three, nucleophiles. The first example of this type of reagent was disclosed in a seminal report in 1979 on the use of ethylene sulfonyl fluoride (ESF) (Figure 5.2) as a Michael acceptor for the addition of amines.[12] Nevertheless, the presence of appropriate reaction conditions or catalysts is needed for selectively transforming a fluoride from the covalent S–F bond to a leaving group.

Due to the operational simplicity and robustness of SuFEx transformations, these hubs have found application in a wide variety of fields such as high-throughput synthesis,[13] library creation,[14] protein tagging,[15] and polymer science,[16] among others.

The recent surge in interest around SuFEx chemistry is due in most part to the need for a more robust 'clickable' sulfonyl electrophile to replace sulfonyl chlorides that can be difficult to tame. The synthetic advantages of S^{VI}–F bonds respect S^{VI}–Cl are based in four contributing factors (Figure 5.3):

1. **Resistance to reduction.** Given the exceptional electronegativity of fluorine, the sulfur(VI)-fluorine bond always cleaves in an heterolytic fashion to form the fluoride ion (Figure 5.3, A).

[10] Smedley, C. J.; Homer, J. A.; Gialelis, T. L.; Barrow, A. S.; Koelln, R. A.; Moses, J. E. *Angew. Chem. Int. Ed.* **2021**, *61*, e202112375.
[11] Sun, S.; Gao, B.; Chen, J.; Sharpless, K. B.; Dong, J. *Angew. Chem. Int. Ed.* **2021**, *60*, 21195.
[12] Krutak, J. J.; Burpitt, R. D.; Moore, W. H.; Hyatt, J. A. *J. Org. Chem*. **1979**, *44*, 3847.
[13] Kitamura, S.; Zheng, Q.; Woehl, J. L.; Solania, A.; Chen, E.; Dillon, N.; Hull, M. V.; Kotaniguchi, M.; Cappiello, J. R.; Kitamura, S.; Nizet, V.; Sharpless, K. B.; Wolan, D. W. *J. Am. Chem. Soc.* **2020**, *142*, 10899.
[14] Liu, Z.; Li, J.; Li, S.; Li, G.; Sharpless, K. B.; Wu, P. *J. Am. Chem. Soc.* **2018**, *140*, 2919.
[15] Jones, L. H. *ACS Med. Chem. Lett.* **2018**, *9*, 584.
[16] Durie, K.; Yatvin, J.; Kovaliov, M.; Crane, G. H.; Horn, J.; Averick, S.; Locklin, J. *Macromolecules* **2018**, *51*, 297.

2. **Thermodynamic stability.** Substitution of the S^{VI}–F center is less preferential in comparison to other halides. This can be rationalized by the higher bond strength of SO_2–F compared to SO_2–Cl (homolytic bond dissociation for SO_2F_2 = ~91 kcal mol^{-1}; SO_2Cl_2 = ~46 kcal mol^{-1}).[9] These factors make S^{VI}–F superior connectors, since they are more recalcitrant toward nucleophilic substitution, hydrolysis, and thermolysis. On the contrary, other S^{VI}-halides suffer from homolytic cleavage that favors other radical reactions (Figure 5.3, B).
3. **Exclusive reaction at sulfur.** Uniquely, S^{VI}–F compounds react as electrophiles at sulfur with high selectivity. Analogous S^{VI}–Cl compounds exhibit competitive reactivity at the chlorine atom for electrophilic halogenations. This divergence in selectivity is due to the greater polarizability of chlorine relative to fluorine (Figure 5.3, C).
4. **The special nature of the fluoride-proton interaction.** Fluoride anions are rarely found 'naked' and they exhibit a unique stabilization in the presence of H^+ due to hydrogen bonding and electrostatic interactions. This can be harvested to accelerate reactions with nucleophiles by choosing appropriate conditions for the activation and release in the S^{VI}–F bonds (Figure 5.3, D).

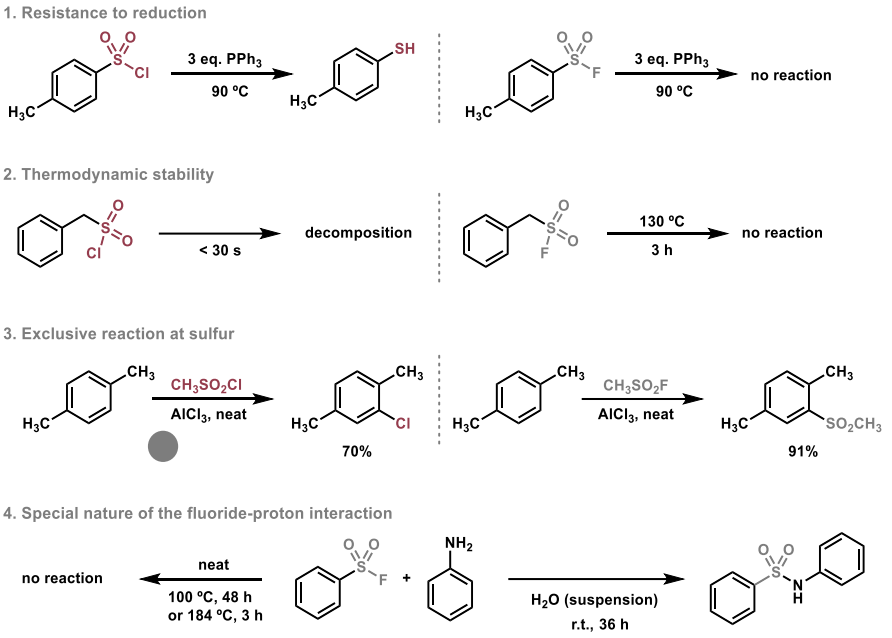

Figure 5.3. Reactions illustrating the differences between sulfonyl fluorides and other sulfonyl halides.[8]

5.1.3 Introduction of –SO_2F

Among the different SuFEx handles, the –SO_2F moiety has received the most attention due to its unique medicinal properties[17] and its ability to act connect two nucleophiles with simplicity and orthogonality. The Sharpless group has shown how gaseous sulfuryl fluoride (SO_2F_2) can be used to install this moiety on various organic molecules, such as phenols and amines, to produce fluorosulfates and sulfamoyl fluorides, respectively (Figure 5.4, A).[9]

[17] Gehringer, M.; Laufer, S. A. *J. Med. Chem.* **2019**, *62*, 5673.

However, while SO_2F_2 is cheap and produces minimal waster, its mild toxicity and difficulty to handle have motivated the search for more practical alternatives. As a first approach, the group of De Borggraeve reported a protocol for the generation of SO_2F_2 *ex situ* from 1,1'-sulfonyldiimidazole (SDI) and KF in the presence of TFA.[18] The setup consists of a two-chamber reactor, in which the generation of the SO_2F_2 takes place in one chamber, while in the other the nucleophile reacts with the incoming gas (Figure 5.4, B).

Alternatively, solid reagents have been developed to avoid the use of gases or specialized setups. The group of Sharpless reported an imidazolium based reagent (FDIT: 1-(fluorosulfonyl)-2,3-dimethyl-1H-imidazol-3-ium trifluoromethanesulfonate) made in two steps from cheap, commercially available starting materials (Figure 5.4, C).[19] The reagent outperformed the reactivity of SO_2F_2 as it could react with a wide range of primary and secondary amines in a selective manner without undergoing disubstitution to form sulfamides. Pfizer independently developed the aniline-based 4-(acetylamino)phenyl]imidodisulfuryl difluoride (AISF) reagent that did not require SO_2F_2 for its preparation (Figure 5.4, C), which is also able to transfer the $–SO_2F$ fragment to nucleophiles.[20]

[18] Veryser, C.; Demaerel, J.; Bieliunas Vidmantas; Gilles, P.; De Borggraeve, W. M. *Org. Lett.* **2017**, *19*, 5244.

[19] Guo, T.; Meng, G.; Zhan, X.; Yang, Q.; Ma, T.; Xu, L.; Sharpless, K. B.; Dong, J. *Angew. Chem. Int. Ed.* **2018**, *57*, 2605.

[20] Zhou, H.; Mukherjee, P.; Liu, R.; Evrard, E.; Wang, D.; Humphrey, J. M.; Butler, T. W.; Hoth, L. R.; Sperry, J. B.; Sakata, S. K.; Helal, C. J.; am Ende, C. W. *Org. Lett.* **2018**, *20*, 812.

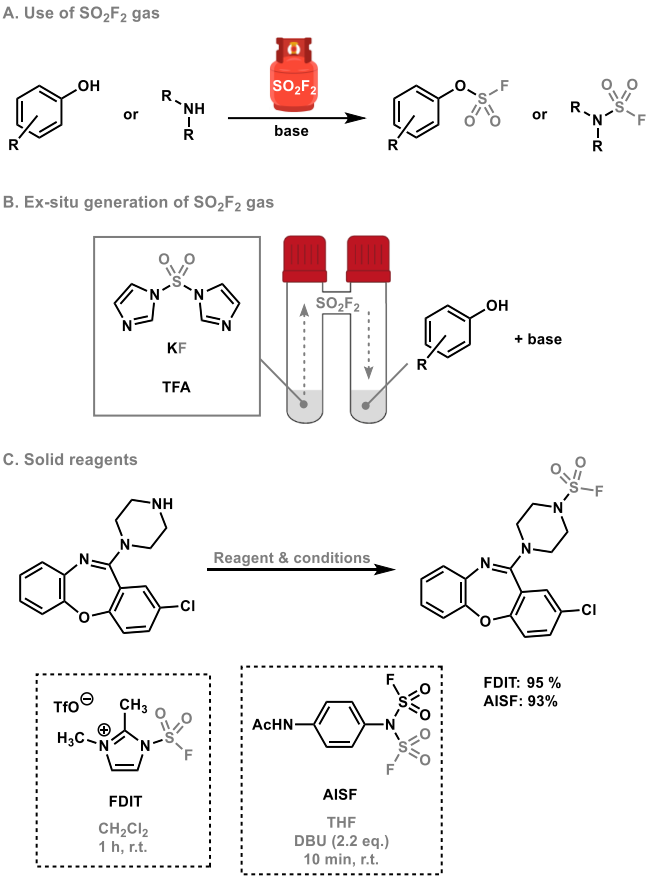

Figure 5.4. Strategies for the introduction of the SO_2F motif.

After its introduction, the new X–SO_2F handle can be further *SuFExed* to connect another nucleophile. For this second ligation, the use of Lewis bases or Lewis acids have been used to forge S^{VI}–N and S^{VI}–O bonds (Figure 5.5).[9,21] For example, fluorosulfates can be coupled with silyl-protected phenols in the presence of catalytic DBU to yield asymmetric sulfates.[9] This strategy takes advantage of the strong Si–F bond formed (BDE Si–F = 130 kcal mol^{-1}) to activate the fluoride and assist in the sulfate formation.

[21] Mahapatra, S.; Woroch, C. P.; Butler, T. W.; Carneiro, S. N.; Kwan, S. C.; Khasnavis, S. R.; Gu, J.; Dutra, J. K.; Vetelino, B. C.; Bellenger, J.; am Ende, C. W.; Ball, N. D. *Org. Lett.* **2020**, *22*, 4389.

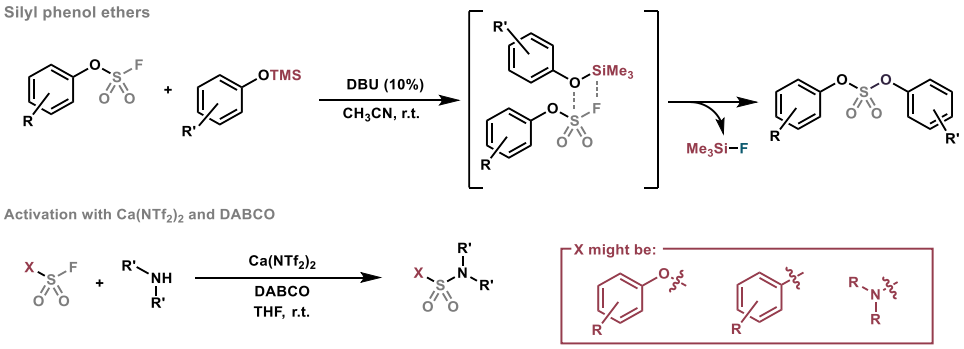

Figure 5.5. Derivatization of the SO_2F handle by the reaction of silyl phenol ethers and amines.

5.1.4 Flow chemistry

Flow chemistry is a technological discipline that takes advantage of microfluidic equipment to perform chemical reactions with unique control over the key reaction parameters.[22] Fundamentally, continuous-flow synthesis consists in pumping reactants through reactors in a continuous manner. In this introduction, some practical elements will be presented to have a panoramic view of this technology.

5.1.4.1 Flow elements

To understand the flow chemistry setup, it is useful to be familiar with the individual devices used in the construction of these modular systems (Figure 5.6).[23]

- **Pumping modules** are used to push the solution of reagents through the system. There are mainly four types:
  - Syringe pumps. Adequate for small volumes (1-20 mL), low system pressure (up to 7 bar), and precise control of flow rate.

[22] Plutschack, M. B.; Pieber, B.; Gilmore, K.; Seeberger, P. H. *Chem. Rev.* **2017**, *117*, 11796.
[23] Britton, J.; Jamison, T. *Nat. Protoc.* **2017**, *12*, 2423.

- HPLC pumps. Adequate for larger volumes (1-20 mL), high system pressure (up to 80 bar), and with less accuracy in the flow rate.
- Peristaltic pumps. Used for continuous feeding (normally for scale-up and multigram reactions) high pressures, slurries, and biphasic mixtures.
- Mass flow controllers. Used to pump gases in multiphase gas-liquid mixtures with a precise flow rate.

- **Reactors** are the core units where chemical reactions take place. There are three main types:
  - Coils. Normally, these tubes are made of a chemical resistant polymer (perfluoroalkoxy alkane (PFA) or fluorinated ethylene propylene (FEP)). Alternatively, for special temperature or volume applications, they can also be made of stainless steel. Normally, they have an internal diameter between 0.2 and 2 mm.
  - Packed beds. They are used for immobilizing heterogeneous catalysts or solid reagents. These units consist of an embedded volume of solid material between two filters. Typically, these cartridges are made of glass, polymer, or stainless steel.
  - Chips. They consist of a series of channels carved on a solid support such as glass, ceramics, or stainless steel. They offer the highest accuracy in terms of reaction control at the expense of low throughput, and can suffer from clogging.
- **Mixers** are used to connect different tubing to facilitate the encounter of the pumped streams of reagents. Depending on the shape, T, Y, and quad mixers can be differentiated.
- **Back-pressure regulators** are devices that maintain a defined pressure upstream of its own inlet. Their main application is to pressurize the system to a defined value.

- **Check valves** are used to prevent the backflow of material by only allowing fluid to flow in one direction.
- **Purification and analysis elements.** There is a plethora of devices which can be coupled to the flow setups, which can aid purification (e.g., molecular sieves column or liquid-liquid separators), or to monitor the reaction mixtures (e.g., in-line NMR, IR, HPLC analysis).
- **Connectors** are used to securely attach the tubing to all the previous elements. All fittings are standardized to ensure the modularity and interchangeability of all components.

Figure 5.6. Common elements and equipment in flow setups.

5.1.4.2 Flow reaction concepts

To help understand the differences between conventional batch processes and flow chemistry, three key concepts must be introduced.[22]

- **Flow rate** is defined as the speed of the stream in terms of volume of fluid per unit of time, and is controlled by the pumping modules.
- **Residence time** is the time that a fluid parcel has spent inside a controlled volume (normally a reactor). Importantly, it is not the same as the reaction time, since it does not take into account the kinetics of a transformation.
- **Fed-batch** consists of an operational setup where a stream of solution from a flow system is fed (supplied) to a conventional reaction flask where another chemical transformation takes place.

5.1.4.3 Advantages of flow processes *vs.* batch

Although flow chemistry "is not the answer to the ultimate question of life, the universe, and everything",[22] it offers some unique advantages over batch process.[24]

These advantages can be summarized in eight points:

1. **Enhanced mass transfer.** The use of microfluidics enhances the efficiency in mixing of the reactants. This parameter is crucial for multiphase reactions, where reactions are kinetically controlled by diffusion, especially considering the confinement of the reagents in the tubes.
2. **Enhanced heat transfer.** Flow reactors have extremely high surface-to-volume ratios in comparison to conventional flasks used in batch processes. Therefore, the large area for heat-exchange reduces the common batch problem of hot spots, facilitating much faster temperature equilibration.
3. **Controlled pressure.** The use of back pressure regulators and the high surface-to-volume ratio enables precise system

[24] Noël, T.; Capaldo, L.; Wen, Z. *Chem. Sci.* **2023**, in press.

pressurization to a desired value regardless of the boiling point of the solvent.

4. **Modularity.** Since all the components can be streamlined, flow setups can be easily modified to accommodate the conditional needs of a particular reaction, aiding multistep syntheses.
5. **Light penetration.** The effective absorption of light is dependent on the distance between the light source and the absorbing species (defined by the Beer-Lambert law). Flow reactors can have very small internal diameter (micrometer to millimeter scale), enabling full irradiation of the entire reaction mixture. This feature is a significant advantage over batch processes, where light often does not penetrate to the center of the reaction volume (centimeter scale).
6. **Safety.** In addition to the enhanced mass and heat transfer, smaller reactor volumes and precise control of the reaction conditions significantly improve the safety of chemical processes.
7. **Scalability.** Either by increasing the number of channels in the reactor (numbering up) or by changing the size of the reactors (sizing up), a laboratory scale transformation can be adapted for production needs.
8. **Automation.** As the reaction parameters can be controlled more accurately and reliably, flow processes are more reproducible. Consequently, flow set-ups have been coupled with analytical techniques for high-throughput experimentation (HTE).

In general, these advantages make flow chemistry ideal for working with dangerous processes, gaseous reagents, heterogeneous mixtures, kinetically controlled transformations, photochemical and electrochemical reactions, scaling-up, and automated systems.[24]

5.2 Target of the project

Considering the currently available methods for the introduction of the -SO_2F handle, we wondered if flow technology could be advantageous for the development of a platform to (i) safely generate and dose SO_2F_2, (ii) increase the speed of the ligation reaction, (iii) enable the SuFEx reaction in a wide range of substrates, and (iv) telescope transformations by taking advantage of the modularity of flow setups.

5.3 Results and discussion

5.3.1 Initial observations on Cl–F exchange

We began our study by identifying SO_2F_2 as an excellent source of –SO_2F due to low cost, high reactivity, and high atom economy. However, SO_2F_2 is a toxic gas which makes its use as a reagent impractical for many chemists. We sought to overcome these problematic SO_2F_2 issues by using microfluidic systems to generate the reactive gas *in situ*, with its release being managed in a controlled and safe manner.

To start, we hypothesized that sulfuryl chloride (SO_2Cl_2) and potassium fluoride could react to produce SO_2F_2 *in situ*. This idea was supported by the greater thermodynamic stability of the S(VI)–F bond (~90.5 kcal mol^{-1}) compared to the S(VI)–Cl bond (~46.0 kcal mol^{-1}), which suggests that this exchange should be easily achievable.

Initial batch experiments confirmed this hypothesis. By mixing sulfuryl chloride and an excess of potassium fluoride in acetonitrile we observed the formation of the sulfuryl chloride fluoride intermediate (SO_2ClF) in 15 min using ^{19}F NMR. The reaction continued, with the double chloride fluoride exchange completed within 2 h to give the desired SO_2F_2 product. This experiment showed that *in situ* generation of the reactive sulfuryl fluoride gas could be achievable from the easy to handle nongaseous sulfuryl chloride and potassium fluoride.

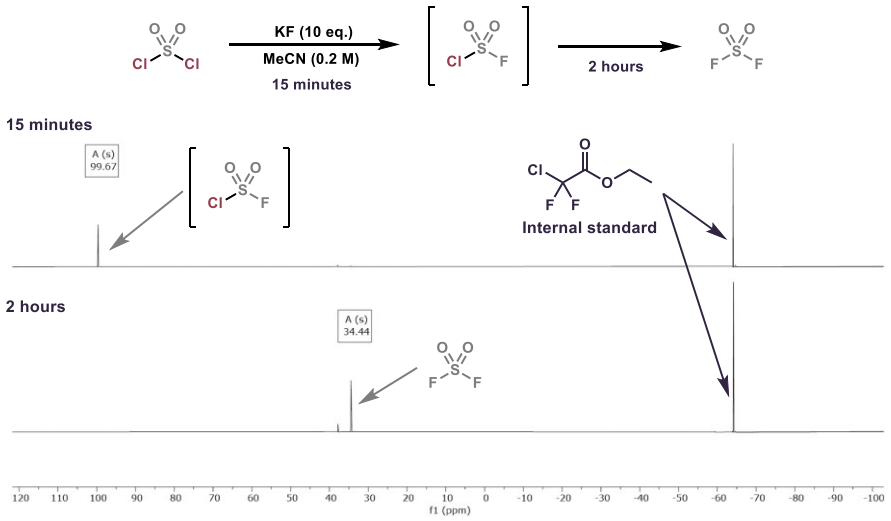

Figure 5.7. ^{19}F NMR studies on the batch formation of SO_2ClF (top), and SO_2F_2 (bottom). Experimental details can be found in section 5.5.

5.3.2 Generation of SO_2F_2 in flow

With these observations in hand, we decided to translate the batch SO_2F_2 generation into a microfluidic setup. As potassium fluoride is a solid reagent, a packed bed reactor was deemed to be an appropriate module for the conversion of SO_2Cl_2. An empty polypropylene (PP) cartridge from a flash chromatography column was used as the vessel in which the packed solids would be loaded. Specifically, the column was filled with a mixture of anhydrous KF and glass beads (425–600 μm) in a weight ratio of 1:1. This allows the reactor to have an empty volume for the reaction. In our case, a 12 g SiO_2 cartridge could be filled with a mixture of ~9.3 g of KF and glass beads, giving an empty volume of 3.8 mL.

Next, we proceeded with the optimization of the *in situ* SO_2F_2 generation. The reactor was loaded with an equimolar solution of SO_2Cl_2 and 1,2-difluorobenzene in acetonitrile using a syringe pump, and the eluent was collected for analysis by ^{19}F NMR to measure the conversion (Table 5.1, heading). A screening of various flow rates revealed that fast flow rates

(greater than 2.0 mL·min^{-1}) deliver a mixture of SO_2FCl and SO_2F_2 (Table 5.1, entries 1–2). Gratifyingly, reducing the flow rate to 0.5 mL·min^{-1} delivered the desired gaseous reagent in excellent purity, with a residence time of approximately 7 min (Table 5.1, entry 3). This significantly reduced reaction time (from 2 h for the reaction carried out under batch conditions) can be explained by the enhanced liquid-to-solid contact. It is important to stress that the 55% ^{19}F NMR yield corresponds to complete conversion of SO_2Cl_2, as during the manipulation of the dissolved SO_2F_2 there are losses due to product evaporation. This was confirmed by using lower flow rates (Table 5.1, entries 4–5), where the same yield was obtained despite the higher residence time.

Table 5.1. Optimization of the SO_2Cl_2 flow rate for the selective formation of SO_2F_2. [a]Yields were determined by ^{19}F NMR using 1,2-difluorobenzene as the internal standard. Experimental details can be found in section 5.5.

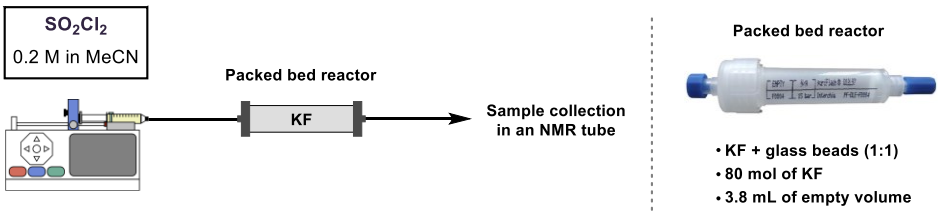

Entry	Flow rate (mL·min^{-1})	Residence time (min)	SO_2ClF[a] (%)	SO_2F_2[a] (%)
1	4.0	1	25	29
2	2.0	2	21	28
3	0.50	7	<1	55
4	0.25	15	0	50
5	0.15	30	0	54

With the optimized flow rate (0.5 mL·min^{-1}), a lifespan assessment of the KF cartridge was performed. To do so, the generation module was connected to a benchtop ^{19}F NMR 60 MHz spectrometer to measure SO_2F_2 formation *in*

situ (Figure 5.8). This would prevent any possible leaks due to the confined system. Using the optimal flow rate of 0.5 mL·min^{-1} with a residence time of 7 min, a 0.2 M solution was pumped through the reactor bed. After 17 mmol of SO_2Cl_2 solution has been injected, conversion suddenly to below 50%, and the formation of SO_2FCl was observed, corresponding to incomplete chloride-fluoride exchange. This was attributed to the cartridge being close to exhaustion (Figure 5.8).

The cartridge contained approximately 80 mmol of KF, so if 17 mmol of SO_2F_2 were generated it means that 43% of the KF had been consumed from the packed bed.

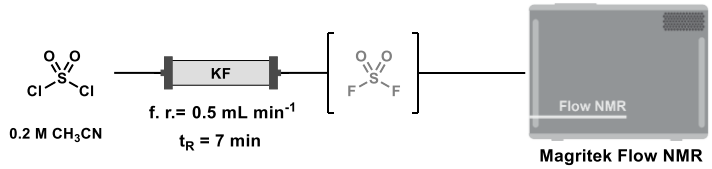

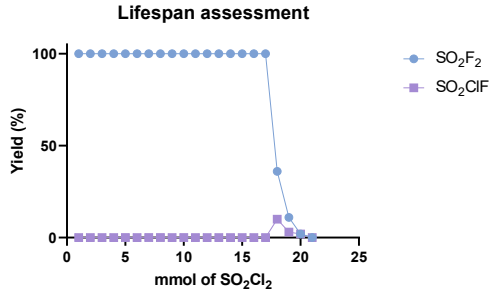

Figure 5.8. In-line SO_2F_2 generation and ^{19}F NMR analysis for the lifespan assessment of the KF packed bed. Yields were determined by ^{19}F NMR using and 1,2-difluorobenzene as the internal standard.

5.3.3 Scope of small molecules

With these results in hand, we turned our attention to coupling the generation of SO_2F_2 with a SuFEx module in which the gaseous reagent would be combined with a nucleophilic partner to react. The chosen module consisted of a 2 mL perfluoroalkoxy alkanes coil (PFA, I.D. = 0.80 mm, O.D. =

1.60 mm) where the SO_2F_2 stream is mixed with a solution of a nucleophile and a base (triethylamine or DBU). These streams are connected to a T mixer and fed by syringe pumps.

A molar ratio of 2:1 of SO_2F_2 and nucleophile was used for the SuFEx reaction. Consequently, the flow of the nucleophile solution was adjusted to have a total residence time of the SuFEx module of 2 min. This short residence time should allow the generation of large libraries of SuFExed compounds with minimal effort and time.

Specifically, we found that several phenols could be cleanly converted into the corresponding fluorosulfates with excellent isolated yields, regardless of the electronic nature of the substituent or its position on the aromatic ring (**1–6**, Scheme 5.1). The use of SO_2F_2 can become problematic when dealing with large-scale reactions, but thanks to the flow set-up, fluorosulfate **1** could easily be obtained on a gram scale (1.73 g) by simply increasing the collection time without loss of chemical efficiency (98%).

We also found that a wide variety of natural products, drugs, and fluorescent tracers could be successfully reacted using our flow protocol. For example, *N*-Boc tyrosine, broxyquinoline, fluorescein, α-tocopherol, estrone, and unprotected amoxicillin were all successfully reacted (**7–12**, Scheme 5.1), demonstrating the excellent functional group tolerance of the approach.

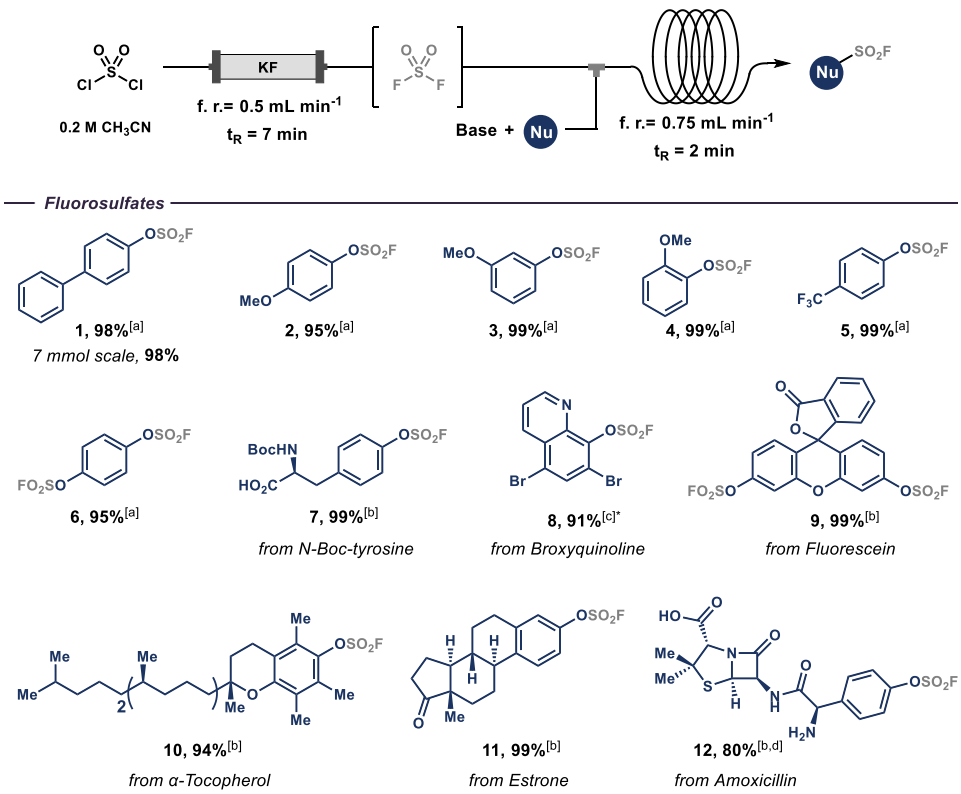

Scheme 5.1. Scope of the SuFEx reactions using phenols as nucleophiles. All yields are those of isolated compounds. Standard conditions for the SO_2F_2 generation: SO_2Cl_2 (2 equiv, 0.2 M in CH_3CN) passed through a 3.8 mL cartridge filled with a 1:1 mixture of KF and glass beads. Standard conditions for the second step: [a] Nucleophile (1 equiv, 0.2 M in CH_3CN), Et_3N (2.5 equiv). [b] Nucleophile (1 equiv, 0.2 M in DMF), Et_3N (2.5 equiv). [c] Nucleophile (1 equiv, 0.2 M in CH_3CN), DBU (4.0 equiv). [d] The compound has been isolated after an acetylation step. *5 equiv of DBU were used. Experimental details can be found in section 5.5.

A range of nitrogen-based nucleophiles could also be used in this strategy to obtain the corresponding sulfamoyl fluorides (Scheme 5.2). For instance, 4- to 7-membered ring secondary amines (**13–17**), heteroaromatic derivatives (**18–20**), and a primary aniline (**21**) were effectively reacted with SO_2F_2. In this case, several pharmaceutically relevant molecules were also submitted to the flow protocol, such as stanozolol, paroxetine, desloratadine, amoxapine, and olanzapine, which rapidly yielded the desired SuFExed analogs (**22–26**).

Additionally, nucleosides such as adenosine and cytidine derivatives (**27**–**29**) proved to be effective substrates, although a fed-batch system using K_2CO_3 as a base had to be employed for fully unprotected cytidine. Finally, we could also use bidentate nucleophiles such as BINOL, catechol, and salicylamide (**30**-**32**) to obtain the corresponding sulfates and sulfamates.

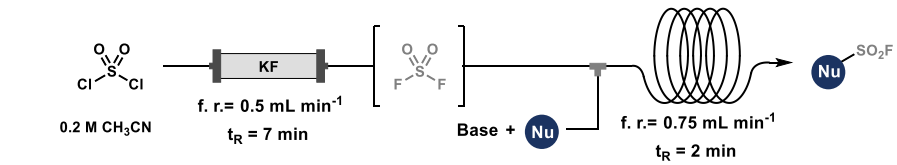

Fluorosulfates

13, n=0, 98%[a]
14, n=1, 99%[a]
15, n=2, 99%[a]
16, n=3, 75%[a]

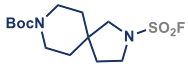

17, 84%[a]

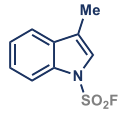

18, 84%[c]

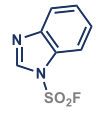

19, 87%[c]

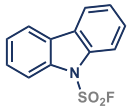

20, 99%[c]

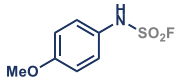

21, 99%[c]

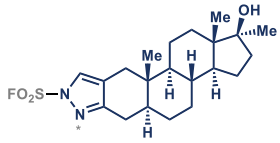

22, 63%, (r.r 2.5:1)[b]

From Stanozolol

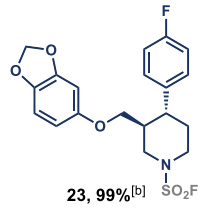

23, 99%[b]

From Paroxetine

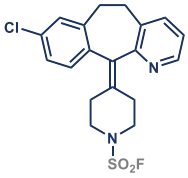

24, 97%[b]

From Desloratadine

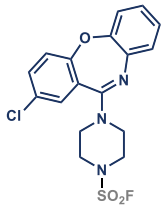

25, 81%[b]

From Amoxapine

26, 69%[e]

From Olanzapine

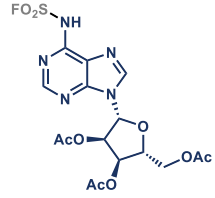

27, 95%[e]

From Adenosine

Sulfates and Sulfamates

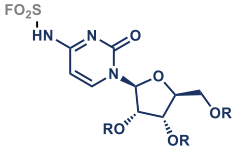

28, R= Ac, 99%[e]
29, R= H, 60%[d,f]

From Cytidine

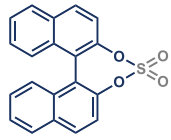

30, 99%[b]

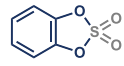

31, 89%[b]

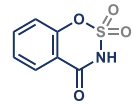

32, 76%[e]

Scheme 5.2. Scope of the SuFEx reactions N-based nucleophiles and bidentate compounds. All yields are those of isolated compounds. Standard conditions for the SO_2F_2 generation: SO_2Cl_2 (2 equiv, 0.2 M in CH_3CN) passed through a 3.8 mL cartridge filled with a 1:1 mixture of KF and glass beads. Standard conditions for the second step: [a] Nucleophile (1 equiv, 0.2 M in CH_3CN), Et_3N (2.5 equiv). [b] Nucleophile (1 equiv, 0.2 M in DMF), Et_3N (2.5 equiv). [c] Nucleophile (1 equiv, 0.2 M in CH_3CN), DBU (4.0 equiv). [d] The compound has been isolated after an acetylation step. [e] Nucleophile (1 equiv, 0.2 M in DMF), DBU (4.0 equiv). [f] Nucleophile (1 equiv, 0.1 M in DMSO), K_2CO_3 (4.0 equiv). Experimental details can be found in section 5.5.

In summary, the developed flow platform enabled the *in situ* generation of gaseous SO_2F_2 and subsequent fast (2 min) SuFEx ligation of a wide variety of substrates with exquisite functional group tolerance. All the products could be isolated without the use of column chromatography, except those which had to be acetylated for isolation purposes (**12** and **29**).

More importantly, we could expand the scope of amine nucleophiles that can be coupled with SO_2F_2, which was previously regarded as poor: "*SO_2F_2 showed a limited substrate scope (cyclic and a few symmetric secondary amines) […] using sulfuryl fluoride (SO_2F_2) gas as the reagent with such primary amines, one gets, at best, useless mixtures*".[19] This was achieved through the use of DBU, which reacts rapidly with SO_2F_2 to form an ionic complex **33** with increased reactivity, similar to the FDIT reagent (1-(fluorosulfonyl)-2,3-dimethyl-1H-imidazol-3-ium trifluoromethanesulfonate)). This allowed the functionalization of electron poor phenols (**8**), and some N-heterocycles (**18**-**20**) and anilines (**21**) which did not react when using triethylamine as base.

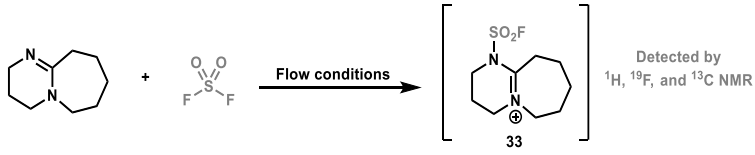

Scheme 5.3. *In situ* formation of a SO_2F-DBU complex. Experimental details can be found in section 5.5.

5.3.4 Telescoping of reactions

Capitalizing on the modular nature of this setup, we wondered if we could couple a second reactor in line to further derivatize the installed SuFEx handles. To do so, an additional syringe pump and a coil were connected to the exit of the second module through use of a T mixer (Scheme 5.4). With this modified setup, three contiguous reactions in-line in a telescoped fashion could be performed: (i) generation of SO_2F_2 in the Cl–F exchange module, (ii) installation of the SuFEx hub in the second module, and (iii) second SuFEx ligation in the third module.

Taking this into account, estrone was chosen to install the –SO_2F handle and (4-iodophenoxy)trimethylsilane to perform the second ligation (Figure 5.4). Gratifyingly, we were able to obtain sulfate **34** in a yield of 67%, with a total residence time of only 3.6 min. Importantly, the flow rates were readjusted to ensure a stoichiometry of SO_2F_2:estrone of 1.1 to 1, which helped to inhibit potential side reactions such as the reaction of excess SO_2F_2 with the second nucleophile.

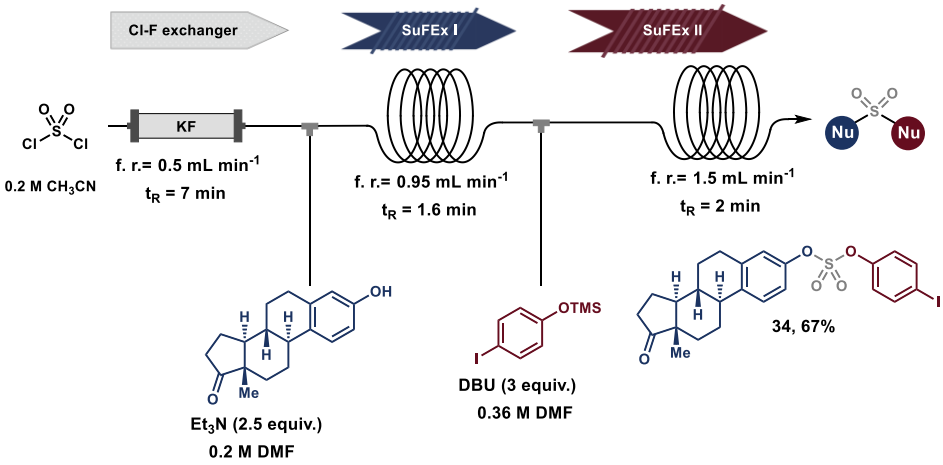

Scheme 5.4. Trimodular flow setup for the telescoped formation of sulfate **34**. Experimental details can be found in section 5.5.

The R–OSO_2F handle is not only useful for SuFEx ligations, but can also be exploited for other transformations such as cross-couplings,[25] deoxyfluorinations,[26] and radiolabeling.[27] To prove the versatility of our system, it was decided to couple a fed-batch module to perform a hydrolysis reaction (Scheme 5.5, A) and a palladium catalyzed cross-coupling (Scheme 5.5, B). Specifically, a stream of fluorosulfate solution was generated and subsequently fed into a vial to perform the next reaction.

For the hydrolysis derivatization, ethyleneglycol acetal-protected estrone was used to avoid undesired condensations. The receiving vial contained a KOH solution in ethanol which afforded hydrogensulfate **35** in 80% yield. Regarding the cross-coupling reaction, estrone was used as nucleophile and the solvent from the vial was changed and phenyl boronic acid, palladium(II) acetate, triphenylphosphine, and cesium carbonate were added. After an overnight at 110 °C, we were able to obtain the resulting Suzuki-Miyaura cross-coupling product **36** in 55% yield.

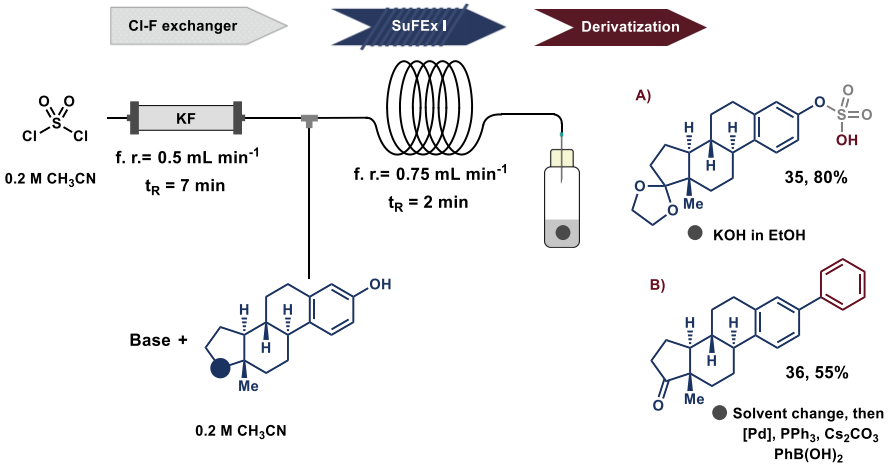

[25] Liang, Q.; Xing, P.; Huang, Z.; Dong, J.; Sharpless, K. B.; Li, X.; Jiang, B. *Org. Lett.* **2015**, *17*, 1942.
[26] Schimler, S. D.; Cismesia, M. A.; Hanley, P. S.; Froese, R. D.; Jansma, M. J.; Bland, D. C.; Sanford, M. S. *J. Am. Chem. Soc.* **2017**, *139*, 1452.
[27] Zheng, Q.; Xu, H.; Wang, H.; Du, W.-G. H.; Wang, N.; Xiong, H.; Gu, Y.; Noodleman, L.; Sharpless, K. B.; Yang, G.; Wu, P. *J. Am. Chem. Soc.* **2021**, *143*, 3753.

Scheme 5.5. Flow-batch setup for the formation hydrolyzed product **35**, and cross-coupled product **36**. A) KOH (10 equiv), EtOH (1M); B) toluene (0.28 M), $Pd(OAc)_2$ (0.05 equiv), PPh_3 (0.125 equiv), Cs_2CO_3 (3 equiv), $PhB(OH)_2$ (1.4 equiv). Experimental details can be found in section 5.5.

5.3.5 Scope of peptides and proteins

Our microfluidic system showed excellent performance with small molecules bearing unprotected functionalities. Inspired by the fact that click reactions are commonly used in biological settings, we decided to investigate their application to peptide modification.

Because of the high reactivity of SO_2F_2 with phenols, we reasoned that tyrosine residues could be selectively modified in the presence of other nucleophilic amino acids. To test this hypothesis, we began our study by performing some competition experiments with protected nucleophilic amino acids. ^{19}F NMR analysis revealed that, indeed, tyrosine was the most reactive amino acid, followed by lysine (Figure 5.9).

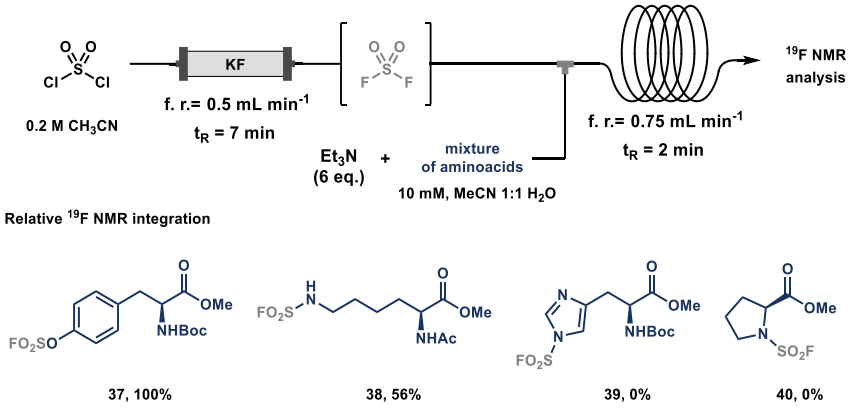

Figure 5.9. Competition experiment of protected amino acids for preliminary test of site selectivity in the SuFEx reaction. Experimental details can be found in section 5.5.

We then decided to test some model pentapeptides in the flow set-up to confirm these observations. The setup of choice was the same as for the scope

of small molecules (Scheme 5.1). However, we changed the solvent of the reaction by using a mixture of acetonitrile and water (1:1 in volume) together with 6 equivalents of triethylamine. Also, due to the diluted conditions and the presence of water, we had to increase the equivalents of SO_2F_2 (40 equiv) to overcome the poor solubility of the gas in the reaction.

As depicted in Scheme 5.6, tyrosine-containing peptides **41** and **42** fully reacted to exclusively modify the phenolic residue in only two min of residence time. On the other hand, lysine and histidine residues in **43** and **44**, exhibited limited reactivity (50% and 5%, respectively). Finally, other nucleophilic amino acids such as proline **45**, aspartic acid or asparagine **46**, serine and cysteine **47**, did not react at all with SO_2F_2.

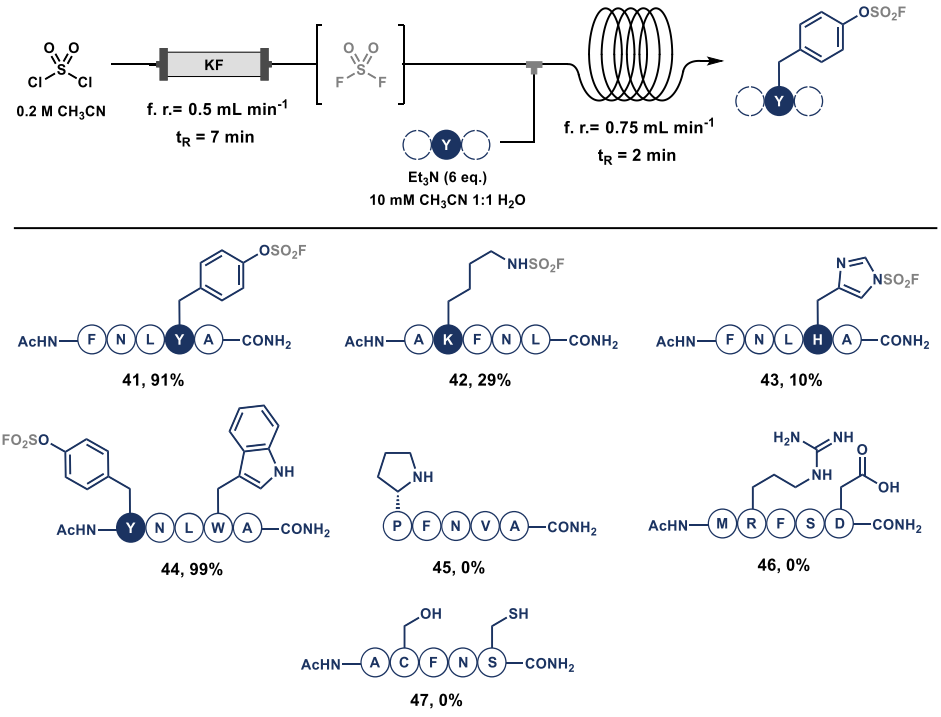

Scheme 5.6. Flow modification of pentapeptides to test residue reactivity. Standard conditions for the SO_2F_2 generation: SO_2Cl_2 (40 equiv, 0.2 M in CH_3CN) passed through a 3.8 mL cartridge filled with a 1:1 mixture of KF and glass beads at f.r. 0.5 mL/min. Peptide (1 equiv, 10 mM in CH_3CN:H_2O 1:1), Et_3N (6 equiv), f.r. 0.25 mL/min, res. time 2 min at room temperature. Experimental details can be found in section 5.5.

The marked selectivity toward tyrosine motivated us to explore the modification of more complex peptide chains (Scheme 5.7). Significantly, the preparation of tyrosine-SO_2F peptides was previously achieved by preforming the unnatural amino acid and subsequent multistep solid phase peptide synthesis (SPPS).[28] However, we pursued the direct modification of the peptide chains.

Cyclic peptides desmopressin **48** and oxytocin **49** were modified at tyrosine as confirmed by MS/MS spectrometry in excellent conversions. Therapeutic drugs such as Angiotensin II **50** and Bivalirudin **51** could be successfully converted to the corresponding fluorosulfates (66% and 30%, respectively). In the case of natural peptides, α-Endorphin **52** was obtained in 87% conversion with partial selectivity due to lysine competition (4.5:1 tyrosine/lysine), and β-Amyloid (1–28) **53** was obtained in low conversion (10%).

[28] Chen, W.; Dong, J.; Li, S.; Liu, Y.; Wang, Y.; Yoon, L.; Wu, P.; Sharpless, K. B.; Kelly, J. W. *Angew. Chem. Int. Ed.* **2015**, *55*, 1835.

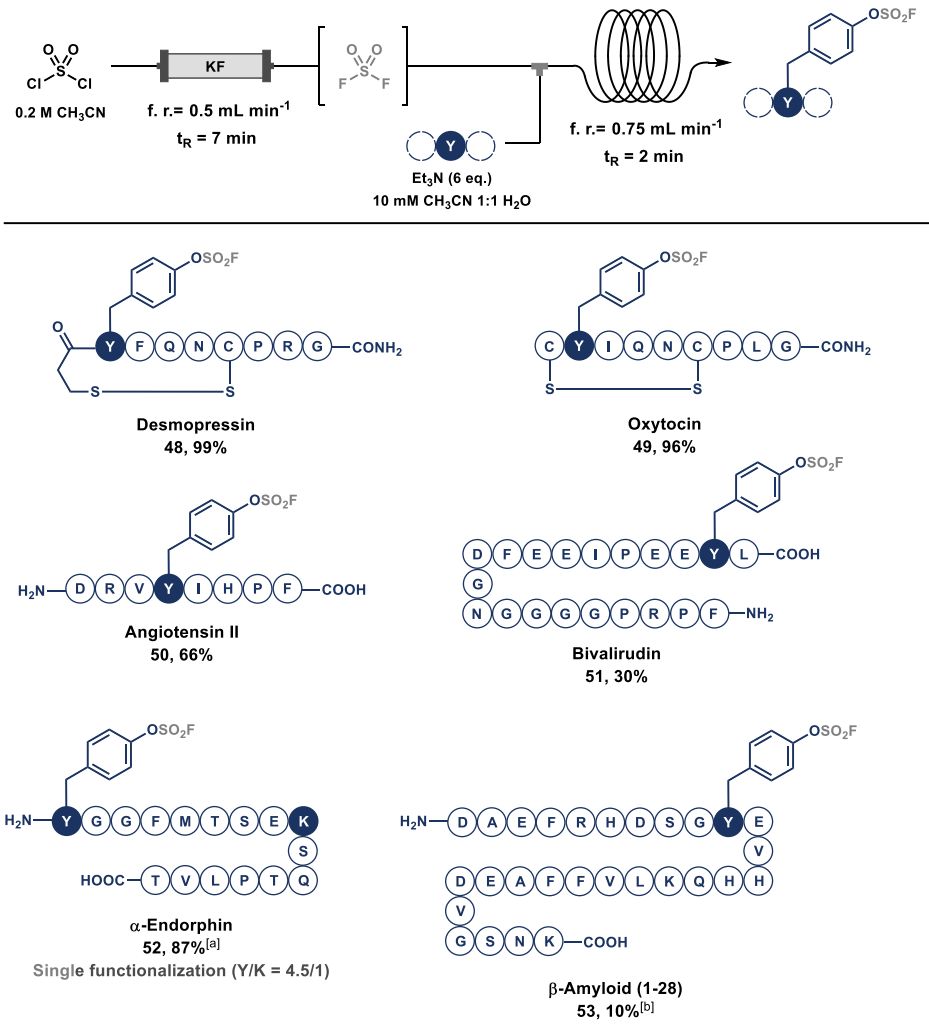

Scheme 5.7. Scope of the SuFEx ligation of peptides in the flow system. Standard conditions for the SO_2F_2 generation: SO_2Cl_2 (40 equiv, 0.2 M in CH_3CN) passed through a 3.8 mL cartridge filled with a 1:1 mixture of KF and glass beads at f.r. 0.5 mL/min. Peptide (1 equiv, 10 mM in CH_3CN:H_2O 1:1), Et_3N (6 equiv), f.r. 0.25 mL/min, res. time 2 min at room temperature. [a] α-Endorphin (6 mM), SO_2F_2 (67 equiv). [b] β-Amyloid (3 mM), SO_2F_2 (133 equiv). Experimental details can be found in section 5.5.

Finally, we set our focus on the direct modification of proteins in flow. As proteins require an aqueous buffer for their reaction and tolerate a low percentage of organic solvent, the flow setup had to be adapted for this purpose. Given that SO_2F_2 comes from the Cl–F exchange module as an

acetonitrile solution, the flow rate of this stream was modified (0.1 mL/min) to be 10% with volume in respect of the protein input (0.9 mL/min). Due of this difference in flow rates, a back pressure regulator (2.5 bar) was installed after the packed-bed column to ensure reliable mixing (Table 5.2, heading).

Myoglobin (~17 KDa, 2 tyrosines in its structure) and β-Casein (~25 KDa, 4 tyrosines in its structure) were selected as candidates for the installation of the SO_2F handle. Next, the optimization of the reaction of myoglobin was conducted pursuing the selective functionalization of one of the two available tyrosine residues (Table 5.2).

Table 5.2. Optimization of Myoglobin SuFEx ligation in flow. Experimental details can be found in section 5.5. Reactions carried out at r.t. otherwise indicated.

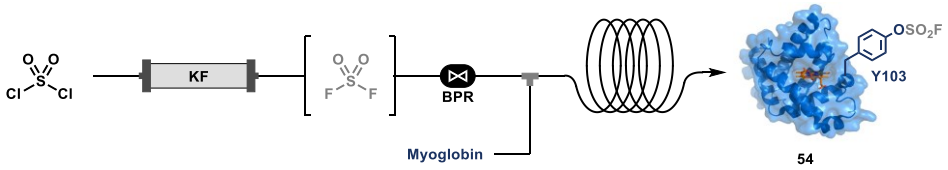

Entry	pH	SO_2F_2 (equiv)	Res. time (min)	Additive (equiv)	Conv. (%)	Functionalization (%)		
						Mono.	Di.	Tri.
1	7.0	10	1.5	-	24	79	21	-
2	7.0	40	1.5	-	25	80	20	-
3	7.7	10	1.5	-	48	69	25	6
4	6.0	10	1.5	-	34	85	15	-
5	5.0	10	1.5	-	8	100	-	-
6	6.0	10	10	-	31	87	13	-
7	5.0	10	1.5	TMG (1)	33	100	-	-
8	6.0	10	1.5	TMG (10) at 37 °C	70	49	33	14

The starting point of the optimization was to use similar conditions to those of the peptides (Scheme 5.6). In this case, a conversion of 24% was obtained with a mixture of mono- and di- functionalization (Table 5.2, entry 1). To our surprise, the increase in SO_2F_2 equivalents did not have any effect on conversion (Table 5.2, entry 2). In contrast, the variation of the pH had a substantial impact on both conversion and selectivity (Table 5.2, entries 3–6). We reasoned that lowering the pH would favor the protonation of competing lysines, thus increasing the selectivity toward tyrosine. Indeed, use of pH = 7.7 (entry 3) gave an increased conversion at the expense of selectivity, while acidic conditions of pH = 5.0 (entry 5) gave perfect selectivity but with lower conversion. Increasing the residence time (Table 5.2, entry 6) had no impact on the outcome of the reaction. Gratifyingly, setting the pH to 5 and adding 1 equivalent of 1,1,3,3-tetramethylguanidine (TMG) as basic activator, we could exclusively install one $–SO_2F$ handle to myoglobin (Table 5.2, entry 7). Digestion of the crude followed by MS/MS analysis revealed that tyrosine 103 was the one of the two possible tyrosines that was modified. At that point, we decided to tune the conditions to obtain a sample with a higher conversion (Table 5.2, entry 8) by increasing the pH, temperature, and the equivalents of TMG.

This study discloses a new bioconjugation reaction, which differs from the classical SuFEx ligations because we directly place the electrophilic handle on the protein. Moreover, we performed the transformation in flow with a residence time of just 1.5 min, representing an incredibly fast process. To the best of our knowledge, this is one of the fastest protein modifications ever reported.[29]

To compare with other methodologies, we decided to reproduce the optimal conditions in conventional setups. Strikingly, the use of a fed-batch system only delivered the modified protein in 16% conversion (Scheme 5.8). Additionally, when opting for a fully batch approach with the H-type reactor,

[29] Boutureira, O.; Bernardes, G. J. L. *Chem. Rev.* **2015**, *115*, 2174.

a complex mixture of products was observed, with no desired SO_2F additions to myoglobin detected.

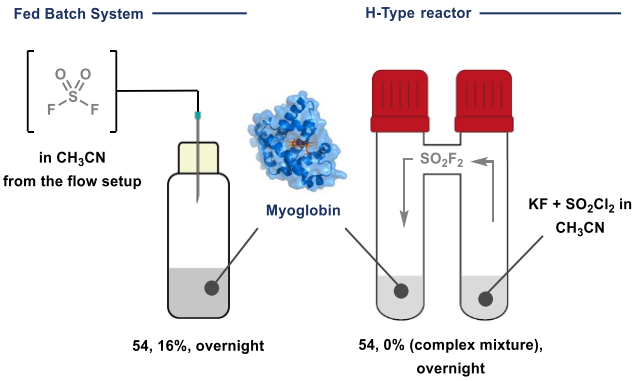

Scheme 5.8. Attempts towards –SO_2F installation in myoglobin with conventional setups. Experimental details can be found in section 5.5.

Remarkably, the microfluidic system outperformed all other traditional setups that were tested. The enhanced mass transfer and the confinement of the gaseous hydrophobic SO_2F_2 result in a fierce mixing of components enabling the SuFEx hub installation in complex macromolecular systems. Also, the controlled dosage of the SO_2F_2 by the pumping system was crucial for achieving the desired selectivity.

With these results in hand, we focused our efforts on modifying β-Casein. As this protein has 4 unique tyrosine residues in its structure, we decided to prime conversion over selectivity. To our delight, minimal modification of previous myoglobin conditions (Table 5.2, entry 8) enabled a 58% conversion of β-Casein with predominantly single functionalization (62%) at three different tyrosine residues (Y180/Y193/Y114 =10.7/2.4/1, determined by digestion and MS/MS analysis), followed by di- (27%) and tri-functionalization (11%).

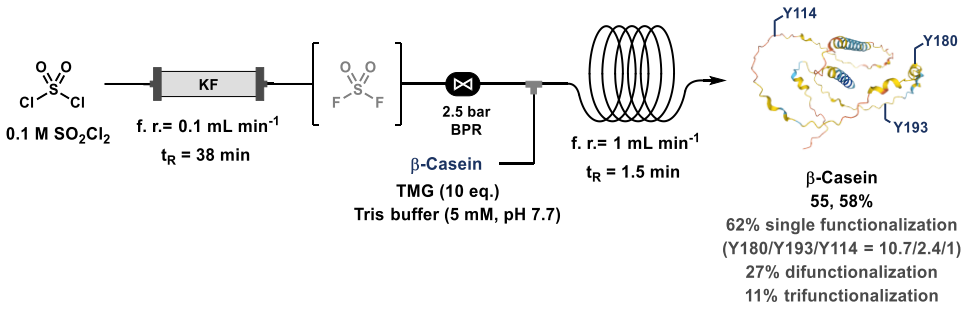

Scheme 5.9. In flow SuFEx ligation of β-casein. Experimental details can be found in section 5.5.

5.4 Conclusions

In this chapter, a new modular flow platform for the installation of the SO_2F handle into small molecules, peptides, and proteins has been described. We did this by developing a microfluidic system for the *in situ* preparation and use of reactive SO_2F_2 gas, providing a practical platform for chemists to access SuFEx chemistry without the common problems associated with its handling and toxicity.

Starting with a simple cartridge of KF, we could transform an acetonitrile solution of cheap and commercially available SO_2Cl_2 into an SO_2F_2 stream. After optimizing the flow rate for the generation of the gaseous reagent, we coupled this Cl–F exchange unit to a second reaction module where the SuFEx reaction took place. With this setup we could successfully modify a wide variety of phenols, amines and nitrogen-heterocycles bearing different functional groups in just 2 min. Also, taking advantage of the modularity of the system, we could exploit the platform to further functionalize the $–SO_2F$ handle.

Being aware of the robustness of the transformation, we used our system for the derivatization of peptides. Initial studies demonstrated a clear selectivity toward the tyrosine residue compared to other nucleophilic amino acids. After tuning of the reaction conditions, we could modify different peptide chains preferentially at the phenolic residue. Finally, we

demonstrated that our flow platform could also be used for the modification of proteins in a new super-fast bioconjugation reaction.

We hope our findings will offer new opportunities for the creation of libraries of compounds, and for the modification of peptides and proteins. We believe that our simple, yet effective, flow platform can be easily implemented in any research laboratory.

5.5 Experimental section

^{1}H (300, 400, and 500 MHz), ^{13}C (75, 101, and 125 MHz) and ^{19}F (282, 376, and 470 MHz) spectra were recorded at ambient temperature using Bruker AV 300-I, AV 400, AV 500-NEO. For continuous NMR analysis, a Benchtop NMR Spinsolve 60 Carbon from Magritek was used. ^{1}H NMR spectra are reported in parts per million (ppm) downfield relative to $CDCl_3$ (7.26 ppm) and all ^{13}C NMR spectra are reported in ppm relative to $CDCl_3$ (77.16 ppm) unless stated otherwise. The multiplicities of signals are designated by the following abbreviations: s (singlet), d (doublet), t (triplet), q (quartet), m (multiplet), dd (doublet of doublets), dt (doublet of triplets), td (triplet of doublets), ddd (doublet of doublet of doublets). Coupling constants (J) are reported in hertz (Hz). NMR data was processed using the MestReNova 14 software package. High resolution mass spectra (HRMS) were collected on an AccuTOF LC, JMS-T100LP Mass spectrometer (JEOL, Japan) or on an AccuTOF GC v 4g, JMS-T100GCV Mass spectrometer (JEOL, Japan), or on a 7200 GC−qTOF (Agilent Technologies). Disposable syringes were purchased from Laboratory Glass Specialist. Syringe pumps were purchased from Chemix Inc. model Fusion 200 Touch. Product isolation was performed manually, using silica (P60, SILICYCLE). TLC analysis was performed using Silica on aluminum foils TLC plates (F254, SILICYCLE) with visualization under ultraviolet light (254 nm and 365 nm) or appropriate TLC staining (Cerium Ammonium Molybdate). Organic solutions were concentrated under reduced pressure on a Büchi rotary evaporator (in vacuo at 40 °C, ~5 mbar).

For the analytical instruments for peptide and protein modification, the reversed phase liquid chromatography (RPLC) and size exclusion chromatography (SEC) analysis were performed on an UltiMate RSLCnano system (Thermo Fisher Scientific, Breda, The Netherlands) equipped with a high-pressure pump with microflow selector and a loading pump (NCS-3500RS), as well as two 10-port, two-position valve and an autosampler. Injection loop of 1 μL and 20 μL were used. The autosampler temperature was

8°C throughout the study. Alternatively, an analytical reverse-phase RPLC coupled to ESI-MS (Agilent 1260 + quadrupole 6120, Column: Eclipse XDB-C18, 4.6 × 150 mm, 5 μm) or an RPLC coupled to ESI-MS (Agilent 1260 + quadrupole LC/MSD XT, Column: AdvanceBio RP-mAb C4, 2.1 × 50 mm, 3.5 μm) were used. The high-resolution mass spectrometry was obtained using a QExactive-Plus Biopharma (Thermo Fisher Scientific, Bremen, Germany). For intact protein analysis, the SEC-MS was performed on a TSKgel SuperSW3000 (1.0 x 300 mm x 4 μm, TOSOH, Japan) column. For RPLC-MS/MS analysis, the peptides and digestion products were separated from the InfinityLab Poroshell 120 EC-C18 (2.1 x 500 mm x 1.9 μm, Agilent, USA) column.

5.5.1 Materials

All reagents and solvents were used as received without further purification. Reagents and solvents were purchased from Sigma Aldrich, TCI, abcr, Bachem, and Fluorochem. Technical solvents were purchased from VWR International and used as received. Empty cartridges used for the packed bed reactor were purchased at Screening Devices (catalog number SD-0000-004). For the analysis of peptides and proteins, Ammonium acetate (AmAc, analytical grade), formic acid (FA, analytical grade > 98%), dithiothreitol (>99.5%), iodoacetamide (>99%), ammonium bicarbonate (>99.5%), urea (>98%) and trypsin from porcine pancreas were purchased from Sigma Aldrich (St. Louis, Missouri, United States). Methanol (MeOH) and acetonitrile (CH_3CN) were purchased from Biosolve (Valkenswaard, The Netherlands). High-purity (HP) water (18.2 MΩ·cm) was produced by a Sartorius (Göttingen, Germany) Arium 611UV Ultrapure-Water System.

(4-iodophenoxy)trimethylsilane[30] and (8*R*,9*S*,13*S*,14*S*)-13-methyl-6,7,8,9,11,12,13,14,15,16-decahydrospiro[cyclopenta[*a*]phenanthrene-17,2'-

[30] D. Amantini, F. Fringuelli, F. Pizzo, L. Vaccaro, *J. Org. Chem.* **2001**, 66, 6734.

[1,3]dioxolan]-3-ol[31] were prepared according to reported literature procedures.

5.5.2 Packed bed reactor preparation

To implement batch SO_2F_2 generation in a microfluidic setup, a packed bed was selected as the appropriate module for the SO_2Cl_2 reaction with KF. The reactor consisted of an empty polypropylene (PP) cartridge from an automated flash chromatography column,[32] which was filled with a mixture of dried KF and glass beads (425 - 600 μm) in a weight ratio of 1:1. Importantly, this mixture was grinded in an agate mortar, and dried overnight at 150 °C under vacuum before filling up the cartridge. In our system, the cartridge could be filled with a mixture of ~9.3 g of KF and glass beads. The empty volume of the reactor was determined to be of ~3.8 mL by weighting the filled cartridge before and after flushing it with acetonitrile.

5.5.3 Peptide analysis

General Analytical method A

For unreacted pure peptides, 20 μL of the purified fractions were directly injected in the RPLC-MS, while for reacted peptides, the amount of solution corresponding to 3 nmol of peptide was diluted in 30 μL H_2O/ CH_3CN 1:1, being then the total sum of volumes injected in the RPLC-MS.

Peptides were analyzed by analytical reverse-phase RPLC coupled to ESI-MS (Agilent 1260 + quadrupole 6120, Column: Eclipse XDB-C18, 4.6 × 150 mm, 5 μm) with solvent A (H_2O + 0.1% FA + 0.01% TFA) and solvent B (CH_3CN + 0.1% FA + 0.01% TFA) via a 10 min gradient from 5% to 95% solvent B.

---

[31] M. P. Leese, H. A. M. Hejaz, M. F. Mahon, S. P. Newman, A. Purohit, M. J. Reed, B. V. L. Potter, *J. Med. Chem.* **2005**, *48*, 5243.

[32] The PP cartridge was purchased form Screening Devices company: 4g, Double Luer Lock Top and Bottom Empty Solid Load Cartridge with Screw Cap, frits, O-ring and end tips, 20p (catalog number SD-0000-004).

General Analytical method B

The SO_2F-based functionalization of various peptides was investigated using RPLC coupled with MS. The concentrations of peptides are 0.2 mg/mL and 10% CH_3CN was used as the dilution solvent when they were analyzed. the measurement was conducted at a flowrate of 250 μL/min using Water/ CH_3CN = 2: 98% with 0.1% FA (A) and Water/CH_3CN = 98: 2% with 0.1% FA (B) as mobile phases. The gradient applied consisted of two steps from 98% B to 80% B in 8 min and from 80% to 40% B in 10 min. After the gradient the column was re-equilibrated for 5 min. The injection volume was 1 μL. The oven was kept at 60 °C. The MS spectrum was acquired using a full MS scan followed by parallel reaction monitoring (PRM) for MS/MS, specifying the masses to fragmentate. The parameters were as follows. Polarity: positive. Microscans: 1. Resolution: 70000. Maximum injection time: 200 ms. Scan range: 300 to 3500. AGC target: 3e6. Capillary temperature: 350 Celsius. Sheath gas flow: 35. Auxiliary gas flow: 10. Spray voltage: 3.5 kV. S-lens RF level: 50. The MS/MS data is obtained by Parallel Reaction Monitoring mode with the conditions of polarity: positive, Default charge: 2, resolution: 17500, AGC target: 3e6, maximum IT: 100 ms, isolation window: 1.0 m/zm (CE)/stepped nce: 35 or 50.

The MS data was visualized with FreeStyle 1.6 software (Thermo Fisher Scientific) and Thermo Biopharma Finder (Thermo Fisher Scientific). The deconvolution results are carried out with UniDec software (University of Arizona, Phoenix, AZ, USA).[33]

The conversion rate (CR) of proteins is calculate by

$$\text{CR (\%)} = \frac{Intensity_{Modified\ proteins}}{Intensity_{unmodified\ proteins} + Intensity_{modified\ proteins}} \text{ x } 100.$$

The conversion rate (CR) of peptides is calculate by

[33] Michael T. Marty, Andrew J. Baldwin, Erik G. Marklund, Georg K. A. Hochberg, Justin L. P. Benesch, and Carol V. Robinson. *Anal. Chem.* **2015**, *87*, 4370.

$$\text{CR (\%)} = \frac{Peak\ areas_{Modified\ peptides}}{Peak\ areas_{unmodified\ peptides} + Peak\ areas_{modified\ peptides}} \text{ x } 100.$$

5.5.4 Protein analysis

General Analytical method C

5 μL of a 250 μM solution of myoglobin in H_2O + 0.1% TFA were analyzed by analytical reverse-phase RPLC coupled to ESI-MS (Agilent 1260 + quadrupole LC/MSD XT, Column: AdvanceBio RP-mAb C4, 2.1 × 50 mm, 3.5 μm) with solvent A (H_2O + 0.1% FA) and solvent B (iPrOH 80% + CH_3CN 10% + H2O 10% + 0.1% FA) via a 10 min gradient from 5% to 95% of solvent B.

General Analytical method D

The SO_2F-based functionalization of various proteins was proved by using native microflow size exclusion chromatography (SEC) coupled to high-resolution mass spectrometry (MS) method.[34] Samples were analyzed as 1.0 mg/mL in200 mM ammonium acetate. For the microflow SEC, it was performed at 15 μL/min with 200 mM ammonium acetate as mobile phase. 1 μL was used as injection volume. The MS spectrum is acquired with HRM-AIF mode. The parameters were as follows. Polarity: positive. In-source CID: 50 eV. Microscans: 10. Resolution: 17500. Maximum injection time: 200 ms. Scan range: 350 to 6000. AGC target: 3e6. Capillary temperature: 275°C. Sheath gas flow: 15. Auxiliary gas flow: 5. Spray voltage: 2.5 kV. S-lens RF level: 200.

Protein digestion and MS/MS analysis

The analysis was performed using mobile phase A 2% CH_3CN + 0.1% FA and B 98% CH_3CN + 0.1%FA and a two-step gradient method from 98% B to 80% B in 27 min and from 80% B to 60% B in 10 min. After the gradient the column was re-equilibrated for 5 min. The analysis was performed at 60 °C.

[34] I. K. Ventouri, S. Veelders, M. Passamonti, P. Endres, R. Roemling, P. J. Schoenmakers, G. W. Somsen, R. Haselberg, A. F.G. Gargano, *Anal. Chim. Acta.* **2023**, *1266*, 341324.

20 μL loop was employed and the μLPickUp mode was used to inject samples. 4 uL of solution were injected. The MS spectrum was acquired with Full MS/ data dependent MS/MS acquisition with Top5 mode. The parameters of full MS were as follows: Polarity: positive. Default charge: 2. Resolution: 70000. Maximum injection time: 100 ms. Scan range: 200 to 2000. AGC target: 3e6. The conditions of dd-MS^2 were as follows: Resolution: 17500. AGC target: 1e5. Maximum injection time: 200 ms. Loop count: 5. TopN: 5. (N)ce/STEPPED NCE: 30. Capillary temperature: 350 Celsius. Sheath gas flow: 35. Auxiliary gas flow: 10. Spray voltage: 3.5 kV. S-lens RF level: 50.

5.5.5 Batch experiments by using a H-type reactor for 4-phenylphenol

We evaluated the feasibility of a batch setup by generating SO_2F_2 *ex situ* from sulfuryl chloride and KF: The setup consists of a two-chamber reactor where in one vessel the generation of the SO_2F_2 takes place, while in the other the nucleophile reacts with the incoming gas. Under these conditions, we observed generally slower reaction times and yields (Table E1, entries 1–6). In order to obtain similar chemical efficiency with respect to our flow setup, we had to increase the equivalents of KF to 13 and greatly extend the reaction time.

Table E1. H-Type reactor experiments for the generation of [1,1'-biphenyl]-4-yl sulfurofluoridate. Yields were determined by ^{19}F NMR analysis using 1,2-difluorobenzene as the internal standard.

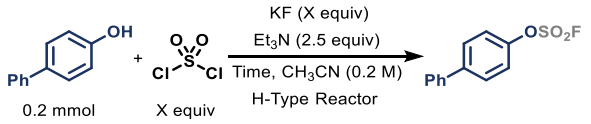

Entry	KF (equiv)	SO_2Cl_2 (equiv)	Time (h)	Yield (%)
1	9	2	2	38
2	9	5	2	18
3	9	2	18	69
4	9	5	18	42
5	13	2	2	38
6	13	5	2	23
7	13	2	18	100
8	13	5	18	92

5.5.6 Installation of the SO_2F motif for small molecules

General Procedure A

In a typical experiment, sulfuryl chloride (810 μL, 10 mmol) was dissolved in dry acetonitrile (50 mL, 0.2 M) in an oven-dried, N_2 filled 100 mL round bottom flask with a rubber septum. The 0.2 M solution of sulfuryl chloride was taken up with a 20 mL syringe and mounted on a syringe pump. The first time a packed bed was used, it was flushed with dry acetonitrile to fill the empty volume with solvent. Then 5 mL of the SO_2Cl_2 were pumped at 0.5 $mL \cdot min^{-1}$ to equilibrate the reactor. Once this procedure was done, the cartridge could be used continuously until its exhaustion.

Parallelly, in a 10 mL vial the nucleophile was charged. Next, solvent and an organic base were subsequently added. This mixture was then taken up with a 5 mL syringe and mounted on a second syringe pump.

To start a reaction, the solution of sulfuryl chloride was constantly pumped through the equilibrated KF packed bed at 0.5 $mL \cdot min^{-1}$ (t_R = ~7 min). The resulting sulfuryl fluoride flow was then mixed with the nucleophile solution (pumped at 0.25 $mL \cdot min^{-1}$) through a PEEK T-mixer. The combined

feeds were connected to a 1.5 mL PFA coil (I.D = 0.8 mm, t_R = 2 min) which served as reactor for the SuFEx event. At the end of the coil, the organic crude was collected in a conical flask. These flow rates ensured a stoichiometry of 2 to 1, SO_2F_2:nucleophile.

Importantly, when the syringe pump of the nucleophile finished pushing the solution, the system was stopped (both syringe pumps), and the syringe of the nucleophile was quickly substituted by another one containing acetonitrile. Then the flow rate of the latter one was set to 0.75 mL·min^{-1} to push the remaining reaction crude of the PFA coil, while the syringe pump of the sulfuryl chloride solution remained stopped.

The collected organic crude was diluted with ethyl acetate, washed with 10% $HCl_{(aq.)}$, and then with brine. Next, the organic phase was dried over Na_2SO_4, filtered, and concentrated under reduced pressure to obtain the SuFExed products.

General Procedure B

In a typical experiment, sulfuryl chloride (810 μL, 10 mmol) was dissolved in dry acetonitrile (50 mL, 0.2 M) in an oven-dried, N_2 filled 100 mL round bottom flask with a rubber. The 0.2 M solution of sulfuryl chloride was taken up with a 20 mL syringe and mounted on a syringe pump. The first time a packed bed was used, it was flushed with dry acetonitrile to fill the empty volume with solvent. Then 5 mL of the SO_2Cl_2 were pumped at 0.5 mL·min^{-1} to equilibrate the reactor. Once this procedure was done, the cartridge could be used continuously until its exhaustion.

Parallelly, in a 10 mL vial containing a magnetic stir bar, the nucleophile was charged. Next, solvent and an organic base were subsequently added, and the vial was capped with a septum.

To start a reaction, the solution of sulfuryl chloride was constantly pumped through the equilibrated KF packed bed at 0.5 mL·min^{-1} (t_R = ~7 min). The resulting sulfuryl fluoride flow was then fed to the vial containing the

nucleophile through a needle. Once the desired amount of SO_2F_2 was fed into the vial, the latter one was left stirring at room temperature.

5.5.7 Characterization Data of Products Direct Coupling

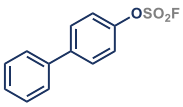

[1,1'-Biphenyl]-4-yl sulfurofluoridate (1). Prepared according to general procedure A, using [1,1'-biphenyl]-4-ol (85.1 mg, 0.5 mmol, 1 equiv) and triethylamine (175 μL, 1.25 mmol, 2.5 equiv) in CH_3CN (2.5 mL, 0.2 M). Compound **1** was obtained as a white solid (124 mg, 98% yield). The spectroscopic data are consistent with those reported previously.[35]

Large scale preparation was achieved by prolonging the reaction time using the same flow setup. According to general procedure A, using [1,1'-biphenyl]-4-ol (1.19 g, 7 mmol, 1 equiv) and triethylamine (2.5 mL, 17.5 mmol, 2.5 equiv) in CH_3CN (35 mL, 0.2 M). Compound **1** was obtained as a white solid (1.73 g, 98% yield).

^{1}H NMR (400 MHz, $CDCl_3$) δ 7.67 (d, *J* = 8.7 Hz, 2H), 7.56 (d, *J* = 7.0 Hz, 2H), 7.47 (t, *J* = 7.3 Hz, 2H), 7.41 (m, 3H). **^{13}C{^{1}H} NMR (101 MHz, $CDCl_3$)** δ 149.5, 142.1, 139.4, 129.1, 128.2, 127.3, 121.3. **^{19}F NMR (376 MHz, $CDCl_3$)** δ 37.64 (s, 1F).

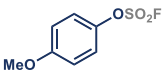

4-Methoxyphenyl sulfurofluoridate (2). Prepared according to general procedure A, using 4-methoxyphenol (62.1 mg, 0.5 mmol, 1 equiv) and triethylamine (175 μL, 1.25 mmol, 2.5 equiv) in CH_3CN (2.5 mL, 0.2 M). Compound **2** was obtained as a colorless oil (98mg, 95% yield). The spectroscopic data are consistent with those reported previously.[36]

^{1}H NMR (400 MHz, $CDCl_3$) δ 7.16 (d, J = 9.2 Hz, 2H), 6.85 (d, J = 9.2 Hz, 2H), 3.72 (s, 3H). **^{13}C{^{1}H} NMR (101 MHz, $CDCl_3$)** δ 159.4, 143.7, 122.1, 115.3, 55.8. **^{19}F NMR (376 MHz, $CDCl_3$)** δ 36.33 (s, 1F).

---

[35] J. Dong, L. Krasnova, M. G. Finn, K. B. Sharpless *Angew. Chem. Int. Ed.* **2014**, *53*, 9430.
[36] Q. Liang, P. Xing, Z. Huang, J. Dong, K. B. Sharpless, X. Li, B. Jiang, *Org. Lett.* **2015**, *17*, 1942.

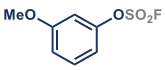

3-Methoxyphenyl sulfurofluoridate (3). Prepared according to general procedure A, using 3-methoxyphenol (62.1 mg, 0.5 mmol, 1 equiv) and triethylamine (175 μL, 1.25 mmol, 2.5 equiv) in CH_3CN (2.5 mL, 0.2 M). Compound **3** was obtained as a colorless oil (103 mg, 99% yield). The spectroscopic data are consistent with those reported previously.[35]

^{1}H NMR (400 MHz, $CDCl_3$) δ 7.36 (t, J = 8.3 Hz, 1H), 6.94 (m, 2H), 6.87 (t, J = 2.5 Hz, 1H), 3.83 (s, 3H). **^{13}C{^{1}H} NMR (101 MHz, $CDCl_3$)** δ 161.0, 150.8, 130.7, 114.4, 112.6, 107.0, 55.7. **^{19}F NMR (376 MHz, $CDCl_3$)** δ 37.64 (s, 1F).

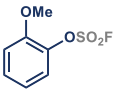

2-Methoxyphenyl sulfurofluoridate (4). Prepared according to general procedure A, using 2-methoxyphenol (62.1 mg, 0.5 mmol, 1 equiv) and triethylamine (175 μL, 1.25 mmol, 2.5 equiv) in CH_3CN (2.5 mL, 0.2 M). Compound **4** was obtained as a colorless oil (103 mg, 99% yield). The spectroscopic data are consistent with those reported previously.[36]

^{1}H NMR (400 MHz, $CDCl_3$) δ 7.42–7.28 (m, 2H), 7.06 (dd, *J* = 8.4, 1.4 Hz, 1H), 6.99 (td, *J* = 7.8, 1.5 Hz, 1H), 3.91 (s, 3H). **^{13}C{^{1}H} NMR (101 MHz, $CDCl_3$)** δ 151.3, 139.1, 129.8, 122.4, 121.0, 113.6, 56.2. **^{19}F NMR (376 MHz, $CDCl_3$)** δ 39.58 (s, 1F).

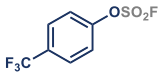

4-(Trifluoromethyl)phenyl sulfurofluoridate (5). Prepared according to general procedure A, using 4-(trifluoromethyl)phenol (81.1 mg, 0.5 mmol, 1 equiv) and triethylamine (175 μL, 1.25 mmol, 2.5 equiv) in CH_3CN (2.5 mL, 0.2 M). Compound **5** was obtained as a colorless oil (122 mg, 99% yield). The spectroscopic data are consistent with those reported previously.[37]

^{1}H NMR (400 MHz, $CDCl_3$) δ 7.78 (d, J = 8.6 Hz, 2H), 7.49 (d, J = 8.5 Hz, 2H). **^{13}C{^{1}H} NMR (101 MHz, $CDCl_3$)** δ 152.1, 131.3 (q, J = 33.4 Hz), 128.1 (q, J = 3.7

[37] P. S. Hanley, M. S. Ober, A. L. Krasovskiy, G. T. Whiteker, W. J. Kruper, *ACS Catal.* **2015**, 5, 5041.

Hz), 123.4 (q, J = 272.5 Hz), 121.8. **^{19}F NMR (376 MHz, $CDCl_3$)** δ 39.58 (s, 1F), -62.76 (s, 3F).

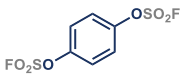

1,4-Phenylene bis(sulfurofluoridate) (6). Prepared according to general procedure A, using hydroquinone (55.1 mg, 0.5 mmol, 1 equiv) and triethylamine (175 μL, 1.25 mmol, 2.5 equiv) in CH_3CN (2.5 mL, 0.2 M). Compound **6** was obtained as a white solid (130 mg, 99% yield). The spectroscopic data are consistent with those reported previously.[35] **^{1}H NMR (400 MHz, $CDCl_3$)** δ 7.50 (s, 4H). **^{13}C{^{1}H} NMR (101 MHz, $CDCl_3$)** δ 149.1, 123.5. **^{19}F NMR (376 MHz, $CDCl_3$)** δ 38.24 (s, 2F).

(*S*)-2-((*tert*-Butoxycarbonyl)amino)-3-4((fluorosulfonyl)oxy)phenyl)propanoic acid (7). Prepared according to general procedure A, using (*tert*-butoxycarbonyl)-L-tyrosine (141.0 mg, 0.5 mmol, 1 equiv) and triethylamine (175 μL, 1.25 mmol, 2.5 equiv) in DMF (2.5 mL, 0.2 M). Compound **7** was obtained as a white solid (181.8 mg, 99% yield). The compound was previously unreported.

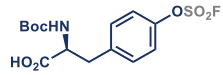

^{1}H NMR (500 MHz, DMSO-*d*$_6$) δ 12.56 (s, 1H), 7.62 – 7.30 (m, 2H), 7.29 – 6.46 (m, 2H), 4.26 – 3.84 (m, 1H), 3.10 (m, 1H), 2.94 – 2.58 (m, 1H), 1.49 – 1.17 (m, 9H).[38] **^{13}C{^{1}H} NMR (126 MHz, DMSO-*d*$_6$)** δ 172.7, 155.7, 148.3, 139.2, 131.2, 120.1, 78.0, 54.5, 36.0, 27.9.[39] **^{19}F{^{1}H} NMR (376 MHz, $CDCl_3$)** δ 37.50 (s, 1F). **HRMS (ESI$^+$):** m/z calculated for $[M+H]^+$, $C_{14}H_{19}FNO_7S^+$: 364.0861, found 364.0865.

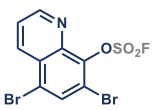

5,7-Dibromoquinolin-8-yl sulfurofluoridate (8). Prepared according to general procedure A, using 5,7-dibromoquinolin-8-ol (151.5 mg, 0.5 mmol, 1 equiv) and DBU (373 μL, 2.5 mmol,

[38] Peaks in ^{1}H-NMR spectrum split in multiple signals due to the presence of N-Boc rotamers. VT-NMR experiments were performed to confirm these observations.

[39] Peaks in ^{13}C-NMR spectrum split in multiple signals due to the presence of N-Boc rotamers. Highest intensity peaks of the rotamers are reported.

5.0 equiv) in CH_3CN (2.5 mL, 0.2 M). The crude mixture was filtered through a short path of silica with EtOAc, then the organic phase was concentrated under reduced pressure to afford compound **8** as a pale yellow crystalline solid (176 mg, 91% yield). The compound was previously unreported.

^{1}H NMR (400 MHz, $CDCl_3$) δ 9.07 (dd, J = 4.2, 1.6 Hz, 1H), 8.54 (dd, J = 8.6, 1.5 Hz, 1H), 8.09 (s, 1H), 7.66 (dd, J = 8.6, 4.2 Hz, 1H). **^{13}C{^{1}H} NMR (101 MHz, $CDCl_3$)** δ 152.9, 144.2, 142.0, 136.1, 133.4, 128.3, 123.9, 122.4, 117.0. **^{19}F NMR (376 MHz, $CDCl_3$)** δ 48.63 (s, 1F). **HRMS (FD):** m/z calculated for $[M]^+$, $C_9H_4Br_2FNO_3S^+$: 382.8257, found 382.8252.

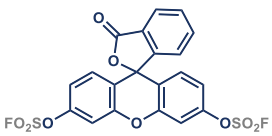

3-Oxo-3*H*-spiro[isobenzofuran-1,9'-xanthene]-3',6'-diyl bis(sulfurofluoridate) (9). Prepared according to general procedure A, using 3',6'-dihydroxy-3*H*-spiro[isobenzofuran-1,9'-xanthen]-3-one (166.2 mg, 0.5 mmol, 1 equiv) and triethylamine (175 μL, 1.25 mmol, 2.5 equiv) in DMF (2.5 mL, 0.2 M). Compound **9** was obtained as a white solid (248 mg, 99% yield). The spectroscopic data are consistent with those reported previously.[40]

^{1}H NMR (400 MHz, $CDCl_3$) δ 8.13 – 8.00 (m, 1H), 7.82 – 7.65 (m, 2H), 7.37 (d, J = 2.4 Hz, 2H), 7.19 (d, J = 7.5 Hz, 1H), 7.11 (dd, J = 8.8, 2.5 Hz, 2H), 7.00 (d, J = 8.9 Hz, 2H). **^{13}C{^{1}H} NMR (101 MHz, $CDCl_3$)** δ 168.6, 152.3, 151.5, 150.7, 136.0, 130.9, 130.3, 125.9, 125.6, 123.9, 119.8, 117.3, 110.5, 80.1. **^{19}F NMR (376 MHz, $CDCl_3$)** δ 38.79 (s, 1F).

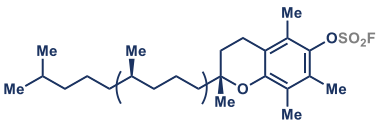

®-2,5,7,8-Tetramethyl-2-((4*R*,8*R*)-4,8,12-trimethyltridecyl)chroman-6-yl sulfurofluoridate (10). Prepared according to general procedure A, usi®(*R*)-2,5,7,8-tetramethyl-2-((4*R*,8*R*)-4,8,12-trimethyltridecyl)chroman-6-ol (215.4 mg, 0.5 mmol, 1 equiv) and triethylamine (175

[40] C. J. Smedley, J. A. Homer, T. L. Gialelis, A. S. Barrow, R. A. Koelln, J. E. Moses, *Angew. Chem. Int. Ed.* **2021**, *61*, e202112375.

μL, 1.25 mmol, 2.5 equiv) in DMF (2.5 mL, 0.2 M). Compound **10** was obtained as yellowish oil (241 mg, 94% yield). The spectroscopic data are consistent with those reported previously.[35]

^{1}H NMR (400 MHz, $CDCl_3$) δ 2.64 (t, *J* = 6.8 Hz, 2H), 2.27 (s, 3H), 2.24 (s, 3H), 2.15 (s, 3H), 1.84 (m, 2H), 1.70–1.52 (m, 3H), 1.52–1.39 (m, 2H), 1.39–1.23 (m, 12H), 1.23–1.05 (m, 7H), 0.90 (m, 12H). **^{13}C{^{1}H} NMR (101 MHz, $CDCl_3$)** δ 151.1, 142.0, 127.6, 126.2, 124.5, 118.5, 75.8, 40.1, 39.5, 37.6, 37.6, 37.5, 32.9, 32.8, 31.0, 28.1, 25.0, 24.6, 24.0, 22.9, 22.8, 21.1, 20.7, 19.9, 19.8, 13.6, 12.8, 12.0. **^{19}F NMR (376 MHz, $CDCl_3$)** δ 41.37 (s, 1F).

(8R,9S,13S,14S)-13-Methyl-17-oxo-7,8,9,11,12,13,14,15,16,17-decahydro-6H-cyclopenta[a]phenanthren-3-yl sulfurofluoridate (11). Prepared according to general procedure A, using (13*S*)-3-hydroxy-13 methyl-6,7,8,9,11,12,13,14,15,16-decahydro-17*H*cyclopenta[*a*]phenanthren-17-one (135.0 mg, 0.5 mmol, 1 equiv) and triethylamine (175 μL, 1.25 mmol, 2.5 equiv) in DMF (2.5 mL, 0.2 M). Compound **10** was obtained as a white solid (174 mg, 99% yield). The spectroscopic data are consistent with those reported previously.[41]

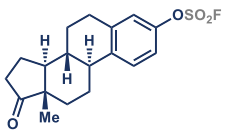

^{1}H NMR (400 MHz, $CDCl_3$) δ 7.38 (d, J = 8.6 Hz, 1H), 7.11 (d, J = 8.6 Hz, 1H), 7.07 (d, J = 2.7 Hz, 1H), 3.15 – 2.90 (m, 2H), 2.53 (dd, J = 18.7, 8.7 Hz, 1H), 2.46–2.38 (m, 1H), 2.32 (m, 1H), 2.18 (m, 1H), 2.13–2.03 (m, 2H), 2.02–1.96 (m, 1H), 1.72 – 1.41 (m, 6H), 0.93 (s, 3H). **^{13}C{^{1}H} NMR (101 MHz, $CDCl_3$)** δ 220.4, 148.2, 140.6, 139.6, 127.4, 120.7, 117.9, 50.4, 47.9, 44.2, 37.8, 35.9, 31.5, 26.1, 25.8, 21.6, 13.8. **^{19}F NMR (376 MHz, $CDCl_3$)** δ 37.42 (s, 1F).

(2S,5R,6R)-6-((*R*)-2-Acetamido-2-(4-(fluorosulfonyl)oxy)phenyl)acetamido)-3,3-dimethyl-7-oxo-4-thia-1-azabicyclo[3.2.0]heptane-2-carboxylic acid (Ac-12)

[41] K. Domino, C. Veryser, B. A. Wahlqvist, C. Gaardbo, K. T. Neumann, K. Daasbjerg, W. M. De Borggraeve, T. Skrydstrup, *Angew. Chem. Int. Ed.* **2018**, *57*, 6858.

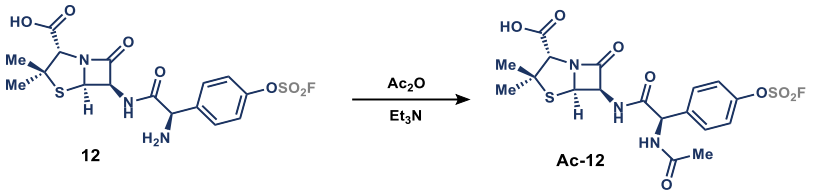

Prepared according to general procedure A, using (2*S*,5*R*,6*R*)-6-(2-amino-2-(4-hydroxyphenyl)acetamido)-3,3-dimethyl-7-oxo-4-thia-1-azabicyclo[3.2.0]heptane-2-carboxylic acid trihydrate (104.9 mg, 0.25 mmol, 1 equiv) and triethylamine (122 μL, 0.875 mmol, 3.5 equiv) in DMF (2.5 mL, 0.2 M). The crude mixture was then subjected to acetylation conditions for of isolation purposes: acetic anhydride (35.4 μL, 0.375 mmol, 1.5 equiv) and triethylamine (70 μL, 0.5 mmol, 2.0 equiv) were directly added to the crude mixture and the solution was left stirring overnight at room temperature. Next, the solvent was evaporated under reduced pressure. The resulting crude was purified by flash column chromatography (hexane:EtOAc 70:30) to afford compound **Ac-12** as a yellowish oil (98 mg, 80% yield). The compound was previously unreported.

^{1}H NMR (400 MHz, acetone-*d*$_6$) δ 8.30 (d, *J* = 7.6 Hz, 1H), 7.98 (d, *J* = 7.8 Hz, 1H), 7.72 (d, *J* = 8.8 Hz, 2H), 7.52 (d, *J* = 8.8 Hz, 2H), 5.95–5.84 (m, 1H), 5.56 (q, *J* = 4.0 Hz, 1H), 5.48 (d, *J* = 4.0 Hz, 1H), 4.32 (s, 1H), 2.09 (s, 1H), 2.02 (s, 3H), 1.54 (s, 3H), 1.48 (s, 3H). **^{13}C{^{1}H} NMR (101 MHz, acetone-*d*$_6$)** δ 173.3, 170.3, 170.2, 169.1, 150.5, 140.7, 130.8, 121.9, 71.1, 68.6, 64.7, 60.0, 56.5, 31.8, 27.0, 22.7. **^{19}F NMR (376 MHz, acetone-*d*$_6$)** δ 36.50 (s, 1F). **HRMS (ESI$^+$):** m/z calculated for $[M+H]^+$, $C_{18}H_{21}FN_3O_8S_2^+$: 490.0749, found 490.0751.

Azetidine-1-sulfonyl fluoride (13). Prepared according to general procedure A, using azetidine hydrochloride (46,8 mg, 0.5 mmol, 1 equiv) and triethylamine (279 μL, 2.0 mmol, 4 equiv) in CH_3CN (2.5 mL, 0.2 M). Compound **13** was obtained as a slightly yellow liquid (68 mg, 98% yield) The compound was previously unreported.

^{1}H NMR (300 MHz, $CDCl_3$) δ 4.19 (td, *J* = 7.9, 2.2 Hz, 4H), 2.39 (p, *J* = 7.9 Hz, 2H). **^{13}C{^{1}H} NMR (75 MHz, $CDCl_3$)** δ 53.1, 15.7. **^{19}F NMR (376 MHz, $CDCl_3$)** δ 27.88 (s, 1F). **HRMS (EI):** m/z calculated for $[M]^+$, $C_3H_6FNO_2S^+$: 139.0098, found 139.0096.

Pyrrolidine-1-sulfonyl fluoride (14). Prepared according to general procedure A, using pyrrolidine (41 μL, 0.5 mmol, 1.0 equiv) and triethylamine (174 μL, 1.25 mmol, 2.5 equiv) in CH_3CN (2.5 mL, 0.2 M). Compound **14** was obtained as a slightly yellow liquid (76 mg, 99% yield) The compound was previously unreported.

^{1}H NMR (400 MHz, $CDCl_3$) δ 3.49 (td, *J* = 6.8, 3.1 Hz, 4H), 2.07 – 1.95 (m, 4H). **^{13}C{^{1}H} NMR (101 MHz, $CDCl_3$)** δ 49.4 (d, *J* = 1.3 Hz), 25.7. **^{19}F NMR (376 MHz, $CDCl_3$)** δ 36.0 (t, *J* = 3.1 Hz, 1F). **HRMS (EI):** m/z calculated for $[M]^+$, $C_4H_8FNO_2S^+$: 153.0254, found 153.0255.

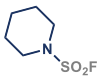

Piperidine-1-sulfonyl fluoride (15). Prepared according to general procedure A, using piperidine (49 μL, 0.5 mmol, 1.0 equiv) and triethylamine (174 μL, 1.25 mmol, 2.5 equiv) in CH_3CN (2.5 mL, 0.2 M). Compound **15** was obtained as a slightly yellow liquid (83 mg, 99% yield) The compound was previously unreported.

^{1}H NMR (400 MHz, $CDCl_3$) δ 3.41 (t, *J* = 5.2 Hz, 4H), 1.70 (p, *J* = 5.6 Hz, 4H), 1.65 – 1.57 (m, 2H). **^{13}C{^{1}H} NMR (101 MHz, $CDCl_3$)** δ 48.1 (d, *J* = 1.2 Hz), 24.7 (d, *J* = 1.3 Hz), 23.2. **^{19}F NMR (376 MHz, $CDCl_3$)** δ 39.74 (s, 1F). **HRMS (EI):** m/z calculated for $[M]^+$, $C_5H_{10}FNO_2S^+$: 167.0411, found 167.0408.

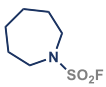

Azepane-1-sulfonyl fluoride (16). Prepared according to general procedure A, using azepane (56 μL, 0.5 mmol, 1.0 equiv) and triethylamine (174 μL, 1.25 mmol, 2.5 equiv) in CH_3CN (2.5 mL, 0.2 M). Compound **16** was obtained as a colorless liquid (68 mg, 75% yield) The compound was previously unreported.

^{1}H NMR (400 MHz, $CDCl_3$) δ 3.51 (td, *J* = 6.0, 2.2 Hz, 4H), 1.65 – 1.73 (m, 4H), 1.69 – 1.60 (m, 4H). **^{13}C{^{1}H} NMR (101 MHz, $CDCl_3$)** δ 49.6 (d, *J* = 1.9 Hz), 28.3 (d, *J* = 1.8 Hz), 26.8. **^{19}F NMR (376 MHz, CDCl3)** δ 46.98 (s, 1F). **HRMS (EI+):** m/z calculated for $[M]^+$, $C_6H_{12}FNO_2S^+$: 181.0567, found 181.0567.

***tert*-Butyl 2-(fluorosulfonyl)-2,8-diazaspiro[4.5]decane-8-carboxylate (17).**

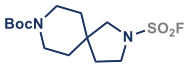

Prepared according to general procedure A, using *tert*-butyl 2,8-diazaspiro[4.5]decane-8-carboxylate (120 mg, 0.5 mmol, 1.0 equiv) and triethylamine (174 μL, 1.25 mmol, 2.5 equiv) in CH_3CN (2.5 mL, 0.2 M). Compound **17** was obtained as a white solid (135 mg, 84% yield). The compound was previously unreported.

^{1}H NMR (400 MHz, $CDCl_3$) δ 3.88 – 3.06 (m, 8H), 2.01 – 1.88 (m, 1H), 1.81 – 1.49 (m, 5H), 1.45 (s, 9H). **^{13}C{^{1}H} NMR (101 MHz, $CDCl_3$)** δ 154.7, 80.2, 56.9, 50.8, 47.8, 43.4, 34.1, 28.4, 23.0. **^{19}F NMR (376 MHz, $CDCl_3$)** δ 36.78 (s, 1F). **HRMS (ESI^+):** m/z calculated for $[M+Na]^+$, $C_{13}H_{23}FN_2O_4SNa^+$: 345.1255, found 345.1260.

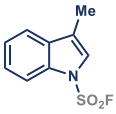

3-Methyl-1*H*-indole-1-sulfonyl fluoride (18). Prepared according to general procedure A, using 3-methylindole (66 mg, 0.5 mmol, 1.0 equiv) and DBU (299 μL, 2.0 mmol, 4.0 equiv) in DMF (2.5 mL, 0.2 M). The resulting organic crude was dissolved in a minimum amount of dichloromethane and pentane was added dropwise until the product crashed out. Next, the solid was filtered and dried to obtain compound **18** as a white solid (90 mg, 84% yield). The compound was previously unreported.

^{1}H NMR (400 MHz, $CDCl_3$) δ 7.89 (d, *J* = 7.8 Hz, 1H), 7.57 (d, *J* = 1.6 Hz, 1H), 7.47 – 7.36 (m, 2H), 7.18 (s, 1H), 2.31 (s, 3H). **^{13}C{^{1}H} NMR (101 MHz, $CDCl_3$)** δ 135.3, 131.7, 125.9, 124.7, 122.64 (d, *J* = 2.3 Hz), 120.78 (d, *J* = 1.7 Hz), 120.0, 113.7, 9.6. **^{19}F NMR (376 MHz, $CDCl_3$)** δ 53.37 (s, 1F). **HRMS (EI):** m/z calculated for $[M]^+$, $C_9H_8FNO_2S^+$: 213.0254, found 213.0255.

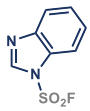

1*H*-Benzo[*d*]imidazole-1-sulfonyl fluoride (19). Prepared according to general procedure A, using 1H-benzo[*d*]imidazole (59.0 mg, 0.5 mmol, 1.0 equiv) and DBU (299 μL, 2.0 mmol, 4.0 equiv) in DMF (2.5 mL, 0.2 M). Compound **19** was obtained as a white solid (87 mg, 87% yield). The compound was previously unreported.

^{1}H NMR (400 MHz, $CDCl_3$) δ 8.27 (s, 1H), 7.92 – 7.77 (m, 2H), 7.51 (tt, *J* = 7.5, 5.8 Hz, 2H). **^{13}C{^{1}H} NMR (101 MHz, $CDCl_3$)** δ 127.0, 126.4, 121.8, 112.6. **^{19}F NMR (376 MHz, $CDCl_3$)** δ 56.49 (s, 1F). **HRMS (ESI+):** m/z calculated for $[M+H]^+$, $C_7H_6FN_2O_2S^+$: 201.0129, found 201.0131.

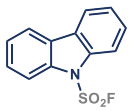

9*H*-Carbazole-9-sulfonyl fluoride (20). Prepared according to general procedure A, using carbazole (83.6 mg, 0.5 mmol, 1.0 equiv) and DBU (299 μL, 2.0 mmol, 4.0 equiv) in DMF (2.5 mL, 0.2 M). Compound **20** was obtained as a white solid (123 mg, 99% yield). The spectroscopic data are consistent with those reported previously.[42]

^{1}H NMR (400 MHz, $CDCl_3$) δ 8.06 (d, *J* = 8.3 Hz, 2H), 7.96 (d, *J* = 7.7 Hz, 2H), 7.56 – 7.50 (m, 2H), 7.46 (t, *J* = 7.5 Hz, 2H). **^{13}C{^{1}H} NMR (101 MHz, $CDCl_3$)** δ 137.4 (d, *J* = 1.8 Hz), 128.1, 126.3, 125.3, 120.4, 114.8. **^{19}F NMR** (376 MHz, $CDCl_3$) δ 52.45 (s, 1F).

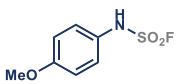

(4-Methoxyphenyl)sulfamoyl fluoride (21). Prepared according to general procedure A, using 4-methoxyaniline (61.6 mg, 0.5 mmol, 1.0 equiv) and DBU (299 μL, 2.0 mmol, 4.0 equiv) in DMF (2.5 mL, 0.2 M). Compound **21** was obtained as a purple syrup (109 mg, 99% yield). The spectroscopic data are consistent with those reported previously.[43]

^{1}H NMR (400 MHz, $CDCl_3$) δ 7.28 (dd, *J* = 8.4, 1.6 Hz, 2H), 7.05 (bs, 1H), 6.99 – 6.91 (m, 2H), 3.85 (s, 3H). **^{13}C{^{1}H} NMR (101 MHz, $CDCl_3$)** δ 159.5, 126.8 (d,

[42] M. H. Jeon, Y.-D. Kwon, M. P. Kim, G. B. Torres, J. K. Seo, J. Son, Y. H. Ryu, S. Y. Hong, J.-H. Chun, *Org. Lett.* **2021**, *23*, 2766.
[43] M. Ochiai, T. Okada, N. Tada, A. Yoshimura, K. Miyamoto, M. Shiro, *J. Am. Chem. Soc.* **2009**, 131, 8392.

J = 1.8 Hz), 126.03 (d, *J* = 2.6 Hz), 115.0, 55.7. **^{19}F NMR (376 MHz, $CDCl_3$)** δ 49.71 (s, 1F).

(1*S*,3a*S*,3b*R*,5a*S*,10a*S*,10b*S*,12a*S*)-1-Hydroxy-1,10a,12a-trimethyl-2,3,3a,3b,4,5,5a,6,10,10a,10b,11,12,12a-

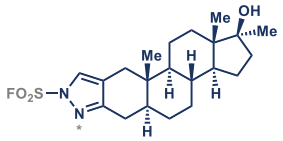

tetradecahydrocyclopenta[5,6]naphtho[1,2-f]indazole-7(1*H*)-sulfonyl fluoride (22). Prepared according to general procedure A, using stanozolol (164 mg, 0.5 mmol, 1.0 equiv) and triethylamine (174 μL, 1.25 mmol, 2.5 equiv) in DMF (2.5 mL, 0.2 M). Compound **22** was obtained as a 1:0.4 mixture of stereoisomers, off-white solid (129 mg, 63% yield). The compound was previously unreported.

^{1}H NMR (400 MHz, $CDCl_3$) δ 7.70 (s, 1H), 7.65 (s, 0.4H), 2.87 (ddd, *J* = 18.1, 5.1, 1.6 Hz, 0.4H), 2.78 – 2.68 (m, 2H), 2.61 – 2.49 (m, 0.4H), 2.44 – 2.29 (m, 1.4H), 2.11 (d, *J* = 15.9 Hz, 1.4H), 1.88 – 1.69 (m, 4.2H), 1.66 – 1.50 (m, 7H), 1.49 – 1.15 (m, 14H), 0.95 – 0.82 (m, 7H), 0.76 (s, 4.2H). **^{13}C{^{1}H} NMR (101 MHz, $CDCl_3$)** δ 158.25, 146.6, 142.4, 129.8, 122.1, 122.0, 121.2, 81.6, 53.5, 53.5, 50.5, 50.4, 45.4, 45.3, 41.9, 41.8, 38.9, 36.5, 36.4, 36.0, 35.9, 34.7, 34.2, 31.5, 31.3, 31.2, 29.1, 28.6, 27.4, 27.2, 25.8, 23.3, 20.8, 20.8, 13.9, 11.6, 11.5. **^{19}F NMR (376 MHz, $CDCl_3$)** δ 55.36 (s, 1F), 53.57 (s, 1F). **HRMS (FD):** m/z calculated for $[M]^+$, $C_{21}H_{31}FN_2O_3S^+$: 410.2039, found 410.2030.

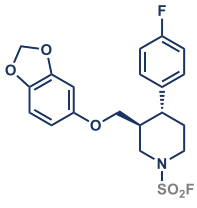

(3*S*,4*R*)-3-((Benzo[*d*][1,3]dioxol-5-yloxy)methyl)-4-(4-fluorophenyl)piperidine-1-sulfonyl fluoride (23). Prepared according to general procedure A, using (3*S*,4*R*)-3-((benzo[*d*][1,3]dioxol-5-yloxy)methyl)-4-(4-fluorophenyl)piperidine hydrochloride (183 mg, 0.5 mmol, 1.0 equiv) and triethylamine (174 μL, 1.25 mmol, 2.5 equiv) in DMF (2.5 mL, 0.2 M). Compound **23** was obtained as a white solid (203 mg, 99% yield). The compound was previously unreported.

^{1}H NMR (400 MHz, $CDCl_3$) δ 7.16 (dd, *J* = 8.4, 5.3 Hz, 2H), 7.01 (t, *J* = 8.5 Hz, 2H), 6.63 (d, *J* = 8.5 Hz, 1H), 6.36 (d, *J* = 2.5 Hz, 1H), 6.14 (dd, *J* = 8.4, 2.5 Hz, 1H), 5.90 – 5.85 (m, 2H), 4.23 (ddd, *J* = 12.8, 4.3, 1.8 Hz, 1H), 4.07 (dq, *J* = 12.7, 3.1 Hz, 1H), 3.62 (dd, *J* = 9.6, 2.8 Hz, 1H), 3.48 (dd, *J* = 9.6, 6.2 Hz, 1H), 3.14 (tdd, *J* = 11.1, 7.3, 3.3 Hz, 2H), 2.75 (td, *J* = 10.8, 7.2 Hz, 1H), 2.26 (dtt, *J* = 11.4, 8.0, 3.5 Hz, 1H), 1.96 (h, *J* = 4.2 Hz, 2H). **^{13}C{^{1}H} NMR (101 MHz, $CDCl_3$)** δ 163.1, 160.7, 153.9, 148.3, 142.0, 137.7 (d, *J* = 3.3 Hz), 128.8 (d, *J* = 7.9 Hz), 115.9 (d, *J* = 21.2 Hz),107.9, 105.6, 101.3, 98.0, 68.1, 50.3, 47.8, 42.8, 41.2, 32.6. **^{19}F NMR (376 MHz, $CDCl_3$)** δ 40.98 (s, 1F), -115.04 – -115.27 (m, 1F). **HRMS (FD):** m/z calculated for $[M]^+$, $C_{19}H_{19}F_2NO_5S^+$: 411.0947, found 411.0944.

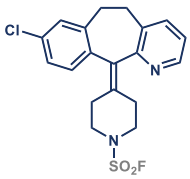

4-(8-Chloro-5,6-dihydro-11*H*-benzo[5,6]cyclohepta[1,2-*b*]pyridin-11-ylidene)piperidine-1-sulfonyl fluoride (24). Prepared according to general procedure A, using 8-chloro-11-(piperidin-4-ylidene)-6,11-dihydro-5H-benzo[5,6]cyclohepta[1,2-*b*]pyridine (155 mg, 0.5 mmol, 1.0 equiv) and triethylamine (174 μL, 1.25 mmol, 2.5 equiv) in DMF (2.5 mL, 0.2 M). Compound **24** was obtained as a yellow solid (191 mg, 97% yield). The compound was previously unreported.

^{1}H NMR (400 MHz, $CDCl_3$) δ 8.36 (dd, *J* = 4.8, 1.6 Hz, 1H), 7.41 (dd, *J* = 7.7, 1.7 Hz, 1H), 7.16 (d, *J* = 2.1 Hz, 1H), 7.13 – 7.04 (m, 3H), 3.67 (ddt, *J* = 23.6, 11.6, 5.3 Hz, 2H), 3.39 – 3.18 (m, 4H), 2.92 – 2.72 (m, 2H), 2.66 (ddd, *J* = 13.9, 9.2, 4.4 Hz, 1H), 2.52 (ddd, *J* = 13.8, 8.9, 4.5 Hz, 1H), 2.46 – 2.39 (m, 2H). **^{13}C{^{1}H} NMR (101 MHz, $CDCl_3$)** δ 156.1, 146.7, 139.7, 137.9, 137.2, 136.0, 134.1, 133.4, 133.3, 130.1, 129.1, 126.3, 122.6, 48.3 (d, *J* = 3.7 Hz), 31.5 (d, *J* = 3.5 Hz), 29.6, 29.4. **^{19}F NMR (376 MHz, $CDCl_3$)** δ 41.33 (s, 1F). **HRMS (ESI^+):** m/z calculated for $[M+H]^+$, $C_{19}H_{19}ClFN_2O_2S^+$: 393.0834, found 393.0845.

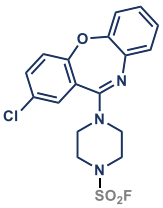

4-(2-Chlorodibenzo[*b,f*][1,4]oxazepin-11-yl)piperazine-1-sulfonyl fluoride (25). Prepared according to general procedure A, using amoxapine (157 mg, 0.5 mmol, 1.0 equiv) and triethylamine (174 μL, 1.25 mmol, 2.5 equiv) in DMF (2.5 mL, 0.2 M). Compound **25** was obtained as a yellow solid (160 mg, 81% yield). The spectroscopic data are consistent with those reported previously.[44] **^{1}H NMR (400 MHz, $CDCl_3$)** δ 7.33 (dd, *J* = 8.7, 2.6 Hz, 1H), 7.20 (d, *J* = 2.6 Hz, 1H), 7.17 – 6.90 (m, 5H), 3.50 (d, *J* = 33.1 Hz, 8H). **^{13}C{^{1}H} NMR (101 MHz, $CDCl_3$)** δ 159.5, 158.3, 151.8, 139.5, 133.2, 130.7, 128.7, 127.3, 126.0, 125.5, 124.5, 123.1, 120.4, 46.6, 46.5. **^{19}F NMR (376 MHz, $CDCl_3$)** δ 39.29 (s, 1F).

2-Methyl-4-(4-methylpiperazin-1-yl)-10*H*-benzo[*b*]thieno[2,3-e][1,4]diazepine-10-sulfonyl fluoride (26). Prepared according to general procedure A, using olanzapine (156 mg, 0.5 mmol, 1.0 equiv) and DBU (299 μL, 2.0 mmol, 4.0 equiv) in DMF (2.5 mL, 0.2 M). Compound **26** was obtained as a yellow solid (136 mg, 69% yield). The compound was previously unreported.

^{1}H NMR (400 MHz, $CDCl_3$) δ 7.37 – 7.27 (m, 2H), 7.17 (dd, *J* = 8.1, 1.5 Hz, 1H), 7.08 (td, *J* = 7.6, 1.6 Hz, 1H), 6.54 (d, *J* = 1.4 Hz, 1H), 3.81 (t, *J* = 10.2 Hz, 2H), 3.60 – 3.50 (m, 2H), 2.50 (ddd, *J* = 10.5, 6.9, 3.2 Hz, 2H), 2.47 – 2.36 (m, 5H), 2.32 (s, 3H). **^{13}C{^{1}H} NMR (101 MHz, $CDCl_3$)** δ 153.9, 145.0, 140.8, 139.3, 131.3 (d, *J* = 2.5 Hz), 130.1, 128.9, 128.2, 128.0 (d, *J* = 2.3 Hz), 124.3, 122.3, 54.8, 46.2, 16.1. **^{19}F NMR (376 MHz, $CDCl_3$)** δ 49.55 (s, 1F). **HRMS (ESI^+):** m/z calculated for $[M+H]^+$, $C_{17}H_{20}FN_4O_2S_2^+$: 395.1006, found 395.1002.

[44] T. Guo, G. Meng, X. Zhan, Q. Yang, T. Ma, L. Xu, K. B. Sharpless, J. Dong, *Angew. Chem. Int. Ed.* **2018**, 57, 2605.

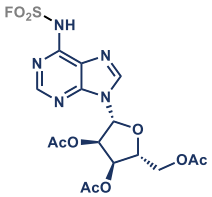

(2*R*,3*R*,4*R*,5*R*)-2-(Acetoxymethyl)-5-(6-((fluorosulfonyl)amino)-9*H*-purin-9-yl)tetrahydrofuran-3,4-diyl diacetate (27). Prepared according to general procedure A, using (2*R*,3*R*,4*R*,5*R*)-2-(acetoxymethyl)-5-(6-amino-9*H*-purin-9-yl)tetrahydrofuran-3,4-diyl diacetate (197 mg, 0.5 mmol, 1.0 equiv) and DBU (299 μL, 2.0 mmol, 4.0 equiv) in DMF (2.5 mL, 0.2 M). The resulting organic crude was dissolved in a minimum amount of dichloromethane and pentane was added dropwise until the product crashed out. Next, the solid was filtered and dried to obtain compound **27** as a pale-yellow solid (226 mg, 95% yield). The spectroscopic data are consistent with those reported previously.[45]

^{1}H NMR (400 MHz, $CDCl_3$) δ 8.65 (s, 1H), 8.39 (s, 1H), 6.24 (d, *J* = 5.5 Hz, 1H), 5.86 (t, *J* = 5.5 Hz, 1H), 5.56 (dd, *J* = 5.6, 4.4 Hz, 1H), 4.48 (td, *J* = 4.4, 3.3 Hz, 1H), 4.46 – 4.32 (m, 2H), 2.15 (s, 3H), 2.13 (s, 3H), 2.08 (s, 3H). **^{13}C{^{1}H} NMR (75 MHz, $CDCl_3$)** δ 170.59, 169.8, 169.6, 151.1, 150.3, 145.2, 142.5, 123.8, 86.9, 80.9, 73.4, 70.7, 63.1, 20.9, 20.6, 20.5. **^{19}F NMR (376 MHz, $CDCl_3$)** δ 53.65 (s, 1F).

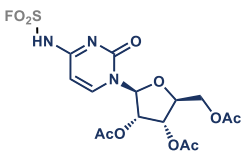

(2*S*,3*S*,4*S*,5*S*)-2-(Acetoxymethyl)-5-(4-((fluorosulfonyl)amino)-2-oxopyrimidin-1(2*H*)-yl)tetrahydrofuran-3,4-diyl diacetate (28). Prepared according to general procedure A, using (2*R*,3*R*,4*R*,5*R*)-2-(acetoxymethyl)-5-(6-amino-2-oxopyrimidin-1(2*H*)-yl)tetrahydrofuran-3,4-diyldiacetate (185 mg, 0.5 mmol, 1.0 equiv) and DBU (299 μL, 2.0 mmol, 4.0 equiv) in DMF (2.5 mL, 0.2 M). The resulting organic crude was dissolved in a minimum amount of dichloromethane and pentane was added dropwise until the product crashed out. Next, the solid was filtered and dried to obtain compound **28** as a beige solid (224 mg, 99% yield). The spectroscopic data are consistent with those reported previously.[45]

45 M. Chrominski, K. Ziemkiewicz, J. Kowalska, J. Jemielity, *Org. Lett.* **2022**, *24*, 4977.

^{1}H NMR (400 MHz, $CDCl_3$) δ 7.77 (d, *J* = 8.1 Hz, 1H), 6.51 (d, *J* = 8.0 Hz, 1H), 5.97 (d, *J* = 4.5 Hz, 1H), 5.41 (t, *J* = 5.2 Hz, 1H), 5.30 (t, *J* = 5.4 Hz, 1H), 4.51 – 4.27 (m, 3H), 2.14 (s, 3H), 2.11 (s, 6H). **^{13}C{^{1}H} NMR (75 MHz, $CDCl_3$)** δ 170.4, 170.1, 169.8, 161.3, 147.6, 143.1, 99.1, 89.1, 80.6, 73.3, 69.9, 62.8, 20.9, 20.6, 20.5. **^{19}F NMR (376 MHz, $CDCl_3$)** δ 27.88 (s, 1F).

(1-((2*S*,3*S*,4*R*,5*S*)-3,4-Dihydroxy-5-(hydroxymethyl)tetrahydrofuran-2-yl)-2-oxo-1,2-dihydropyrimidin-4-yl)sulfamoyl fluoride (29)

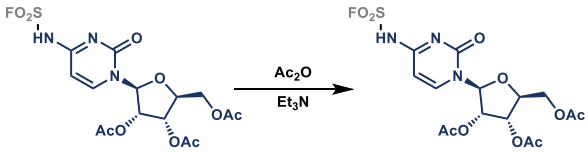

Prepared according to general procedure B, using 4-Amino-1-[(2*R*,3*R*,4*S*,5*R*)-3,4-dihydroxy-5-(hydroxymethyl)oxolan-2-yl]pyrimidin-2(1*H*)-one (66.8 mg, 0.25 mmol, 1.0 equiv) and K_2CO_3 (138 mg, 1.0 mmol, 4.0 equiv) in DMSO (1 mL, 0.2 M). The crude mixture was then subjected to acetylation conditions for of isolation purposes: acetic anhydride (35.4 μL, 0.375 mmol, 1.5 equiv) and triethylamine (70 μL, 0.5 mmol, 2.0 equiv) were directly added to the crude mixture and the solution was left stirring overnight at room temperature. Next, the crude was diluted with water and extracted multiple times with dichloromethane. Then, the organic phase was dried over Na_2CO_3, filtered, and concentrated under reduced pressure. The resulting crude was purified by flash column chromatography (CH_2Cl_2:MeOH 98:2) to afford compound **28** as a beige solid (52 mg, 60% yield). The spectroscopic data are consistent with those reported previously.[45]

^{1}H NMR (400 MHz, $CDCl_3$) δ 7.77 (d, *J* = 8.1 Hz, 1H), 6.51 (d, *J* = 8.0 Hz, 1H), 5.97 (d, *J* = 4.5 Hz, 1H), 5.41 (t, *J* = 5.2 Hz, 1H), 5.30 (t, *J* = 5.4 Hz, 1H), 4.51 – 4.27 (m, 3H), 2.14 (s, 3H), 2.11 (s, 6H). **^{13}C{^{1}H} NMR (75 MHz, $CDCl_3$)** δ 170.4, 170.1, 169.8, 161.3, 147.6, 143.1, 99.1, 89.1, 80.6, 73.3, 69.9, 62.8, 20.9, 20.6, 20.5. **^{19}F NMR (376 MHz, $CDCl_3$)** δ 27.88 (s, 1F).

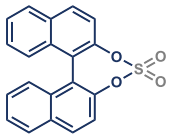

Dinaphtho[2,1-d:1',2'-f][1,3,2]dioxathiepine 4,4-dioxide (30). Prepared according to general procedure A, using 1,1′-Bi-2-naphthol (143.2 mg, 0.5 mmol, 1 equiv) and triethylamine (175 μL, 1.25 mmol, 2.5 equiv) in CH_3CN (2.5 mL, 0.2 M). Compound **30** was obtained as white solid (172.3 mg, 99% yield).

^{1}H NMR (400 MHz, $CDCl_3$) δ 8.04 (dd, J = 16.8, 9.0 Hz, 2H), 7.91 (d, J = 8.2 Hz, 2H), 7.62 (d, J = 9.1 Hz, 1H), 7.57 (d, J = 8.9 Hz, 1H), 7.53 – 7.41 (m, 3H), 7.33 – 7.27 (m, 2H), 7.18 – 7.08 (m, 1H). **^{13}C{^{1}H} NMR (101 MHz, $CDCl_3$)** δ 147.0, 146.2, 133.0, 132.8, 132.6, 132.3, 132.1, 131.8, 128.9, 128.6, 128.3, 127.6, 127.5, 127.3, 127.0, 126.6, 123.0, 122.7, 120.1, 118.8. **HRMS (FD):** m/z calculated for $[M]^+$, $C_{20}H_{12}O_4S^+$: 348.0456, found 348.0460.

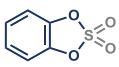

Benzo[*d*][1,3,2]dioxathiole 2,2-dioxide (31). Prepared according to general procedure A, using pyrocatechol (55.1 mg, 0.5 mmol, 1 equiv) and triethylamine (175 μL, 1.25 mmol, 2.5 equiv) in CH_3CN (2.5 mL, 0.2 M). Compound **31** was obtained as colorless crystalline solid (76.8 mg, 89% yield). The spectroscopic data are consistent with those reported previously.[35]

^{1}H NMR (400 MHz, $CDCl_3$) δ 7.23 (s, 4H). **^{13}C{^{1}H} NMR (101 MHz, $CDCl_3$)** δ 142.8, 125.5, 112.0.

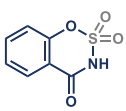

Benzo[*e*][1,2,3]oxathiazin-4(3*H*)-one 2,2-dioxide (32). Prepared according to general procedure A, using salicylamide (68.6 mg, 0.5 mmol, 1 equiv) and DBU (298 μL, 2.0 mmol, 4.0 equiv) in CH_3CN (2.5 mL, 0.2 M). Compound **32** was obtained as white solid (94 mg, 94% yield). The spectroscopic data are consistent with those reported previously.[46]

^{1}H NMR (400 MHz, d_6-DMSO) δ 7.93 (dd, J = 7.8, 1.7 Hz, 1H), 7.68 (td, J = 7.8, 1.7 Hz, 1H), 7.39 (bs, 1H), 7.34 (t, J = 7.6 Hz, 1H), 7.29 (d, J = 8.3, 1H). **^{13}C{^{1}H}**

[46] A. Kamal, A. B. Rao, P. B. Sattur, *J. Org. Chem*. **1988**, *53*, 4112.

NMR (101 MHz, *d*$_6$-DMSO) δ 166.0, 153.0, 135.3, 128.5, 124.9, 117.8, 115.9. **HRMS (GC-EI):** m/z calculated for $[M]^+$, $C_7H_5NO_4S^+$: 198.9934, found 198.9938.

1-(Fluorosulfonyl)-2,3,4,6,7,8,9,10-octahydro-1H-pyrimido[1,2-a]azepin-5-ium (33). Prepared according to general procedure A, using DBU (298 μL, 2.0 mmol, 4.0 equiv) in CH_3CN (2.5 mL, 0.2 M). Compound **33** was obtained as a pale-yellow solid after workup and evaporation of the organic phase.

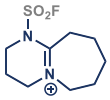

^{1}H NMR (400 MHz, $CDCl_3$) δ 3.65 – 3.43 (m, 2H), 3.42 – 3.30 (m, 2H), 3.22 (qd, J = 6.3, 2.1 Hz, 2H), 2.60 – 2.50 (m, 2H), 1.77 (p, J = 5.9 Hz, 4H), 1.67 (dp, J = 15.3, 5.5 Hz, 4H). **^{13}C{^{1}H} NMR (75 MHz, $CDCl_3$)** δ 178.0, 49.9, 44.7, 40.6 (d, J = 1.9 Hz), 36.9, 29.9, 28.3, 27.0, 23.3. **^{19}F NMR (376 MHz, $CDCl_3$)** δ 52.42 (s, 1F).

5.5.8 Telescoped transformations

Sulfate formation

Sulfuryl chloride (810 μL, 10 mmol) was dissolved in dry acetonitrile (50 mL, 0.2 M) in an oven-dried N_2 filled 100 mL round bottom flask with a rubber septum. The 0.2 M solution of sulfuryl chloride was taken up with a 20 mL syringe and mounted on a syringe pump. The first time a packed bed was used, it was flushed with dry acetonitrile to fill the empty volume with solvent. Then 5 mL of the SO_2Cl_2 were pumped at 0.5 mL·min^{-1} to equilibrate the reactor. Once this procedure was done, the cartridge could be used continuously until its exhaustion. Parallelly, in a 10 mL vial, (13*S*)-3-hydroxy-13-methyl-6,7,8,9,11,12,13,14,15,16-decahydro-17*H*cyclopenta[*a*]phenanthren-17-one (135.0 mg, 0.5 mmol, 1 equiv) and triethylamine (139 μL, 1 mmol, 2 equiv) were dissolved in DMF (2.5 mL, 0.2 M). This mixture was then taken up with a 5 mL syringe and mounted on a second syringe pump. Next, in a 10 mL vial, (4-iodophenoxy)trimethylsilane (292 mg, 1 mmol, 2 equiv) and DBU (224 μL,

1.5 mmol, 3 equiv) were dissolved in DMF (2.78 mL, 0.36 M). This mixture was then taken up with a 5 mL syringe and mounted on a third syringe pump.

To start the reaction, the solution of sulfuryl chloride was constantly pumped through the equilibrated KF packed bed at 0.5 mL·min^{-1} (t_R = ~7 min). The resulting sulfuryl fluoride flow was then mixed with the first feeding solution containing (13*S*)-3-hydroxy-13-methyl-6,7,8,9,11,12,13,14,15,16-decahydro-17*H*cyclopenta[*a*]phenanthren-17-one (pumped at 0.45 mL·min^{-1}) through a PEEK T-mixer. The combined feeds were connected to a 1.5 mL PFA coil (I.D = 0.8 mm, t_R = 1.6 min) whichh served as reactor for the SuFEx event. Next, the ensuing fluorosulfate was mixed with the second feeding solution containing (4-iodophenoxy)trimethylsilane (pumped at 0.55 mL·min^{-1}) throwhichother PEEK T-mixer. The combined feeds were connected to a 3 mL PFA coil (I.D = 0.8 mm, t_R = 2 min) which served as reactor for the sulfate formation. At the end of the coil, the organic crude was collected in a conical flask.The collected solution was diluted with ethyl acetate, washed with 10% $HCl_{(aq.)}$, and then with brine. Next, the organic phase was dried over Na_2SO_4, filtered, and concentrated under reduced pressure. The resulting crude was purified by flash column chromatography (Hexane:AcOEt 8:2) to afford compound **34** as an off-white solid (185 mg, 67% yield). The spectroscopic data are consistent with those reported previously.[47]

4-Iodophenyl ((8R,9S,13S,14S)-13-methyl-17-oxo-7,8,9,11,12,13,14,15,16,17-decahydro-6H-cyclopenta[a]phenanthren-3-yl) sulfate (34)

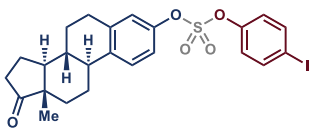

^{1}H NMR (400 MHz, $CDCl_3$) δ 7.74 (d, *J* = 8.8 Hz, 2H), 7.32 (d, *J* = 8.6 Hz, 1H), 7.15 – 6.99 (m, 4H), 2.92 (dd, *J* = 9.0, 4.3 Hz, 2H), 2.51 (dd, *J* = 18.8, 8.7 Hz, 1H), 2.40 (dt, *J* = 14.0, 3.7 Hz, 1H), 2.29 (td, *J* = 10.7, 4.4 Hz, 1H), 2.22 – 1.91 (m, 4H), 1.78 – 1.40 (m, 6H), 0.91 (s, 3H). **^{13}C{^{1}H} NMR (101 MHz,**

[47] G.-F. Zha, Q. Zheng, J. Leng, P. Wu, H.-L. Qin, K. B. Sharpless, Palladium-Catalyzed Fluorosulfonylvinylation of Organic Iodides. *Angew. Chem. Int. Ed.* **2017**, *56*, 4849.

$CDCl_3$) 220.6, 150.4, 148.4, 139.7, 139.2, 139.2, 127.1, 123.3, 121.0, 118.1, 92.2, 50.5, 48.0, 44.2, 37.9, 35.9, 31.6, 29.5, 26.2, 25.8, 21.7, 13.9.

Hydrolysis of fluorosulfate

(8*R*,9*S*,13*S*,14*S*)-13-Methyl-6,7,8,9,11,12,13,14,15,16-decahydrospiro[cyclopenta[*a*]phenanthrene-17,2'-[1,3]dioxolan]-3-yl hydrogen sulfate (35)

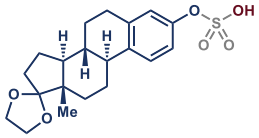

(8*R*,9*S*,13*S*,14*S*)-13-methyl-6,7,8,9,11,12,13,14,15,16-decahydrospiro[cyclopenta[*a*]phenanthrene-17,2'-[1,3]dioxolan]-3-ol (157 mg, 0.500 mmol, 1 equiv) was suspended in dry MeCN (2.5 mL), Et_3N (175 μL, 1.25 mmol, 2.5 equiv) was added and suspension was sonicated until all solids were solubilized. The corresponding fluorosulfate was prepared in accordance with the general procedure A. The ensuing reaction mixture was then collected in a nitrogen-filled RBF and sparged for 10 min to remove residual SO_2F_2. Solvent was removed under reduced pressure. Subsequently, 1 molar solution of KOH in absolute EtOH (5 mL, 5 mmol, 10 equiv) was added to the solid residue, and the mixture was stirred for 30 miwhichuring which formation of a jelly mixture was observed. Subsequently, 5 mL of a 1 molar KOH solution in EtOH were added to have a homogenwhich mixture, which was diluted with water (10 mL) and extracted with EtOAc (3x15 mL). Combined organic layers were dried over anhydrous Na_2SO_4, and solvent was removed under the reduced pressure to afford 160 mg (81%) of product in form of a white solid. The compound was previously unreported.

^{1}H NMR (400 MHz, CD_3OD) δ 7.23 (d, *J* = 8.5 Hz, 1H), 7.03 (dd, *J* = 8.5 Hz, 2.4 Hz, 1H), 7.00 (d, *J* = 2.4 Hz, 1H), 3.96-3.82 (m, 4 H), 2.91-2.83 (m, 2H), 2.39-2.33 (m, 1H), 2.24-2.17 (m, 1H), 2.04-1.97 (m, 1H), 1.95-1.90 (m, 1H), 1.85-1.72 (m, 3H), 1.68-1.61 (m, 1H), 1.56-1.51 (m, 1H), 1.50-1.26 (m, 4H), 0.89 (s, 3H). **^{13}C NMR (101 MHz, CD_3OD)** δ 151.7, 138.8, 138.0, 127.0, 122.5, 120.5, 119.7, 66.2, 65.6, 50.7, 47.3, 45.3, 40.4, 35.2, 31.9, 30.6, 28.2, 27.3, 23.3, 14.8. **HRMS (ESI):** m/z calculated for $[M+H]^+$, $C_{20}H_{27}FO_6S^+$: 395.1523, found 395.1522.

Cross-coupling

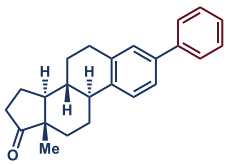

(8*R*,9*S*,13*S*,14*S*)-13-Methyl-3-phenyl-6,7,8,9,11,12,13,14,15,16-decahydro-17*H*-cyclopenta[*a*]phenanthren-17-one (36)

Prepared according to a modified version of general procedure A, using (13*S*)-3-hydroxy-13-methyl-6,7,8,9,11,12,13,14,15,16-decahydro-17*H*cyclopenta[*a*]phenanthren-17-one (135.0 mg, 0.5 mmol, 1 equiv) and triethylamine (175 μL, 1.25 mmol, 2.5 equiv) in DMF (2.5 mL, 0.2 M), crude estrone fluorosulfate derivate **11**, was collected in a vial. Then, the solvent was removed under reduced pressure, and phenylboronic acid (85 mg, 0.7 mmol, 1.4 equiv), diacetoxypalladium (5.6 mg, 0.025 mmol, 0.05 equiv), triphenylphosphine (16.4 mg, 0.63 mmol, 0.125 equiv), cesium carbonate (489 mg, 1.5 mmol, 3 equiv), and toluene (1.8 mL) were added. Then, a magnetic stir bar was charged into the vial, and the reaction was heated up to 110 °C for 24 h. Next, the reaction was diluted with dichloromethane, washed with 10% HCl(aq.), and then with brine. The organic phase was dried over Na_2SO_4 filtered, and concentrated under reduced pressure. The resulting crude was purified by flash column chromatography (hexanes:EtOAc 90:10) to afford compound **36** as a white solid (91 mg, 55% yield). The spectroscopic data are consistent with those reported previously.[48]

^{1}H NMR (400 MHz, $CDCl_3$) 7.50 (d, *J* = 7.2 Hz, 2H), 7.36 – 7.21 (m, 6H), 2.91 (dd, *J* = 9.1, 4.2 Hz, 2H), 2.52 – 2.34 (m, 2H), 2.27 (m, 1H), 2.16 – 1.83 (m, 4H), 1.71 – 1.28 (m, 6H), 0.84 (s, 3H). **^{13}C{^{1}H} NMR (101 MHz, $CDCl_3$)** δ 221.0, 141.1, 139.0, 138.9, 137.0, 128.8, 127.8, 127.2, 127.1, 125.9, 124.7, 50.6, 48.1, 44.5, 38.3, 36.0, 31.7, 29.7, 26.7, 25.9, 21.7, 14.0.

[48] X.-J. Li, J.-L. Zhang, Y. Geng, Z. Jin *J. Org. Chem.* **2013**, *78*, 5078.

5.5.9 Optimization of the SuFEx process for peptides

We also performed a method optimization under conditions amenable to functionalize peptides – aqueous solutions and low concentrations. The results of this screening are summarized in the Table E2.

Table E2. Optimization of the SuFEx reaction under aqueous and diluted conditions. [a] Yield determined by ^{19}F NMR analysis using 1,2-difluorobenzene as standard.

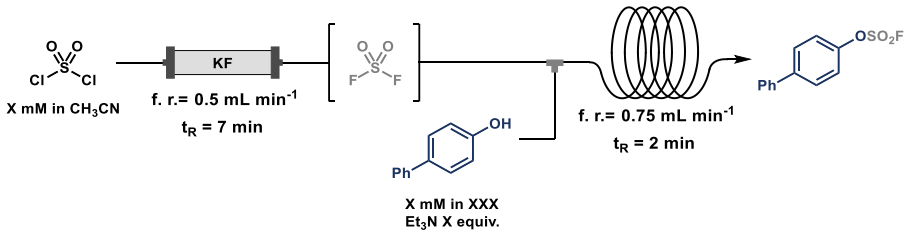

Entry	$[SO_2F_2]$ mM	[Phenol] mM	ACN : H_2O	Et_3N	Yield[a]
1	200	200 mM	4 : 1	2.5	82%
2	200	200 mM	1 : 1	2.5	79%
3	200	10 mM	1 : 1	2.5	75%
4	10	10 mM	1 : 1	2.5	-
5	20	10 mM	1 : 1	2.5	-
6	200	10 mM	1 : 1	6	99%

5.5.10 Myoglobin SuFEx ligation using a fed-batch approach

With the previously optimized conditions from our flow system, we decided to test the reaction in a fed-batch setup (Scheme S2).

In a typical experiment, sulfuryl chloride (404 μL, 5 mmol) was dissolved in dry acetonitrile (50 mL, 0.1 M) in an oven-dried, N_2 filled 100 mL round bottom flask closed with a rubber septum. The 0.1 M solution of sulfuryl chloride was taken up with a 20 mL syringe and mounted on a syringe pump. The first time a packed bed was used, it was flushed with dry acetonitrile to fill the empty volume with solvent. Then 5 mL of the SO_2Cl_2 were pumped at

0.1 mL·min^{-1} to equilibrate the reactor. Once this procedure was done, the cartridge could be used continuously until its exhaustion.

Parallelly, in a 10 mL vial containing a magnetic stir bar, equine myoglobin (16.9 mg, 2.5 μmol, 1 equiv) was charged. Next, aqueous acetate buffer (2.5 mL, 10 mM, pH 5) and 1,1,3,3-tetramethylguanidine (10 μL of a 0.25 M aqueous solution, 2.5 μmol, 1 equiv) were subsequently added to the vial.

To start the reaction, the solution of sulfuryl chloride was constantly pumped through the equilibrated KF packed bed at 0.1 mL·min^{-1} (t_R = ~38 min). The resulting sulfuryl fluoride flow was then fed to the vial containing the myoglobin in solution. Once the SO_2F_2 (0.27 mL, 27 μmol, 11 equiv) was fed into the vial, the latter was capped, and the mixture was left stirring overnight at room temperature. RPLC-MS analysis revealed a conversion of 16% to the monofunctionalized product following general analytical method C.

5.5.11 Myoglobin SuFEx ligation using the H-type reactor

With the previously optimized conditions from our flow system for the protein solution, we decided to test the reaction in a batch setup using a H-type reactor with an excess of SO_2F_2.

For this experiment, a COware gas reactor (SigmaAldrich, reference STW1) was used. Both chambers were charged with a magnetic stir bar and then purged with N_2. One chamber was dedicated to the generation of gaseous SO_2F_2, and it was charged with KF (151 mg, 2.6 mmol, 1040 equiv) and CH_3CN (2.4 mL, 0.2 M). The other chamber was charged with myoglobin (16.6 mg, 2.5 μmol, 1 equiv), acetate buffer (2.5 mL, 10 mM, pH 5) and 1,1,3,3-tetramethylguanidine (10 μL of a 0.25 M aqueous solution, 2.5 μmol, 1 equiv). The reaction was started by the addition of SO_2Cl_2 (33 μL, 0.4 mmol, 160 equiv) to the SO_2F_2 generation chamber. Then the reactor was left stirring overnight. RPLC-MS analysis, following general analytical method C, revealed full

conversion, but no yield of the targeted product and a complex mixture of byproducts.

5.5.12 Installation of the SO_2F motif for peptides

General Procedure C

In a typical experiment, sulfuryl chloride (810 μL, 10 mmol) was dissolved in dry acetonitrile (50 mL, 0.2 M) in an oven-dried N_2 filled 100 mL round bottom flask with a rubber septum. The 0.2 M solution of sulfuryl chloride was taken up with a 20 mL syringe and mounted on a syringe pump. The first time a packed bed was used, it was flushed with dry acetonitrile to fill the empty volume with solvent. Then 5 mL of the SO_2Cl_2 were pumped at 0.5 $mL \cdot min^{-1}$ to equilibrate the reactor. Once this procedure was done, the cartridge could be used continuously until its exhaustion. Parallelly, in a 5 mL vial containing a magnetic stir bar, the peptide was charged. Next, a CH_3CN 1 : 1 H_2O mixture and Et_3N (6 equiv) were added, and the vial was capped with a septum. To start a reaction, the solution of sulfuryl chloride was constantly pumped through the equilibrated KF packed bed at 0.5 $mL \cdot min^{-1}$ (t_R = ~7 min). The resulting sulfuryl fluoride flow was then mixed with the nucleophile solution (pumped at 0.25 $mL \cdot min^{-1}$) through a PEEK T-mixer. The combined feeds were connected to a 1.5 mL PFA coil (I.D = 0.8 mm, t_R = 2 min) which served as reactor for the SuFEx event. At the end of the coil, the crude was collected and subsequently analyzed by RPLC-MS to determine conversion.

Ac-F-N-L-Y-A-NH_2 (41)

Prepared according to general procedure C, using Ac-F-N-L-Y-A-NH_2 trifluoroacetate salt (7.8 mg, 10 μmol, 1 equiv), water (0.5 mL), acetonitrile (0.5 mL), and triethylamine (8.4 μL, 60 μmol, 6 equiv). Conversion was determined to be 91% by RPLC-MS following general analytical procedure A.

Ac-A-K-F-N-L-NH_2 (42)

Prepared according to general procedure C, using Ac-A-K-F-N-L-NH_2 trifluoroacetate salt (3.2 mg, 5 μmol, 1 equiv), water (0.25 mL), acetonitrile (0.25 mL), and triethylamine (4.2 μL, 30 μmol, 6 equiv). Conversion was determined to be 29% by RPLC-MS following general analytical procedure A.

Ac-F-N-L-H-A-NH_2 (43)

Prepared according to general procedure C, using Ac-F-N-L-H-A-NH_2 trifluoroacetate salt (1.6 mg, 2.5 μmol, 1 equiv), water (0.125 mL), acetonitrile (0.125 mL), and triethylamine (2.1 μL, 15 μmol, 6 equiv). Conversion was determined to be 10% by RPLC-MS following general analytical procedure A.

Ac-Y-N-L-W-A-NH_2 (44)

Prepared according to general procedure C, using Ac-Y-N-L-W-A-NH_2 trifluoroacetate salt (8.0 mg, 10 μmol, 1 equiv), water (0.5 mL), acetonitrile (0.5 mL), and triethylamine (8.4 μL, 60 μmol, 6 equiv). Conversion was determined to be 99% by RPLC-MS following general analytical procedure A.

P-F-N-V-A-NH_2 (45)

Prepared according to general procedure C, using P-F-N-V-A-NH_2 trifluoroacetate salt (2.7 mg, 5 μmol, 1 equiv), water (0.25 mL), acetonitrile (0.25 mL), and triethylamine (4.2 μL, 30 μmol, 6 equiv). Conversion was determined to be 0% by RPLC-MS following general analytical procedure A.

Ac-M-R-F-S-D-NH_2 (46)

Prepared according to general procedure C, using Ac-M-R-F-S-D-NH_2 trifluoroacetate salt (3.5 mg, 5 μmol, 1 equiv), water (0.25 mL), acetonitrile (0.25 mL), and triethylamine (4.2 μL, 30 μmol, 6 equiv). Conversion was determined to be 0% by RPLC-MS following general analytical procedure A.

Ac-A-C-F-N-S-NH_2 (47)

Prepared according to general procedure C, using Ac-A-C-F-N-S-NH_2 trifluoroacetate salt (2.9 mg, 5 μmol, 1 equiv), water (0.25 mL), acetonitrile (0.25 mL), and triethylamine (4.2 μL, 30 μmol, 6 equiv). Conversion was determined to be 0% by RPLC-MS following general analytical procedure A.

Desmopressin (48)

Prepared according to general procedure C, using desmopressin acetate salt (5.7 mg, 5 μmol, 1 equiv), water (0.25 mL), acetonitrile (0.25 mL), and triethylamine (4.2 μL, 30 μmol, 6 equiv). Conversion was determined to be 99% by RPLC-MS/MS following general analytical procedure B. MS/MS analysis: LC-MS/MS gives a peptide coverage of 66.67% (the covered sequence was in red font below). and probes the reaction was selective exclusively for Tyr2. The sequence of Desmopressin is shown below, the site of modification (Y) is highlighted in bold red. Deamino-^{1}C **Y** F Q N C P R G^{9}-NH_2

Oxytocin (49)

Prepared according to general procedure C, using oxytocin (3.0 mg, 3.0 μmol, 1 equiv), water (0.15 mL), acetonitrile (0.15 mL), and triethylamine (10 μL of 1.8 M solution in MeCN, 18 μmol 6 equiv). Conversion was determined to be 96% by RPLC-MS/MS following general analytical procedure C. MS/MS analysis: LC-MS/MS analysis behaves good peptide coverage (66.67%, the covered sequence was in red font below) and probes the reaction was selective exclusively for Tyr2. The sequence of oxytocin is shown below, the site of modification (Y) is highlighted in bold red. ^{1}C Y I Q N C P L G^{9}-NH_2

Angiotensin II (50)

Prepared according to general procedure C, using Angiotensin II (2.6 mg, 2.5 μmol, 1 equiv), water (0.125 mL), acetonitrile (0.125 mL), and triethylamine (2.1 μL, 15 μmol, 6 equiv). Conversion was determined to be 66% by RPLC-MS/MS following general analytical procedure B. MS/MS analysis: LC-MS/MS

analysis behaves good peptide coverage (87.5%, the covered sequence was in red font below) and probes the reaction was selective exclusively for Tyr4. The sequence of angiotensin is shown below, the site of modification (Y) is highlighted in bold red. ^{1}D R V Y I H P F^{8}

Bivalirudin (51)

Prepared according to general procedure C, using Bivalirudin (5.7 mg, 2.5 μmol, 1 equiv), water (0.125 mL), acetonitrile (0.125 mL), and triethylamine (2.1 μL, 15 μmol, 6 equiv). Conversion was determined to be 30% by RPLC-MS following general analytical procedure A. MS/MS analysis: LC-MS/MS analysis behaves good peptide coverage (80.00%, the covered sequence was in red font below) and probes the reaction was selective exclusively for Tyr19. The sequence of bivalirudin is shown below, the site of modification (Y) is highlighted in bold red. ^{1}F P R P G G G G N G D F E E I PE EY L^{20}

α-Endorphin (52)

Prepared according to general procedure C, using α-Endorphin (1.0 mg, 0.6 μmol, 1 equiv), water (0.050 mL), acetonitrile (0.050 mL), and triethylamine (10 μL of 0.36 M solution in MeCN, 3.6 μmol, 6 equiv). Conversion was determined to be 87% by RPLC-MS/MS following general analytical procedure B.

MS/MS analysis

LC-MS/MS analysis behaves good peptide coverage (50.00%, the covered sequence was in red font below) and probes the reaction was selective for Tyr1, although functionalization at Lys9 was also observed. The sequence of endorphin is shown below, the site of modification (Y) is highlighted in bold red. ^{1}Y G G F M T S E K S Q T P L V T^{16}

β-Amyloid (1–28) (53)

Prepared according to general procedure C, using β-Amyloid (1–28) (1.0 mg, 0.3 μmol, 1 equiv), water (0.050 mL), acetonitrile (0.050 mL), and triethylamine (5 μL of 0.36 M solution in MeCN, 1.8 μmol, 6 equiv). Conversion was determined to be 10% by RPLC-MS/MS following general analytical procedure B. MS/MS analysis: LC-MS/MS analysis behaves good peptide coverage (46.43%, the covered sequence was in red font below) and probes the reaction was selective exclusively for Tyr10. The sequence of amyloid is shown below, the site of modification (Y) is highlighted in bold red. ^{1}D A E F R H D S G Y E V H H Q K L V F F A E D V G S N K$^{28.}$

5.5.13 Installation of the SO_2F motif in proteins

General Procedure D

In a typical experiment, sulfuryl chloride (404 μL, 5 mmol) was dissolved in dry acetonitrile (50 mL, 0.1 M) in an oven-dried N_2 filled 100 mL round bottom flask with a rubber septum. The 0.1 M solution of sulfuryl chloride was taken up with a 20 mL syringe and mounted on a syringe pump. The first time a packed bed was used, it was flushed with dry acetonitrile to fill the empty volume with solvent. Then 5 mL of the SO_2Cl_2 were pumped at 0.1 mL·min^{-1} to equilibrate the reactor. Once this procedure was done, the cartridge could be used continuously until its exhaustion.

Parallelly, in a 5 mL vial containing a magnetic stir bar protein was charged. Next, aqueous buffer, and 1,1,3,3-tetramethylguanidine were subsequently added to the vial.

To start a reaction, the solution of sulfuryl chloride was constantly pumped through the equilibrated KF packed bed at 0.1 mL·min^{-1} (t_R = ~38 min). The resulting sulfuryl fluoride flow was then mixed with the protein solution (pumped at 0.9 mL·min^{-1}) through a PEEK T-mixer. The combined feeds were connected to a 1.5 mL PFA coil (I.D = 0.8 mm, t_R = 1.5 min) which

served as reactor for the SuFEx event. At the end of the coil, the aqueous crude was collected in vial. Crucially, after the packed bed reactor, a 2.8 bar back pressure regulator was installed to ensure the consistency in the mixing between the SO_2F_2 and the protein feed.

Importantly, when the syringe pump of the protein solution finished pushing, the system was stopped (both syringe pumps), and the syringe of the protein was quickly substituted by another one containing aqueous buffer. Then the flow rate of the latter one was set to 1 mL·min^{-1} to push the remaining reaction crude out of the PFA coil, while the syringe pump of the sulfuryl chloride solution remained stopped. The collected crude was then analyzed by RPLC-MS to determine conversion.

Equine myoglobin (54)

Prepared according to general procedure D, using myoglobin (16.9 mg, 2.5 μmol, 1 equiv), acetate buffer (2.5 mL, 10 mM, pH 5), and 1,1,3,3-Tetramethylguanidine (10 μL of a 0.25 M aqueous solution, 2.5 μmol, 1 equiv). Conversion was determined to be 33% by RPLC-MS following general analytical procedure A. MS/MS analysis: LC-MS/MS analysis gave full peptide coverage (100%, the covered sequence is reported in red font below) and probes the reaction was selective exclusively for Tyr103. The sequence of myoglobin is shown below, with the identified peptide functionalization sites underlined.

^{1}GLSDG EWQQV LNVWG KVEAD IAGHG QEVLI
RLFTG HPETL EKFDK FKHLK TEAEM KASED
LKKHG TVVLT ALGGI LKKKG HHEAE LKPLA
QSHAT KHKIP IK**Y**LE FISDA IIHVL HSKHP
GDFGA DAQGA MTKAL ELFRN DIAAK YKELG
FQG^{153}

Y^{103} L E F I S D A I I H V L H S K

β-Casein from bovine milk (55)

Prepared according to general procedure D, using β-Casein (25.0 mg, 2.5 μmol, 1 equiv), tris buffer (2.5 mL, 5 mM, pH 7.7), and 1,1,3,3-Tetramethylguanidine (100 μL of a 0.25 M aqueous solution, 2.5 μmol, 10 equiv). The reaction mixture was directly analyzed by native SEC-MS method without any pretreatment. Conversion rate was determined to be 58% by the mass intensity following general analytical procedure D. MS/MS analysis: LC-MS/MS analysis gives a peptide coverage of 86.6% (the covered sequence was in red font below) and probes the reaction was selective exclusively for Tyr 114, Tyr180, Tyr193. The sequence of β-casein is shown below, with the identified peptide functionalization sites underlined.

^{1}RELEE LNVPG EIVES LSSSE ESITR INKKI EKFQS
EEQQQ TEDEL QDKIH PFAQT QSLVY PFPGP IPNSL
PQNIP PLTQTP VVVP PFLQP EVMGV SKVKE AMAPK
HKEMP FPK**Y**P VEPFT ESQSL TLTDV ENLHL PLPLL
QSWMH QPHQP LPPTV MFPPQ SVLSL SQSKV LPVPQ
KAVP**Y** PQRDM PIQAF LL**Y**QE PVLGP VRGPF PIIV^{209}

Y^{114} P V E P F T E S Q S L
A V P Y^{180} P Q R
L L Y^{193} Q E P V L G P V R G P F P I I V

CHAPTER VII

General Conclusions

UNIVERSITAT ROVIRA I VIRGILI
REAGENTS AND METHODOLOGIES FOR THE INTRODUCTION OF THIOFLUOROALKYL AND FLUOROSULFUR MOTIFS
Miguel Bernús Pérez

7.1 General Conclusions

The present thesis has developed methodologies and reagents for the incorporation of thiofluoroalkyl and fluorosulfur motifs, which hold significance in the field of medicinal chemistry. The approaches employed in this work utilize cost-effective starting materials and simple experimental setups, providing accessible solutions for any synthetic laboratories. Overall, the initial objectives set forth have been successfully achieved. The specific conclusions for each chapter are summarized below:

Chapter III: Evaluation of medicinal chemistry properties of thiofluoroalkyl fragments.

This chapter presents a comprehensive study of the lipophilicity and acid properties of 2-thiofluoroalkyl (SR_F) and 2-sulfonyl fluoroalkyl (SO_2R_F) substituted pyridines. Generally, thiofluoroalkyl motifs are known to enhance lipophilicity. However, this work highlights the intricate interplay between the degree of fluorination and the molecular topology in this parameter. Through collaboration with computational chemists, a rationale has been proposed to explain the observed trends in lipophilicity: it has been observed that the introduction of fluorine has a dual effect of polarizing the molecule and increasing its hydrophobic surface. In navigating this delicate balance, we have established a scale of different SR_F and SO_2R_F motifs that can be effectively generalized to aid in the selection of these fragments for fine-tuning the physicochemical properties of drug candidates.

Chapter IV: Development of electrophilic thiopolifluoroalkylating reagents.

In this chapter two saccharin-based reagents to introduce SCF_2CF_2H and SCF_2CF_3 have been disclosed. These electrophilic agents are synthesized in multigram scale without the need of column chromatography. In this work, the installation of 2-thiofluoroalkyl (SR_F) motifs has been proved in a wide

range of nucleophiles to forge heteroatom- and carbon-SR_F bonds, including natural products and blockbuster drugs. In addition, the thiofluoroalkyl handles have been further derivatized to access other functionalities. In general, these reagents expand the synthetic toolbox to access new thiofluoroalkyl fragments in a direct fashion.

Chapter V: A Modular Flow Platform for SuFEx ligation.

This chapter discloses a modular flow platform for the installation of the -SO_2F handle into small molecules, peptides, and proteins. The presented system overcomes some actual limitations of the previously available systems as the direct use of toxic and gaseous SO_2F_2, or expensive engineered reagents. Moreover, the microfluidic system enables the click ligation in just two minutes in a wide range of phenols and amino functionalities, and can be coupled with other modules to telescope transformations. Due to the robustness of the system, the same platform can be used to modify tyrosine residues in peptides and proteins. In general, these findings offer a simple solution for accessing libraries of compounds containing -SO_2F handles.

UNIVERSITAT ROVIRA I VIRGILI
REAGENTS AND METHODOLOGIES FOR THE INTRODUCTION OF THIOFLUOROALKYL AND FLUOROSULFUR MOTIFS
Miguel Bernús Pérez

UNIVERSITAT ROVIRA I VIRGILI
REAGENTS AND METHODOLOGIES FOR THE INTRODUCTION OF THIOFLUOROALKYL AND FLUOROSULFUR MOTIFS
Miguel Bernús Pérez

UNIVERSITAT
ROVIRA i VIRGILI